Steam gasification of tropical lignocellulosic agrowaste : impact of biomass characteristics on the gaseous and solid by-products

Lina Maria Romero Millan

Université Fédérale

Toulouse Midi-Pyrénées

THÈSE

en vue de l'obtention du

DOCTORAT DE L'UNIVERSITÉ DE TOULOUSE

délivré par

IMT - École Nationale Supérieure des Mines d'Albi-Carmaux

Cotutelle Internationale avec "Universidad Nacional de Colombia", Colombie

---

Présentée et soutenue par

Lina Maria ROMERO MILLAN

Le 28 Novembre 2018

Steam gasification of tropical lignocellulosic agrowaste: Impact of biomass characteristics on the gaseous and solid by-products

---

École doctorale et discipline ou spécialité :
MEGEP : Génie des procédés et de l'Environnement

Unité de recherche :
Centre RAPSODEE, UMR CNRS 5302, IMT Mines Albi

Directeur(s) de Thèse :
Ange NZIHOU, Professeur, IMT Mines Albi
Fabio Emiro SIERRA VARGAS, Professeur, Universidad Nacional de Colombia

Membres du jury :
Laurence LECOQ, Professeur, IMT Atlantique - DSEE *(Présidente)*
Claire COURSON, Maître de Conférence, ICPEES Université de Strasbourg *(Rapporteur)*
Marco CASTALDI, Professeur, The City College of New York *(Examinateur)*
Maria Fernanda GOMEZ GALINDO, Professeur, Univ. de la Sabana Colombia *(Examinateur)*
Carlos Alberto GUERRERO FAJARDO, Professeur, Univ. Nacional de Colombia *(Examinateur)*

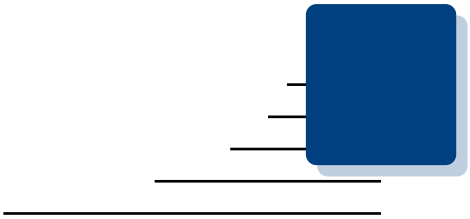

Acknowledgment

Firstly, I would like to express my sincere gratitude to my supervisors, Professor Fabio Sierra and Professor Ange Nzihou, for their continuous support of my research, for their patience, motivation, and knowledge. Their guidance and persistent help were essential for the successful development of my work. Both professors gave me the opportunity to join their research teams, and develop my research work in the framework of a cotutelle agreement between the National University of Colombia (Colombia) and the "IMT Mines Albi-Carmaux" institute (France). This has been a grateful experience to me, from both personal and professional point of view.

Also, I gratefully acknowledge the members of my Ph.D. committee for their time and valuable comments and feedback.

I owe a great gratitude to COLCIENCIAS and the Colombian national program for doctoral formation, for the doctoral scholarship granted for the development of my Ph.D. (CV 647-2014)

My sincere thanks also goes to the research, technical, and administrative staff of the National University of Colombia, and the RAPSODEE research laboratory. Thanks for their kind support during my research activities, their guidance, and expertise. It has been a pleasure to me to work with such talented and committed teams. Their suggestions and contributions, as well as the technical discussions, were always extremely valuable and inspiring.

Thanks to all my colleagues and friends for their inspiration, friendship, and support. Their motivation and enthusiasm helped me to successfully complete this process. I am grateful for the time spent together.

Last but not the least, I would like to thank my family: my parents and my sisters, for their encouragement and patience during all these years. Without their support, this achievement would not be possible.

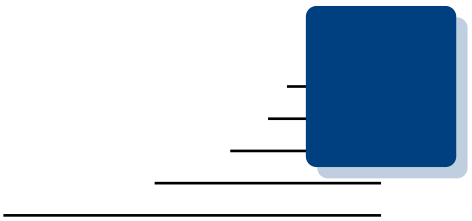

Contents

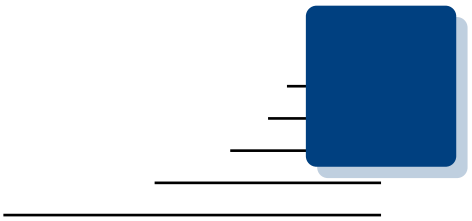

Abstract

In the context of most developing countries, steam gasification could be a very interesting process for both energy generation in isolated areas and the production of value-added products from lignocellulosic agrowaste. Considering that the availability of agricultural residues is often seasonal, gasification facilities should operate with different feedstocks. In consequence, this work is focused on the understanding of the impact of biomass characteristics on the gasification process and the properties of the gaseous and solid by-products. Three lignocellulosic agrowastes with different macromolecular structure and inorganic composition were selected for this study: Coconut shells (CS), bamboo guadua (BG) and oil palm shells (OPS).

The thermal decomposition kinetics of the selected feedstocks was analyzed in a thermogravimetric scale under inert and steam atmosphere. Despite the differences in their macromolecular composition, inorganics showed to be the most important parameter influencing the steam gasification reactivity and kinetics of the samples. The beneficial impact of AAEM was confirmed, as well as the inhibitory effect of Si and P. More specifically, the ratio K/(Si+P) proved to be suitable to describe and compare the steam gasification behavior of lignocellulosic agrowastes. In accordance, a new kinetic modeling approach was proposed to predict the gasification behavior of samples, from the knowledge of their inorganic composition.

The validity of the ratio K/(Si+P) to classify and predict the biomass steam gasification behavior was also confirmed from experiments in a lab-scale fluidized bed gasifier. Samples with K/(Si+P) above 1 exhibited higher gasification reactivities compared to samples with ratios below 1, resulting in greater gas yields and higher gas efficiencies. Moreover, inorganics impacted not only the gasification rate of the samples, but also the properties of the gasification solid by-products. In particular, higher gasification reactivities were related to higher char surface areas and contents of oxygenated surface functional groups. A temperature of 850°C, a gasification time of 1 hour, and a steam fraction of 30% in the reacting atmosphere proved to be the most suitable conditions for the simultaneous production of fuel gases for energy applications, and a valuable char that could be valorized in soil amendment applications.

The gasification model and experimental results presented in this work might be an important reference for real gasification applications working with different kind of residues, when both the gaseous and solid by-products valorization is intended. Moreover, in the presented context, steam gasification of lignocellulosic agrowaste may improve the energy access in rural isolated areas, and simultaneously promote the development of productive projects that could generate new incomes for local communities.

Keywords: Steam gasification, Gasification reactivity, Inorganic composition, Lignocellulosic agrowaste, Syngas, Biochar.

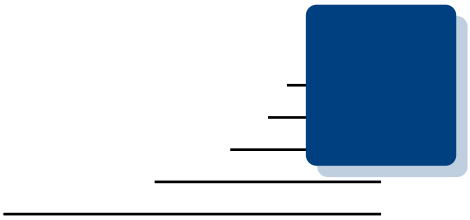

Spanish abstract / Resumen

En el contexto económico de una gran parte de países en vía de desarrollo, la gasificación con vapor de agua de residuos agrícolas y agroindustriales puede ser considerada como un proceso de especial interés para la producción simultanea de energía en regiones aisladas, y productos de valor agregado. Teniendo en cuenta que la disponibilidad de los residuos agrícolas no es constante y depende de la estacionalidad de los cultivos, diferentes tipos de biomasa deben ser utilizados para asegurar el funcionamiento de las instalaciones de gasificación. En este sentido, el presente trabajo está enfocado en la comprensión del impacto de las características de la biomasa en el proceso de gasificación, y en las propiedades de los subproductos sólidos y gaseosos. Tres residuos agrícolas lignocelulósicos con diferente composición macromolecular e inorgánica fueron seleccionados para este estudio: cáscara de coco (CS), bambú guadua (BG) y cuesco de palma (OPS).

La cinética de la descomposición térmica de los materiales seleccionados fue estudiada a escala termogravimétrica en atmosfera inerte y de vapor de agua. A pesar de las diferencias en la estructura macromolecular de las muestras, la composición inorgánica es el parámetro con mayor influencia en la reactividad y la cinética de gasificación. El impacto positivo de los metales alcalinos y alcalino-térreos fue confirmado, al igual que el efecto inhibidor del Si y P. En particular, la relación K/(Si+P) es considerada apropiada para describir el comportamiento de los materiales durante el proceso de gasificación con vapor de agua. En consecuencia, un nuevo modelo cinético de gasificación a partir de la composición inorgánica de la biomasa es propuesto.

Igualmente, la validez de la relación K/(Si+P) para clasificar y predecir el comportamiento de las biomasas fue confirmada a mayor escala, en un reactor de lecho fluidizado a escala de laboratorio. Las muestras con relación K/(Si+P) superior a 1 mostraron una reactividad a la gasificación superior a la de las muestras con relación inferior a 1, y en consecuencia, una mayor producción de gas y un rendimiento energético más elevado. Asimismo, se observó que la composición inorgánica tiene a su vez una importante influencia en las propiedades del sub-producto sólido. En particular, una

mayor reactividad a la gasificación está relacionada con una mayor área superficial y una mayor cantidad de grupos funcionales en los carbonizados.

El modelo de gasificación y los resultados experimentales presentados pueden ser considerados como una importante referencia para aplicaciones reales de gasificación que trabajen con diferentes tipos de residuos. Asimismo, en el contexto de los países en vías de desarrollo, la gasificación con vapor de agua de biomasas lignocelulósicas se presenta como una alternativa para mejorar el acceso a la energía de zonas rurales aisladas, promoviendo a la vez el desarrollo de actividades productivas que generen nuevos ingresos para las comunidades locales.

Palabras claves: Gasificación con vapor de agua, Reactividad, Composición inorgánica, Biomasa lignocelulósica, Syngas, Biochar.

French abstract / Résumé

Dans le contexte économique de la plupart des pays en voie de développement, la gazéification sous vapeur d'eau de résidus agricoles lignocellulosiques pourrait être un procédé intéressant, à la fois pour la génération d'énergie dans des régions isolées et pour la production des produits à valeur ajoutée. Étant donné que la disponibilité des résidus agricoles est souvent saisonnière, différents types de biomasse doivent être utilisés pour assurer le fonctionnement des installations de gazéification. A cet égard, ce travail est axé sur la compréhension de l'impact des caractéristiques de la biomasse sur le procédé de gazéification et les propriétés des sous-produits gazeux et solides. Trois biomasses lignocellulosiques à composition macromoléculaire et inorganique différentes ont été sélectionnées pour cette étude : coques de noix de coco (CS), bambou guadua (BG) et coques de palmier à huile (OPS).

La cinétique de décomposition thermique des biomasses a été étudiée une échelle thermogravimétrique sous atmosphère inerte et sous vapeur d'eau. Malgré les différences dans la structure macromoléculaire des échantillons, la composition inorganique s'est avérée être le paramètre le plus important influençant la réactivité et la cinétique de gazéification. L'impact bénéfique des métaux alcalins et alcalino-terreux a été confirmé, ainsi que l'effet inhibiteur du Si et du P. Plus précisément, le ratio K/(Si + P) est considéré approprié pour décrire et comparer le comportement des biomasses pendant la gazéification sous vapeur d'eau. En conséquence, une nouvelle approche pour la modélisation de la cinétique de gazéification à partir de la composition inorganique de l'échantillon a été proposée.

La validité du ratio K/(Si + P) pour classifier et prédire le comportement des biomasses a également été confirmée par des expériences dans un réacteur à lit fluidisé à l'échelle laboratoire. Les échantillons avec un ratio K/(Si + P) au-dessus de 1 ont montré des réactivités de gazéification supérieures à celles des échantillons dont le ratio était inférieur à 1, et donc, une production de gaz et un rendement énergétique plus élevés. De plus, la composition inorganique a non seulement impacté le taux de gazéification des échantillons, mais également les propriétés du sous-produit solide. En particulier, une réactivité de gazéification plus élevée est liée à des chars avec une surface spécifique

et un nombre de groupes fonctionnels plus importants. Une température de 850°C, un temps de gazéification d'une heure, et une fraction de vapeur de 30% dans l'agent de réaction ont été identifiées comme les conditions les plus adaptées à la production simultanée de gaz combustible et de char pouvant être valorisé dans des applications agricoles.

Le modèle de gazéification sous vapeur d'eau et les résultats expérimentaux présentés dans ce travail peuvent être une référence pour des applications réelles de gazéification travaillant avec différents types de résidus. Par ailleurs, dans le contexte présenté, la gazéification sous vapeur d'eau de déchets lignocellulosiques peut améliorer l'accès à l'énergie des zones rurales isolées, en promouvant simultanément le développement de projets productifs susceptibles de générer de nouveaux revenus pour les communautés locales.

Mots-clés: Gazéification sous vapeur d'eau, Réactivité, Composition inorganique, Biomasse lignocellulosique, Syngas, Biochar.

English extended abstract

Introduction

Agricultural and agroindustrial wastes represent one of the most abundant and inexpensive resources on earth, considering that billion tons of these residues are generated every year all around the world. However, most of them are nor valorized and often remain underexploited. In several locations, agrowastes could even represent an environmental risk, as they are not disposed properly, causing problems such as air and soil pollution. In this regard, considering their low cost and abundance, agroresidues may constitute an interesting and renewable source for the production of biofuels and value-added products.

In the particular case of developing countries, the valorization of agricultural and agroindustrial residues may also represent an opportunity to improve energy security and provide business opportunities for several communities, generally situated in rural areas. Nevertheless, it has been observed that the sustainability of energy supply projects in these areas usually depends on the development of associated productive activities that could improve the income levels perceived by the communities.

In this context, the selection of the appropriate valorization pathways of agrowastes could provide rural communities in developing countries the opportunity to improve their access to electricity, and simultaneously generate additional incomes.

In relation to lignocellulosic agrowastes, pyro-gasification can be considered as a very interesting process, taking into account that it converts a solid residue in fuel gases that can be used for the production of heat or power, and a solid by-product that could also be valorized in several applications. In particular, steam as gasifying agent produces fuel gases with a considerably high heating value, and a porous carbon material that could have similar properties to activated carbons. These characteristics suggest that steam gasification could be an interesting process for the simultaneous valorization of gasification gaseous and solid by-products, as presented in figure 6.

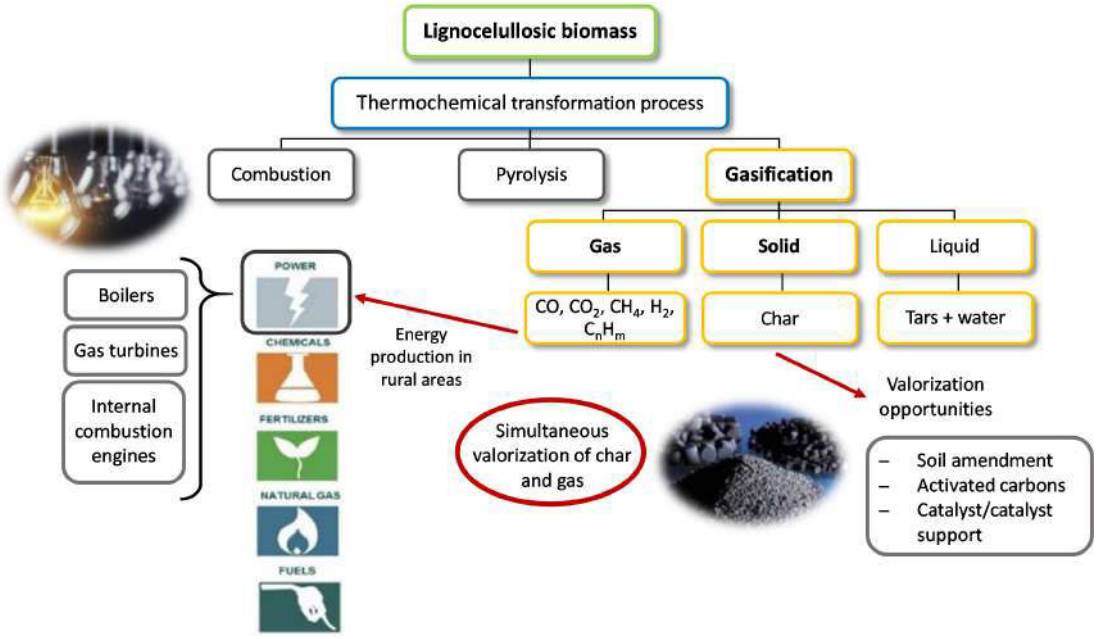

Figure 1: Possible thermochemical transformation processes for lignocellulosic agrowastes. Gasification by-products and valorization pathways

However, the valorization of lignocellulosic agrowastes in energy applications may have several challenges, as it must consider the specific local conditions, such as the relevant crops and agricultural practices, crop rotation, climate, residues volume, and energy requirements of local communities.

In this regard, one of the most important challenges is probably the fact that the availability of agrowastes is not constant over the year and often depends on seasonal crops. Consequently, gasification facilities should work using different kind of residues with several characteristics, to ensure a constant operation. Depending on their origin and nature, the composition and structure of lignocellulosic residues varies and should be taken into account for their transformation process and subsequent valorization possibilities. In this context, the main objective of this work is to analyze the steam gasification behavior of different lignocellulosic agrowastes, and understand the impact of their characteristics on the process by-products properties and valorization pathways.

Although the present research project was motivated by the social and energy context of Colombia and other tropical developing countries, the results of this work may be also valid in developed countries with a large production of agrowastes, where the implementation of appropriate strategies for their treatment are also required.

This PhD thesis was developed in the framework of an international cooperation (cotutelle agreement) between the university "Universidad Nacional de Colombia" in Colombia, and the "IMT Mines Albi-Carmaux" institute in France. The research project in Colombia is entitled "Use of gasification by-products from lignocellulosic biomasses for agroindustrial applications". In France, the project is entitled "Steam gasification of tropical lignocellulosic agrowaste: Impact of biomass characteristics on the gaseous and solid by-products".

The present manuscript has been structured in 7 chapters, in the form of a scientific paper, already published, submitted, or in intent of submission. A brief description of the structure, objectives, and main results of each chapter is presented below.

Chapter 1. Literature review

The objective of this first chapter is to provide the elements required to understand the choices and research directions developed in this work. In this respect, the basic concepts related to the gasification of lignocellulosic biomasses are described, as well as the progress of the current research on he valorization pathways of gasification by-products. Particular attention is given to the process solid residue and its properties.

At first, Section 1.2 describes the main characteristics of lignocellulosic biomass as a suitable raw material for thermochemical transformation processes. Special attention is given to agricultural and agroindustrial residues. Then, the different stages involved in the pyro-gasification process are detailed, describing the associated chemical reactions and their main by-products. Moreover, the impact of operating parameters like temperature, reaction agent, and biomass composition, on the transformation process is discussed. Finally, the most commonly used technologies for pyro-gasification are detailed and compared.

For its part, section 1.3 is dedicated to the description of the pyro-gasification solid by-product, also called char. At first, the influence of the process parameters on the char yield and physico-chemical properties is discussed. Then, an overview of the main char characteristics and their interest for subsequent applications and valorization pathways is presented. Finally, attention is given to the recent research developments in relation to the valorization of chars in several applications. In particular, their use in environmental and agricultural applications is of particular interest in the context of both developed and developing countries.

Chapter 2. Materials and experimental methods

This chapter summarizes the materials and experimental methods used in this study. Considering that the main objective of this work is to understand the impact of biomass characteristics on the steam gasification process and by-products, section 2.2 presents the selection criteria of the lignocellulosic residues to be analyzed and their main characteristics. Coconut shells (CS), oil palm shells (OPS) and bamboo guadua (BG), a bamboo species native from Central and South America were selected for this study, considering their inorganic and macromolecular composition.

For its part, section 2.3 describes the characteristics of two experimental devices initially considered for the development of gasification tests. From the analysis of the advantages and disadvantages of each technology and device, the most appropriate setup to achieve the objectives of the present work was selected. Thus, the steam gasification tests of the analyzed biomasses were carried out in a fluidized bed reactor at a laboratory scale. The selected device allows the accurate control of the process parameters, in order to make a precise comparison between the feedstocks and their gasification by-products.

To better analyze the differences between the selected lignocellulosic residues, a kinetic study of the pyro-gasification process was carried out at a thermogravimetric scale. In this respect, section 2.4 is dedicated to the description of the experimental methods used

to analyze the thermal decomposition behavior of biomasses, under inert atmosphere, and under steam as a gasifying agent.

Finally, Section 2.5 presents the experimental procedure and the operating conditions used for the steam gasification experiments of the selected feedstocks, and the sampling of their gasification by-products. The experimental methodology and the techniques used to evaluate the physico-chemical properties of the raw biomass and the produced char are also summarized.

Chapter 3. Kinetic analysis of tropical lignocellulosic agrowaste pyrolysis

In this chapter, the thermal decomposition behavior of coconut shells (CS), oil palm shells (OPS), and bamboo guadua (BG), the three selected biomasses for this work, was analyzed under inert atmosphere at thermogravimetric scale.

A non-isothermal approach using a combined kinetics parallel reaction model was proposed, assuming that the decomposition of the three main macromolecular components of the samples takes place independently. In this respect, the mathematical deconvolution of the derivative thermogravimetric curves (DTG) using Fraser-Suzuki functions was performed. This mathematical treatment allowed the description of the biomass pyrolysis as the sum of the decomposition of its three macromolecular constituents: hemicellulose, cellulose and lignin.

Considering that the calculated apparent activation energy of each biomass component evidenced no dependence on the reaction extent in all the conversion range, master plots approach was used to identify their decomposition mechanism. In this regard, model-free isoconversional methods proved to be suitable to determine the pyrolysis kinetic parameters of lignocellulosic agrowastes with different macromolecular compositions, and H/C and O/C ratios near 1.5 and 0.8 respectively.

In particular, this study has shown that even when the elemental composition of the samples is very similar, their macromolecular constituents can have an important impact on their decomposition rate, and especially on the apparent activation energy associated with the pyrolysis process. In this respect, considering the role of lignin for the stability of the lignocellulosic structure, it has been observed that the activation energy of the samples is in the order BG Ea <CS Ea <OPS Ea, consistent with their lignin content (BG <CS <OPS).

The validation of the kinetic approach proposed in this work showed a very good agreement with the experimental results, with a fitting error below 10%. Therefore, the kinetic model presented can be considered as a valuable tool for reactor design, and for the development and scale-up of pyrolysis and gasification processes using tropical lignocellulosic agrowastes as a feedstock.

Chapter 4. Steam gasification of tropical agrowastes: a new modeling approach based on their inorganic content

In this chapter, the steam gasification and co-gasification reactivity and global kinetics of the three selected biomasses was analyzed at a thermogravimetric scale, with temperatures ranging from 750°C to 900°C, and steam partial pressures from 3 to 10 kPa. An isothermal experimental approach was used for this analysis, considering that the beginning of the steam gasification reactions can be controlled by switching the atmosphere from inert to reactive after the isothermal regime is established.

Moreover, model-free isoconversional methods and the generalized master-plots approach were used to determine the kinetic parameters and the most suitable reaction model that better describe the steam gasification process of the samples. In this regard, in order to better understand and compare the differences between the analyzed biomasses, their gasification behavior was described using a nth order reaction model with respect to the reacting solid.

It has been found that despite the differences in the macromolecular composition of the samples, inorganics is the most important parameter influencing the biomass gasification reactivity and kinetics. In particular, the experimental results confirmed the beneficial impact of alkali and alkaline earth metals, principally K, on the gasification reactivity, as well as the inhibitory effect of Si, Al, and P. In accordance, a linear relationship was found between the reactivity of the samples and their inorganic ratio K/(Si+P), for all the studied experimental conditions.

Furthermore, from the kinetic analysis, it was possible to notice that the identified reaction model that describes the steam gasification process is also related to the inorganic composition of the samples. More precisely, a linear and inverse relationship between the identified order of reaction n and the inorganic ratio K/(Si+P) of the biomass was found.

Accordingly, a new steam gasification kinetic model that considers the inorganic composition of the feedstocks was proposed. For all the analyzed samples and gasification conditions, a good agreement was found between the model and the experimental results, with fitting errors below 10%. This value was considered reasonable, taking into account the heterogeneity of the biomasses and the incertitude in the measurement of their inorganic composition.

As a result, the proposed kinetic model could constitute a valuable tool for reactor design, and for the development and scale-up of steam gasification facilities using lignocellulosic residues. Moreover, considering that the availability of agrowastes is not constant, this approach could be also useful in applications where different kind of residues should be gasified at the same time.

Chapter 5. Impact of feedstock characteristics on the steam gasification of lignocellulosic agrowastes

The analysis of the steam gasification process of lignocellulosic agrowastes was also carried out in a fluidized bed reactor at a laboratory scale. In this chapter, various operating conditions were evaluated in order to understand their impact on the gasification process, product yield, and particularly, on syngas production and quality, in terms of composition and calorific value.

At first, the impact of the steam quantity on the gasification products distribution was analyzed in order to determine the most suitable conditions for the production of combustible gases for energy applications. In particular, experimental results showed that steam fractions between 15% and 30% in the gasifying agent promote the production of fuel gases. In contrast, higher values were associated with an increase in the tar production, resulting in a negative impact on the process efficiency.

In consequence, the steam gasification analysis and comparison of the selected samples were performed using 30% of steam in the gasifying agent. For the three studied

biomasses, the experimental results showed that in the analyzed temperature range, a rise in the process temperature is associated with a higher gasification reactivity, an increase in the amount of gas produced, and therefore, a higher efficiency of the process.

Even though the process parameters showed similar effects on the gasification behavior of the three samples, remarkable differences were identified between them, mainly related to their mineral composition. In accordance to the results of the kinetic analysis of the process, presented in chapter 4, the beneficial impact of alkali and alkaline earth metals, as well as the inhibitory effect of Si, Al, and P on the steam gasification process was confirmed. In particular, the validity of the inorganic ratio K/(Si+P) to classify and predict the steam gasification behavior of lignocellulosic agrowaste was verified. Under the same experimental conditions, gasification of samples with K/(Si+P) above 1 resulted in higher gas yields and gas efficiencies compared to samples with K/(Si+P) below 1.

In contrast, no remarkable differences were observed between the analyzed samples in terms of gas composition and heating value. In this regard, with a high heating value between 10 and 12 MJ/m^3, and a H_2/CO ratio between 2.5 and 4, the steam gasification gas produced from lignocellulosic feedstocks with H/C and O/C ratio near 1.5 and 0.8 respectively, could be considered suitable for energy applications using boilers, gas turbines, or internal combustion engines.

In this regard, the experimental observations presented in this chapter could be an important reference for real gasification applications working with different kind of lignocellulosic residues. In particular, the presented results provide useful information to adapt the process parameters and conditions to the available feedstocks and the application requirements.

Chapter 6. Physico-chemical characterization of steam gasification chars from tropical lignocellulosic agrowastes

This chapter is dedicated to the analysis of the physico-chemical properties of steam gasification chars or *biochars* produced from the three selected biomasses. After each gasification test described in chapter 5, the resulting chars were recovered and characterized, in order to understand the impact of the process parameters and raw biomass characteristics on their properties.

The biochars chemical composition, specific surface area, structure, and surface chemistry were determined and compared. In accordance with the results presented in chapters 4 and 5, the gasification chars characterization proved that the inorganic composition of the raw samples impacts also the physico-chemical properties of the gasification solid by-product. In particular, the experimental results showed that inorganics have an important influence on the gasification reactivity of the samples, and in consequence, an impact on the porous structure development and surface chemistry of the gasification chars.

The comparison between chars produced under the same experimental conditions showed that for samples with inorganic ratio K/(Si+P) above 1, the beneficial impact of AAEM (specially K) on the steam gasification reactions resulted also in higher surface area development and oxygen-containing functional groups in the char surface, in comparison to samples with inorganic ratio below 1. In particular, as a result of

the steam gasification reaction mechanism, a relationship between the char specific surface area and the total quantity of oxygen-containing functional groups was found. Furthermore, the pore size distribution of gasification chars seems to be related to the nature and the macromolecular composition of the raw feedstocks.

In general, the analyzed gasification chars are highly microporous carbonaceous materials, with specific surface areas between 500 and 1000 m^2/g. A dominance of acidic oxygenated functional groups in the char surface, with pH_{PZC} values below 3 was observed in all cases. In this regard, according to the observed characteristics, similar of those of several activated carbons, steam gasification chars could be considered as an interesting by-product that may be valorized in applications where the adsorption or retention of cations is required. Moreover, the significant inorganic content of chars may also suggest their valorization in soil amendment and remediation applications.

The experimental observations presented in this work could be an important reference for real gasification applications working with different kind of residues, when the simultaneous valorization of the gaseous and solid by-products is intended. According to the nature and composition of the samples, the gasification parameters and conditions could be adapted in order to obtain the by-products proportion required by each application, with the char needed characteristics.

Chapter 7. Characterization of agrowaste steam gasification chars for soil amendment applications

Considering the characterization results presented in chapter 6 for the steam gasification solid by-product, this chapter is dedicated to the analysis of the char properties, in order to determine their suitability to be used in soil amendment and remediation applications.

In this regard, steam gasification chars from coconut shells, oil palm shells, and bamboo guadua, produced at 850°C with a steam fraction of 30% in the gasifying agent were selected for this study. These conditions proved to be adequate for the simultaneous production of syngas with a relatively high process efficiency, and a porous carbon material with desirable properties for several applications.

The experimental results confirmed that the three analyzed chars showed an interesting potential to be used in soil amendment applications. In particular, their high pH values between 9 and 11, and their significant acid neutralization capacity above 62 cmol H^+/kg, suggest the char capacity for the improvement of acidic soil characteristics. Moreover, their cation exchange capacity values between 11 and 45 cmol/kg may enhance the nutrient retention and fertility of several kinds of soils.

In general, it has been observed that the inorganic composition of the samples impacts in a very important way the char properties with regard to soil applications. Particularly, BG chars, with an ash content above 30%, exhibited the highest cation exchange and acid neutralization capacities, in comparison to chars with lower ash content (coconut shells and oil palm shells).

Moreover, the mineral release analysis of the three gasification chars at different pH values revealed that these materials could be a non negligible source of macro and micro-nutrients, that may also impact the soil fertility and crop yield. More specifically,

thanks to their high mineral content, coconut shells and bamboo guadua chars may supply up to 100% and 20% of the K and P needs of some low-input crops.

Although the behavior of chars in real applications may differ from the one observed during the laboratory characterization, the results presented in this chapter give an useful insight regarding a promising valorization pathway for steam gasification chars from different lignocellulosic agrowastes, adapted to both developed and developing countries.

General conclusion

In the current world energy, environmental, and economic context, agricultural and agroindustrial wastes represent an interesting, low-cost, and renewable resource for the production of biofuels and value-added products in both developing and developed countries.

In particular, considering the great variety of lignocellulosic agrowaste sources, the understanding of the biomass organic and inorganic composition impact on the pyro-gasification behavior is of great importance to adapt the process parameters to the available feedstocks and application requirements. Moreover, the understanding of the influence of biomass characteristics on the pyro-gasification by-products is also essential to determine their most suitable valorization pathways.

In general, the results presented in this work have contributed to a better understanding of the steam gasification process of lignocellulosic agrowastes, and highlighted the important role of inorganics in their gasification behavior and by-products properties. In accordance, the design and operation of agrowaste gasification facilities should take into account the organic and inorganic composition of the feedstocks, in order to properly adapt the process parameters to ensure the production of the required by-products yield and properties.

Moreover, the present research showed that steam gasification could be considered as a suitable technique for the simultaneous valorization of lignocellulosic residues in energy applications, and the production of value-added products, that could represent an opportunity to implement productive activities in the context of both developing and developed countries.

French extended abstract / Résumé Long

Introduction

Avec des milliards des tonnes produites chaque année, les déchets agricoles et agroindustriels peuvent être considérés comme l'une des ressources le plus abondantes au monde. Cependant, la plupart de ces résidus ne sont pas utilisés et restent souvent sous-exploités. Dans certains endroits, la mauvaise disposition des déchets agricoles et agroindustriels peut même entrainer la contamination des sols par le ruissellement de lixiviats, et de l'air, par la décomposition des déchets, représentant un risque environnemental.

À cet égard, en raison de leur faible coût et de leur abondance, les résidus agricoles peuvent représenter une source intéressante et renouvelable pour la production de biocarburants et de produits à valeur ajoutée.

Dans le cas particulier des pays en voie de développement, la valorisation énergétique de ces déchets pourrait contribuer à améliorer la sécurité de l'approvisionnement d'énergie dans plusieurs communautés, généralement situés dans des zones rurales. Cependant, il a été constaté que la mise en place de projets productifs associés à l'approvisionnement d'énergie, visant la génération de revenus supplémentaires pour les communautés, est nécessaire pour assurer la pérennité des projets.

Dans ce contexte, le choix d'un procédé de conversion énergétique des déchets adapté, peut offrir aux communautés rurales des pays en voie de développement la possibilité d'améliorer leur accès à l'énergie, et à la fois, de générer des revenus alternatifs.

En ce qui concerne les résidus lignocellulosiques, la pyro-gazéification est un procédé particulièrement intéressant, car il permet de produire à la fois un gaz combustible qui peut être utilisé pour la génération d'électricité ou de chaleur, et un sous-produit solide qui peut également être valorisé dans des diverses applications. En particulier, l'utilisation de vapeur d'eau comme atmosphère de gazéification produit un gaz avec un haut pouvoir calorifique, et un solide poreux avec des propriétés similaires à celles des charbons actifs. Ceci suggère que la gazéification sous vapeur d'eau pourrait être un

procédé d'intérêt pour la valorisation simultanée des sous-produits gazeux et solides, comme présenté dans la figure 2.

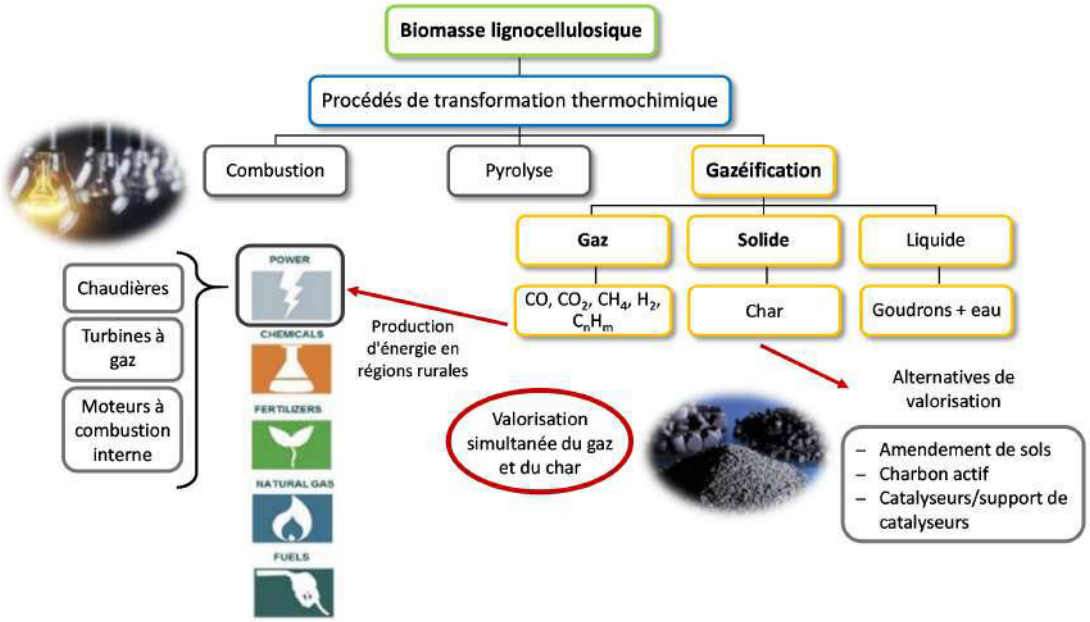

Figure 2: Procédés de transformation thermochimique des résidus agricoles lignocellulosiques. Sous-produits de la gazéification et voies de valorisation.

Néanmoins, la valorisation des résidus lignocellulosiques agricoles pour des applications énergétiques présente plusieurs défis, car il est nécessaire de tenir compte de diverses conditions, telles que les cultures et leur rotation, les pratiques agricoles, le climat, le volume des résidus, et les besoins énergétiques des communautés locales.

À cet égard, l'un des défis les plus importants est probablement le fait que la disponibilité des biomasses n'est pas constante tout au long de l'année et dépend souvent des cultures saisonnières. Par conséquent, afin d'assurer leur fonctionnement continu, les installations de gazéification doivent travailler avec divers types de résidus, présentant différentes caractéristiques. Selon leur origine et leur nature, la composition et la structure des biomasses varient et peuvent impacter leur comportement au cours de la gazéification, ainsi que les possibles voies de valorisation de leurs sous-produits.

Dans ce contexte, le principal objectif de la thèse est donc d'étudier la gazéification sous vapeur d'eau de différents résidus agricoles lignocellulosiques, et de comprendre l'impact de leurs caractéristiques sur le procédé et les propriétés des sous-produits, ainsi que sur leurs possibles voies de valorisation.

Bien que ce projet de recherche a été motivé par le contexte social et énergétique de la Colombie et d'autres pays tropicales en voie de développement, les résultats de ce travail sont également valides dans le cadre des pays développés avec une production importante de résidus agricoles et agroindustriels, qui ont également besoin de mettre en place des stratégies adaptées pour leur traitement.

Ce travail de thèse a été développé dans le cadre d'une cotutelle internationale entre l'université "Universidad Nacional de Colombia" en Colombie, et l'institut "IMT Mines Albi-Carmaux" en France. Le projet de recherche en Colombie est intitulé "Use of

gasification by-products from lignocellulosic biomasses for agroindustrial applications". En France, le projet est intitulé "Gazéification sous vapeur d'eau de résidus agricoles: Impact des caractéristiques de la biomasse sur les propriétés des sous-produits gazeux et solides".

La structure générale du manuscrit, composé de sept chapitres est présentée dans la figure 3. Les chapitres 3 au 7 ont été rédigés sous la forme d'articles scientifiques, déjà publiés ou en vue de publication dans des journaux scientifiques internationaux.

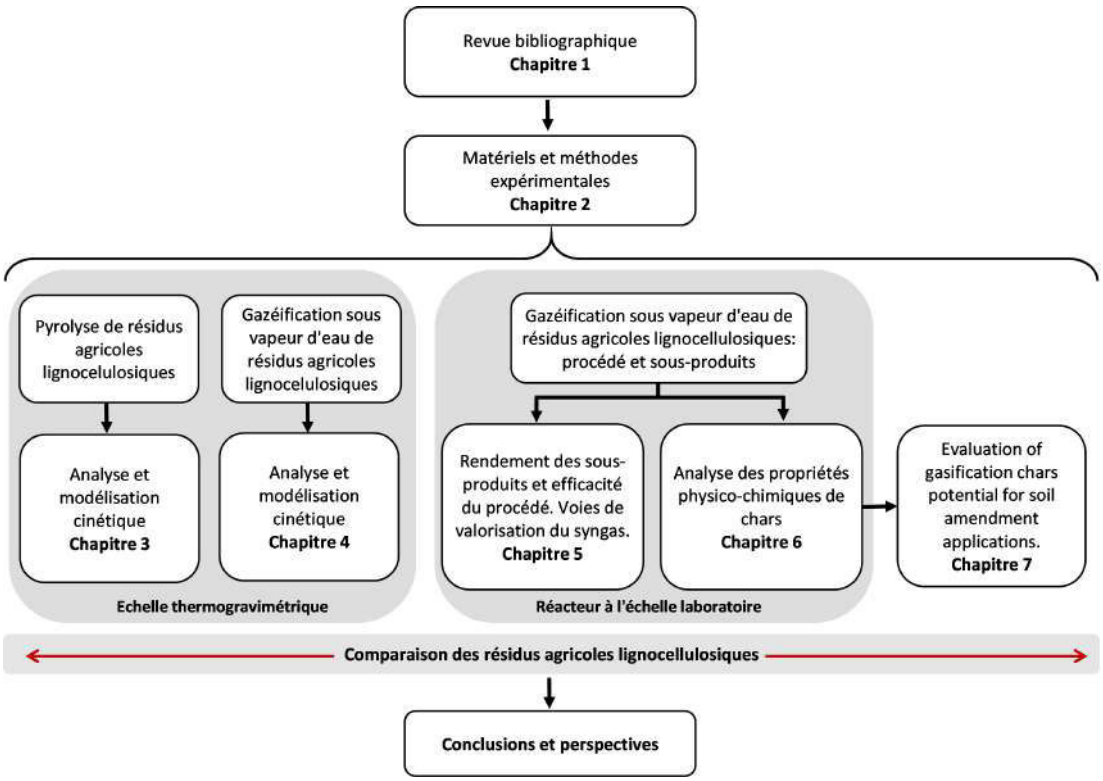

Figure 3: Structure du manuscrit

Chapitre 1. Revue bibliographique

L'objectif de ce premier chapitre est de donner les éléments nécessaires pour comprendre les choix et les orientations de recherche développés dans le présent travail. A cet égard, les concepts de base relatifs à la gazéification de biomasses lignocellulosiques sont décrits, ainsi que les progrès de la recherche actuelle sur les voies de valorisation des sous-produits. Une attention particulière est adressée au résidu solide de la gazéification et ses propriétés.

Dans un premier temps, la section 1.2 décrit les principales caractéristiques de la biomasse lignocellulosique en tant que matière première approprié pour les procédés de transformation thermochimique. Une attention particulière est accordée aux résidus agricoles et agro-industriels. Ensuite, les différentes étapes du procédé de pyro-gazéification sont détaillées, en décrivant les réactions chimiques associées et leurs principaux sous-produits. Un accent spécial est porté sur les différents paramètres opératoires qui impactent le procédé, tels que la température, l'agent de réaction, et la composition la biomasse.

Également, les technologies les plus couramment utilisées pour la pyro-gazéification sont décrites et comparées.

Pour sa part, la section 1.3 est dédiée à la description du sous-produit solide issu du procédé de pyro-gazéification, aussi appelé char. Particulièrement, l'influence des paramètres opératoires du procédé sur son rendement et ses propriétés physico-chimiques est discutée dans un premier temps. Ensuite, une description des principales caractéristiques des chars et de leur intérêt vis-à-vis de différentes applications et voies de valorisation est présentée. Enfin, l'attention est portée sur les progrès récents de la recherche en relation avec la valorisation des chars dans plusieurs applications. Notamment, leur utilisation dans des applications environnementales et agricoles s'avère particulièrement intéressante dans le cadre des besoins des pays en voie de développement.

Chapitre 2. Matériels et méthodes expérimentales

Ce chapitre récapitule les matériaux et les méthodes expérimentales utilisés au cours de cette étude.

Étant donné que l'objectif principal de ce travail est de comprendre l'impact des caractéristiques de la biomasse sur le procédé de gazéification sous vapeur d'eau et les propriétés de ses sous-produits, la section 2.1 présente les critères de sélection des résidus lignocellulosiques à analyser et leurs principales caractéristiques physico-chimiques. Les coques de noix de coco (CS), les coques de palmier à huile (OPS), et le bambou guadua (BG), une espèce de bambou originaire de l'Amérique centrale et du sud ont été choisis pour cette étude en tenant compte de leur composition inorganique et macromoléculaire.

D'autre part, la section 2.2 décrit les caractéristiques de deux dispositifs expérimentaux considérés dans un premier temps pour le développement des tests de gazéification. Une analyse des avantages et des inconvénients de chaque technologie et appareil a permis de choisir la configuration expérimentale la plus adaptée pour atteindre les objectifs de ce travail. Ainsi, les tests de gazéification sous vapeur d'eau des biomasses sélectionnées ont été réalisés avec un réacteur à lit fluidisée à l'échelle laboratoire. Ceci permet de contrôler de façon précise les paramètres opératoires de la gazéification afin de faire une comparaison entre les biomasses et ses sous-produits.

Pour mieux analyser les différences entre les résidus lignocellulosiques choisis, une étude cinétique de leur pyro-gazéification a été effectuée à l'échelle thermogravimétrique. A cet égard, la section 2.4 est dédiée à la description des méthodes expérimentales utilisées pour analyser le comportement de la décomposition thermique des biomasses, sous atmosphère inerte et sous vapeur d'eau comme agent de gazéification.

Enfin, la section 2.5 présente la procédure expérimentale et les conditions opératoires utilisées avec le réacteur à lit fluidisée, pour le développement des tests de gazéification sous vapeur d'eau, ainsi que l'échantillonnage des sous-produits obtenus. La méthodologie expérimentale et les techniques utilisées pour évaluer les propriétés physico-chimiques de la biomasse brute et du char produit sont également présentées de manière synthétique.

Chapitre 3. Analyse cinétique de la pyrolyse de résidus agricoles

Dans ce chapitre, le comportement de la décomposition thermique des coques de noix de coco (CS), coques de palmier à huile (OPS), et bambou guadua (BG), les trois biomasses sélectionnées pour ce travail, a été étudié à l'échelle thermogravimétrique (TGA).

Une approche non-isotherme utilisant un modèle de réactions parallèles est proposée en tenant compte des trois principaux composants macromoléculaires des échantillons: hémicellulose, cellulose et lignine. A cet égard, une méthode de déconvolution des courbes DTG (première dérivée de la perte de masse) a été mise en place avec des fonctions mathématiques de Fraser-Suzuki. Ceci a permis de décrire avec un bon accord le comportement de la pyrolyse de la biomasse, comme étant la somme de la décomposition de ses trois constituants macromoléculaires, ici appelés "pseudo-composants".

L'analyse cinétique est ensuite basée sur de méthodes mathématiques appelées "model-free methods", adaptées aux donnés thermogravimétriques. Ces méthodes se sont avérées adéquates pour la détermination des paramètres cinétiques de la pyrolyse des biomasses avec différentes compositions macromoléculaires.

En particulier, cette étude a montré que même lorsque la composition élémentaire des échantillons est très similaire, ses constituants macromoléculaires peuvent avoir un impact sur leur vitesse de décomposition, et notamment sur l'énergie d'activation associée à la pyrolyse. A cet égard, en considérant le rôle de la lignine pour la stabilité de la structure lignocellulosique, il a été observé que l'énergie d'activation des échantillons est dans l'ordre BG E_a < CS E_a < OPS E_a, en cohérence avec leur contenu de lignine (BG < CS < OPS).

La validation de l'approche cinétique proposée dans ce travail montre un très bon accord avec les résultats expérimentaux, avec une erreur inférieure à 10%. Par conséquent, le modèle cinétique présenté peut représenter un outil important dans le futur, pour l'analyse et la conception des procédés de pyrolyse et gazéification à une plus grande échelle, en utilisant de résidus lignocellulosiques.

Chapitre 4. Analyse cinétique de la gazéification sous vapeur d'eau de résidus agricoles

Dans ce chapitre, l'analyse de la gazéification sous vapeur d'eau des biomasses d'étude et leurs mélanges a été faite à une échelle thermogravimétrique, avec des températures entre 750°C et 900°C, et pressions partielles de vapeur entre 3 kPa et 10 kPa. Une approche expérimentale isotherme a été mise en place pour cette étude, afin de contrôler de manière précise le début de la phase de gazéification des échantillons aux températures d'étude, et de comparer leur comportement.

La détermination des paramètres cinétiques du procédé est basée sur des méthodes d'isoconversion ou "model-free isoconversional methods", permettant de calculer l'énergie d'activation sans une hypothèse préalable du modèle de réaction, qui pourrait conduire au calcul des paramètres cinétiques inexacts. A cet égard, l'approche "master-plots" a été utilisé pour l'identification du modèle de réaction le plus approprié pour chaque condition expérimentale. Ainsi, afin de comparer les échantillons, le modèle de réaction est décrit en fonction d'un ordre n de par rapport au solide.

Il a été constaté que malgré les différences dans la composition macromoléculaire des échantillons, leur composition inorganique est le paramètre principal qui influence

leur réactivité. En relation avec ceci, les résultats expérimentaux ont confirmé l'effet bénéfique des métaux alcalins et alcalino-terreux, principalement celui du K, sur la réactivité à la gazéification sous vapeur d'eau des biomasses, ainsi que l'effet inhibiteur d'éléments comme le Si, l'Al et le P. En particulier, une relation linéaire a été observé entre la réactivité des échantillons et leur ratio inorganique K/(Si+P), pour toutes les conditions expérimentales étudiées.

D'autre part, l'étude de la cinétique du procédé a également permis d'observer une relation entre le mécanisme réactionnel décrivant la gazéification sous vapeur d'eau des biomasses et leur composition inorganique. Particulièrement, une relation linéaire inverse a été constaté être l'ordre de la réaction par rapport au solide, et le ratio inorganique (K/Si+P) de chaque biomasse ou mélange de biomasses.

De ce fait, un nouveau modèle cinétique tenant compte de la composition inorganique de biomasses a été proposé pour décrire le procédé de gazéification sous vapeur d'eau. La validation expérimentale du modèle a montré des erreurs inférieures à 10%, considérées raisonnables en tenant compte de l'hétérogénéité des biomasses et des incertitudes dans la détermination de leur composition inorganique.

En conséquence, le modèle cinétique proposé permet de prédire avec un bon accord le comportement de la gazéification de différents types de biomasses lignocellulosiques à partir de leur composition inorganique. Ces résultats peuvent être considérés comme un outil important pour la conception des procédés de gazéification à une plus grande échelle, en utilisant différents types de résidus lignocellulosiques.

Chapitre 5. Impacts des caractéristiques de la biomasse sur le procédé de gazéification sous vapeur d'eau

L'étude du procédé de gazéification sous vapeur d'eau de résidus lignocellulosiques agricoles a également été faite dans un réacteur a lit fluidise à l'échelle laboratoire. Dans ce chapitre, différents paramètres opératoires ont été évalués afin de comprendre leur impact sur le procédé, rendement des sous-produits, et notamment, sur la production du gaz et sa qualité, en termes de composition et pouvoir calorifique.

Dans un premier temps, la variation de la quantité de vapeur d'eau utilisée pour la gazéification a permis d'identifier les conditions pour lesquelles la production de gaz est privilégiée. En particulier, les résultats expérimentaux ont montré que des fractions de vapeur entre 15% et 30% dans l'agent de gazéification favorisent la production des gaz combustibles. En revanche, des valeurs supérieures sont associées à une augmentation de la production de goudrons, avec un impact défavorable sur l'efficacité du procédé. En conséquence, l'analyse comparative des trois biomasses d'étude a été faite pour une fraction de vapeur de 30%.

Également, il a été observé que l'augmentation de la température du procédé est associée à des réactivités de gazéification supérieures, et donc à une augmentation de la quantité de gaz produit, et de l'efficacité du procédé.

Bien que les conditions opératoires aient montré des effets similaires sur la gazéification des trois biomasses, des différences importantes ont été identifiées entre elles, principalement liées avec leur composition minérale. En cohérence avec les résultats de l'étude cinétique, l'effet bénéfique des métaux alcalins et alcalino-terreux, ainsi que l'effet inhibiteur du Si, Al et P sur les réactions de gazéification a été mis en évidence.

Particulièrement, la validité du ratio K/(Si+P) pour classifier et décrire le comportement de la gazéification des biomasses lignocellulosiques a été confirmée. Les échantillons avec un ratio inorganique K/(Si+P) supérieur à 1 ont montré une production de gaz et une efficacité du procédé supérieure en comparaison avec les échantillons avec un ratio inférieur a 1, sous les mêmes conditions expérimentales.

D'autre part, l'analyse de la composition du gaz produit n'a pas montré des différences importantes entre les trois biomasses d'étude. Avec un pouvoir calorifique entre 10 et $12\,MJ/m^3$ et un ratio H_2/CO entre 2.5 et 4, le gaz produit à partir de la gazéification sous vapeur des résidus agricoles avec des ratios H/C et O/C proches de 1.5 et 0.8 respectivement, est compatible avec des applications de production d'énergie utilisant des chaudières, moteurs à combustion interne, ou turbines à gaz.

Les observations expérimentales présentées dans ce chapitre peuvent être une référence importante pour des installations réelles de gazéification, permettant d'adapter les paramètres opératoires aux biomasses de travail, et au rendement des sous-produits souhaité en fonction de l'application envisagée.

Chapitre 6. Propriétés physico-chimiques de chars issus du procédé de gazéification sous vapeur d'eau

Ce chapitre est dédié à l'analyse des propriétés physico-chimiques du char issu de la gazéification sous vapeur d'eau des biomasses d'étude. A la fin des tests de gazéification décrits dans le chapitre 5, le char résultant a été récupère et caractérisé afin de comprendre l'impact des conditions opératoires et des caractéristiques de la biomasse d'origine sur ses propriétés.

La composition chimique des chars, ainsi que leur surface spécifique, structure, et chimie de surface ont été déterminés. En accord avec les résultats présentés dans les chapitres 4 et 5, la caractérisation des chars a montré que la composition inorganique des échantillons impacte également les propriétés du sous-produit solide de la gazéification. Particulièrement, la réactivité de la biomasse influence d'une manière importante le développement de la surface spécifique des chars et leur chimie de surface.

La comparaison des chars produits avec les mêmes conditions expérimentales montre que pour les échantillons avec un ratio inorganique K/(Si+P) supérieure à 1, l'effet bénéfique du K et des métaux alcalins et alcalino-terreux est associé avec un développement supérieur de la surface spécifique des chars, ainsi qu'avec une quantité plus importante de groupes oxygénés dans leur surface, en comparaison avec les échantillons avec un ratio inférieur a 1. Également, du fait du mécanisme réactionnel entre la vapeur d'eau et l'échantillon en cours de la gazéification, une relation a été observée entre la surface spécifique et la quantité totale mesurée des groupes oxygénés dans la surface des chars. D'autre part, la distribution de la taille des pores des échantillons a montré être en relation avec la nature et la composition macromoléculaire de la biomasse d'origine.

En général, les chars analysés sont des matériaux carbonés hautement microporeux, avec des surfaces spécifiques comprises entre 500 et $1000\,m^2/g$. Une dominance de groupes fonctionnels oxygénés acides dans la surface du charbon, avec des valeurs de pH_{PZC} inférieures à 3, a été observée dans tous les cas. En conséquence, en fonction des propriétés observées, proches de celles de certains charbons actifs, les chars issus de la gazéification sous vapeur d'eau peuvent être considérés comme un sous-produit intéressant qui pourrait être valorisé dans des applications d'adsorption. De plus, le

contenu inorganique significatif des chars suggère également leur valorisation dans des applications agricoles, pour l'amendement des sols.

Les observations expérimentales présentées dans ce travail pourraient constituer une référence importante pour les applications réelles de gazéification utilisant différents types de résidus, lorsque la valorisation simultanée des sous-produits gazeux et solides est recherché. En fonction de la nature et de la composition des échantillons, les paramètres et les conditions de la gazéification pourraient être adaptés pour obtenir la proportion requise de sous-produits, avec les caractéristiques nécessaires.

Chapitre 7. Caractérisation des chars vis-à-vis de leur utilisation dans des applications d'amendement de sols

En tenant compte des résultats de caractérisation présentés dans le chapitre 6 pour les chars issus de la gazéification sous vapeur des biomasses d'étude, ce chapitre est dédié à l'analyse des propriétés des chars vis-à-vis de leur utilisation dans des applications agricoles et d'amendement des sols.

Pour cette étude, des chars de coques de noix de coco, coques de palmier à huile, et bambou, produits à 850°C avec une fraction de 30% de vapeur d'eau dans l'agent de gazéification ont été choisis. Comme observé dans les chapitres précédants, ces conditions opératoires se sont avérées adéquates pour la production simultanée de syngaz, avec une efficacité de procédé élevée, et de char avec des propriétés physico-chimiques d'intérêt pour des nombreuses applications.

Les résultats expérimentaux ont confirmé que les trois échantillons analysés ont un potentiel intéressant pour des applications agricoles. Notamment, leur pH élevé, compris entre 9 et 11, et leur capacité de neutralisation acide supérieure à 62 cmolH^+/kg, suggèrent leur possible utilisation pour le traitement des sols acides. De plus, leur capacité d'échange cationique comprise entre 11 et 45 cmol/kg, supérieure a celle de plusieurs types de sol, pourrait également contribuer à l'amélioration de la rétention des nutriments et la fertilité des sols.

En général, il a été constaté que le contenu inorganique des chars impacte de manière très importante leurs propriétés. En particulier, les chars de bambou guadua, avec un taux de cendres supérieur à 30%, ont montré des capacités d'échange cationique et de neutralisation acide supérieures a celles des chars avec des taux des cendres inférieurs (coques de noix de coco et coques de palmier a huile).

D'autre part, l'analyse des tests de lixiviation des minéraux contenus dans la matrice des chars à différentes valeurs de pH, a révélé que ces matériaux pourraient également constituer une source non négligeable de nutriments, pouvant améliorer la fertilité des sols et le rendement de différents types de cultures. Spécifiquement, grâce à leur important contenu inorganique, les chars de bambou et coques de noix de coco, pourraient fournir jusqu'à 100% et 20% des besoins en K et P pour certains cultures.

Malgré le fait que le comportement des chars dans des applications réelles peut être différent de celui observé en cours des caractérisations, le présent travail donne un aperçu très utile sur une voie de valorisation prometteuse pour les sous-produits solides de la gazéification sous vapeur d'eau des résidus agricoles.

Conclusions

Dans le cadre du contexte énergétique, environnemental et économique actuel, les résidus agricoles at agroindustriels représentent une source intéressante, renouvelable, et à faible cout, pour la production de biocarburants et produits à valeur ajoutée, dans des pays développés et en voie de développement.

En particulier, compte tenu de la grande diversité des sources des résidus lignocellulosiques, la compréhension de l'impact de la composition organique et inorganique de la biomasse sur le comportement de la pyro-gazéification a une grande importance, afin d'adapter les paramètres du procédé aux matériaux disponibles et aux applications envisagées. De plus, la compréhension de l'influence des caractéristiques de la biomasse sur les sous-produits de la pyro-gazéification est également essentielle pour déterminer les voies de valorisation les plus appropriées.

En général, les résultats obtenus dans le présent travail ont contribué à une meilleure compréhension du procédé de gazéification sous vapeur d'eau des résidus lignocellulosiques agricoles, et ont mis en évidence le rôle important des inorganiques dans le rendement et les propriétés des sous-produits issus du procédé. En conséquence, la conception et l'exploitation des installations de gazéification des déchets agricoles doivent tenir compte de la composition organique et inorganique des matières premières, afin d'adapter correctement les paramètres du procédé et obtenir le rendement requis des sous-produits, avec les caractéristiques nécessaires à leur valorisation.

De plus, ce travail a montré que la gazéification sous vapeur d'eau peut être considérée comme une technique appropriée pour la valorisation simultanée des résidus lignocellulosiques dans des applications énergétiques et dans la production de produits à valeur ajoutée. Ceci, pourrait représenter l'opportunité de créer des revenus additionnels associés à la production d'énergie pour des communautés rurales dans des pays en voie de développement.

General introduction

Social and scientific context of the research

Each year, billion tons of agricultural and agroindustrial wastes are generated all around the world, representing one of the most abundant and inexpensive resources on earth [1]. However, most of these residues are not valorized and often remain underexploited. In several locations, agrowastes could represent an environmental risk, as they are not always disposed properly, causing problems like air and soil pollution. In this regard, due to their low cost and abundance, agroresidues may represent an interesting and renewable source for the production of biofuels and value-added products.

Figure 4: Population without access to electricity (millions). Data: IEA, 2017.

In the particular case of developing countries, the valorization of agricultural and agroindustrial wastes could also represent an opportunity to provide energy security and business opportunities for several communities.

In relation to this, it is worth noting that according to International Energy Agency [2], around 1.1 billion people in the world still lack access to electricity and cooking facilities (15% of the total global population). Most of them live in rural areas in developing countries, as observed in figure 4, and may have access to important amounts of agrowastes, particularly in the case of tropical countries, where the climate conditions favor the agricultural and farming activities [3]. In this regard, agrowaste could represent a valuable resource to provide energy solutions to rural communities, considering that crop production and processing usually take place in rural areas.

In the case of Colombia, according to the Colombian Energy and Mining Planning Unit - UPME, even though the global energy access is above 96%, there are still more than 470.000 homes that do not have access to electricity, principally in rural areas [4]. On the other side, considering its geographic location and climate conditions, it has been estimated that the agricultural and agroindustrial activities in the country produce more than 70 million tons of wastes every year, from coffee, banana, coconut, oil palm, rice, sugar cane, corn, and other crops [5]. As observed in figure 5, the comparison of the energy needs with the agrowaste resources location reveals that most of the agricultural residues in the country are produced close to areas with low electrification levels.

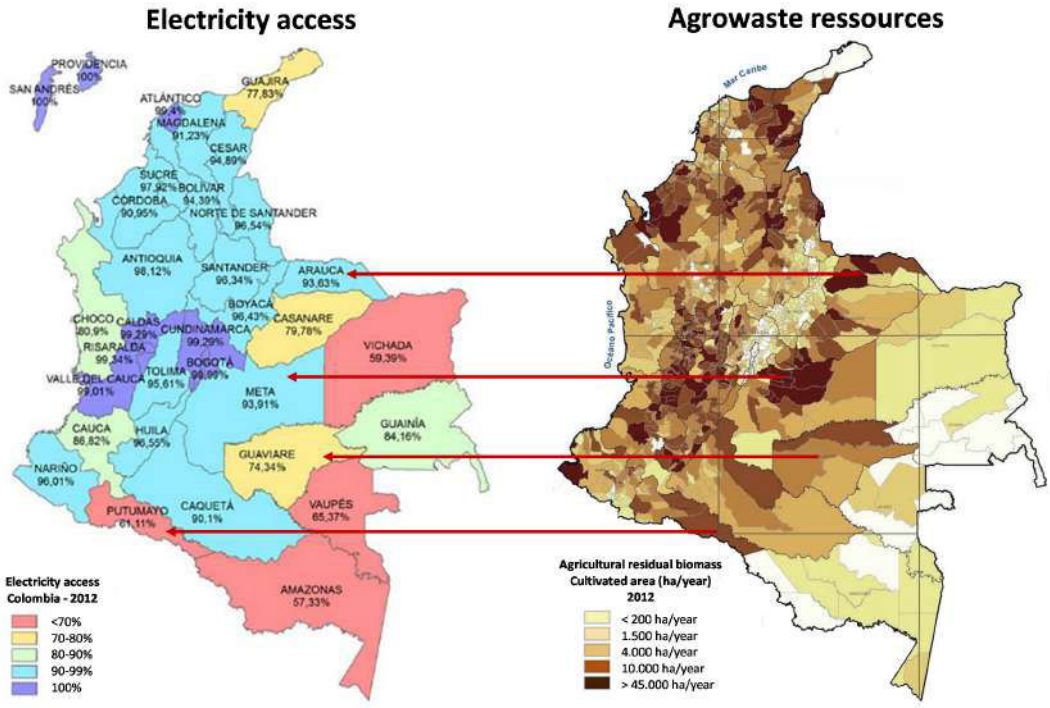

Figure 5: Comparison between Colombian energy needs and agrowaste available resources

Thus, these observations suggest that agrowaste valorization in energy applications could be a valuable solution for energy supply in most Colombian rural communities.

Moreover, considering the situation of several developing countries located in tropical areas, agrowaste energy valorization may contribute to the global access to electricity.

However, energy access is not the only concern for communities, considering that energy supply projects should be sustainable in time. In this context, the term sustainability refers to whether or not the project services and structures continue working over an extended period of time after their installation. In relation to this, several authors have documented numerous unsuccessful cases related to energy supply projects for poor communities, showing that different cultural and societal factors can hinder the implementation of these kind of initiatives. Among these reported unsuccessful cases, nearly 80% correspond to technologies using biomass as energy source [6, 7]. One of the most determinant factors that influence the sustainability of energy projects in developing countries is possibly the fact that commonly, no productive activities are associated to the projects and then, no particular improvements of the life quality, and principally, of the income levels are perceived by communities.

In relation to this and considering the characteristics of agrowastes, the selection of the appropriate valorization pathways could provide rural communities the opportunity to improve their access to energy and simultaneously generate additional incomes.

In this regard, agricultural residues can be valorized via physical, chemical, and biological treatments according to their nature and characteristics. Notably, lignocellulosic agrowastes are suitable for thermochemical conversion processes, considering their low moisture and high carbon contents [8]. In relation to this, combustion, pyrolysis, and gasification are the most common processes used for lignocellulosic biomass valorization. Therefore, the choice of the most suitable process will depend on the final products required for each application and their intended uses.

In particular, combustion refers to the exothermic oxidation of biomass at relatively high temperatures. In accordance, hot flue gases are the main product of this process, that can be used directly or indirectly for cooking, heating applications, or electricity production [9].

For its part, pyrolysis is related to the thermal decomposition of the feedstocks in the absence of oxygen or a reacting atmosphere. This process produces gas, liquid and solid by-products in different proportions, depending on its operation parameters. The main product of slow pyrolysis is char or charcoal, while fast pyrolysis produces mainly bio-oils. The process by-products can be easily transported for further use in combustion or gasification facilities, or refined into chemicals in the case of bio-oils [10].

In contrast, gasification consists in the partial oxidation of biomass under the presence of an oxidant agent like steam, air, oxygen, or carbon dioxide. This process is a very interesting alternative in the presented context, as it converts a solid residue in fuel gases that can be used for heat or power generation, and a solid by-product, usually considered as a residue, that could also be valorized (figure 6). In this case, fuel gases can be used in a more efficient way, with less emissions, compared to the combustion of raw biomasses [8]. In particular, steam as gasifying agent produces considerably high heating value fuel gases, and a porous carbon material that could have similar properties to activated carbons [11, 12]. These characteristics suggest that steam gasification could be an interesting process for the simultaneous valorization of gasification gaseous and solid by-products.

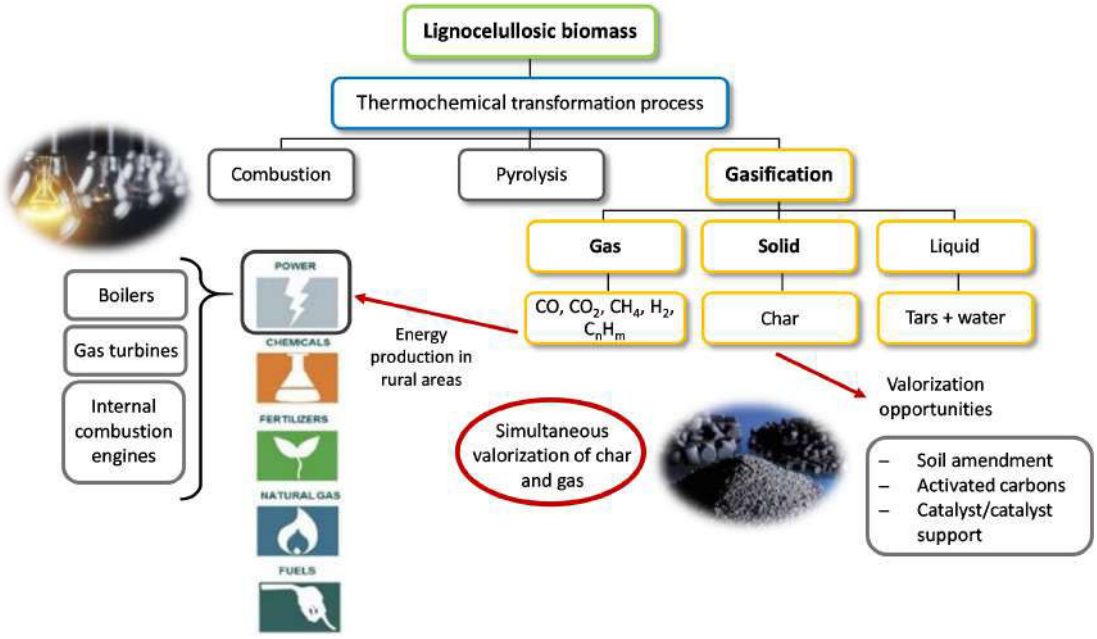

Figure 6: Possible thermochemical transformation processes for lignocellulosic agrowastes. Gasification by-products and valorization pathways.

Nevertheless, agrowaste valorization for energy applications has several challenges, as it must take into account the specific local conditions, such as the relevant crops and agricultural practices, climate, crop rotation and availability, residues volume, and energy requirements of local communities.

In this regard, one of the most important challenges is probably the fact that the availability of agrowastes is not constant and often depends on seasonal crops. Consequently, gasification facilities should work with different kind of residues with several characteristics, to ensure a constant operation. Depending on their origin and nature (e.g. type of crop, plant part, treatment, harvesting method, etc), the composition and structure of lignocellulosic residues varies and should be taken into account in their transformation process and subsequent valorization possibilities.

In consequence, the understanding of the impact of the feedstock characteristics on the gasification behavior and by-products is of great importance, in order to properly adapt the process conditions to the specific requirements of each application.

Although this research project was inspired in the social and energy context of Colombia and several developing countries in tropical regions, the results obtained are also applicable to developed countries, where great amounts of agrowastes are generated as well, with the associated treatment and valorization requirements.

In accordance, the **main objective** of this work is to analyze the steam gasification behavior of different lignocellulosic agrowastes, and understand the impact of their characteristics on the process by-products properties and valorization pathways.

The associated **specific objectives** are listed below:

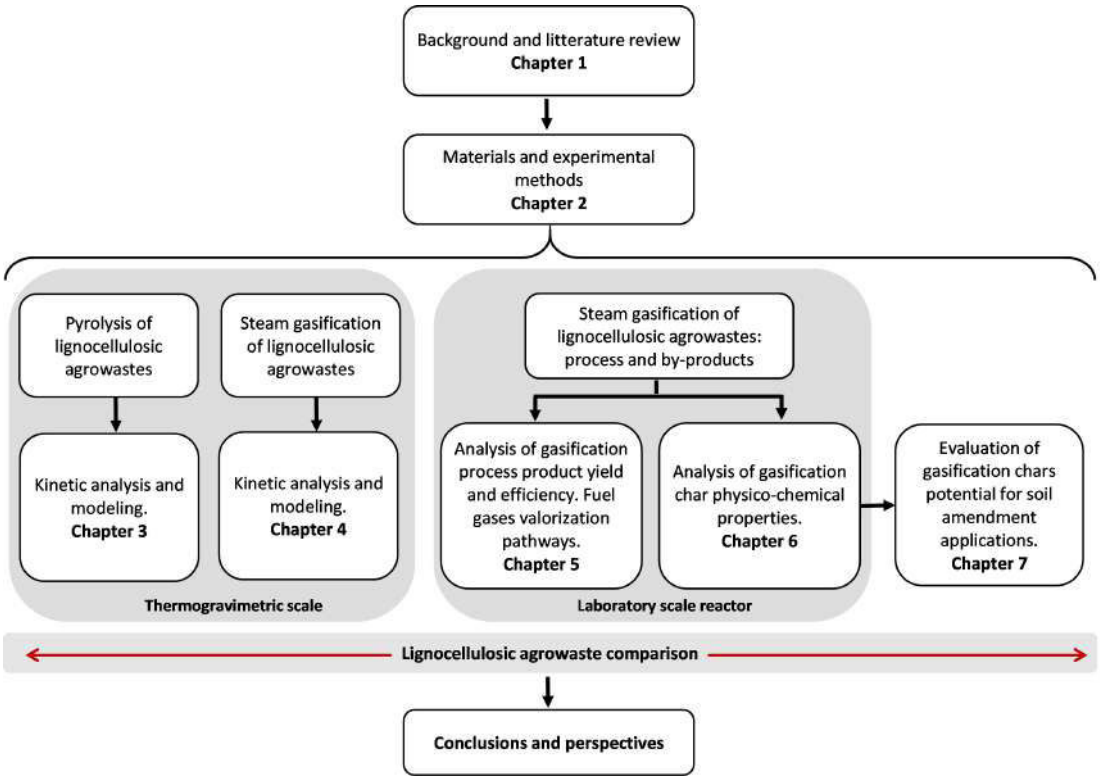

Figure 7: Structure of the manuscript

1. To determine the physico-chemical characteristics of selected biomasses from the perspective of their chemical composition, energy content, and structure.
2. To identify the influence of biomass characteristics and gasification parameters on syngas quality and its use as fuel gas.
3. To identify the influence of biomass characteristics and gasification parameters on the textural properties and structure of biochars.
4. To analyze the effect of surface properties and structure of chars in their capacity to be used in agroindustrial applications

This work was developed in the framework of an international cooperation between Colombia (Universidad Nacional de Colombia), and France (IMT - Mines Albi - Carmaux)

Manuscript structure

The present manuscript has been structured in 7 chapters, as summarized in figure 7. Each chapter is in the form of a scientific paper, already published, submitted or in intent of submission.

Chapter 1 is dedicated to the literature review, presenting the relevant background related to the gasification of lignocellulosic biomass, and the current research progress

on the valorization pathways of its gaseous and solid by-products. Attention is given to lignocellulosic agrowastes.

Chapter 2 describes the materials used in the present study and summarizes the experimental methods employed. At first, the procedure and criteria considered for the choice of the most appropriate feedstocks to be analyzed is described. Hence, three lignocellulosic agrowastes with different macromolecular and inorganic composition were selected: coconut shells (CS), bamboo guadua (BG), and oil palm shells (OPS). Moreover, the evaluation of two different experimental devices for gasification experiments is discussed, as well as the selection criteria of the most appropriated one. Finally, the methodology and experimental plan for the analysis of steam gasification process is presented, as well as the procedures applied for the characterization of the process gaseous and solid by-products.

Chapter 3 is dedicated to the analysis of the thermal decomposition behavior of the selected feedstocks under inert atmosphere, based on non-isothermal thermogravimetric analysis. An approach using a combined kinetics parallel reaction model and model-free isoconversional methods was employed. The influence of the biomass nature in the thermal decomposition behavior was discussed, comparing the calculated kinetic parameters of the studied materials.

Chapter 4 analyses the steam gasification behavior of the selected feedstocks and their blends, using an isothermal thermogravimetric analysis. The influence of the gasification temperature and steam partial pressure on the gasification reactivity of biomasses was discussed. Also, the impact of biomass and blends composition on the gasification reactivity and kinetics was analyzed. An approach using model-free isoconversional methods and generalized master plots was employed to determine the gasification kinetic parameters of the samples and compare their decomposition behavior. A new steam gasification kinetic model based on the inorganic composition of the samples is proposed.

Chapter 5 focuses on the steam gasification behavior and product distribution of the three selected samples and their blends. The mass and energy distribution of the gasification by-products was compared for the analyzed feedstocks. Also, the influence of the biomass organic and inorganic composition on the gasification product yield and gas efficiency is discussed. A focus on the permanent gaseous by-products is done, analyzing its composition, heating value, and possible suitable applications in the presented context.

Chapter 6 is dedicated to the analysis of the physico-chemical properties of the steam gasification chars produced from the selected feedstocks. The organic and inorganic composition of the chars were analyzed, as well as the distribution of minerals in their surface. In addition, the surface area, pore structure, and surface chemistry were also evaluated and compared. Finally, the relationship between the char structure and surface chemistry was discussed for the three samples.

Finally, **chapter 7** presents the evaluation of the physico-chemical properties of selected steam gasification chars produced from coconut shells, oil palm shells and bamboo guadua, in order to determine their suitability to be used in soil amendment and remediation applications. The pH and buffering capacities of chars were analyzed, as well as their cation exchange capacity (CEC) and mineral release at different pH

conditions. Accordingly, the agronomical implications of the observed gasification char properties were discussed, providing new insights to steam gasification chars valorization pathways.

The general conclusions related to the present work are summarized, and perspectives are proposed for future research work in order to complement the current investigations.

Bibliography

[1] Camille Foster. *Agricultural wastes. Charateristics, types and management*. Ed. by Camille Foster. Nova Science, 2015, p. 281 (cit. on p. 1).

[2] Iea - International Energy Agency. *WEO-2017 Special Report: Energy Access Outlook*. Tech. rep. 2030 (cit. on p. 2).

[3] Kifayat Ullah, Vinod Kumar Sharma, Sunil Dhingra, Giacobbe Braccio, Mushtaq Ahmad, and Sofia Sofia. "Assessing the lignocellulosic biomass resources potential in developing countries: A critical review." In: *Renewable & Sustainable Energy Reviews* 51 (2015), pp. 682–698 (cit. on p. 2).

[4] Unidad De Planeación Minero Energética (Upme) Ministerio de Minas y Energía. *Plan Indicativo De Expansión De Cobertura De Energía Eléctrica 2013-2017*. 57. Bogotá, 2013, p. 141 (cit. on p. 2).

[5] Universidad Indsutrial de Santander, Unidad de Planeación Minero Energética - UPME, Meteorologia y Estudios A Instituto de Hidrologia, and Mbientales - Ideam. *Atlas del potencial energético de la biomasa residual en Colombia*. 2011, p. 180 (cit. on p. 2).

[6] Julia Terrapon-Pfaff, Carmen Dienst, Julian Koenig, and Willington Ortiz. "A cross-sectional review: Impacts and sustainability of small-scale renewable energy projects in developing countries." In: *Renewable & Sustainable Energy Reviews* 40 (2014), pp. 1–10 (cit. on p. 3).

[7] Ana María González, Harrison Sandoval, Pilar Acosta, and Felipe Henao. "On the acceptance and sustainability of renewable energy projects-a systems thinking perspective." In: *Sustainability (Switzerland)* 8.11 (2016) (cit. on p. 3).

[8] J. a. Ruiz, M. C. Juárez, M. P. Morales, P. Muñoz, and M. a. Mendívil. "Biomass gasification for electricity generation: Review of current technology barriers." In: *Renewable and Sustainable Energy Reviews* 18 (2013), pp. 174–183 (cit. on p. 3).

[9] Prabir Basu. *Combustion and gasification in fluidized beds*. Ed. by Taylor & Francis Group. CRC Press. 2006, p. 467 (cit. on p. 3).

[10] Prabir Basu. *Biomass Gasification and Pyrolysis. Practical Design.* First Edit. Oxford: Elsevier, 2010, p. 364 (cit. on p. 3).

[11] Prabir Basu. "Gasification Theory." In: *Biomass Gasification, Pyrolysis and Torrefaction*. Elsevier Inc., 2013. Chap. Chapter 7, pp. 199–248 (cit. on p. 3).

[12] J F Kwiatkowski. *Activated Carbon: Classifications, Properties and Applications*. 2011 (cit. on p. 3).

Chapter

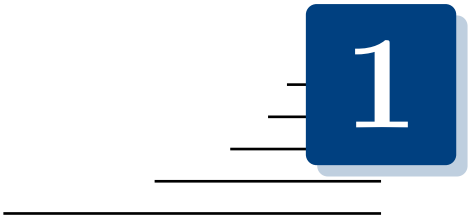

Background and literature review

1.1 Introduction

The aim of this chapter is to provide the relevant background information related to the gasification of lignocellulosic biomass, and the current research progress on the valorization pathways of its gaseous and solid by-products. This literature review is essential to understand the choices and research directions developed in the present work. In this regard, the chapter has been structured in two main sections.

Section 1.2 is dedicated to the biomass pyro-gasification principal concepts. At first, the main characteristics of lignocellulosic biomass, as a suitable feedstock for pyro-gasification process are described. Attention is given to agricultural and agroindustrial residues. Then, the different processes involved in biomass pyro-gasification, as well as their principal by-products are discussed. The most common technologies used are also described and compared.

For its part, section 1.3 is dedicated to the description of the pyro-gasification solid by-product. At first, the influence of the process parameters on the char yield and physico-

chemical properties is discussed. Then, an overview of the char main characteristics and their interest for subsequent applications is presented. Finally, attention is given to the current research progress on char valorization in several applications.

1.2 Biomass pyro-gasification basics

1.2.1 Lignocellulosic biomass

A unique definition of the term *biomass* does not exist in the literature. However, it generally refers to any organic material derived from plants or animals. Biomass is usually considered as a sustainable and renewable energy resource, as it is constantly being formed by the interactions of CO_2, air, water, soil, and sunlight with animals and plants [1].

Among the ones coming from botanical sources (plants), lignocellulosic biomass is the most abundant resource. Lignocellulosic material is the non-starch, fibrous part of plants, constituted mainly by hemicellulose, cellulose and lignin. A brief description of these three constituents is presented below [2]:

Cellulose

As the primary structural component of plant cell walls, cellulose is a long chain polymer with a high degree of polymerization (∼10.000) and a large molecular weight. Due to its substantial degree of crystallinity, it functions as a rigid and high strength component of the cell wall, providing the skeletal structure of the plants. Cellulose can be represented by the generic formula $(C_6H_{10}O_5)n$.

Hemicellulose

Unlike cellulose, which is crystalline and strong, hemicellulose has a random and amorphous structure with little strength. In general, it is a group of carbohydrates with a low degree of polymerization (∼80-200). The composition of hemicellulose varies depending on the plant source, but may be represented by the generic formula $(C_5H_8O_4)n$.

Lignin

Lignin is a very complex molecule containing cross-linked polymers of phenolic monomers. It is located in the layers of cell walls, forming with hemicellulose, an amorphous matrix around cellulose fibers, protecting them against biodegradation. In accordance, lignin acts as a cementing agent of plant constituents, giving structural support and resistance against microbial and chemical attack.

The proportion of these polymers varies from one plant species to another, based on the biomass type and origin, as observed in table 1.1.

In general, lignocellulosic biomass may be broadly classified as follows:

- Virgin biomass: Related to forest biomass, grasses and plants without particular transformation (e.g. wood).
- Waste biomass: Harvest related residues or waste generated after processing harvested materials, or from any other productive activity (e.g. bagasse, rice husk, coconut shells, demolition wood, etc).

Table 1.1: Cellulose, hemicellulose and lignin content of lignocellulosic biomass [3]

	Cellulose (%)	**Hemicellulose (%)**	**Lignin (%)**
Hardwood	45-47	25-40	20-25
Softwood	40-45	25-29	30-60
Grasses	25-40	35-50	10-30
Corn cobs	45	35	15
Switchgrass	45	31	12
Wheat straw	30	50	15

- Energy crops: Plants cultivated for the purpose of producing energy.

In this work, special attention is given to waste biomass, considering that these lignocellulosic materials have an interesting valorization potential in energy applications, or for the production of value-added products. In particular, agricultural and agroindustrial residues are largely available and cheap, and their valorization may imply not only an economic gain but also an environmental benefit.

Agricultural and agroindustrial waste

Agricultural and agroindustrial waste can be defined as the residues from the growing and processing of raw agricultural products. They are mostly available in the countries with large agricultural sector and food production. In the European Union, the production of crop residues is estimated at 258 million tons per year [4], while in the case of developing countries, agroresidues potential is estimated at more than 2900 million tons per year [5]. Residues like rice straw and husk, sugarcane bagasse, maize straw and cobs, wheat straw, coconut shells and coir, and oil palm residues are some of the most abundant. The elemental composition of some agrowastes is presented in table 1.2.

Table 1.2: Composition of some lignocellulosic agrowastes from literature [6, 7].

	Wheat straw	**Rice straw**	**Corn stover**	**Rape stalk**	**Cotton stalk**	**Sugarcane bagasse**	**Hazelnut shell**
Elemental composition (wt.%)							
C	42.4	40.6	44.1	43.1	45.8	43.8	52.3
H	5.4	5.3	5.6	5.8	5.9	5.8	6.5
O	41.7	40.5	41.6	42.4	41.7	47.1	26.8
N	0.6	0.9	1.0	0.8	1.1	0.4	5.2
Ash	9.2	11.9	7.4	6.8	4.9	2.9	4.3
Macromolecular composition (wt.%)							
Hemicellulose	21.8	18.2	17.0	14.2	13.0	22.6	15.7
Cellulose	38.4	41.3	37.2	41.9	38.3	41.3	22.9
Lignin	21.1	18.1	22.8	19.9	27.5	18.3	51.5

The production of residues depends on several factors like the type of crop, crop rotation, climate conditions, cultivated area, and agricultural practices. These variables must be taken into account to determine the valorization potential of agrowastes in each location.

In this regard, lignocellulosic agrowastes may constitute a very interesting resource for energy applications taking into account their low cost, availability, and the fact that they do not compete with food production. Moreover, considering that the wrong disposal of these residues could cause problems like air and soil pollution, the energy valorization of agrowastes may also represent an environmental benefit.

1.2.2 Pyro-gasification process and reactions

Among the alternatives available for lignocellulosic biomass conversion and valorization, pyro-gasification is a thermochemical process, where a carbon-based material is converted into fuel gases, accompanied by a small fraction of liquid and solid by-products [8]. Unlike combustion, where the sample is completely oxidized, pyro-gasification uses non-stoichiometric quantities of oxidizing agents like steam, air, or oxygen to rearrange the molecular structure of the feedstock by means of different heterogeneous reactions [9].

Pyro-gasification, usually referred as gasification, is a very complex sequence of processes, which can be classified in three different individual steps: drying, pyrolysis and gasification. The main chemical reactions occurring during the pyro-gasification process are summarized in table 1.3. Each individual step is briefly described below:

Table 1.3: Main chemical reactions involved in biomass gasification process [8, 10]

Reaction type	Reaction	Heat of reaction
Pyrolysis		
R1 (Devolatilization)	$\text{Biomass} \longrightarrow \text{Char} + \text{tars} + H_2O + \text{light gases}$	Endothermic
Char combustion		
R2 (Partial oxidation)	$C + 0.5\,O_2 \longrightarrow CO$	-111 kJ/kmol
R3 (Total oxidation)	$C + O_2 \longrightarrow CO_2$	-394 kJ/kmol
Char gasification		
R4 (Boudouard)	$C + CO_2 \longleftrightarrow 2\,CO$	+173 kJ/kmol
R5 (Water-gas)	$C + H_2O \longleftrightarrow CO + H_2$	+131 kJ/kmol
R6 (Hydrogasification)	$C + 2\,H_2 \longleftrightarrow CH_4$	-78.4 kJ/kmol
Homogeneous reactions		
R7 (Shift reaction)	$CO + H_2O \longleftrightarrow CO_2 + H_2$	-41.2 kJ/kmol
R8 (Methanation)	$2\,CO + 2\,H_2 \longrightarrow CH_4 + CO_2$	-247 kJ/kmol
R9 (Methanation)	$CO + 3\,H_2 \longleftrightarrow CH_4 + H_2O$	-206 kJ/kmol
Tar conversion reactions [a]		
R10 (Steam reforming)	$C_nH_m + n\,H_2O \longrightarrow (m/_2{}^+ n)H_2 + n\,CO_2$	Endothermic
R11 (Dry reforming)	$C_nH_m + n\,CO_2 \longrightarrow 2\,n\,CO_2 + m/2H_2$	Endothermic

[a] C_nH_m represents light hydrocarbons

Drying

In this first stage, the water contained in the biomass (free water and bound water) is released by effect of heat. This endothermic process occurs at temperatures below 200°C.

Pyrolysis

This step corresponds to the thermal decomposition or devolatilization of the organic material in the absence of oxygen, at temperatures between 300°C and 800°C. The pyrolysis process produces gas, liquid and solid by-products in different proportions, depending on the feedstock composition (e.g. hemicellulose, cellulose and lignin), heating rate, temperature, and time [11]. The produced gases are mainly composed of H_2, CO_2, CO,CH_4, and C_nH_m, while the liquid phase is mainly constituted of water and condensable hydrocarbons, also named tars. For its part, the solid by-product or char consist of almost pure carbon with a fraction of inorganic material originally present in the feedstock. The production of char is maximized at low temperatures and slow heating rates [12]. In contrast, fast heating rate conditions favor the production of liquids [13].

The composition of the biomass and particularly its macromolecular constituents have an important impact on the pyrolysis product yield, considering that each component has a different decomposition behavior. From thermogravimetric analysis, several authors have identified the decomposition temperature range for hemicellulose, cellulose and lignin, as the mains constituents of lignocellulosic biomass [14].

Hemicellulose has been reported as the less stable constituent, with low decomposition temperatures between 200°C and 350°C, followed by cellulose, with a decomposition range between 300°C and 400°C. In contrast, lignin pyrolysis occurs in a wide temperature range, from 200°C to 800°C, due to its high aromaticity [14]. In accordance, several authors describe the biomass decomposition behavior as the superposition of the three main components.

Nevertheless, considering that the hemicellulose, cellulose, and lignin are not isolated in the biomass structure, interactions between them may occur during the pyrolysis process. In relation to this, Lui et al. [15], studied the interactions between the biomass components, concluding that lignin impacts in an important extent the hemicellulose and cellulose decomposition rates. Similarly, Mendu et al. [16] found that high lignin biomasses show well-differentiated peaks for hemicellulose and cellulose decomposition, unlike low lignin samples.

Regarding the product yield, hemicellulose and cellulose are the main source of volatiles during pyrolysis. Hemicellulose releases mainly non-condensable gases, while cellulose is the primary source of tars. In relation to its aromatic nature, lignin degrades slowly and contributes to the char yield [11]. In this regard, the macromolecular composition of the samples is probably the main factor responsible for the differences observed between the pyrolysis behavior and products of different feedstocks. Nevertheless, the interactions between macromolecular components during the thermochemical decomposition processes still need further investigations.

Gasification

Gasification consists in the partial oxidation of char under the presence of an oxidant agent like steam, air, oxygen, or carbon dioxide. Gasification process typically occurs at high temperatures, in the range of 700°C to 1300°C [17]. The gasification agent reacts with the char, converting it into gas by means of different heterogeneous reactions, summarized in table 1.3. In accordance, the main product of gasification process is a

fuel gas composed of H_2, CO_2, CO,CH_4,and C_nH_m. For their part, tars and char are the liquid and solid by-products of the process, respectively.

The heating value of the produced gas is significantly affected by the choice of the gasifying agent, as presented in table 1.4.

Table 1.4: Heating value of produced gas based on the gasifying agent [8]

Gasifying agent	**Heating value (MJ/Nm3)**
Air	4-7
Steam	10-18
Oxygen	12-28

If air is used, the nitrogen will dilute the produced gas, resulting in a lower heating value. In contrast, oxygen gasification has the highest heating value followed by steam gasification. However, the high cost of oxygen production limits the use of this agent in most gasification facilities [18, 19]. Despite the fact that several reactions occur simultaneously during a gasification process, R4 and R5 are considered as the main reactions in the case of CO_2 or steam gasification respectively.

Besides the differences in the produced fuel gas heating value, the reacting atmosphere also impacts the gas composition and product yield of the gasification process. For instance, steam gasification enhances the production of hydrogen, while CO_2 favors the production of CO and reduces the H_2 and CH_4 yields [10]. Moreover, in several applications, the gasification is carried out using a mixture of air, oxygen, steam, or carbon dioxide.

Some technical challenges associated to the use of steam and CO_2 as reacting atmospheres should be taken into account. In particular, energy requirements associated to the production of steam, or the CO_2 separation and storage, may increase the final energy costs of the process. In consequence, the gasification parameters should be analyzed for each particular application, and adapted to the required gas composition and product yield. In this regard, the main advantages and technical challenges associated to air, steam and CO_2 as gasifying agents are presented in table 1.5.

Furthermore, as observed in table 1.3, most of the reactions involved in the gasification process are endothermic and then, require an energy supply to maintain the temperature of the process. This energy may be provided internally in the reactor, by a controlled partial oxidation of the feedstock, considering that oxidation reactions (R2 and R3) are exothermic. In this case, the process is known as direct or autothermal gasification. In contrast, if the heat is externally supplied, the process is called indirect or allothermal gasification [20, 21].

Several authors have investigated the effect of operating parameters and conditions on the performance of the biomass gasification process. Parameters like temperature and gasifying agent have shown an important impact on the produced gas composition and product yield [22, 23]. Moreover, the impact of the indigenous inorganic elements of the raw materials on the steam gasification reactivity has been also reported [24, 25]

Table 1.5: Advantages and technical challenges of different gasifying agents. Adapted from [10]

Gasifying agent	
1. Air	
Advantages	1. Provides heat to the process through partial combustion 2. Yields moderate char and tar contents
Technical challenges	1. Provides low heating value gases with large amounts of N_2 2. The process temperature depends on the amount of air supplied
1. Steam	
Advantages	1. Yields a high heating value syngas 2. Yields a hydrogen-rich syngas
Technical challenges	1. Requires indirect or external heat supply 2. Yields a high tar content in the produced gas 3. May require catalytic tar reforming 4. The steam production requires additional energy supply
3. Carbon dioxide	
Advantages	1. Yields a high heating value syngas 2. Yields CO rich gas with low contents of CO_2
Technical challenges	1. Requires indirect or external heat supply 2. Requires a CO_2 separation/production system 3. May require catalytic tar reforming

Lignocellulosic biomass from agricultural and agroindustrial activities exhibit different amounts and compositions of inorganic elements that influence its gasification behavior. In particular, alkali and alkaline earth metals (AAEM) such as K, Na, Ca and Mg, could have a catalytic effect on the gasification reactions [24].

In this regard, several authors have proposed different reaction mechanisms to describe the catalytic effect of alkali carbonates during CO_2 gasification [26]. The R4 reaction sequence via the metal M proposed by McKee is presented below [27]:

$$\begin{gathered} M_2CO_3 + 2\,C \longrightarrow 2\,M + 3\,CO \\ 2\,M + CO_2 \longrightarrow M_2O + CO, \text{ or} \\ M_2O + CO_2 \longrightarrow M_2CO_3 \\ C + CO_2 \longrightarrow 2\,CO \end{gathered}$$

In the case of steam gasification, the R5 reaction sequence is also considered as an oxygen transfer mechanism via the metal M [27, 28]:

$$\begin{gathered} M_2CO_3 + 2\,C \longrightarrow 2\,M + 3\,CO \\ 2\,M + 2\,H_2O \longrightarrow 2\,MOH + H_2 \\ 2\,MOH + CO \longrightarrow M_2CO_3 + H_2 \\ 2\,C + 2\,H_2O \longrightarrow 2\,CO + 2\,H_2 \end{gathered}$$

Among the AAEM, K has been reported to be the most active species in steam and carbon dioxide gasification [28]. In contrast, elements like Si, Al and P may inhibit this beneficial effect, as they tend to react with AAEM to form alkali silicates [29].

In this regard, it is important to point out that the biomass inorganic content may influence in a significant way the biomass combustion and gasification behavior[24]. However, a better description and understanding of the interactions between the biomass mineral constituents and their influence in the gasification process are still required.

1.2.3 Pyro-gasification by-products

As aforementioned, combustible gases are the main product of pyro-gasification process. However, a liquid and a solid phase are also produced in different proportions, depending on the process parameters and feedstocks. The main characteristics of the gasification by-products are presented below:

Gases

Pyro-gasification gas is principally composed of CO and H_2. CO_2 is the third component followed by CH_4 and light hydrocarbons, present in minor concentrations. The gasifying agent impacts in an important way the composition and heating value of the produced gas [30]. For instance, the H_2 content can be increased if steam is used as the gasifying agent. In contrast, the use of CO_2 enhances the production of CO and reduces the H_2 and CH_4 fractions [31]. Alternatively, mixtures of steam or CO_2 with air or O_2 can be also used as gasifying atmosphere, impacting also the component fractions in gas [32].

In accordance, produced gas from lignocellulosic biomass can be used in boilers, internal combustion engines, or gas turbines for power generation [18]. Moreover, depending on its composition, it can be also converted to advanced chemicals through Fisher-Tropsh synthesis and oxo-synthesis processes [33]. In particular, the H_2/CO ratio of the gas gives an insight to its possible valorization pathways.

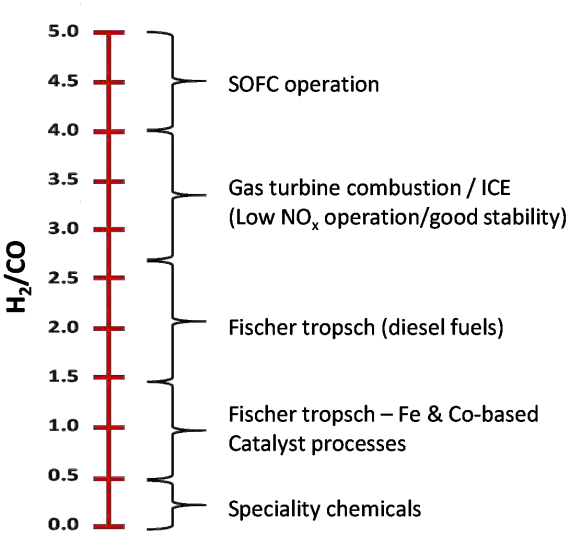

Figure 1.1: Gas valorization pathways according to the H_2/CO ratio. Adapted from [31]

As presented in figure 1.1, H_2/CO ratios between 4 and 6 are suitable for solid oxide fuel cells (SOFC) operation, while values between 4 and 2.5 are mostly recommended in gas turbines and internal combustion engines applications. Finally, H_2/CO ratios below 2 are more suited for Fisher-Tropsh (FT) synthesis processes [31, 34].

In this regard, depending on the intended application, the process gasifying agent is a very important parameter to consider that may be adapted to obtain the required H_2/CO ratio.

Liquids

Gasification liquid by-products, generally known as tars, are defined as a complex mixture of condensable hydrocarbons with molecular weight higher than benzene [35]. These compounds are a main concern for gasification process, as they can condense and clog pipes and equipment, and produce metallic corrosion. In accordance, the presence of tars in the gas is associated to its usefulness. In applications where the raw gas is burned directly without cooling, there is no need of gas cleaning. However, if a use in internal combustion engines or gas turbines is intended, tar conversion or removal is compulsory [36].

For energy applications, internal combustion engines require syngas with tar levels of maximum $100\,mg/m^3$, while gas turbines require less than $10\,mg/m^3$, in order to avoid equipment damages [37]. Moreover, in the case of advanced chemicals production applications, the tar limits are even more stringent, with upper values as low as $0.02\,mg/m^3$. To meet these requirements and face tar problems, several syngas conditioning methods have been developed. They are mainly classified in primary or secondary methods depending on the location where tars are removed. Primary methods are related with the gas treatment inside the gasification reactor, whereas secondary methods are performed outside the gasifier, and can be physical or chemical [38].

Solids

Char or *biochar* is the solid residue from biomass pyro-gasification process. Pyrolysis chars are mainly composed of carbon, while gasification chars may contain important amounts of inorganic material, depending on the progress of the gasification reactions [39]. Biochars could have several valorization pathways according to their physico-chemical characteristics: combustion for energy recovery, catalyst or catalyst supports, soil amendment materials, adsorbents, and activated carbon precursors [40, 41]. A focus on the pyrolysis and gasification chars physico-chemical properties and possible valorization pathways is presented in section 1.3.

1.2.4 Pyro-gasification technologies

The sequence of pyro-gasification reactions and the characteristics of the process by-products depend in an important extent on the reactor type used. Various works on design improvements have been done for enhancing the performance of gasification devices. However, they are generally classified in fixed-bed and fluidized-bed reactors [17]:

Fixed-bed reactors

Fixed-bed reactors are also known as moving-bed reactors and can be classified in updraft (counter-current) gasifiers and downdraft (co-current) gasifiers (Figure 1.2).

- In updraft gasifiers, the feedstock is fed by the top, while the oxidizing agent is introduced from the bottom, as observed in 1.2a. Then, the gases rise through the bed and are recovered at the top of the reactor. The biomass is moving in the opposite direction and passes first through the drying zone, then, the pyrolysis zone, the reduction zone, and finally, the combustion zone. These reactors are easy to operate, but may produce gases with an important content of tars (typically 10% to 20% by weight of the feed) [1].
- In a downdraft gasifier, the biomass is fed from the top, while the oxidizing agent is fed at the sides. In this reactor, the gas is moving in the same direction as the biomass and is recovered at the bottom of the reactor as observed in 1.2b. Since the pyrolysis products pass through the combustion high-temperature zone, the tar cracking reactions are favored, resulting in a low tar gas production (<1 g/Nm^3) [1].

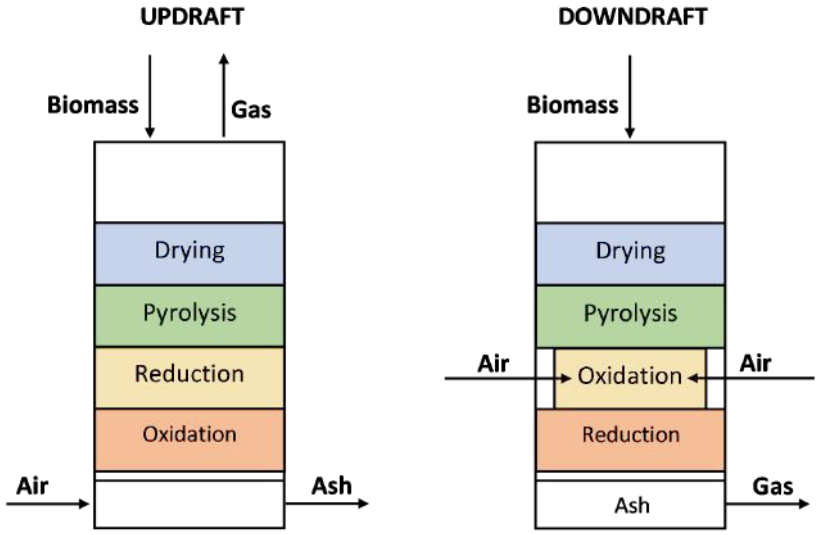

Figure 1.2: Fixed-bed reactors designs. a) Updraft (counter-current), b) Downdraft (co-current). Adapted from [8]

Fluidized-bed reactors

The fluidized bed reactors have some advantages over fixed-beds, regarding the mixing and temperature uniformity, the high reaction rates, high heat and mass transfer, and the possibility to be built in large scales [42]. A fluidized bed is composed of fine solids that are kept suspended in a liquid-like state by the action of the gasifying agent, injected from the bottom of the reactor with a sufficient pressure. Fluidized-bed gasifiers can be mainly classified in bubbling and circulating reactors.

- In a bubbling fluidized bed reactor, the velocity of the upward flowing gasifying agent is around 1-3 m/s and the expansion of the bed occurs only at the lower part of the gasifier, as presented in figure 1.3a. Considering the low gas velocities, the bed materials remain in the reactor. Gasifiers operating at temperatures below 900°C are preferred in order to avoid ash agglomeration. However, bubbling fluidized bed reactor can work at temperatures above 1000°C in the case of low ash feedstocks.

- In a circulating fluidized bed, the solids circulate around a loop that is characterized by intense mixing, as shown in figure 1.3b. This design exhibits great gasification efficiencies and high carbon conversions, thanks to the increase in the residence time of the particles and gases inside the reactor. The velocity of the upward flowing gasifying agent is around 5-10 m/s to ensure the circulation of the solids. Moreover, the operation temperatures are between 800°C and 1000°C in order to avoid ash agglomeration.

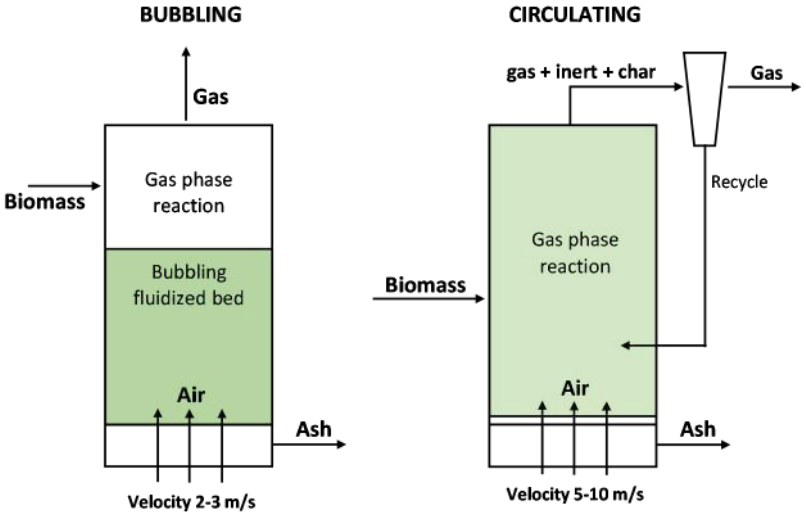

Figure 1.3: Fluidized-bed reactors design. a) Bubbling bed gasifier, b) Circulating fluidized gasifier. Adapted from [42]

The advantages and technical challenges identified for the described gasifier designs are summarized in table 1.6.

1.3 Focus on pyro-gasification chars properties

As extensively discussed in the literature, pyro-gasification process operating conditions influence in a great extent the physico-chemical properties of the solid by-products. More specifically, parameters like heating rate, temperature, and reacting atmosphere should be carefully chosen in accordance to the required char yield and properties.

1.3.1 Influence of process parameters

Heating rate

In a pyro-gasification process, the heating rate has an important impact on the quantity of char recovered and its properties. In particular, pyrolysis can be classified in slow and fast, according to the heating rate. It has been widely observed in the literature, that low heating rates (∼20°C/min) favor the production of char, while high heating rates (>10°C/s) maximize the production of liquids [24, 43]. These differences may be explained by the fact that a slow heating allows the slow release of volatiles and the occurrence of secondary char formation reactions that increase the resulting solid yield[40]. In this regard, it has been reported that the highest recovered char quantities,

Table 1.6: Advantages and technical challenges of the principal reactor designs. Adapted from [10]

Gasifier design	
1. Fixed-bed	
Advantages	1. Simple and reliable desing 2. Suitable for wet biomass gasification 3. Economically viable at small scales 4. Downdraft reactor yields gases with low tar content
Technical challenges	1. Operates at longer residence times 2. Non-uniform temperature distribution 3. Low cold-gas efficiency 4. Limited to low biomass processing capacity 5. Updraft reactor yields gases with high tar contents
2. Fluidized-bed	
Advantages	1. Short biomass residence time 2. High biomass processing capacity 3. Uniform temperature distribution 4. Yields low char contents 5. High cold-gas efficiencies
Technical challenges	1. Yields high particulate dust contents in syngas 2. Yields high tar contents 3. Economically viable only at medium and large scales

between 20% and 40% are obtained for slow pyrolysis process, followed by fast pyrolysis, and finally by gasification, with approximately 15% and 10%, respectively [41].

The differences between chars prepared under both conditions has been widely described in the literature. In general, it has been observed that high heating rate chars have higher specific surface areas, as a result of the extremely fast release of volatiles from the carbon structure, that breaks the carbon matrix [44]. In consequence, these chars have shown higher reactivities to gasification or combustion reactions, mostly related to their open structure [45].

Temperature

The pyro-gasification temperature impacts in a very important way the biochar quantity and quality. Some of the char properties that are widely influenced by the process temperature are the elemental composition, fixed carbon content, surface area, pore volume, heating value, pH, and cation exchange capacity [40].

Considering that higher pyrolysis temperatures are associated to greater biomass decomposition extents, pyrolysis chars show a decrease in the H/C and O/C ratios with the temperature increase, indicating higher carbon percentages, but lower surface functionalities in the char surface. Likewise, greater surface areas and pore volumes have been observed by several authors for high temperature chars.

Furthermore, the amount of char that can be obtained from pyro-gasification depends mainly on the process temperature and residence time. Higher temperatures result

higher decomposition extents and lower char yields, as well as longer residence times. In this regard, the effect of the temperature on some of the most relevant properties of pyrolysis biochars is summarized in figure 1.4.

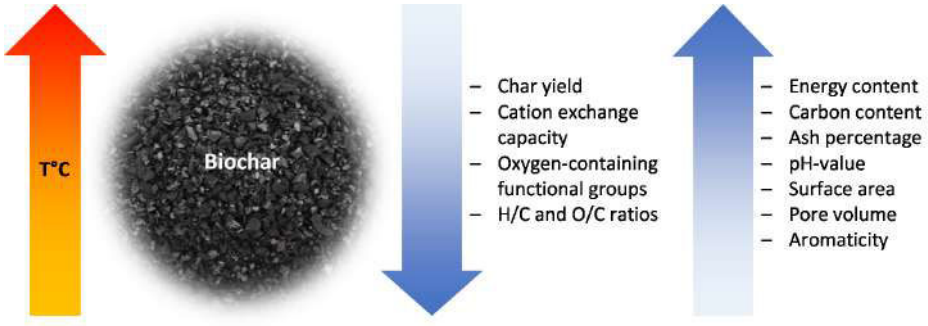

Figure 1.4: Effects of the temperature on biochar properties. Adapted from [40, 46]

As observed, depending on the intended applications of the chars, some properties can be improved with the temperature rise, while others may be deteriorated. In consequence, the choice of the process temperature may be done considering the expected applications and the required char characteristics. Moreover, the quantity of char recovered from a process is also an important point to consider for the economic design of a particular char valorization activity.

Reacting atmosphere

The reacting atmosphere is a very important parameter to consider in pyro-gasification processes, as it has a significant impact on the chars structure and surface chemistry. As stated previously, under inert atmosphere, the biomass decomposition occurs only as a result of the temperature increase, and no particular reactions take place.

In contrast, in the presence of a reacting agent, heterogeneous reactions between the char and the gaseous phase create a porous network in the char and integrates surface functionalities [47]. In this regard, several authors have reported that gasification chars produced with steam or CO_2 exhibit considerably higher surface areas in comparison to pyrolysis-only chars [48]. Values between 2 and 400 m^2/g have been reported in the literature for pyrolysis chars produced at different temperatures, while values near 700 m^2/g or higher have been observed for CO_2 and steam gasification chars [49, 50].

More specifically, Klinghoffer et al. [51] investigated in detail the physico-chemical properties of woody chars produced with air, CO_2, and steam as gasifying agents. Different characteristics were observed for the three samples, considering that the reaction mechanism differs from one agent to another. CO_2 chars exhibited a higher microporosity in comparison to steam gasification chars. In this regard, Guizani et al.[52] suggested that steam molecules diffuse more deeply in the biochar matrix and enhance the formation of larger pores.

Regarding the char surface chemistry, pyrolysis chars produced at high temperatures does not exhibit significant amounts of surface functional groups, as a result of the sample devolatilization. In contrast, when a reacting atmosphere is present, chemisorption of oxygen and hydrogen may occur on the char structure, creating surface complexes [47].

In this regard, gasification chars may have interesting properties that could suggest their valorization in several applications.

As presented in this section, the process parameters impact in a very important way the physico-chemical properties of the resulting chars. Therefore, gasification conditions should be carefully selected according to the required by-products characteristics and intended applications.

1.3.2 Pyro-gasification chars physico-chemical properties

This section gives a broad overview of the main physico-chemical properties of pyro-gasification chars and their interest for subsequent applications:

Elemental composition

The knowledge of the C,H,N,S and O content of the char gives a first insight to its possible applications. In particular, the atomic ratios H/C and O/C are used as a measure of the aromaticity and decomposition extent in the case of pyrolysis chars [53]. Higher gasification temperatures are associated to an increase in the char carbon content, and a decrease in the H/C and O/C ratios, due to the devolatilization of functional structures containing oxygen and hydrogen.

In contrast, steam and CO_2 gasification chars may exhibit higher hydrogen and oxygen contents in comparison to pyrolysis chars produced at the same temperature, considering that gasification reactions could result in the functionalization of the char surface, as aforementioned [49].

In relation to the inorganic composition, chars could contain different amounts of minerals, depending on the indigenous inorganic content of the parent materials. As a large part of the ash remains in the char after the pyro-gasification process, the increase of the temperature and residence time will be also associated to an increase in the char inorganic content [40]. For some applications, the presence of minerals in the char structure could be beneficial, as in the case of soil remediation and heavy metal adsorption [54], while for others, the ash content could generate operational problems like slagging, fouling and corrosion [55]. In this regard, the organic and inorganic composition of pyro-gasification chars are important parameters to consider in the choice of their most suitable valorization pathways.

Specific surface area and porosity

The char specific surface area is usually determined by the BET analysis, assessed using N_2 adsorption at 77K. This property is a very important parameter to identify the possible uses of a char. High specific surface areas are required for char applications as adsorbent, catalyst, or catalyst support [56].

In addition to the surface area, the pore size distribution and pore volume of chars play and important role in their performance in several applications. Biochars may contain different proportions of micropores (<2nm), mesopores (2-50nm), and macropores (>50nm) depending on the process parameters, as aforementioned, and on the parent material [47]. In adsorption applications, favorable pore size distribution for a targeted molecule, makes the internal surface accessible and enhances the adsorption process [57]. For instance, according to the pore size, microporous carbons can be used for gas applications, like gas separation and purification. In contrast, mesoporous

and macroporous materials are suitable for liquid phase applications, such as water purification [57].

Surface oxygen-containing functional groups

As a result of the thermal decomposition of the biomass structure, high temperature pyrolysis chars show low H/C and O/C ratios, indicating a more aromatic structure and less surface functional groups in comparison to chars produced at low temperatures [58]. Aromatic structures have a great thermodynamic stability, and are associated to a significant char recalcitrance, useful in soil amendment and carbon sequestration applications [49].

However, the content of oxygen and hydrogen in the char structure also plays an important role in the char performance in several applications. More specifically, oxygen-containing functional groups in the char structure are highly reactive and could affect their adsorption ability. Moreover, the type and amount of functional groups influence the char alkalinity and their ability to exchange cations and neutralize acidity in soil amendment applications [59].

Figure 1.5 shows an example of oxygenated functional groups that can potentially exist on the char surface.

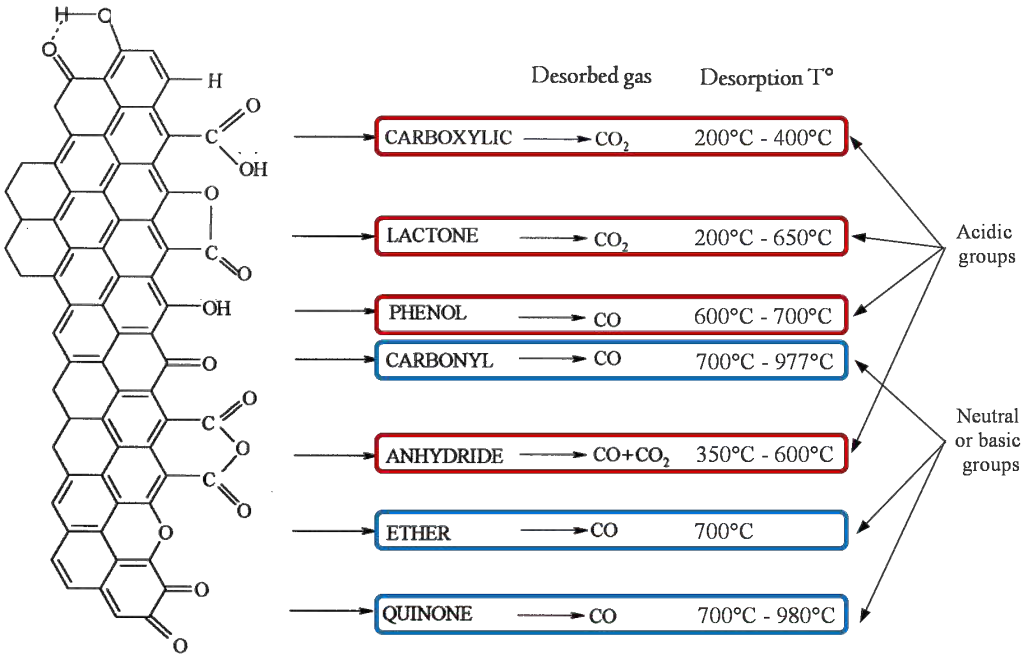

Figure 1.5: Oxygen functional groups and thermal stability. Adapted from [60]

In relation to the character of these groups, carboxylic acids, hydroxyl, lactone and phenol groups are known as acidic surface functional groups [61, 62], while carbonyl, quinone and pyrone-like functional groups are reported to be neutral or basic [63].

More specifically, oxygen-containing functional groups, specially the acidic ones, have shown to be responsible for the amphoteric character of chars. In particular, in aqueous phase, the char surface may be positively or negatively charged, depending on the pH of the surrounding solution. Then, the carbon may have the capacity to interact with

positive or negative charges. The pH at the point of zero charge or pH_{PCZ} is a measure of this ability. The pH_{PCZ} is defined as the pH at which the char surface has zero charge. In this regard, if the pH_{PCZ} of a carbon is higher than the pH of the solution, its surface will be positively charged and will enhance interactions with anions. In contrast, if the pH_{PCZ} is lower than the solution pH, the surface will be negatively charged and will favor cationic interactions[57].

Surface functional groups can be analyzed qualitatively and quantitatively using different techniques like Boehm titration, Fourier transform spectroscopy (FTIR), X-ray photoelectron spectroscopy (XPS), or thermal programmed desorption (TPD). The latter one is particularly interesting as it is relatively simple and allows a quantitative determination based on the thermal stability of each functionality. It consist on the heating of the sample in an inert atmosphere, analyzing the CO and CO_2 released. As observed in figure 1.5, the nature of each group can be determined according to the emitted gas and its desorption temperature.

In this regard, the accurate characterization of surface functionalities on chars is of great importance to determine their possible uses and applications.

pH-value

The char pH is also a very important parameter to consider, particularly for agricultural applications, as it can help to adjust the soil pH and increase its buffering capacity. The alkalinity of chars depends mainly on the raw material and the treatment temperature. Generally, pH increases with the pyro-gasification temperature, due to the material devolatilization and the loss of acidic complexes existing in the raw biomass [46].

Moreover, the increase in the ash content, usually basic in nature, results in higher pH values [64]. The existence of alkaline minerals in the char matrix also enhance the char acid neutralization capacity, making this material suitable for the amendment of acidic soils [65].

Cation exchange capacity

The cation exchange capacity (CEC) is a relevant char property usually evaluated for environmental applications. It is related to the char capacity to hold and exchange cations (e.g. K^+, Na^+, Ca^{2+}, Mg^{2+} and $NH_4{}^+$), and is usually associated to soil fertility [66]. CEC depends directly on the char surface structure, oxygen containing functional groups (e.g. $-COOH$, $-OH$), and mineral content [64]. In particular, it is the result of the negative charges on the char surface.

High cation exchange capacities have been observed for low-temperature pyrolysis chars, considering their low devolatilization extent. In contrast, a decrease in the CEC with the increase of the pyrolysis temperature has been reported by several authors [67]. In the particular case of steam and CO_2 gasification chars, as the heterogeneous gasification reactions could result in the functionalization of the char surface, CEC comparable to low-temperature pyrolysis chars may be observed [67, 68].

1.3.3 Pyro-gasification chars applications

As observed in section 1.3.2, depending on the production parameters, biochars from agrowastes have a wide range of physico-chemical properties that could be interesting for several applications. The environmental and industrial applications of biochar in

the areas of energy production, carbon sequestration, soil amendment, and advanced materials production have been widely discussed in the literature in the recent years, and will depend on the material properties. The most common pyro-gasification chars applications are summarized in figure 1.6

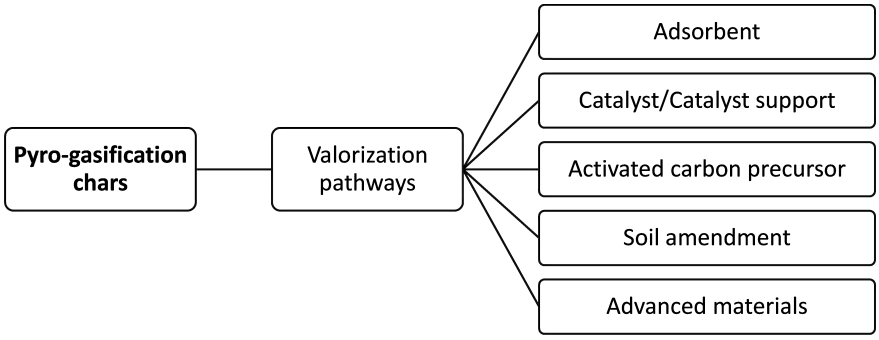

Figure 1.6: Common applications of pyro-gasification chars

Adsorbent

The inherent high specific surface area of biochars is of great interest in adsorption applications. According to their pore size distribution, biochars could be used in gas or liquid phase applications, for the removal of several kinds of pollutants. Different studies have investigated the effectiveness of biochars in the removal of organic contaminants from water [69], flue gases treatment [70], and syngas tar removal [71].

According to different authors, the adsorption performance of biochars depend on the parent material used for their production. Xu el al. [72] compared the methyl violet adsorption behavior of different biochars, suggesting that the adsorption characteristics of biochar are influenced by the number of negative charges in its surface. Moreover, the mineral content and composition of the chars played an important role on their adsorption ability. In particular, mineral-rich biochars proved to be suitable for heavy metal adsorption in water and soils [64], considering the interactions between metals and the charged minerals in the char surface. The higher the negative charge of the char surface, the more pronounced the electrostatic adsorption of heavy metals.

The ability of biochars to adsorb organic contaminants has also been highlighted by different authors. Several studies have reported that for this application the presence of minerals is not beneficial, and thus, de-ashing treatments could be required. The removal of minerals can greatly influence the surface characteristics of the biochar and then, impact its adsorption properties [64].

Similarly, biochars have proved to be suitable for the adsorption of light aromatic hydrocarbons and light polycyclic aromatic tars from syngas. Reported studies showed that biochars can achieve an adsorption performance of almost 87% for some tars compounds, and almost 95% if combined with other techniques [73, 74]. In relation to this, Hu et al [75], found that higher surface areas, smaller particle sizes and an important proportion of micropores, are related to better adsorption performances. Also, the average pore diameter influenced the tar adsorption capacity, depending on the type of model compound.

Catalyst precursor

The use of biochar from agrowastes as catalyst precursor or catalyst support has also been widely discussed in the literature, considering the physico-chemical properties of biochar and its relative low cost [40]. In catalysis applications, both the surface area and the functional groups are important criteria. In this regard, the proper choice of pyro-gasification conditions may allow the production of biochars with the required characteristics for catalytic applications.

In particular, several authors have reported the promising behavior of biochar as a catalyst for gasification syngas cleaning applications [76]. El-Rub et al. [77] compared biomass chars with other typical catalysts used for tar decomposition, concluding that char has a great potential to convert different tar compounds like phenol and naphthalene. For their part, Chen at al. [78] analyzed the catalytic performance of biochars from different agrowastes, varying the temperature, residence time and particle size. They concluded that the tar conversion rate was improved at higher temperatures and with smaller particle sizes. In contrast, no significant differences were observed between the materials analyzed. Tar conversion percentages up to 98% have been reported for some tar compounds using biochar from different feedstocks [79].

Recent applications of biochars as catalysts for biodiesel production have been also reported. Dehkhoda et al. [80] studied the esterification and transesterification of vegetable oils over sulfonated biochar, concluding that chars with high specific surface areas lead to high biodiesel production yields. The observed conversion percentages demonstrated the char potential as solid acid catalyst for biodiesel production.

Moreover, biochars have also been used as catalysis supports for different applications. In relation to syngas conditioning and tar removal, different authors have studied the performance of char supported Ni and Fe-based catalyst. Conversions up to 97% at 800°C have been reported for real syngas using wood and coal chars [81]. The carbon structure and porosity have also shown a significant role in the tar conversion process, improving the interactions between the syngas and the catalyst surface.

Activated carbon precursor

For some applications, the biochar pore structure and surface functionalities may not be sufficient to ensure their outstanding performance. In this case, biochar could be used as a renewable and low cost precursor for activated carbon production. According to the intended applications, activated carbons could be produced by physical or chemical activation, enhancing the material porous structure and including the desired functional groups in its surface.

For physical activation, steam or CO_2 are generally used as activating agents. Other gases like NH_3, O_2 or their mixtures may also be employed. Typical activation temperatures have been reported near between 800°C and 1000°C [82]. The physical activation process of biochars from agrowastes produces carbon porous materials with surface areas up to $1000\,m^2/g$ and a well developed microporous structure.

For its part, chemical activation uses different chemicals as activating agents. Reagents like HCl, HNO_3, KOH, K_2CO_3, H_3PO are generally used [41], resulting also in the production of highly porous materials, with high specific surface areas and functional

complexes [82]. Although chemical activation is less time and energy intensive, environmental concerns related to the use of chemicals should be considered.

Physical and chemical biochar-based activated carbons have found several applications for gases and liquids treatments. Different authors have analyzed the use of activated biochars for air pollution control and NO_x removal [70], water treatment and purification [83], gas storage [84, 85], capacitors [86] and medical applications [87, 88]. The applications are determined by the characteristics of the materials such as surface area, pore structure, pore volume and chemical composition.

Soil amendment

Recent studies have highlighted the beneficial effects of the use of pyro-gasification chars in soil amendment applications. In particular, biochars show high stability and an important ability to retain plant nutrients compared to several kind of soils [40].

Application of biochars to low-quality soils is mainly associated to an improvement in their soil cation exchange capacity (CEC), microbial activity and nutrient retention [68]. In fact, an increase in the cation exchange capacity of soils is related to the improvement of the soil ability to retain nutrients, most of them cations (e.g. K^+, Na^+, Ca^{2+}, and Mg^{2+}), and avoid their leachability [89]. Moreover, considering that chars from agrowastes usually have considerable amounts of minerals, these materials could be a source of nutrients to soils (e.g. K, Ca, Na, Mg, and P), increasing their availability and reducing the traditional fertilizers requirements [68]. The bio-availability of biochar nutrients to plants depends on two principal factors: the occurrence form and distribution of mineral species, and the morphological structure of chars [90].

Furthermore, mineral-rich biochars have also proved their capacity to immobilize heavy metals in soils, reducing their availability for plant uptake [64]. In the literature, several mechanisms have been proposed in relation to metal sorption by biochars. They include electrostatic interactions, cation exchange, metal complexation, and metal precipitation [91]. Different studies have shown that both carbon and mineral fractions of biochar contribute to heavy metals retention. More specifically, for biochars with low mineral content, the sorption of heavy metals is mainly associated to surface oxygen containing functional groups. In contrast, for mineral-rich biochars, interactions between heavy metals and the char mineral fraction are the dominant factor, and could be associated to up to 90% of the metal retention and removal [64].

In relation to organic pollutants, several authors have also underlined the capacity of pyro-gasification chars to reduce contaminant exposure in soils. Generally, soil pollutants can accumulate and produce negative effects on soil organisms and other living beings [92]. Recent studies have found that the reduction of bioaccessible polycyclic aromatic hydrocarbons (PAHs) in soils after the application of biochars varied from 27% to 80%, depending on the char precursor and quantity applied [93]. Similarly, Kotowski et al. [94] also validated the suitability of biochars and biochar-based activated carbons for the immobilization of freely dissolved and bioaccessible PAHs. Higher effectiveness were observed for materials with higher specific surface areas and pore volumes.

Moreover, in agricultural applications, the soil pH is an important parameter to consider. Acidic soils may present several problems to plant growth and crop yields, mainly related to aluminum (Al) and manganese (Mn) toxicity to plants, and an important deficiency of essential nutrients like phosphorous (P), potassium (K), calcium (Ca) and magnesium

(Mg) [95]. In this regard, considering that most biochars have a basic nature and a significant acid neutralization capacity, their application to acidic soils may result in an increase in the pH value and an improvement in the soil ability to resist acidification [65].

1.4 Conclusion

From the literature review, it was possible to conclude that pyro-gasification is a very interesting process for the valorization of agricultural and agroindustrial wastes. In particular, this process produces fuel gases that can be used for the generation of heat or power, and a solid by-product with interesting properties for several applications. Notably, steam gasification is of particular interest, as it produces high heating value fuel gases, and a carbon-rich highly porous material, with similar characteristics to activated carbons.

Despite the fact that different process parameters impact in an important way the gasification by-products yield and properties, biomass is possibly the most important one to consider when the valorization of lignocellulosic agrowastes is intended. In fact, considering that agroresidues come from a wide variety of sources and are often seasonal, gasification facilities should deal with a large range of materials with different characteristics and chemical compositions.

As highlighted with the literature review, the chemical composition of the feedstocks may influence their pyrolysis and gasification behavior, and the physico-chemical properties of the solid by-products. Hence, a better understanding of the impact of biomass characteristics on the steam gasification behavior and by-products is essential for process design, operation, and optimization using agrowastes. Moreover, it could be of particular interest to adapt the process parameters to each feedstock in order to obtain the required gas and char properties for the intended applications.

Nevertheless, even if previous studies have provided good insights regarding the impact of biomass composition on its pyrolysis and gasification behavior, further investigations are still required. Particularly, the yield and by-product properties obtained from the gasification of different feedstocks requires in-depth investigation and comparison, as well as the co-gasification of different biomasses.

In relation to the solid by-products, the valorization pathways may depend on their physico-chemical properties. In this regard, considering the important inorganic content of most lignocellulosic agrowastes, the analysis of char use in soil amendment applications may be an interesting alternative that requires further investigations.

Bibliography

[1] Prabir Basu. *Biomass Gasification and Pyrolysis. Practical Design.* First Edit. Oxford: Elsevier, 2010, p. 364 (cit. on pp. 10, 18).

[2] Vinay Sharma and Arindam Kuila. *Lignocellulosic biomass production and industrial applications*. Ed. by Vinay Sharma and Arindam Kuila. March. Wiley, 2017, p. 304 (cit. on p. 10).

[3] Pratima Bajpai. *Pretreatment of lignocellulosic biomass for biofuel production*. Vol. 34. 2016, p. 86 (cit. on p. 11).

[4] Palmiro Poltronieri and Oscar Fernando D'Urso. *Biotransformation of Agricultural Waste and By-Products: The Food, Feed, Fibre, Fuel (4F) Economy*. 2016, pp. 1–357 (cit. on p. 11).

[5] Kifayat Ullah, Vinod Kumar Sharma, Sunil Dhingra, Giacobbe Braccio, Mushtaq Ahmad, and Sofia Sofia. "Assessing the lignocellulosic biomass resources potential in developing countries: A critical review." In: *Renewable & Sustainable Energy Reviews* 51 (2015), pp. 682–698 (cit. on p. 11).

[6] Wenjuan Niu, Lujia Han, Xian Liu, Guangqun Huang, Longjian Chen, Weihua Xiao, and Zengling Yang. "Twenty-two compositional characterizations and theoretical energy potentials of extensively diversified China's crop residues." In: *Energy* 100 (2016), pp. 238–250 (cit. on p. 11).

[7] Vaibhav Dhyani and Thallada Bhaskar. "A comprehensive review on the pyrolysis of lignocellulosic biomass." In: *Renewable and Sustainable Energy Reviews* 129 (2018), pp. 695–716 (cit. on p. 11).

[8] Prabir Basu. "Gasification Theory." In: *Biomass Gasification, Pyrolysis and Torrefaction*. Elsevier Inc., 2013. Chap. Chapter 7, pp. 199–248 (cit. on pp. 12, 14, 18).

[9] A.A.P. Susastriawan, Harwin Saptoadi, and Purnomo. "Small-scale downdraft gasifiers for biomass gasification: A review." In: *Renewable and Sustainable Energy Reviews* 76 (Sept. 2017), pp. 989–1003 (cit. on p. 12).

[10] Yohan Richardson, Martin Drobek, Anne Julbe, Joël Blin, and François Pinta. *Recent Advances in Thermo-Chemical Conversion of Biomass*. Elsevier, 2015, pp. 213–250 (cit. on pp. 12, 14, 15, 20).

[11] Prabir Basu. "Pyrolysis." In: *Biomass Gasification, Pyrolysis and Torrefaction*. Second Edi. London: Elsevier Inc., 2013. Chap. Chapter 5, pp. 147–176 (cit. on p. 13).

[12] Tanmya Rout, Debalaxmi Pradhan, R.K. Singh, and Namrata Kumari. "Exhaustive study of products obtained from coconut shell pyrolysis." In: *Journal of Environmental Chemical Engineering* (Feb. 2016) (cit. on p. 13).

[13] Kiky C. Sembiring, Nino Rinaldi, and Sabar P. Simanungkalit. "Bio-oil from Fast Pyrolysis of Empty Fruit Bunch at Various Temperature." In: *Energy Procedia* 65 (2015), pp. 162–169 (cit. on p. 13).

[14] Haiping Yang, Rong Yan, Hanping Chen, Dong Ho Lee, and Chuguang Zheng. "Characteristics of hemicellulose, cellulose and lignin pyrolysis." In: *Fuel* 86.12-13 (Aug. 2007), pp. 1781–1788 (cit. on p. 13).

[15] Qian Liu, Zhaoping Zhong, Shurong Wang, and Zhongyang Luo. "Interactions of biomass components during pyrolysis: A TG-FTIR study." In: *Journal of Analytical and Applied Pyrolysis* 90.2 (2011), pp. 213–218 (cit. on p. 13).

[16] Venugopal Mendu, Anne E Harman-Ware, Mark Crocker, Jungho Jae, Jozsef Stork, Samuel Morton, Andrew Placido, George Huber, and Seth Debolt. "Identification and thermochemical analysis of high-lignin feedstocks for biofuel and biochemical production." In: *Biotechnology for biofuels* 4 (2011), pp. 1–13 (cit. on p. 13).

[17] Chistopher Higman and Maarten Van der Burgt. *Gasification*. Ed. by Elsevier. Second Edi. 2008, p. 452 (cit. on pp. 13, 17).

[18] J. a. Ruiz, M. C. Juárez, M. P. Morales, P. Muñoz, and M. a. Mendívil. "Biomass gasification for electricity generation: Review of current technology barriers." In: *Renewable and Sustainable Energy Reviews* 18 (2013), pp. 174–183 (cit. on pp. 14, 16).

[19] Manuel Campoy, Alberto Gómez-Barea, Fernando B Vidal, and Pedro Ollero. "Air-steam gasification of biomass in a fluidised bed: Process optimisation by enriched air." In: *Fuel Processing Technology* 90 (2008), pp. 677–685 (cit. on p. 14).
[20] V Belgiorno, G De Feo, Della Rocca, and R M A Napoli. "Energy from gasification of solid wastes." In: *Waste Management* 23 (2003), pp. 1–15 (cit. on p. 14).
[21] Gong Cheng, Qian Li, Fangjie Qi, Bo Xiao, Shiming Liu, Zhiquan Hu, and Piwen He. "Allothermal gasification of biomass using micron size biomass as external heat source." In: *Bioresource Technology* 107 (2012), pp. 471–475 (cit. on p. 14).
[22] Feng Yan, Si-Yi Luo, Zhi-Quan Hu, Bo Xiao, and Gong Cheng. "Hydrogen-rich gas production by steam gasification of char from biomass fast pyrolysis in a fixed-bed reactor: Influence of temperature and steam on hydrogen yield and syngas composition." In: *Bioresource Technology* 101 (2010), pp. 5633–5637 (cit. on p. 14).
[23] Elango Balu, Uisung Lee, and J.N. Chung. "High temperature steam gasification of woody biomass – A combined experimental and mathematical modeling approach." In: *International Journal of Hydrogen Energy* 40.41 (2015), pp. 14104–14115 (cit. on p. 14).
[24] Colomba Di Blasi. "Combustion and gasification rates of lignocellulosic chars." In: *Progress in Energy and Combustion Science* 35.2 (2009), pp. 121–140 (cit. on pp. 14–16, 19).
[25] Capucine Dupont, Sylvain Jacob, Khalil Ould Marrakchy, Céline Hognon, Françoise Labalette, Maguelone Grateau, and Denilson Da Silva Perez. "How inorganic elements of biomass influence char steam gasification kinetics." In: *Energy* 109 (2016), pp. 430–435 (cit. on p. 14).
[26] Douglas W. McKee. "Mechanisms of the alkali metal catalysed gasification of carbon." In: *Fuel* 62.2 (Feb. 1983), pp. 170–175 (cit. on p. 15).
[27] D W Mckee. "Gasification of graphite in CO2 and water vapor- the catalytic effect of metal salts." In: *Carbon* 20.I (1982), pp. 59–66 (cit. on p. 15).
[28] Ange Nzihou, Brian Stanmore, and Patrick Sharrock. "A review of catalysts for the gasification of biomass char, with some reference to coal." In: *Energy* 58 (Sept. 2013), pp. 305–317 (cit. on pp. 15, 16).
[29] Kentaro Umeki, Antero Moilanen, Alberto Gómez-Barea, and Jukka Konttinen. "A model of biomass char gasification describing the change in catalytic activity of ash." In: *Chemical Engineering & Technology* 207-208 (2012), pp. 616–624 (cit. on p. 16).
[30] Samsudin Anis and Z. a. Zainal. "Tar reduction in biomass producer gas via mechanical, catalytic and thermal methods: A review." In: *Renewable and Sustainable Energy Reviews* 15 (2011), pp. 2355–2377 (cit. on p. 16).
[31] Heidi C. Butterman and Marco J. Castaldi. "CO2 as a Carbon Neutral Fuel Source via Enhanced Biomass Gasification." In: *Environmental Science & Technology* 43.23 (2009), pp. 9030–9037 (cit. on pp. 16, 17).
[32] Maria Puig-Arnavat, Joan Carles Bruno, and Alberto Coronas. "Review and analysis of biomass gasification models." In: *Renewable & Sustainable Energy Reviews* 14 (2010), pp. 2841–2851 (cit. on p. 16).
[33] Ningbo Gao, Aimin Li, and Cui Quan. "A novel reforming method for hydrogen production from biomass steam gasification." In: *Bioresource Technology* 100 (2009), pp. 4271–4277 (cit. on p. 16).

[34] Xueping Song and Zhancheng Guo. "Technologies for direct production of flexible H2/CO synthesis gas." In: *Energy Conversion and Management* 47.5 (2006), pp. 560–569 (cit. on p. 17).

[35] T.A Milne, E.J Evans, and N Abatzoglou. *Biomass Gasifier Tars: Their Nature, Formation, and Conversion*. Tech. rep. Golden, Colorado: NREL, 1998, p. 203 (cit. on p. 17).

[36] Prabir Basu. "Tar Production and Destruction." In: *Biomass Gasification, Pyrolysis and Torrefaction*. Elsevier, 2013. Chap. Chapter 6, pp. 177–198 (cit. on p. 17).

[37] P. Hasler and Th. Nussbaumer. "Gas cleaning for IC engine applications from fixed bed biomass gasification." In: *Biomass and Bioenergy* 16.6 (June 1999), pp. 385–395 (cit. on p. 17).

[38] Lopamudra Devi, Krzysztof J. Ptasinski, and Frans J J G Janssen. "A review of the primary measures for tar elimination in biomass gasification processes." In: *Biomass and Bioenergy* 24 (2002), pp. 125–140 (cit. on p. 17).

[39] D Dias, N Lapa, M Bernardo, D Godinho, I Fonseca, M Miranda, F Pinto, and F Lemos. "Properties of chars from the gasification and pyrolysis of rice waste streams towards their valorisation as adsorbent materials." In: *Waste Management* 65 (2017), pp. 186–194 (cit. on p. 17).

[40] Sonil Nanda, Ajay K. Dalai, Franco Berruti, and Janusz A. Kozinski. "Biochar as an Exceptional Bioresource for Energy, Agronomy, Carbon Sequestration, Activated Carbon and Specialty Materials." In: *Waste and Biomass Valorization* 7.2 (Apr. 2016), pp. 201–235 (cit. on pp. 17, 19–22, 26, 27).

[41] Kezhen Qian, Ajay Kumar, Hailin Zhang, Danielle Bellmer, and Raymond Huhnke. "Recent advances in utilization of biochar." In: *Renewable and Sustainable Energy Reviews* 42 (Feb. 2015), pp. 1055–1064 (cit. on pp. 17, 20, 26).

[42] Prabir Basu. *Combustion and gasification in fluidized beds*. Ed. by Taylor & Francis Group. CRC Press. 2006, p. 467 (cit. on pp. 18, 19).

[43] A V Bridgwater, D Meier, and D Radlein. "An overview of fast pyrolysis of biomass." In: *Organic Geochemistry* 30 (1999), pp. 1479–1493 (cit. on p. 19).

[44] E Cetin, B Moghtaderi, R Gupta, and T F Wall. "Influence of pyrolysis conditions on the structure and gasification reactivity of biomass chars." In: *Fuel* 83 (2004), pp. 2139–2150 (cit. on p. 20).

[45] S Septien, F J Escudero Sanz, S Salvador, and S Valin. "The effect of pyrolysis heating rate on the steam gasification reactivity of char from woodchips." In: *Energy* 142 (2018), pp. 68–78 (cit. on p. 20).

[46] Kathrin Weber and Peter Quicker. "Properties of biochar." In: *Fuel* 217 (2018), pp. 240–261 (cit. on pp. 21, 24).

[47] Roop Chand Bansal and Meenakshi Goyal. *Activated Carbon Adsorption*. CRC Press, May 24, 2005 (cit. on pp. 21, 22).

[48] Vittoria Benedetti, Francesco Patuzzi, and Marco Baratieri. "Gasification Char as a Potential Substitute of Activated Carbon in Adsorption Applications." In: *Energy Procedia* 105 (2017), pp. 712–717 (cit. on p. 21).

[49] Veronika Hansen, Dorette Müller-Stöver, Jesper Ahrenfeldt, Jens Kai Holm, Ulrik Birk Henriksen, and Henrik Hauggaard-Nielsen. "Gasification biochar as a valuable by-product for carbon sequestration and soil amendment." In: *Biomass and Bioenergy* 72.1 (2015), pp. 300–308 (cit. on pp. 21–23).

[50] Naomi Klinghoffer, Marco J. Castaldi, and Ange Nzihou. "Beneficial use of ash and char from biomass gasification." In: *19th Annual North American Waste-to-Energy Conference, NAWTEC19*. Lancaster, Pennsylvania, 2011, pp. 13–17 (cit. on p. 21).

[51] Naomi Klinghoffer, Marco J. Castaldi, and Ange Nzihou. "Catalyst Properties and Catalytic Performance of Char from Biomass Gasification." In: *I&EC* (2012), pp. 13113–13122 (cit. on p. 21).

[52] C. Guizani, F.J. Escudero Sanz, M. Jeguirim, R. Gadiou, and S. Salvador. "The effects of textural modifications on beech wood-char gasification rate under alternate atmospheres of CO2 and H2O." In: *Fuel Processing Technology* 138 (2015), pp. 687–694 (cit. on p. 21).

[53] J Gaunt and A Cowie. *Biochar*. 2013, pp. 317–336. arXiv: arXiv:1011.1669v3 (cit. on p. 22).

[54] Ling Zhao, Xinde Cao, Wei Zheng, Qun Wang, and Fan Yang. "Endogenous minerals have influences on surface electrochemistry and ion exchange properties of biochar." In: *Chemosphere* 136 (2015), pp. 133–139 (cit. on p. 22).

[55] Siim Link, Patrik Yrjas, and Leena Hupa. "Ash melting behaviour of wheat straw blends with wood and reed." In: *Renewable Energy* 124 (2018), pp. 11–20 (cit. on p. 22).

[56] Wu-Jun Liu, Fan-Xin Zeng, Hong Jiang, and Xue-Song Zhang. "Preparation of high adsorption capacity bio-chars from waste biomass." In: *Bioresource technology* 102.17 (Sept. 2011), pp. 8247–52 (cit. on p. 22).

[57] J F Kwiatkowski. *Activated Carbon: Classifications, Properties and Applications*. 2011 (cit. on pp. 22–24).

[58] Roberto Conti, Alessandro G Rombolà, Alberto Modelli, Cristian Torri, and Daniele Fabbri. "Evaluation of the thermal and environmental stability of switchgrass biochars by Py-GC-MS." In: *Journal of Analytical and Applied Pyrolysis* 110 (2014), pp. 239–247 (cit. on p. 23).

[59] Lokesh P Padhye. "Influence of surface chemistry of carbon materials on their interactions with inorganic nitrogen contaminants in soil and water." In: *Chemosphere* 184 (2017), pp. 532–547 (cit. on p. 23).

[60] J L Figueiredo, M F R Pereira, M M A Freitas, and J J M Orfá. "Modification of the surface chemistry of activated carbon." In: *Carbon* 37 (1999), pp. 1379–1389 (cit. on p. 23).

[61] Jakub Ederer, Pavel Janoš, Petra Ecorchard, Václav Štengl, Zuzana Bělčická, Martin Šťastný, Ognen Pop-Georgievski, and Vlastimil Dohnal. "Quantitative determination of acidic groups in functionalized graphene by direct titration." In: *Reactive and Functional Polymers* 103 (June 2016), pp. 44–53 (cit. on p. 23).

[62] Larissa A. Alves, Arthur H. De Castro, Fernanda G. De Mendonça, and João P. De Mesquita. "Characterization of acid functional groups of carbon dots by nonlinear regression data fitting of potentiometric titration curves." In: *Applied Surface Science* 370 (2016), pp. 486–495 (cit. on p. 23).

[63] M. A. Montes-Morán, D. Suárez, J. A. Menéndez, and E. Fuente. "On the nature of basic sites on carbon surfaces: An overview." In: *Carbon* 42.7 (2004), pp. 1219–1224 (cit. on p. 23).

[64] Xiaoyun Xu, Yinghao Zhao, Jingke Sima, Ling Zhao, Ondřej Mašek, and Xinde Cao. "Indispensable role of biochar-inherent mineral constituents in its environmental applications: A review." In: *Bioresource Technology* 241 (Oct. 2017), pp. 887–899 (cit. on pp. 24, 25, 27).

[65] Ren-yong Shi, Zhi-neng Hong, Jiu-yu Li, Jun Jiang, M Abdulaha-Al Baquy, Renkou Xu, and Wei Qian. "Mechanisms for Increasing the pH Buffering Capacity of an Acidic Ultisol by Crop Residue-Derived Biochars." In: *Journal of Agricultural and Food Chemistry* 65 (2017), pp. 8111–8119 (cit. on pp. 24, 28).

[66] K Y Chan, A Downie, : S Joseph, and A Cowie. "Effects of biochar from slow pyrolysis of papermill waste on agronomic performance and soil fertility." In: *Plant Soil* 327 (2010), pp. 235–246 (cit. on p. 24).

[67] C. Banik, M. Lawrinenko, S. Bakshi, and D.A. Laird. "Impact of pyrolysis temperature and feedstock on surface charge and functional group chemistry of biochars." In: *Journal of Environmental Quality* 47.3 (2018), pp. 452–461 (cit. on p. 24).

[68] James W. Lee, Michelle Kidder, A. C. Buchanan, Charles T Garte, and Robert Brown. "Characterization of Biochars Produced from Cornstovers for Soil Amendment." In: *Environ. Sci. Technol.* 44 (2010), pp. 7970–7974 (cit. on pp. 24, 27).

[69] Xiaofei Tan, Yunguo Liu, Guangming Zeng, Xin Wang, Xinjiang Hu, Yanling Gu, and Zhongzhu Yang. "Application of biochar for the removal of pollutants from aqueous solutions." In: *Chemosphere* 125 (2015), pp. 70–85 (cit. on p. 25).

[70] A A Abdulrasheed, A A Jalil, S Triwahyono, M A A Zaini, Y Gambo, M Ibrahim, and Johor Bahru. "Surface modification of activated carbon for adsorption of SO 2 and NO X : A review of existing and emerging technologies." In: *Renewable & Sustainable Energy Reviews* 94 (2018), pp. 1067–1085 (cit. on pp. 25, 27).

[71] Yafei Shen. "Chars as carbonaceous adsorbents / catalysts for tar elimination during biomass pyrolysis or gasi fi cation." In: 43 (2015), pp. 281–295 (cit. on p. 25).

[72] Ren-Kou Xu, Shuang-Cheng Xiao, Jin-Hua Yuan, and An-Zhen Zhao. "Adsorption of methyl violet from aqueous solutions by the biochars derived from crop residues." In: *Bioresource Technology* 102 (2011), pp. 10293–10298 (cit. on p. 25).

[73] Anchan Paethanom, Shota Nakahara, Masataka Kobayashi, Pandji Prawisudha, and Kunio Yoshikawa. "Performance of tar removal by absorption and adsorption for biomass gasification." In: *Fuel Processing Technology* 104 (2012), pp. 144–154 (cit. on p. 25).

[74] Anchan Paethanom and Kunio Yoshikawa. "Influence of Pyrolysis Temperature on Rice Husk Char Characteristics and Its Tar Adsorption Capability." In: *Energies* 5.12 (2012), pp. 4941–4951 (cit. on p. 25).

[75] Xiulan Hu, Toshiaki Hanaoka, Kinya Sakanishi, Takuya Shinagawa, Satoshi Matsui, Mitsushiro Tada, and Toshihiko Iwasaki. "Removal of Tar Model Compounds Produced from Biomass Gasification Using Activated Carbons." In: *Journal of the Japan Institute of Energy* 86 (2007), pp. 707–7011 (cit. on p. 25).

[76] Thana Phuphuakrat, Tomoaki Namioka, and Kunio Yoshikawa. "Tar removal from biomass pyrolysis gas in two-step function of decomposition and adsorption." In: *Applied Energy* 87.7 (July 2010), pp. 2203–2211 (cit. on p. 26).

[77] Z. Abu El-Rub, E.A. Bramer, and G. Brem. "Experimental comparison of biomass chars with other catalysts for tar reduction." In: *Fuel* 87.10-11 (Aug. 2008), pp. 2243–2252 (cit. on p. 26).

[78] Yi Chen, Young-hao Luo, Yi Su, and Wen-guang Wu. "Experimental Investigation on Tar Formation and Destruction in a Lab-Scale Two-Stage Reactor." In: *Energy & Fuels* 23 (2009), pp. 4659–4667 (cit. on p. 26).

[79] Lina Maria Romero Millan and Fabio Emiro Sierra Vargas. "Artículo de revisión Materiales carbonosos para el acondicionamiento de gas de síntesis y remoción

de alquitranes Carbon materials for syngas conditioning and tar removal Este documento posee una licencia Creative Commons Reconocimiento-No Comercial 4.0 I." In: *Ingeniería Mecánica* 20.2 (2017), pp. 99–107 (cit. on p. 26).

[80] Amir Mehdi Dehkhoda, Alex H. West, and Naoko Ellis. "Biochar based solid acid catalyst for biodiesel production." In: *Applied Catalysis A: General* 382.2 (July 2010), pp. 197–204 (cit. on p. 26).

[81] Yafei Shen, Peitao Zhao, Qinfu Shao, Dachao Ma, Fumitake Takahashi, and Kunio Yoshikawa. "In-situ catalytic conversion of tar using rice husk char-supported nickel-iron catalysts for biomass pyrolysis/gasification." In: *Applied Catalysis B: Environmental* 152-153 (June 2014), pp. 140–151 (cit. on p. 26).

[82] Xiao-fei Tan, Shao-bo Liu, Yun-guo Liu, Yan-ling Gu, Guang-ming Zeng, Xin-jiang Hu, Xin Wang, Shao-heng Liu, and Lu-hua Jiang. "Biochar as potential sustainable precursors for activated carbon production: Multiple applications in environmental protection and energy storage." In: *Bioresource Technology* 227 (2017), pp. 359–372 (cit. on pp. 26, 27).

[83] E Menya, P W Olupot, H Storz, M Lubwama, and Y Kiros. "Production and performance of activated carbon from rice husks for removal of natural organic matter from water: A review." In: *Chemical Engineering Research and Design* 1.2 (2018), pp. 271–296 (cit. on p. 27).

[84] Hazimah Madzaki, Wan Azlina, and Wan Ab Karimghani. "ScienceDirect Carbon Dioxide Adsorption on Sawdust Biochar." In: *Procedia Engineering* 148 (2016), pp. 718–725 (cit. on p. 27).

[85] T Ramesh, N Rajalakshmi, and K S Dhathathreyan. "Activated carbons derived from tamarind seeds for hydrogen storage." In: *Journal of Energy Storage* 4 (2015), pp. 89–95 (cit. on p. 27).

[86] Yupeng Guo, Jurui Qi, Yanqiu Jiang, Shaofeng Yang, Zichen Wang, and Hongding Xu. "Performance of electrical double layer capacitors with porous carbons derived from rice husk." In: *Materials Chemistry and Physics* 80 (2003), pp. 704–709 (cit. on p. 27).

[87] Sinan Cem Uzunget, Togay Evrin, Baglan Uzunget, Kemal Ertürk, Egemen Akıncıoğlu, Saffet Özdemir, and Atila Korkmaz. "Evaluation of activated charcoal and lipid emulsion treatment in model of acute rivaroxaban toxicity." In: *American Journal of Emergency Medicine* 36 (2017), pp. 1346–1349 (cit. on p. 27).

[88] Nozha Brahmi, Nadia Kouraichi, Hafedh Thabet, and Mouldi Amamou. "Influence of activated charcoal on the pharmacokinetics and the clinical features of carbamazepine poisoning." In: *The American Journal of Emergency Medicine* 24 (2006), pp. 440–443 (cit. on p. 27).

[89] Donald L Sparks. *Environmental soil chemistry*. Second edi. Elsevier Science & Technology Books, 2003, p. 367 (cit. on p. 27).

[90] Zhaoying Kong, Sui Boon Liaw, Xiangpeng Gao, Yun Yu, and Hongwei Wu. "Leaching characteristics of inherent inorganic nutrients in biochars from the slow and fast pyrolysis of mallee biomass." In: *Fuel* 128 (July 2014), pp. 433–441 (cit. on p. 27).

[91] Hongbo Li, Xiaoling Dong, Evandro B Da Silva, Letuzia M De Oliveira, Yanshan Chen, and Lena Q Ma. "Mechanisms of metal sorption by biochars: Biochar characteristics and modifications." In: *Chemosphere* 178 (2017), pp. 466–478 (cit. on p. 27).

[92] B J Reid, K C Jones, and K T Semple. "Bioavailability of persistent organic pollutants in soils and sediments: a perspective on mechanisms, consequences and assessment." In: *Environmental Pollution* 108 (2000), pp. 103–112 (cit. on p. 27).

[93] Sardar Khan, Muhammad Waqas, Fenghua Ding, Isha Shamshad, Hans Peter, H Arp, and Gang Li. "The influence of various biochars on the bioaccessibility and bioaccumulation of PAHs and potentially toxic elements to turnips (Brassica rapa L.)" In: *Journal of Hazardous Materials* 300 (2015), pp. 243–253 (cit. on p. 27).

[94] Michał Kołtowski, Isabel Hilber, Thomas D. Bucheli, Barbara Charmas, Jadwiga Skubiszewska-Zięba, and Patryk Oleszczuk. "Activated Biochars Reduce the Exposure of Polycyclic Aromatic Hydrocarbons in Industrially Contaminated Soils." In: *Chemical Engineering Journal* 310 (Feb. 15, 2017), pp. 33–40 (cit. on p. 27).

[95] Somchai Butnan, Jonathan L Deenik, Banyong Toomsan, Michael J Antal, and Patma Vityakon. "Biochar characteristics and application rates affecting corn growth and properties of soils contrasting in texture and mineralogy." In: *Geoderma* 237-238 (2015), pp. 105–116 (cit. on p. 28).

Chapter

2

Materials and experimental methods

2.1 Introduction

This chapter aims to describe the materials used in the present study and the experimental procedures employed. Considering that the main objective of this research work is to understand the impact of the biomass characteristics on the steam gasification process and by-products, the section 2.2 presents the selection criteria of the lignocellulosic residues to be analyzed, and their main physico-chemical characteristics. For its part, in the framework of the international cooperation between Colombia and France, the section 2.3 describes the evaluation of two different experimental devices considered for the gasification experiments, and the selection criteria of the most appropriate setup to achieve the objectives of the present work.

Section 2.4 is dedicated to the description of the experimental methods used to analyze the thermal decomposition behavior and kinetics of the selected biomasses, under inert atmosphere, and under steam as gasifying agent. Finally, section 2.5 presents

the experimental procedure followed for the steam gasification tests of the selected feedstocks, and the sampling of the gasification by-products. Also, the experimental methodology used to evaluate the physico-chemical properties of the raw biomass and the produced char is summarized.

2.2 Selection of gasification feedstocks

In order to understand the influence of the biomass characteristics in the gasification process and the properties of its gaseous and solid by-products, three lignocellulosic agrowastes with different physico-chemical characteristics were selected for this study, among several residual biomasses from Colombian agricultural and agroindustrial activities.

From the literature review, the organic and inorganic composition of different lignocellulosic agrowastes were analyzed and compared, in order to determine the most suitable feedstocks for the present study. The characteristics of some of the most representative Colombian crop residues compared are presented in tables 2.1 and 2.2.

Table 2.1: Organic composition of some representative crop residues reported in the literature [1–6]

	Rice husk	**Corncob**	**Sugarcane bagasse**	**Coconut shells**	**Oil palm shells**	**Bamboo guadua**
Elemental composition (wt. % dry basis)						
C	36.9	43.6	47.1	50.2	49.6	47
H	5.0	5.8	6.1	5.7	6.02	5.6
O	37.9	48.6	0.5	43.4	41.9	43
N	0.4	0.7	42.5	0.0	0.4	0.3
S	0.0	0.0	1.0	0.0	0.1	0.1
Ash	20.5	1.2	2.6	1.1	1.8	5.7
High heating value (MJ/Kg dry basis)						
HHV	15.3	16.9	14.7	20.5	20.1	18.8
Molecular composition (wt. % dry basis)						
Cellulose	31.3	42.5	41.3	32.5	30.4	53.9
Hemicellulose	24.3	31.5	22.6	20.5	12.7	13.5
Lignin	14.3	15.5	18.3	36.5	49.8	25.1

In accordance, from the analyzed feedstocks, coconut shells (CS), bamboo guadua (BG), and oil palm shells (OPS) were chosen, taking into account their organic and inorganic composition and their high heating value. Moreover, the great availability of these residues in Colombia and several other developing countries was also considered.

Regarding the composition of the selected samples, the reported elemental analysis shows very similar results for the three feedstocks. In contrast, the comparison of their macromolecular and inorganic composition reveals some remarkable differences.

In relation to the macromolecular composition, it can be noted that coconut shells (CS) and oil palm shells (OPS), as endocarp residues, have high lignin contents in comparison to bamboo guadua (BG), considered as a grass. In particular, OPS exhibit

the highest lignin content with nearly 50%, followed by CS and BG, with 36.5% and 25% respectively. For its part, BG shows the highest cellulose percentage with a value of 54%.

Table 2.2: Major inorganic composition of some representative crop residues reported in the literature [1–5, 7, 8]

	Inorganic composition (mg/kg biomass)					
Major elements	**Rice husk**	**Corncob**	**Sugarcane bagasse**	**Coconut shells**	**Oil palm shells**	**Bamboo guadua**
Al	-	162.1	-	73.0	31.6	10.0
Ca	416.9	249.3	1518.0	1501.0	173.7	252.0
K	2107.2	5408.4	2682.0	1965.0	1477.7	9902.0
Mg	374.88	404.7	6261.0	389.0	262.9	218.0
Mn	25.11	9.9	9.0	1.1	15.8	2.0
Na	30.6	29.3	93.0	1243.0	10.7	3.0
P	78.3	-	284.0	94.0	115.4	482.0
Si	51323.3	-	17340.0	256.0	5510.0	12731.0

- Not reported

Moreover, it can be observed that bamboo guadua (BG) has a higher ash percentage in comparison to coconut shells (CS) and oil palm shells (OPS), indicating an important amount of mineral content in this biomass. From table 2.2 it can be noted that CS contain mainly K, Ca and Na, while OPS and BG are principally composed of Si, P, and also K.

As already stated, the inorganic elements present in the biomass are reported as an influential parameter in the steam gasification reactivity [9]. In particular, alkali and alkaline earth metals (AAEM) like K, Ca, Na and Mg, could have a catalytic impact on biomass gasification [10]. In contrast, elements like Si, P and Al may react with AAEM and inhibit their beneficial effect [11]. In this regard, two of the selected samples are Si rich, while the other one contains mainly AAEM. More specifically, among the high lignin content samples, coconut shells (CS) exhibit an important amount of AAEM, contrary to oil palm shells (OPS). For its part, bamboo guadua (BG) shows the highest AAEM content of the three samples, but also an important amount of Si and P.

In consequence, as the selected feedstocks show interesting differences in their macromolecular and inorganic content, the comparison of their gasification behavior will contribute to the understanding of the influence of the biomass characteristics on the gasification process of lignocellulosic agrowastes, and the properties of their gaseous and solid by-products.

According to the Colombian context, a brief description of the selected samples (figure 2.1) is presented below:

Coconut shells (CS):

Cocos nucifera palms are grown in tropical countries, as they require a warm climate and high humidity for successful development. Generally, coconut palm is considered a very versatile plantation, as almost every part of the plant can be used for different applications. Nevertheless, in Colombia, coconut shells are considered a material with

little or non-economic value and have been traditionally used for handicraft making or discharged in soils. The amount of this residue is not negligible in the country, considering that about 18.400 hectares of land are being used for coconut palm plantations, with a production near 116.000 tons, according to the Colombian Ministry of Agriculture and the Food and Agriculture Organization of the united Nations [12].

Bamboo guadua (BG):

Bamboo guadua (*Guadua Angustifolia Kunth*) is a woody bamboo species native from Central and South America, considered as the largest bamboo in America and the third largest in the world [6]. In Colombia, Bamboo guadua grows in the Andean region, between 500 and 1500 meters above the sea level, and ambient temperature between 17°C and 26°C [13, 14].

This biomass is a sustainable natural resource that has been used by native and rural communities as construction material or firewood. Taking into account its high growing rate, Bamboo Guadua could represent an interesting material for energy purposes in Colombian rural areas. However, energetic applications of this biomass have not been studied in detail. Reported studies related with bamboo as energy source have been mainly performed with other bamboo species [15–17].

Oil palm shells (OPS):

Palm kernel shells are the shell fractions left after the crushing of the kernel nut in the oil palm extraction process from the *Eleais Guineensis* palm. Taking into account that Colombia has become the largest palm oil producer in Latin America and the fourth largest producer in the world after Indonesia, Malaysia and Thailand [18], the amount of residual wastes produced is not negligible. In Colombia, there are about 475.000 hectares planted with oil palms, with a production of near one million tons of crude palm oil per year (1.85% of the world production).

Accordingly, near 220.000 tons of palm kernel shells are generated as a residue in the country [19]. Due to the huge quantities of residual biomass generated, one of the biggest problems of oil production industry is the management of wastes, which can be extremely harmful if discharged on the land, as they can degrade and pollute soil, water sources, and air. In Colombia, raw palm kernel shells are usually burnt in boilers for steam production, or disposed as a cover for plantation roads; without giving any value to this residue [20].

Figure 2.1: Selected gasification feedstocks. a) Coconut shells, b) Bamboo guadua, c) Oil palm shells

2.3 Evaluation of the gasification experimental setup

To analyze the gasification behavior of the selected samples, and the properties of their gaseous and solid by-products, two different experimental reactors were considered in a first stage to perform the gasification tests:

- An autothermal pilot-scale downdraft reactor at the Colombian National University (Universidad Nacional de Colombia).
- A lab-scale fluidized bed reactor at RAPSODEE research center (IMT Mines-Albi).

Both experimental devices are equipped with the required control and monitoring systems to analyze the gasification process. However, considering that the reactor technologies and scales are different, the most appropriate experimental setup should be selected. For this purpose, preliminary tests were performed with both reactors using the three selected feedstocks.

A brief description of both experimental devices is presented below, as well as the advantages and disadvantages identified for each one:

2.3.1 Autothermal pilot scale downdraft reactor

With a height of 2.28 m and an external diameter of 0.34 m, the fixed bed downdraft gasifier is constructed in steel with an internal refractory lining acting as thermal insulation. Ten K-type thermocouples along the gasifier wall allow the monitoring of the temperature profile inside the reactor. All the setup is supported by three load cells for weight measurement, indicating the biomass consumption during the process. The temperature and mass change readings are collected using a National Instruments data acquisition system.

According to the design of the gasifier, the produced gas outlet is at the bottom of the reactor. A gas conditioning unit is provided downstream to clean the syngas, including a wet cyclone and two fiber filters that remove tars and particulate matter. A flare point on the outlet piping is used to burn gases before being released into the atmosphere and also to check their combustibility. An infrared Cubic Gasboard 3100P gas analyzer is used to determine the content of CO, CO_2, H_2, CH_4 and C_nH_m in the gas. The fixed bed downdraft gasifier setup and the characteristic temperature profile inside the reactor during a gasification test is presented in figure 2.2.

It was possible to observe that unlike the pyrolysis and combustion zone, the temperature in the reduction area, is relatively constant during all the gasification experiment. From the preliminary experimental tests, the advantages and disadvantages identified for this experimental device are listed below:

Advantages

- Pilot scale reactor: experimental conditions close to those of a real gasification application.
- Autothermal reactor: No electrical input is required to reach the gasification temperature and operate the reactor.

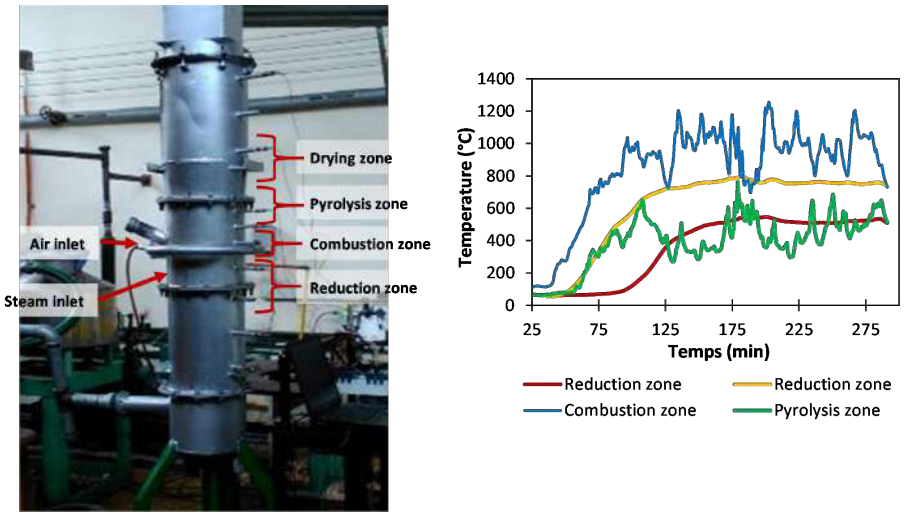

Figure 2.2: Fixed bed downdraft reactor experimental setup and characteristic temperature profile during a gasification test.

- Temperature monitoring: The reactor setup allows the complete monitoring of the temperature profile along the reactor height, and consequently, the distinction of the different reaction zones.

Disadvantages

- Reactor capacity: Significant amounts of biomass are required for each experimental test (>15 kg).
- Control of gasification parameters: Gasification parameters like temperature and heating rate cannot be directly controlled and depend mainly on the equivalence ratio (ER) of the process.
- Gasification agent: The steam gasification atmosphere cannot be accurately controlled, even with a steam feeding point in the gasification zone.
- Char recovery: The complete reactor disassembly is required for the recovery of char. Additionally, as the reactor zones are not well differentiated in this kind of reactor, heterogeneous chars from different zones may be recovered.

2.3.2 Laboratory scale fluidized bed reactor

The fluidized bed reactor with a height of 60 cm and the internal diameter 6 cm, is made of stainless steel and is externally heated with an electrical furnance composed of two radiative covers. A porous disk in the bottom holds the biomass sample and allows the gasification atmosphere to pass through. 10 K-type thermocouples along the gasifier height allow the monitoring of the temperature profile inside the reactor. The thermal regulation is ensured by an Eurotherm controller connected to a thermocouple in the center of the reactor. The reacting agent and fluidizing inert gas are regulated by calibrated flow mass controllers.

At the exit of the gasifier, a gas conditioning unit including 7 impinger bottles with isopropanol allows the condensation of tars and water. For its part, the volume of

produced permanent gases is determined with a gas meter, before being released to the atmosphere. Tedlar®. bags are used for gas sampling in order to analyze their composition (CO, CO_2, H_2, CH_4 and C_nH_m). For this purpose, a micro-GC (MyGC Agilent) is used.

The fluidized bed experimental setup is presented in figure 2.3, as well as the temperature profile inside the reactor.

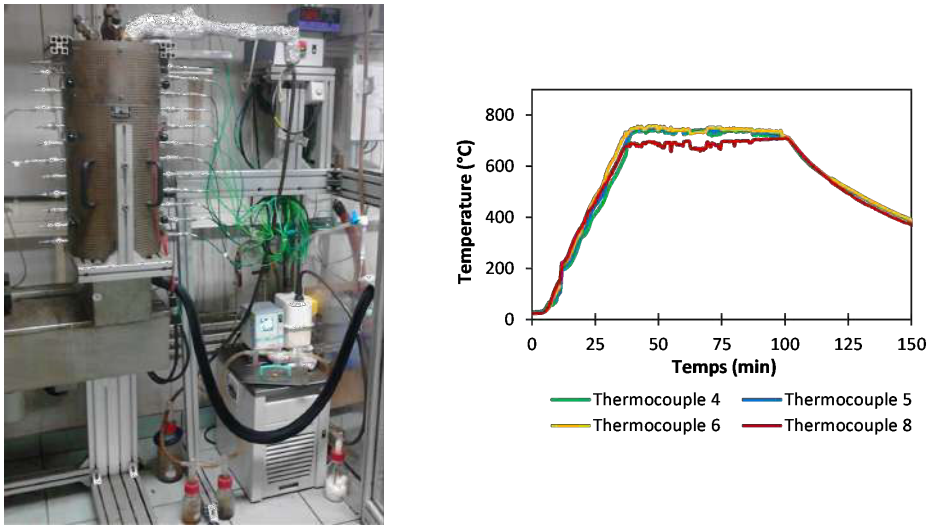

Figure 2.3: Fluidized bed gasifier experimental setup and characteristic temperature profile inside the reactor.

According to the reactor technology, separate reaction zones cannot be distinguished, unlike the fixed bed downdraft gasifier. Thus, an homogeneous temperature is observed along the reactor height. The advantages and disadvantages identified for this experimental device are summarized below:

Advantages

- Reactor capacity: Reduced amounts of biomass are required for gasification experiments (<100 g)
- Control of gasification parameters: Gasification parameters like temperature, heating rate, and gasifying agent can be accurately controlled, considering that the reactor is externally heated.
- Temperature monitoring: The reactor setup allows the complete monitoring of the temperature profile along the reactor height.
- Experimental preparation time: short biomass and reactor preparation times are required prior to the gasification tests, in comparison to the pilot-scale reactor.
- Char recovery: The recovered gasification char could be considered homogeneous, as there are not different reaction zones inside the reactor.

Disadvantages

- Laboratory scale reactor: Experimental results cannot be directly extrapolated to pilot or industrial facilities.

- Char recovery: Only small char quantities can be recovered from each experiment.
- Mass measurement: The mass consumption during the gasification experiments cannot be monitored.

From the preliminary tests it was observed that both gasification systems allow the complete analysis of the gasification process and resulting by-products. However, in addition to the reactor scale, the main differences identified were related to the control of the process parameters and the recovery of chars for further analysis.

In particular, several difficulties were encountered to control the gasification temperature in the autothermal reactor, considering that it depends on the development of the reactions in the combustion zone, and then, on the air quantity supplied to the system. In accordance, a precise air regulation is required. Moreover, in a downdraft reactor the combustion gases act also as gasifying agents, making the accurate control of the reaction atmosphere difficult, even with a steam feeding point in the reduction zone. In contrast, as the fluidized bed reactor is externally heated, the gasifying atmosphere and temperature can be easily controlled and modified.

In this regard, taking into account that the accurate control of the process parameters is required for comparison purposes between the feedstocks, the experimental gasification tests for this study will be performed using the laboratory-scale fluidized bed reactor. Moreover, as the selected reactor is smaller than the fixed bed gasifier, lower biomass quantities are required for the experimental analysis, reducing the time and costs associated to the biomass transport and preparation.

2.4 Biomass thermal decomposition behavior and kinetics

Thermogravimetric analysis (TGA) of the studied samples were performed in order to determine their pyrolysis and steam gasification behavior and kinetics. Regarding the pyrolysis analysis, non-isothermal tests were carried out from 25°C to 800°C, according to the experimental program summarized in figure 2.4a. The non-isothermal approach allowed the evaluation of the pyrolysis behavior of the samples in a wide temperature range.

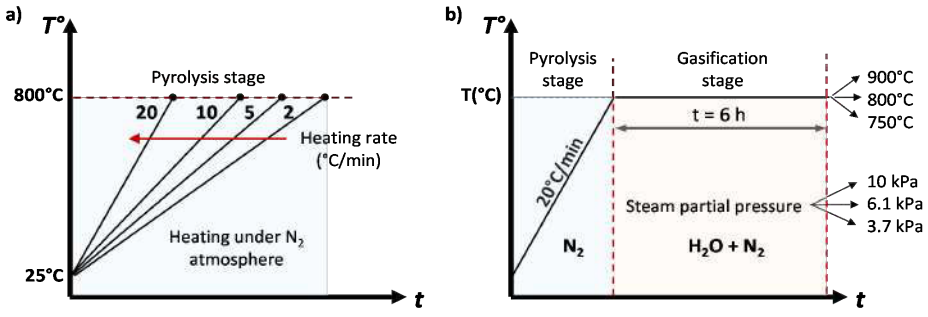

Figure 2.4: Thermogravimetric analysis experimental program. a) pyrolysis, b) steam gasification

In the case of steam gasification analysis, isothermal tests were performed at different temperatures, with three steam partial pressures, as presented in the experimental program in figure 2.4b. The heat-up stage is carried out under nitrogen in order to better control the beginning of the gasification reactions by switching the atmosphere from inert to reactive, when the isothermal regime is established.

In accordance, the analysis procedure of the experimental results should be adapted to the isothermal or non-isothermal approach. In this regard, the kinetic analysis of the pyrolysis and gasification process is developed using model-free isoconversional methods, described in detail in chapter 3 for biomass pyrolysis, and chapter 6 for steam gasification.

2.5 Steam gasification experiments

2.5.1 Methodology and experimental plan

As already stated, pyrolysis and steam gasification experiments were carried out in the semicontinous lab-scale fluidized bed gasifier described in section 2.3, in order to analyze the gasification process of the selected feedstocks, and the resulting by-products. Especial attention was given to fuel gases and char. Before the experimental tests, the raw biomasses were ground and sieved to a size range between 2 mm and 4 mm.

80 g of biomass were placed inside the reactor and heated to the gasification temperature at a heating rate of 20°C/min, under nitrogen. When the gasification temperature was reached, the atmosphere was switched to a mixture of H_2O/N_2 and was maintained during all the gasification stage. A total flow rate of 0.7 m^3/h was used for all the experiments. Preliminary tests were performed to ensure that particle fluidization is attained during the experiments. Information regarding the characterization of fluidizing velocity in this reactor could be found by Ducousso [21] and Klinghoffer [22]. It is important to note that in this work no inert bed materials were used. After each test, the reactor was cooled down to room temperature under nitrogen. The remaining char was collected and weighted, as well as the impinger bottles and pipes, in order to determine the quantity of water and tars condensed. Considering that the nitrogen flow supplied to the process is known and constant for each experiment, the total volume of permanent gases produced can be deduced from the gas volume measured using the gas meter. The experimental program and conditions are presented in figure 2.5.

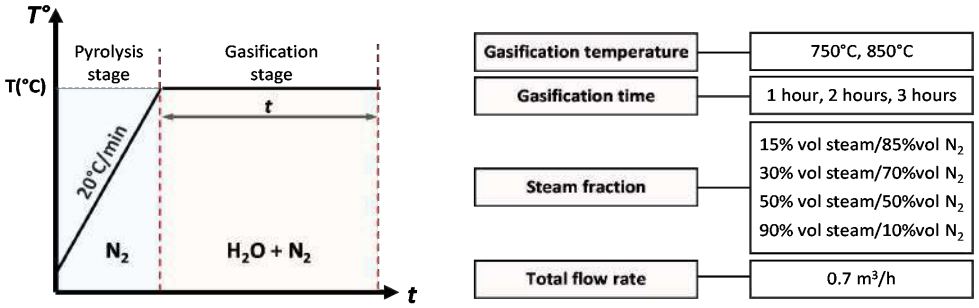

Figure 2.5: Pyrolysis and steam gasification experimental program

Pyrolysis-only tests were also performed in order to determine the gas, solid, and liquid yields at the end of the heating period (pyrolysis stage) for each gasification temperature. For all the experimental conditions, a mass balance was established in order to determine the product yield associated to the pyrolysis and gasification stage, according to figure 5.3.

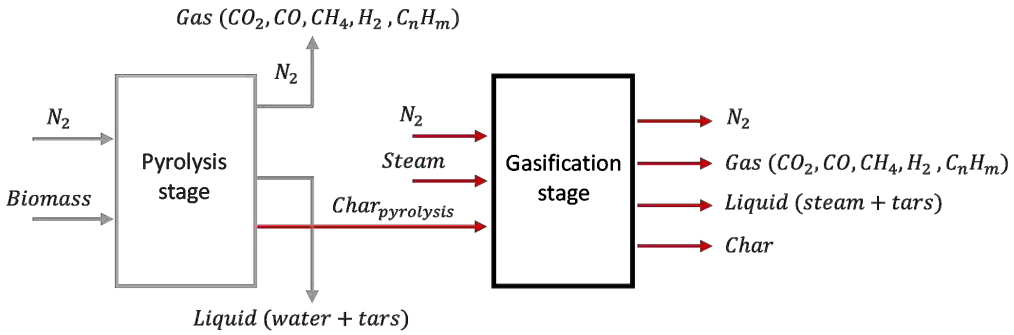

Figure 2.6: Inlet and outlet streams to and from the reactor during the gasification stage.

More specifically, the gas, liquid, and solid mass measured for the pyrolysis tests are subtracted from the gasification experiments to obtain the product yields associated only to the gasification stage.

For all the experimental conditions, gas and char samples were collected for further analysis. In particular, a calibrated MyGC Agilent micro-GC was used to determine the produced gas composition and heating value.

Regarding the gasification chars, the characterization plan and techniques used to determine their physico-chemical characteristics are presented in section 2.5.2. The analysis procedure of the steam gasification experimental results is detailed in chapter 5

2.5.2 Biomass and steam gasification char characterization

In order to understand the impact of biomass characteristics on the steam gasification chars properties and possible valorization pathways, the complete physico-chemical characterization of both raw biomass and char is needed. For this purpose, different analytical techniques were used.

In the case of the raw feedstocks, the knowledge of their organic and inorganic composition is of great interest, as well as their calorific value. Accordingly, the biomass characterization methods are presented in figure 2.7.

Likewise, regarding the gasification chars, their organic and inorganic composition, as well as their textural properties, structure, and surface chemistry were analyzed and compared. The characterization plan and techniques used are summarized in table 2.3.

In accordance to the manuscript structure, the experimental procedures and devices used for each presented technique are precisely detailed in the corresponding chapter, indicated in the last column of the table.

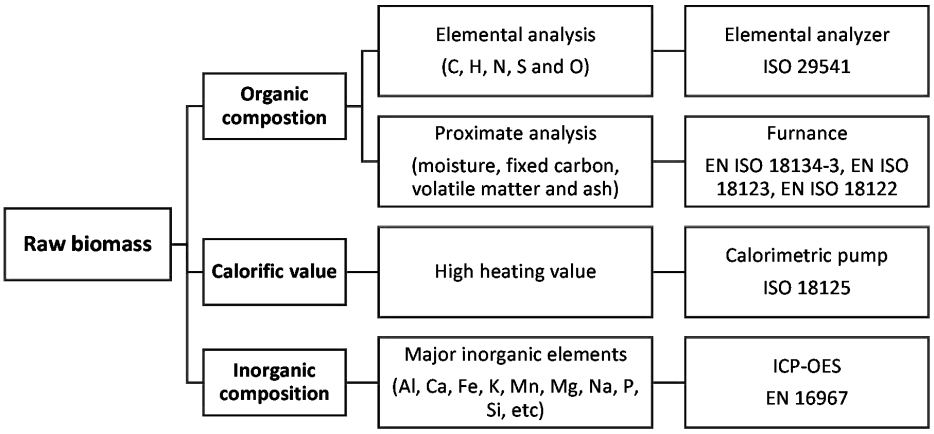

Figure 2.7: Raw biomass characterization methods [23–28]

Table 2.3: Gasification chars characterization methods

	Information	Technique	Chapter
Organic composition	C, H, N, S and O content	Elemental analysis according to ISO 29541	Chapter 6
	Moisture, volatile matter, fixed carbon, and ash	Proximate analysis according to EN ISO 18134-3, EN ISO 18123, EN ISO 18122	
Calorific value	High heating value	ISO 18125	Chapter 6
Inorganic composition	Quantitative mineral composition of the samples	ICP-OES	Chapter 6
	Mineral distribution in the char surface	SEM-EDX	
	Speciation of crystalline minerals	XRD	
Textural properties	Specific surface area	N_2 adsorption	Chapter 6
	Pore size distribution		
	Pore volume		
Carbon structure	Global carbon structure	XRD	Chapter 6
	Carbon nanostructure	TEM	
Surface chemistry	Surface oxygen-containing functional groups	TPD	Chapter 6
	pH_{PZC}	Acid titration	Chapter 7
	Cation exchange capacity	Sodium acetate displacement method	
	Acid neutralization capacity	Acid-base titration according to NF EN 14429 standard	
pH	pH in water solution		Chapter 7

In particular, the techniques described in chapter 6 give a general insight to the properties of the steam gasification chars produced from lignocellulosic agrowastes, and contribute to the understanding of the impact of the process parameters and biomass characteristics on the gasification chars. For their part, the techniques applied in chapter 7 are mostly associated to the establishment of the potential of the analyzed materials to be used in environmental and agricultural applications.

2.6 Summary

This chapter presented the materials and experimental techniques used in this research study. In accordance, the general methodology employed for the development of the experimental activities is illustrated in figure 2.8. The precise procedures and devices are detailed in the corresponding chapter, as well as the analytical methods used to treat and exploit the obtained results.

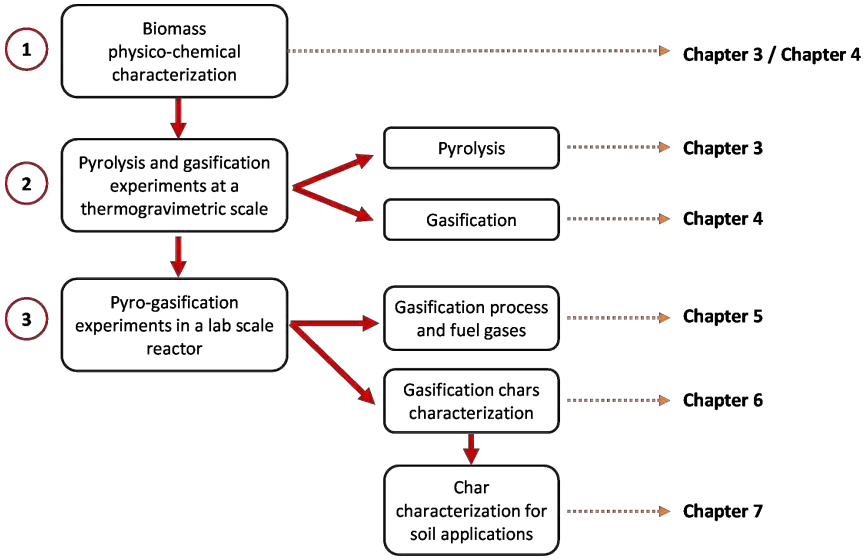

Figure 2.8: General methodology used for the development of the experimental activities and associated chapters

Bibliography

[1] Akeem M. Azeez, Dietrich Meier, Jürgen Odermatt, and Thomas Willner. "Fast pyrolysis of African and European lignocellulosic biomasses using Py-GC/MS and fluidized bed reactor." In: *Energy and Fuels* 24.3 (2010), pp. 2078–2085 (cit. on pp. 38, 39).

[2] Alneira Cuéllar and Ismael Muñoz. "Fibra de guadua como refuerzo de matrices poliméricas - Bamboo fiber reinforcement for polymer matrix." In: *Dyna* 77.162 (2010), pp. 137–142 (cit. on pp. 38, 39).

[3] Jesus A García, Manuel P García, and Keshav C Das. "Determinación de los parámetros cinéticos de degradación térmica de los subproductos de las plantas de beneficio mediante análisis termogravimétrico y calorimetría de barrido diferencial." In: *Revista Palmas* (2008) (cit. on pp. 38, 39).

[4] Vaibhav Dhyani and Thallada Bhaskar. "A comprehensive review on the pyrolysis of lignocellulosic biomass." In: *Renewable and Sustainable Energy Reviews* 129 (2018), pp. 695–716 (cit. on pp. 38, 39).

[5] Tasneem Abbasi and S. A. Abbasi. "Biomass energy and the environmental impacts associated with its production and utilization." In: *Renewable and Sustainable Energy Reviews* 14.3 (2010), pp. 919–937 (cit. on pp. 38, 39).

[6] Lydia Fryda, Claudia Daza, Jan Pels, Arno Janssen, and Robin Zwart. "Lab-scale co-firing of virgin and torrefied bamboo species Guadua angustifolia Kunth as a fuel substitute in coal fired power plants." In: *Biomass and Bioenergy* 65 (June 2014), pp. 28–41 (cit. on pp. 38, 40).

[7] Shuping Zhang, Yinhai Su, Kuan Ding, Shuguang Zhu, Houlei Zhang, Xinzhi Liu, and Yuanquan Xiong. "Effect of inorganic species on torrefaction process and product properties of rice husk." In: *Bioresource Technology* 265 (2018), pp. 450–455 (cit. on p. 39).

[8] Wen Cao, Liejin Guo, Xuecheng Yan, Deming Zhang, and Xiangdong Yao. "Assessment of sugarcane bagasse gasification in supercritical water for hydrogen production." In: *International Journal of Hydrogen Energy* 43 (2018), pp. 13711–13719 (cit. on p. 39).

[9] Colomba Di Blasi. "Combustion and gasification rates of lignocellulosic chars." In: *Progress in Energy and Combustion Science* 35.2 (2009), pp. 121–140 (cit. on p. 39).

[10] Jose M Encinar, Juan F Gonzalez, Juan J Rodriguez, and Maria J Ramiro. "Catalysed and uncatalysed steam gasification of eucalyptus char: influence of variables and kinetic study." In: *Fuel* 80 (2001), pp. 2025–2036 (cit. on p. 39).

[11] M Perander, N Demartini, A Brink, J Kramb, O Karlström, J Hemming, A Moilanen, J Konttinen, and M Hupa. "Catalytic effect of Ca and K on CO 2 gasification of spruce wood char." In: *Fuel* 150 (2015), pp. 464–472 (cit. on p. 39).

[12] Food and Agriculture Organisation of the United Nations. *FAO statistical yearbook 2014: Latin America and the Caribbean*. Santiago de Chile, 2014, p. 878 (cit. on p. 40).

[13] Paula Andrea Rugeles-Silva, Andrés Mauricio Posso-Terranova, Ximena Londoño, Nancy Barrera-Marín, and Jaime Eduardo Muñoz-Florez. "Caracterización Molecular de la Guadua Angustifolia Kunth Mediante Marcadores Moleculares." In: *Acta Agronómica* 61.4 (2012), pp. 325–330 (cit. on p. 40).

[14] Christoph Kleinn and David Morales-Hidalgo. "An inventory of Guadua (Guadua angustifolia) bamboo in the Coffee Region of Colombia." In: *European Journal of Forest Research* 125.4 (Apr. 2006), pp. 361–368 (cit. on p. 40).

[15] Thanasit Wongsiriamnuay, Nattakarn Kannang, and Nakorn Tippayawong. "Effect of operating conditions on catalytic gasification of bamboo in a fluidized bed." In: *International Journal of Chemical Engineering* 2013 (2013) (cit. on p. 40).

[16] Po-Chih Kuo, Wei Wu, and Wei-Hsin Chen. "Gasification performances of raw and torrefied biomass in a downdraft fixed bed gasifier using thermodynamic analysis." In: *Fuel* 117 (Jan. 2014), pp. 1231–1241 (cit. on p. 40).

[17] Dengyu Chen, Dong Liu, Hongru Zhang, Yong Chen, and Qian Li. "Bamboo pyrolysis using TG–FTIR and a lab-scale reactor: Analysis of pyrolysis behavior, product properties, and carbon and energy yields." In: *Fuel* 148 (May 2015), pp. 79–86 (cit. on p. 40).

[18] Federación Nacional de Cultivadores de Palma de Aceite - Fedepalma. *Anuario Estadístico de la agroindustria de la palma de aceite en Colombia y en el mundo - 2014*. Tech. rep. Bogotá - Colombia: Fedepalma, 2014, p. 176 (cit. on p. 40).
[19] Humberto Escalante, Janneth Orduz, Henry J. Zapata, Maria Cecilia Cardona, and Martha Duarte. "Potencial energético de la biomasa residual." In: *Atlas del Potencial Energético de Biomasa Residual en Colombia*. Ed. by Ministerio de Minas y Energia - Republica de Colombia. 2010. Chap. Anexo E, pp. 155–172 (cit. on p. 40).
[20] Jesus a. García N. and Edgar E. Yañez A. "Generación y uso de biomasa en plantas de beneficio de palma de aceite en Colombia - Power generation and use of biomass at palm oil mills in Colombia." In: *Revista Palmas* 31.2 (2010), pp. 41–48 (cit. on p. 40).
[21] Marion Ducousso. "Gasification biochar reactivity toward methane cracking." Doctoral thesis. Université de Toulouse, 2015, p. 276 (cit. on p. 45).
[22] Naomi Klinghoffer. "Utilization of char form biomass gasification in catalytic applications." Tesis doctoral. Columbia University, 2013, p. 145 (cit. on p. 45).
[23] ISO 29541:2010. *Solid mineral fuels - Determination of total carbon, hydrogen and nitrogen content - Instrumental method*. 2010 (cit. on p. 47).
[24] EN ISO 18134-3. *Solid biofuels - Determination of moisture content - Oven dry method - Part 3: Moisture in general analysis sample*. 2015 (cit. on p. 47).
[25] EN ISO 18123. *Solid biofuels - Determination of the content of volatile matter*. 2015 (cit. on p. 47).
[26] ISO 18122:2015. *Solid biofuels - Determination of ash content*. 2015 (cit. on p. 47).
[27] EN 16967:2015. *Biocombustibles solides - Détermination des éléments majeurs - Al, Ca, Fe, Mg, P, K, Si, Na et Ti - International standard*. 2015 (cit. on p. 47).
[28] ISO 18125:2017. *Solid biofuels - Determination of calorific value*. 2017 (cit. on p. 47).

Chapter

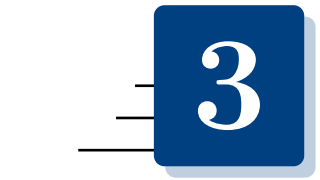

Kinetic analysis of tropical lignocellulosic agrowaste pyrolysis

This chapter was published as a research paper in an international journal. Reference: Romero Millan LM, Sierra Vargas FE, Nzihou A. Kinetic Analysis of Tropical Lignocellulosic Agrowaste Pyrolysis. BioEnergy Res 2017. doi:10.1007/s12155-017-9844-5.. The final publication is available at Springer via http://dx.doi.org/10.1007/s12155-017-9844-5

Abstract

The thermal behavior of three Colombian agricultural residues was studied by non-isothermal thermogravimetric analysis (TGA) at various heating rates. An approach using a combined kinetics parallel reaction model and model-free isoconversional methods proved to be suitable to determine the pyrolysis kinetic parameters of biomasses with different macromolecular composition and H/C and O/C ratios near 1.5 and 0.8 respectively. Fraser-Suzuki functions representing the derivative TGA (DTG) of hemicellulose, cellulose and lignin showed a very good agreement with the experimental data. The calculated apparent activation energy of biomass pseudo-components evidenced no de-

pendence on the reaction extent in all the conversion range, validating the use of master plots for decomposition mechanism identification. Pseudo-hemicellulose, pseudo-cellulose and pseudo-lignin showed to be close to a second order kinetic model, a random scission or an Avrami-Erofeev model, and a high order kinetic model, respectively. Comparing the three feedstocks, the apparent activation energy of the pseudo-components was in the order: bamboo guadua $E_a <$ coconut shells $E_a <$ oil palm shells E_a. The results show that even when samples elemental composition is very similar, macromolecular constituents, in particular lignin, could have an impact in the biomass decomposition rate and apparent activation energy. For the three studied materials, the model fitting error below 10% showed that the calculated kinetic parameters are suitable for the description and prediction of the biomasses thermal decomposition.

3.1 Introduction

Thanks to their climate variety, tropical regions have a great biodiversity and the appropriate conditions for the development of agroindustrial activities. Agroindustry produces large amounts of low cost residues, which can be used for biofuels production or transformed in value added products. However, in most tropical developing countries, these residues are not valorized and represent an environmental risk, as they are not always disposed properly. According to different studies, the agro-residues potential in developing countries is higher than 2900 million tons per year [1]. In Colombia, according to the Colombian Energy and Mining Planning Unit - UPME, more than 70 million tons of wastes are produced every year from agroindustrial activities [2]. In this context, the valorization of these residues from an energetic point of view or for the production of value-added products represents an alternative for their treatment and disposal, and for strengthening the local economy.

Three Colombian lignocellulosic biomasses were chosen for this study: oil palm shells (OPS), coconut shells (CS) and bamboo guadua (BG). OPS are the shell fractions left after the crushing of the kernel nut in the oil palm extraction process from the Eleais guineensis palm. This biomass is considered an important waste of the Colombian oil palm extraction industry, with near 220.000 tons generated every year [2]. In the country, raw oil palm shells are usually burnt in boilers for steam production in palm oil facilities, or disposed as a cover for palm plantation roads, without giving any value to this residue [3].

Furthermore, CS from cocos nucifera palm, are considered a material with little or non-economic value from the Colombian alimentary industry, and have been traditionally used for handicraft making or discharged in soils. The amount of this residue is not negligible in the country, considering that near 119.000 tons of this fruit are produced in Colombia every year, according to the statistics from the Food and Agriculture Organization of the United Nations [4].

Finally, BG – Guadua angustifolia Kunth, is a native woody bamboo species from South and Central America [5, 6]. It has been traditionally used in Colombia as a construction material or firewood. With a high growing rate, BG could represent an interesting material for energy purposes in Colombia and other tropical countries, either from crops or as a residue from the construction industry. Energetic applications of this biomass have not been studied in detail. Reported studies related to bamboo as energy source have been mainly performed with other bamboo species [7–9].

Considering that the three selected biomasses have a heating value above 18 MJ/kg and a great availability [5, 10, 11], it could be interesting to explore their potential to be used as a source of energy, or as a feedstock for the production of value-added materials in Colombia and other tropical countries.

Pyrolysis is the first step in the conversion of biomass into biofuels, adsorbent materials, and value added chemicals [12–15]. This thermochemical conversion process, constitutes the previous stage of combustion and gasification, and should be properly understood for the valorization of different materials through thermochemical conversion processes. In particular, the knowledge of the pyrolysis kinetic parameters is very important to analyze the thermal decomposition process of residual biomasses, predict their conversion, and determine their possible valorization pathways.

Thermogravimetric analysis (TGA) has been widely used for the study of lignocellulosic biomass decomposition kinetics, either from isothermal and non-isothermal approaches. Several pyrolysis kinetic studies using non-isothermal data have focused on model-free methods to estimate the biomass kinetic parameters, as they allow the evaluation of the activation energy without knowing the decomposition reaction model [16, 17]. However, considering that the biomass pyrolysis is an extremely complex process due to the morphologies of its components and their interaction, the model free-procedure is not always sufficient for the identification of the complete kinetic triplet [18].

Most biomass pyrolysis analysis have reported different activation energy values for several kinds of lignocellulosic biomasses, usually considering only a global decomposition approach [19–22]. Works based on model-free isoconversional methods, showed that there is a clear dependence of activation energy on the reaction extent, suggesting that the pyrolysis process includes many different reactions occurring at the same time. Under these circumstances, an interesting alternative for the analysis of complex conversions is a parallel reaction approach, separating the individual processes by derivative TGA (DTG) peak deconvolution [23], followed by the kinetic analysis of the resulting individual curves. Few studies have been reported for biomass pyrolysis kinetic analysis using DTG deconvolution [24–26]. In particular, bamboo guadua, coconut shells and oil palm shells kinetic analysis using this alternative approach has not been reported yet.

According to this, the aim of this work is to study the pyrolysis characteristics and kinetics of three tropical lignocellulosic biomasses, from a non-isothermal thermogravimetric analysis. A three parallel reaction model was employed, using a DTG peak deconvolution procedure, followed by a model-free isoconversional approach and generalized master plots. The influence of the biomass nature in its thermal decomposition characteristics was discussed, comparing the calculated kinetic parameters of the selected materials.

3.2 Materials and methods

3.2.1 Materials

Tropical feedstocks used in this study were collected in Colombia, South America. Oil palm shells were provided by a palm oil extraction plant in the Meta region (N4°16′0″ O73°29′0″, 500 meters above sea level, average temperature 27°C and 2858 mm of precipitation throughout the year). Coconut shells from coconuts coming from the

Nariño region (N1°10′0″ O77°16′0″, 0 to 400 meters above the sea level and 28°C of average temperature) were provided by a food processing industry. Both OPS and CS are considered as an industrial residue.

Table 3.1: Heating value and chemical composition of studied biomasses.

		OPS	CS	BG
Elemental Analysis (wt. % daf)	C	46.7±0.2	46.8 ±0.2	42.7±0.3
	H	6.5±0.1	5.8 ±0.1	5.4±0.1
	O*	46.2±0.1	47.1 ±0.1	51.5±0.1
	N	0.6±0.1	0.3 ±0.1	0.4±0.1
	O/C	0.7±0.1	0.7±0.1	0.9±0.1
	H/C	1.7±0.1	1.5±0.1	1.5±0.1
Proximate analysis (wt. %)	Moisture	9.5±0.4	10.2±0.2	9.0±0.3
	Volatile Matter	69.9±0.3	71.4±0.3	68.3±0.2
	Fixed Carbon*	19.0±0.3	17.1±0.2	18.1±0.3
	Ash	1.6±0.2	1.3±0.1	4.6±0.4
High Heating value (MJ/kg)	HHV	19.6±0.2	18.7±0.3	18.0±0.3
Molecular composition (wt % daf)	Cellulose	30.4	32.5	53.9
	Hemicellulose	12.7	20.5	13.5
	Lignin	49.8	36.5	25.1

* Calculated by difference

For its part, 3 to 4 years old bamboo guadua coming from a bamboo forest in the Quindío region (N4°32′0″ O75°42′0″, 800 to 1200 meters above sea level and 23°C of average temperature) was obtained from a furniture and handicraft construction site, where biomass was indoor stored.

Raw materials were milled and sieved to a size range of 1mm to 2mm before thermogravimetric analysis. CHNS composition of samples was determined using a Themoquest NA 2000 elemental analyzer. Moisture, volatiles and ash content were calculated according to the standards EN ISO 18134-3, EN ISO 18123 and EN ISO 18122, respectively. The high heating value was calculated using an IKA C 5000 automated bomb calorimeter. The samples chemical composition and heating value are presented in table 3.1 as an average of three replicates. Molecular composition of the biomasses is referred to literature reported values [27–29].

3.2.2 Thermogravimetric analysis

Thermogravimetric analysis (TGA) of selected materials were performed using a Mettler Toledo TGA 2 SF analyzer. Approximately 30 mg of each sample were placed in an alumina crucible and heated from 25°C to 800°C, with 2, 5, 10 and 20°C/min as heating rates. Experiments were conducted under a nitrogen atmosphere, using a flow rate of 50 ml/min. To verify the repeatability of TGA experiments, each run was conducted two times and averaged; then, the mean standard deviation was calculated. A blank experiment was made for each heating rate to exclude buoyancy effects. Experimental runs were first performed at 2°C/min, followed by 5°C/min, 10°C/min and 20°C/min. Duplicates were done following the same order described. For each experimental

condition, the standard deviation was below 0.6% for the investigated temperature range. This value was considered reasonable to ensure the repeatability of the obtained mass loss curves.

3.2.3 Kinetic study

Theoretical background

Thermogravimetric analysis has been extensively used to study the kinetics of biomass pyrolysis and to determine the reaction mechanisms controlling this process. Generally, the basis of a kinetic study is a series of experiments where the degree of conversion of a material is measured as a function of time and temperature. According to this, the degree of conversion or reaction extent is usually defined as in Eq. 3.2.1.

$$\alpha = \frac{m_0 - m}{m_0 - m_f} \tag{3.2.1}$$

Where m_0 is the initial mass of the sample, m_f the final mass, and m the current mass at a given temperature or time. The reaction rate $d\alpha/dt$ depends on the temperature T and the degree of conversion α, as shown in Eq. 3.2.2. In this expression, $f(\alpha)$ is the reaction model function representing how the solid state decomposition process occurs, and $k(T)$ the Arrhenius equation, representing the temperature dependence of the process.

$$\frac{d\alpha}{dt} = k(T)f(\alpha) \tag{3.2.2}$$

$$k(T) = A\exp\left(\frac{-E_a}{RT}\right) \tag{3.2.3}$$

From the Arrhenius equation (Eq. (3.2.3)), the reaction rate expression can be rearranged as follows:

$$\frac{d\alpha}{dt} = A\exp\left(\frac{-E_a}{RT}\right)f(\alpha) \tag{3.2.4}$$

Finally, for linear non-isothermal thermogravimetric analysis, the reaction rate is expressed as in Eq. 3.2.5, where β is the heating rate used to perform the experiment in K/min.

$$\frac{d\alpha}{dT} = \frac{A}{\beta}\exp\left(\frac{-E_a}{RT}\right)f(\alpha) \tag{3.2.5}$$

In the case of biomass decomposition, the most commonly accepted reaction model functions $f(\alpha)$ and their integral forms are presented in table 3.2.

Three parallel reaction model

Thermal decomposition of lignocellulosic biomass is quite complex, considering that it is constituted by different components, mainly hemicellulose, cellulose and lignin.

Table 3.2: Most common reaction mechanisms used in solid-state kinetic analysis related to biomass thermal decomposition [18, 30]

	Model	$f(\alpha)$	$g(\alpha)$
Order based	Or1 - First order	$1-\alpha$	$-\ln(1-\alpha)$
	Or2 - Second order	$(1-\alpha)^2$	$[1/(1-\alpha)]-1$
	Or3 - Third order	$(1-\alpha)^3$	$(1/2)\left[1/(1-\alpha)^2\right]-1$
Diffusion	D1 – One dimensional	$1/(2\alpha)$	α^2
	D2 –Two dimensional	$[-\ln(1-\alpha)]^{-1}$	$\alpha+(1-\alpha)\ln(1-\alpha)$
	D3 – Three dimensional	$(3/2)(1-\alpha)^{2/3}\left[1-(1-\alpha)^{1/3}\right]^{-1}$	$\left[1-(1-\alpha)^{1/3}\right]^2$
	D5 – Three dimensional	$(3/2)(1-\alpha)^{4/3}\left[(1-\alpha)^{-1/3}-1\right]^{-1}$	$\left[(1-\alpha)^{-1/3}-1\right]^2$
Power law	Pn – Power law	$n(\alpha)^{(n-1)/n}$	$\alpha^{1/n}$
Nucleation and growth	An – Avrami Erofeev	$n(1-\alpha)\left[-\ln(1-\alpha)\right]^{(n-1)/n}$	$\left[-\ln(1-\alpha)\right]^{1/n}$
Geometrical contraction	R2 – Contracting area	$2(1-\alpha)^{1/2}$	$1-(1-\alpha)^{1/2}$
	R3 – Contracting volume	$3(1-\alpha)^{2/3}$	$1-(1-\alpha)^{1/3}$
Random scission	L2 – Random scission L=2	$2(\alpha^{1/2}-\alpha)$	–

Accordingly, pyrolysis can be described with a parallel reaction model (PRM), assuming that the three main components of the biomass react independently [31]. Three pseudo-components representing the hemicellulose, cellulose and lignin are then considered in this approach. The total reaction rate is expressed as the addition of each pseudo-components reaction rate, as in Eq. 3.2.6.

$$\frac{d\alpha}{dT}=\sum_{i=1}^{3}c_i\frac{d\alpha_i}{dT} \tag{3.2.6}$$

It is important to note that modeled pseudo-components do not represent the real proportion of biomass constituents, as interactions between them can exist [32]. However, the pseudo-components proportion should be in accordance with each biomass molecular composition.

In order to model these three parallel reactions, the biomass DTG curves were deconvoluted, representing each pseudo-component reaction rate as a mathematical function of temperature. Global DTG curves were then considered as the addition or overlap of pseudo-components DTG profile. Gaussian, Lorentzian and Fraser-Suzuki functions were used in this study.

Gaussian function [26]:

$$\left(\frac{d\alpha}{dT}\right)_i=a\exp\left[-\frac{1}{2}\left(\frac{T-b}{c}\right)^2\right] \tag{3.2.7}$$

Where a is the amplitude in 1/K; b is the peak temperature in K, and c the width of the curve in K.

Lorentzian function [26]:

$$\left(\frac{d\alpha}{dT}\right)_i = \frac{a}{1+\left(\frac{T-b}{c}\right)^2} \tag{3.2.8}$$

Where a is the amplitude in 1/K; b is the peak temperature in K, and c the width of the curve in K.

Fraser-Suzuki function [33]:

$$\left(\frac{d\alpha}{dT}\right)_i = a\exp\left[-\frac{\ln 2}{d^2}\ln\left[1+2d\left(\frac{T-b}{c}\right)\right]^2\right] \tag{3.2.9}$$

Where a is the amplitude in 1/K; b is the peak temperature in K, c the half width of the curve in K, and d is the asymmetry of the curve.

Least squares method and an optimization algorithm were used to determine the function parameters that best fit each biomass experimental decomposition profile. The fit error was determined with equation 3.2.10, where $d\alpha/dT$ are the experimental and calculated values of the decomposition rate, and N is the total number of experimental points [32]. According to this, the smaller the fit error, the better fit to the experimental data.

$$Fit\ error(\%) = 100\left(\frac{\sqrt{\sum_{i=1}^{N}\left(\left(\frac{d\alpha_i}{dT}\right)_{exp}-\left(\frac{d\alpha_i}{dT}\right)_{calc}\right)^2}}{\sqrt{N}\left(\frac{d\alpha_i}{dT}\right)_{exp,max}}\right) \tag{3.2.10}$$

Once the best fit was determined, isoconversional model-free methods were used for kinetic analysis, as presented in section 3.2.3.

Isoconversional model-free approach

In this study, different isoconversional model-free methods were used to determine the Arrhenius parameters from experiments performed with four different heating rates. In particular, three isoconversional methods were compared: Friedman, Flynn-Wall-Ozawa (FWO) and Kissinger-Akahira-Sunose (KAS). Friedman is defined as a differential method, while FWO and KAS are integral methods [18, 34]. All of them are well known and widely used for thermal decomposition kinetics analysis. The activation energy value at a constant α can be calculated from the slope of the isoconversional Arrhenius plots, according to the expressions summarized in table 4.3.

$$\lambda(\alpha) = \frac{f(\alpha)}{f(\alpha)_{\alpha=0.5}} = \frac{d\alpha/dt}{(d\alpha/dt)_{0.5}}\frac{\exp(E_a/RT)}{\exp(E_a/RT_{0.5})} \tag{3.2.11}$$

If the apparent value of E_a does not vary in a significant way with α, the process can be described by a single step kinetics and then, generalized master plots can be used to determine the most suitable reaction mechanism associated and as a result, the

pre-exponential factor A. The reduced-generalized reaction rate expression in equation 3.2.11, needs the previous knowledge of activation energy value [35].

Table 3.3: Kinetic model-free methods used in this study

Method	Expression	Isoconversional Arrhenius plot
Friedman	$\ln(d\alpha/dt) = \ln[Af(\alpha)] - E_a/RT$	$ln(\beta\ d\alpha/dT)$ Vs $1/T$
KAS	$\ln(\beta/T^2) = \ln[A\ R/E_a\ g(\alpha)] - E_a/RT$	$\ln(\beta/T^2)$ Vs $1/T$
FWO	$log\beta = log[A\ Ea/R\ g(\alpha)] - 2.315 - 0.4567E_a/RT$	$Log\beta$ Vs $1/T$

KAS - **K**issinger-**A**kahira-**S**unose, FWO - **F**lynn-**W**all-**O**zawa

The most suitable $f(\alpha)$ model can be identified as the best match between the experimental $\lambda(\alpha)$ values and the theoretical master plots presented in Figure 3.1 [36].

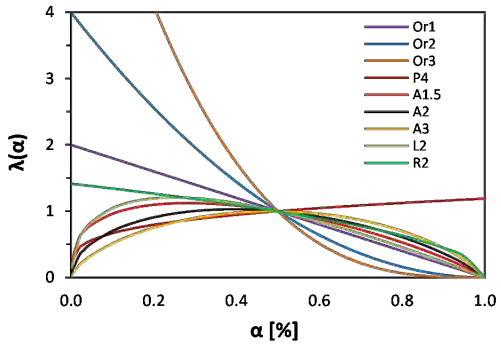

Figure 3.1: Generalized master plots of the different kinetic models in table, constructed according to Eq.

3.3 Results and discussion

3.3.1 Biomass composition and thermal decomposition characteristics

In reference to the biomasses chemical composition presented in table 3.1, it is possible to observe that the three selected materials have similar C and H contents, with H/C ratio between 1.5 and 1.7. In contrast, the molecular composition has remarkable differences, particularly related to lignin content. OPS and CS are endocarp biomasses with relatively high lignin content (50% and 36% respectively). In contrast, BG has lignin content below 25% and a high proportion of cellulose (> 50%).

Regarding the thermal decomposition behavior, the TG and DTG curves of biomasses are presented in Fig. 3.2. For the three samples, it is possible to distinguish four decomposition stages. The first one (stage I), registered before 200°C is related to the moisture and light volatiles release. The second and the third one (stage II and stage III), from 200°C to 330°C, and from 300°C to 380°C, correspond mainly to the hemicellulose and cellulose decomposition; and the last one (stage IV), from 380°C, is mainly related to lignin decomposition. These decomposition ranges found are in accordance with reported values for cellulose, hemicellulose, lignin, and other lignocellulosic biomasses [12, 37].

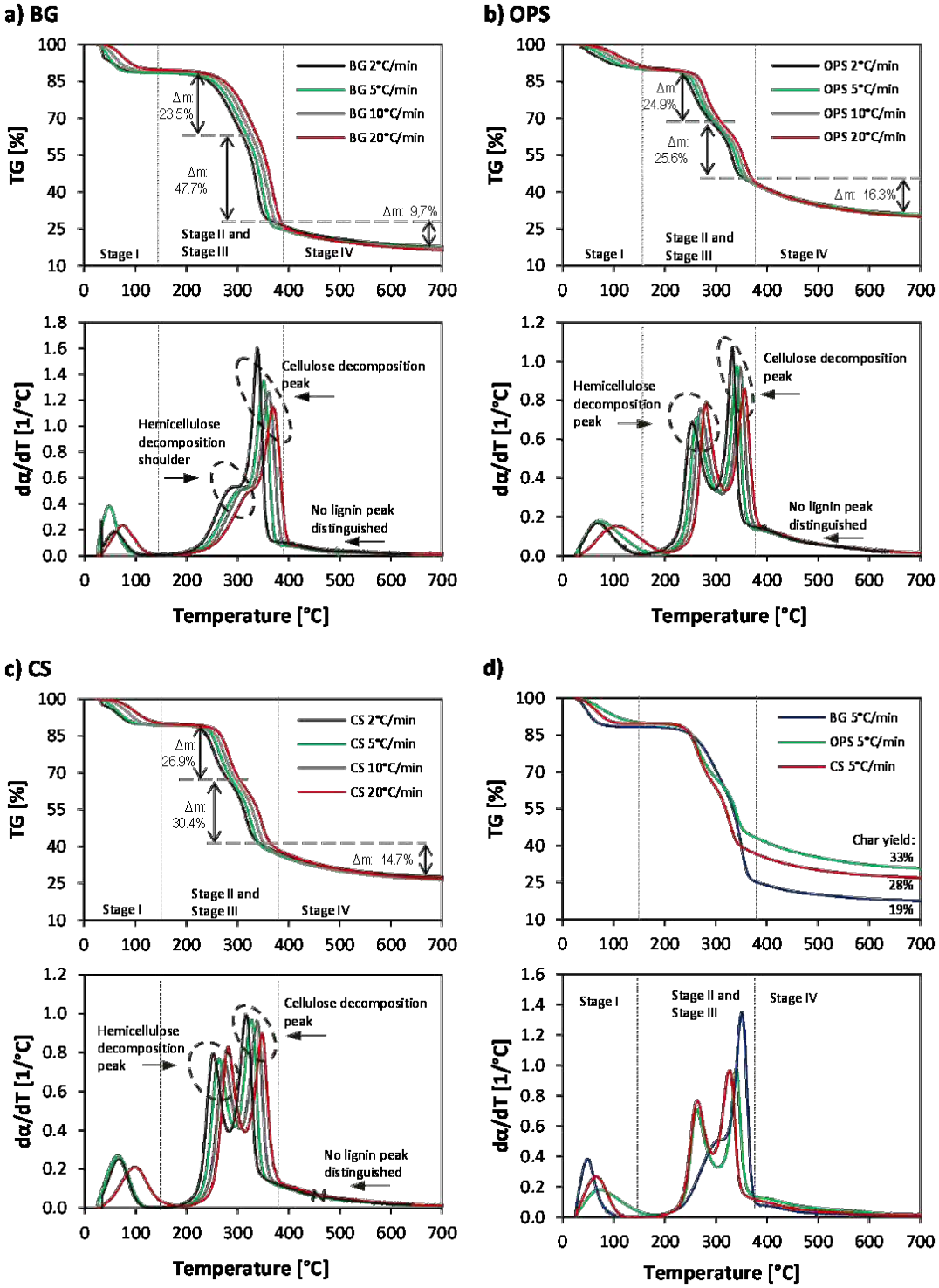

Figure 3.2: TG and DTG curves at 2, 5, 10, and 20°C/min. a) Oil palm shells (OPS), b) Coconut shells (CS), c) Bamboo guadua (BG), d) Comparison of TG and DTG curves at 5°C/min. Mass loss values and char yield are presented in a dry basis

It is possible to notice from the TG curves that the mass loss in each stage is in agreement with the fraction of hemicellulose, cellulose and lignin of the samples. In a dry basis, the three biomasses, with similar hemicellulose content, showed a similar mass loss during the second decomposition stage. This value, higher than their reported hemicellulose composition was expected, taking into account that during this stage some light volatiles can also be released. Regarding the third stage, BG showed the greatest mass loss, in accordance with its high cellulose content (53.9%). In the same way, the comparison of the TG curves, presented in Fig. 3.2d showed that the char yield at the end of the test was different for each biomass. OPS solid residue was 33%, while CS and BG solid yield was 28% and 19% respectively. These differences could be related to the molecular composition of the samples. It is known that lignin contributes in an important way to the solid yield in biomass decomposition [12], explaining the fact that OPS, with the highest lignin content, registered the lowest mass loss, followed by CS and BG.

Moreover, significant differences can be observed between the DTG curves. In the case of OPS and CS, two distinct peaks can be identified for hemicellulose and cellulose decomposition; while for BG, the hemicellulose decomposition is represented by a shoulder next to the cellulose peak. It should also be noted that as lignin decomposition range occurs over a wide temperature range from 150°C to 800°C [38], no specific lignin peak could be distinguished. Regarding the cellulose decomposition rate, endocarp biomasses showed lower values compared with BG. Taking into account that lignin is the binding agent of biomass fibers, higher lignin contents could be related to lower cellulose decomposition rates, and with the well differentiated decomposition peaks for hemicellulose and cellulose. In relation to this, Lui et al [39], studied the interaction between biomass components during pyrolysis. They concluded that lignin has a strong effect in hemicellulose and cellulose decomposition. Mendu et al. [40] also found that high lignin biomasses show well differentiated peaks for hemicellulose and cellulose decomposition.

3.3.2 DTG curves deconvolution

Biomass DTG curves were deconvoluted, representing each pseudo-component with Gaussian, Lorentzian and Fraser Suzuki functions. As Gaussian and Lorentzian functions are symmetric, they were particularly inadequate to fit the OPS and CS decomposition patterns, with an error greater than 13% and 15% respectively.

In contrast, Fraser-Suzuki function allowed the fitting of asymmetric curves, giving a good agreement with experimental data. In all cases, the fit error was lower than 3%. Parejon et al [23], found that Fraser-Suzuki function is the mathematical algorithm that better fits the decomposition rate patterns of complex processes. Fig. 3.2 presents the results of the Fraser-Suzuki deconvolution fitting of BG, CS and OPS at a heating rate of 10 °C/min. Table 3.4 summarizes the final parameters that better fitted each experimental data set.

From the deconvolution results, the pseudo-hemicellulose, pseudo-cellulose and pseudo-lignin fractions of biomass samples were calculated. BG values were 32%, 49% and 19%, respectively. CS values were 28%, 29% and 42%; and finally, OPS values were 26%, 24% and 50%. It should be noted that even when modeled pseudo-components do not represent the real proportion of biomass constituents, their fractions show the different nature of the studied samples in terms of their molecular composition.

Table 3.4: Fitting results of Fraser-Suzuki deconvolution of selected biomasses. (P-HC pseudo-hemicellulose; P-C pseudo-cellulose; P-L pseudo-lignin)

		BG			CS			OPS		
°C/min	**Parameters**	**P-HC**	**P-C**	**P-L**	**P-HC**	**P-C**	**P-L**	**P-HC**	**P-C**	**P-L**
2	**a (1/°K)**	-0.450	-1.460	-0.110	-0.620	-0.795	-0.169	-0.520	-0.840	-0.220
	b (°K)	283.0	337.7	359.0	251.0	315.0	293.0	251.5	328.5	301.0
	c (°K)	57.0	23.0	180.0	36.5	26.0	175.0	35.8	20.5	182.0
	d (-)	-0.200	-0.420	0.210	0.350	-0.300	0.555	0.360	-0.400	0.630
	Fit error (%)		1.8			2.0			2.1	
5	**a (1/°K)**	-0.428	-1.266	-0.073	-0.620	-0.795	-0.165	-0.550	-0.788	-0.184
	b (°K)	297.5	350.5	370.5	262.5	327.5	304.0	262.0	339.2	309.0
	c (°K)	56.0	25.5	186.0	37.0	26.0	180.0	34.7	22.0	184.0
	d (-)	-0.200	-0.400	0.200	0.350	-0.300	0.555	0.390	-0.345	0.630
	Fit error (%)		1.6			1.2			1.5	
10	**a (1/°K)**	-0.440	-1.180	-0.075	-0.620	-0.797	-0.165	-0.600	-0.776	-0.185
	b (°K)	308.5	360.8	380.5	272.5	338.0	312.5	269.8	347.1	319.5
	c (°K)	56.0	26.5	190.0	37.0	26.0	185.0	33.5	21.0	190.0
	d (-)	-0.200	-0.400	0.200	0.330	-0.300	0.560	0.420	-0.295	0.620
	Fit error (%)		1.9			1.0			1.8	
20	**a (1/°K)**	-0.420	-1.040	-0.075	-0.660	-0.734	-0.165	-0.630	-0.682	-0.180
	b (°K)	318.8	371.7	391.0	281.5	347.8	319.0	279.5	356.4	325.7
	c (°K)	56.0	29.0	196.0	38.0	26.0	190.0	36.0	24.0	196.0
	d (-)	-0.200	-0.370	0.210	0.350	-0.300	0.570	0.360	-0.280	0.630
	Fit error (%)		2.0			1.7			2.1	

3.3.3 Kinetic analysis

For the selected biomasses, decomposition rate curves ($d\alpha/dT$ Vs T) of each pseudo-component were analyzed using isoconversional model-free methods, in order to determine their kinetic triplet E_a, A and $f(\alpha)$. Friedman, KAS and FWO Arrhenius plots for OPS, CS and BG pseudo-components showed a good linear fit in all the conversion range between 0.1 and 0.9. In all cases, R^2 values were higher than 0.9871, as presented in table 3.5, where the maximum and minimum R^2 values are summarized. The high correlation coefficients R^2 obtained, suggest that the three isoconversional methods used are reliable and accurate for the apparent activation energy calculation.

Table 3.5: R^2 correlation coefficient of isoconversional Arrhenius plots for the three studied biomasses

		Pseudo-hemicellulose			Pseudo-cellulose			Pseudo-lignin		
		Fried.	**KAS**	**FWO**	**Fried.**	**KAS**	**FWO**	**Fried.**	**KAS**	**FWO**
BG	**R^2 Min**	0.9977	0.9982	0.9982	0.9942	0.9986	0.9988	0.9906	0.9871	0.9981
	R^2 Max	0.9997	1.0000	1.0000	1.0000	1.0000	1.0000	0.9976	0.9992	0.9993
CS	**R^2 Min**	0.9971	0.9990	0.9984	0.9977	0.9989	0.9989	0.9950	0.9946	0.9950
	R^2 Max	0.9997	1.0000	1.0000	0.9996	0.9997	0.9998	0.9991	0.9994	0.9995
OPS	**R^2 Min**	0.9973	0.9983	0.9984	0.9940	0.9977	0.9971	0.9903	0.9918	0.9938
	R^2 Max	1.0000	1.0000	1.0000	0.9991	0.9997	1.0000	0.9999	0.9999	0.9999

Biomass pseudo-components E_a was determined from the slope of the isoconversional plots regression lines, according to the Friedman, KAS and FWO methods, presented in table 4.3. The calculated E_a values are shown in Fig. 3.3, as a function of the reaction extent.

It is possible to observe that in all cases the dependence of E_a on α is quite low. The apparent activation energy remained almost constant in all the conversion range, indicating that pseudo-components thermal decomposition follow a single stage process and no complex reactions occur [30]. In relation to this, table 3.6 summarizes the mean activation energy value found for the three biomasses pseudo-components, using the described isoconversional methods. It should be noted that the relative standard deviation of the activation energy was always lower than 8% (σ = 13.5 kJ/mol), with values even below 2% (σ = 3.2 kJ/mol).

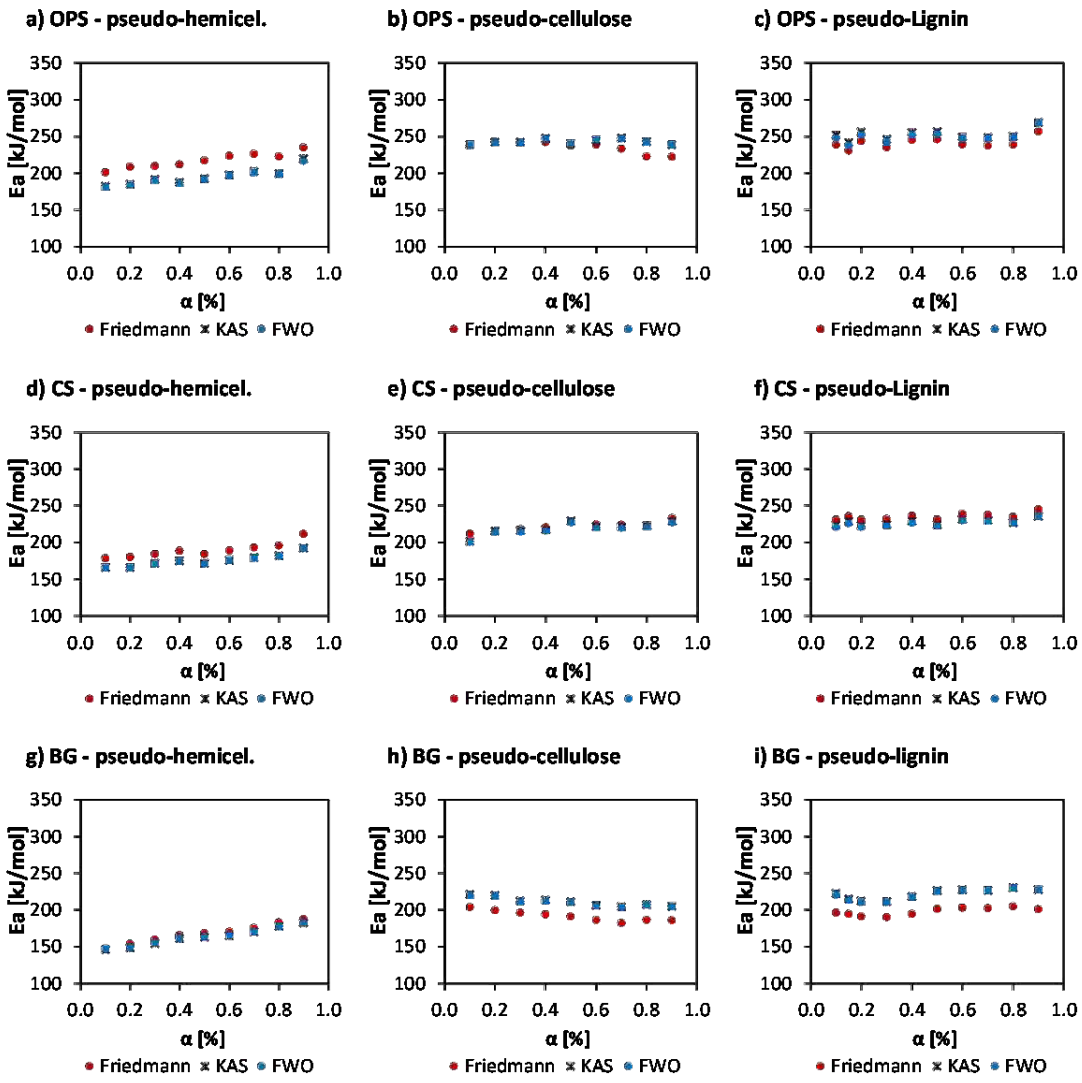

Figure 3.3: Apparent activation energy values of BG, CS and OPS pseudo - components, as a function of reaction extent

Table 3.6: Mean activation energy values of OPS, CS and BG pseudo-components, calculated using Friedman, KAS and FWO model-free methods.

	Apparent activation energy - E_a (kJ/mol), σ(kJ/mol)								
	Pseudo-hemicellulose			**Pseudo-cellulose**			**Pseudo-lignin**		
	Friedman	**KAS**	**FWO**	**Friedman**	**KAS**	**FWO**	**Friedman**	**KAS**	**FWO**
BG	167.8 σ=1.1	163.2 σ=12.2	164.2 σ=11.9	191.0 σ=7.1	211.3 σ=6.2	210.7 σ=5.8	198.4 σ=5.8	221.2 σ=7.0	221.0 σ=7.5
CS	189.9 σ=10.0	175.9 σ=8.2	175.9 σ=8.0	222.5 σ=6.8	219.8 σ=6.5	218.5 σ=6.3	235.8 σ=4.4	228.3 σ=3.9	226.9 σ=4.8
OPS	217.0 σ=10.5	195.8 σ=11.4	194.6 σ=10.7	234.1 σ=7.8	240.0 σ=3.3	240.9 σ=3.2	237.3 σ=7.6	249.5 σ=5.8	248.2 σ=6.5

Friedman, KAS and FWO approaches gave similar apparent activation energy values with absolute deviation below 11% in all cases. These results show that all the three methods are convenient for the calculation of the activation energy of the samples pseudo-components decomposition. In particular, it can be said that for biomasses with H/C and O/C near 1.6 and 0.8, any of the presented methods is suitable for the determination of pyrolysis kinetic parameters, despite the differences in hemicellulose, cellulose and lignin fractions and their decomposition behavior.

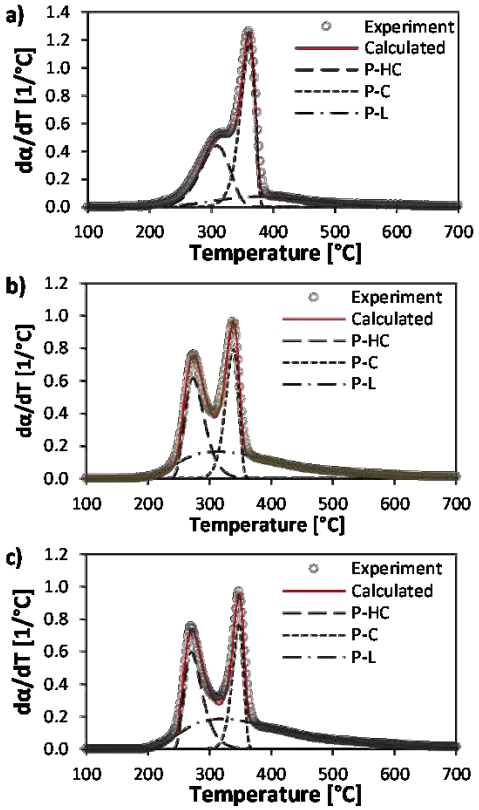

Figure 3.4: Comparison between experimental curves and Fraser-Suzuki deconvolution results of a) BG at 10°C/min. b) CS at 10°C/min. c) OPS at 10°C/min. P-HC pseudo-hemicellulose; P–C pseudo–cellulose; P–L pseudo–lignin

The highest absolute deviation between the methods was found for the mean Ea calculated with Friedman and FWO for OPS pseudo-hemicellulose (22.4 kJ/mol – 10.5%). In contrast, the results obtained with KAS and FWO were very close, with deviations below 1%. These differences are related to the mathematical approach of the isoconversional methods and the treatment of the experimental data, considering that Friedman is a differential method while FWO and KAS are integral.

From table 3.6 it is also possible to notice that for the three biomasses, pseudo-components decomposition followed nearly the same behavior, as E_a is in the order: E_a pseudo-hemicellulose < E_a pseudo-cellulose < E_a pseudo-lignin. Keeping in mind that E_a is the minimum energy required to start a reaction, the lower pseudo-hemicellulose E_a value means that this component degrades easier than the two others.

Accordingly, it is possible to see from Fig. 3.4 that pseudo-hemicellulose decomposition starts at a lower temperature than that of pseudo-cellulose and pseudo-lignin. For its part, pseudo-lignin decomposition over a large temperature range indicates that this component degrades slowly, and is harder to decompose than pseudo-hemicellulose and pseudo-cellulose. The high E_a values associated with pseudo-lignin could be related to its aromatic nature and the fact that this component is the cementing agent of biomass fibers. Lignin is a complex three-dimensional polymer with a large variety of chemical functions which differ in thermal stability and decompose in a broad temperature range [41], interacting with cellulose and hemicellulose. These interactions during biomass decomposition may explain the fact that calculated pseudo-lignin activation energy is higher than isolated lignin reported values, which can be in the range of 37 kJ/mol to 160 kJ/mol, depending on the analyzed lignin type [42, 43].

The apparent activation energies obtained with the three employed methods were in accordance with different biomass pseudo-component values in the literature. Reported pseudo-hemicellulose activation energy is between 86 kJ/mol and 180 kJ/mol; pseudo-cellulose between 140 kJ/mol and 210 kJ/mol; and pseudo-lignin between 62 kJ/mol and 230 kJ/mol [24, 44–47]. However, it can be observed that there are some differences between the three studied biomass samples. In particular, OPS is the material that presented the highest activation energy for the three pseudo-components, followed by CS and then by BG. OPS pseudo-hemicellulose E_a is near 15% and 20% higher than CS and BG in that order. OPS pseudo-cellulose value is greater than CS and BG in around 10% and 17%; and pseudo-lignin value in around 5% and 10% respectively.

This behavior could be possibly explained by the interactions between the biomass components and structure, during thermal decomposition. As the binding agent for biomass structure, lignin could have an impact in the required energy to decompose hemicellulose and cellulose. In relation to this, OPS have the highest lignin content between the studied biomasses and presented the highest E_a values; while BG has the lowest lignin content and the lowest E_a for the three pseudo-components. Thus, it is possible to infer that even when the three studied materials are mainly constituted by the same components, biomass structure plays a role in their decomposition characteristics [48, 49].

According to this, the most suitable decomposition reaction model for each biomass pseudo-component was determined using the generalized master plots procedure, which is valid only for single stage process analysis, where there is no dependence of E_a on α [18]. Experimental data were normalized to α=0.5 using Eq. 3.2.6, and compared

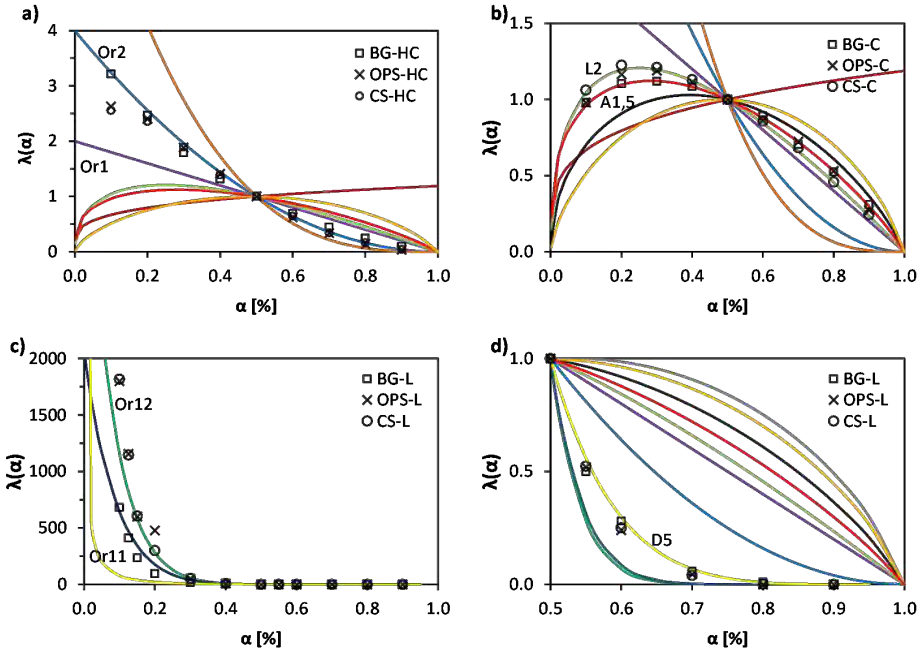

Figure 3.5: Comparison between the experimental and theoretical master plots for the three biomass pseudo-components. a) pseudo-hemicellulose, b) pseudo-cellulose, c) pseudo-lignin, d) pseudo-lignin ($0.5<\alpha<1.0$)

with theoretical master plots in Fig. 3.1. Activation energy in Eq. 3.2.6 is the mean value calculated for each pseudo-component using the mentioned three isoconversional methods.

Fig. 3.5a, shows that for the three biomasses, pseudo-hemicellulose matches closely the theoretical plot of a second order kinetic model (Or2), except at low conversion ($\alpha < 0.2$), where the decomposition model of OPS and CS pseudo-hemicellulose is between first order and second order. For its part, BG is close to a second order kinetic model in all the decomposition range. These differences at low conversion could be possibly due to interactions between the hemicellulose and the other biomass components. Similar approaches to other types of lignocellulosic biomasses have concluded that pseudo-hemicellulose decomposition follows an order based kinetic model with n between 1.5 and 4 [50].

Master plots in Fig. 3.5b, show that pseudo-cellulose decomposition is in agreement with a random scission or an Avrami Erofeev kinetic model, for the three studied biomasses. Notably, BG pseudo-cellulose matches better with an A1.5 Avrami Erofeev nucleation and growth model, while OPS and CS pseudo-cellulose are closer to a L2 random scission model. Theoretical master plots of both models are close and are related to narrow reaction profiles, as seen in Fig. 3.4, where pseudo-cellulose decomposition range is narrower compared with pseudo-hemicellulose and pseudo-lignin. In general, Avrami Erofeev models assume that reaction or decomposition is due to the appearance of random nuclei and their subsequent growth; while random scission is related to the arbitrary break of polymer chains into smaller segments [30, 51]. As the shape of both

models is very close, it is not easy to consistently distinguish between them, in spite of the differences in their theoretical background. According to this, from a mathematical point of view, both of these models could describe the pseudo-cellulose decomposition mechanism. Similar studies reported for cellulose in the literature, have concluded that both Avrami-Erofeev and random scission models could be suitable for the description of the cellulose thermal decomposition [22, 36, 52].

Finally, as seen in Fig. 3.5c, pseudo-lignin decomposition does not match with any known theoretical kinetic model. Due to the complexity of the lignin structure and its interactions with the other biomass components [45, 49, 50], it is not easy to fully understand its decomposition mechanism. As the cementing agent of biomass, lignin could interact with hemicellulose and cellulose in different ways according to the biomass structure and operating conditions. Moreover, lignin decomposes in a wide range of temperature and with low decomposition rate, making it difficult to completely model its corresponding reaction mechanism. At low conversion (α<0.5), pseudo-lignin decomposition could be modeled by an order reaction mechanism, with n between 11 and 12 (Fig. 3.5c). From α=0.5 to α=0.9, decomposition is near a three dimension diffusion mechanism. Particularly, a D5 model (Zhuravlev, Lesokin, Tempelman), as presented in Fig. 3.5d. Other reported studies have described pseudo-lignin decomposition with a third order reaction model [24], or even a high order model with $n > 12$ [22]. The proposed models, however, do not fit completely the pseudo-lignin the decomposition, due to its complexity.

With the knowledge of the most suitable reaction model for each pseudo-component, pre-exponential factor A values were calculated. Taking into account that the difference between the apparent activation energy calculated with the Friedman, KAS and FWO methods is not significant, E_a of each biomass pseudo-component was defined as the mean value of the activation energy estimated with the three methods. Furthermore, Friedman method was chosen for the evaluation of the pre-exponential factor.

The dependence of ln(A) on α, presented in Fig. 3.6, is similar to that of the activation energy, remaining almost constant during all the conversion range ($0.1 < \alpha < 0.9$). The relative standard deviation was in all cases inferior to 8% with values of even 2%. Accordingly, the mean values of E_a and A for the three biomasses are summarized in table 3.7.

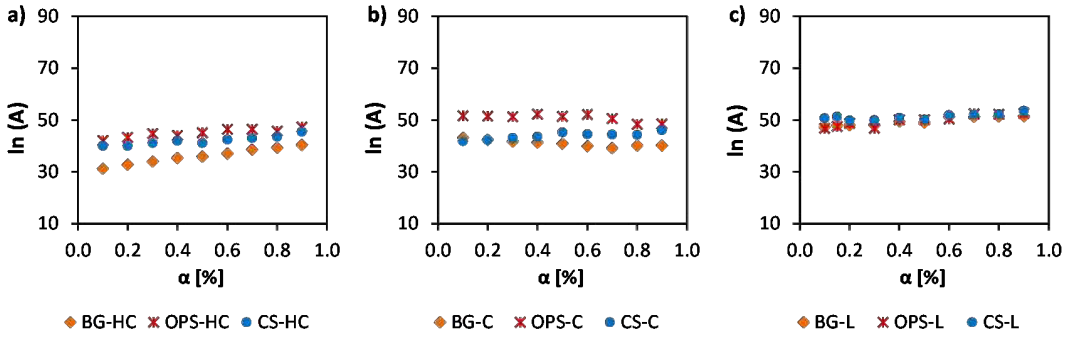

Figure 3.6: Pseudo-component dependence of ln(A) on the reaction extent. a) pseudo-hemicellulose, b) pseudo-cellulose, c) pseudo-lignin

Table 3.7: Average E_a and A values calculated for BG, CS and OPS pseudo-components

	Pseudo-hemicellulose		Pseudo-cellulose		Pseudo-lignin	
Biomass	**Ea (kJ/mol)**	**A (s^{-1})**	**Ea (kJ/mol)**	**A (s^{-1})**	**Ea (kJ/mol)**	**A (s^{-1})**
BG	165.1	2.62E+14	204.3	2.30E+16	214.5	1.02E+18
CS	180.6	5.83E+16	220.3	2.30E+18	230.3	1.47E+21
OPS	202.4	6.33E+18	238.1	3.50E+19	245.0	8.83E+21

These kinetic parameters were validated and used to reproduce the experimental decomposition curves of each biomass from 2 to 20°C/min. For the three studied materials, a good agreement was found between the experimental data and the computed decomposition behavior, with fitting errors below 10% in all cases. Fig. 3.7 shows the modeled decomposition rate of the three biomasses and pseudo-components at a heating rate of 10°C/min.

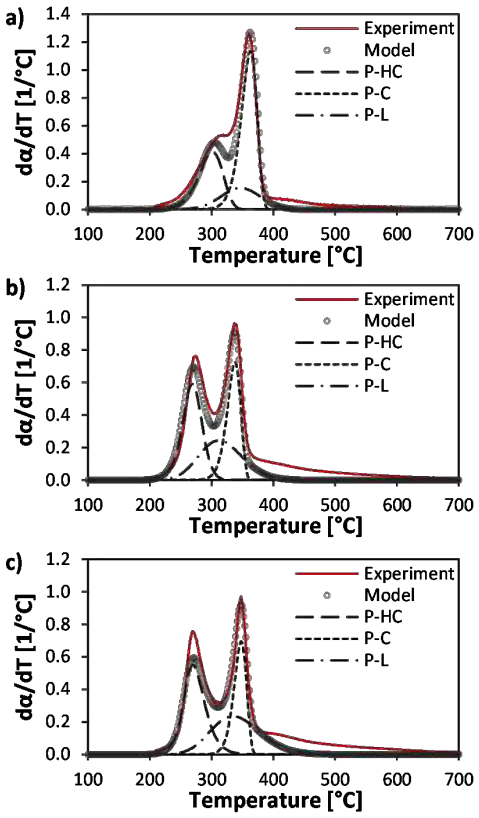

Figure 3.7: Comparison between experimental and modelled decomposition curves of a) BG at 10°C/min. b) CS at 10°C/min. c) OPS at 10°C/min. Modelled curves generated using the calculated E_a and A values presented in Table 3.7 for biomasses and their pseudo-components.

It is possible to observe from this figure that there is a gap between experimental and modeled data at temperatures above 400°C, for the three biomasses. Comparing these results with Fraser-Suzuki fitting presented in Fig. 3.4, it can be noticed that the behavior of modeled pseudo-hemicellulose and pseudo-cellulose is in good agreement with the deconvolution patterns initially proposed. As a result, a good agreement is also obtained between modeled and experimental decomposition at temperatures below 400°C. In contrast, it is clear that the main differences observed are related to pseudo-lignin. This is principally due to the complexity of modeling the pseudo-lignin decomposition behavior in the investigated temperature range. In spite of this, the fitting error below 10% for the three materials showed that the calculated kinetic parameters using model-free isoconversional methods are suitable for the description of the biomasses thermal decomposition.

3.4 Conclusion

In this study, the thermal decomposition of three lignocellulosic biomasses with different macromolecular composition but nearly the same H/C and O/C fraction was investigated. Bamboo guadua (BG), coconut shells (CS) and oil palm shells (OPS) were used.

In general, the approach presented in this paper using a parallel reaction model using Fraser-Suzuki deconvolution and model-free isoconversional methods proved to be suitable to determine the pyrolysis kinetic parameters of biomasses with H/C and O/C near 1.5 and 0.8. Despite the differences in the hemicellulose, cellulose and lignin fraction of biomasses, any of the presented isoconversional methods can be used to calculate and predict the pseudo-components activation energy and pre-exponential factor, and to estimate their decomposition mechanism. This information could constitute a valuable tool for reactors design and for the development and scale-up of pyrolysis and gasification processes using tropical lignocellulosic agrowastes as a feedstock.

The apparent activation energy of biomass pseudo-components, followed the same behavior for the three studied materials: pseudo-hemicellulose E_a < pseudo-cellulose E_a < pseudo-lignin E_a. Regarding the decomposition mechanism, pseudo-hemicellulose and pseudo-cellulose were well described by a second order model, and a random-scission or an A1.5 Avrami-Erofeev model, respectively. For its part, pseudo-lignin decomposition did not completely match with any known theoretical model, and was described by a combination of a high order model with n between 11 and 12, and a third dimension diffusion model. Lignin behavior was possibly due to the complexity of its structure and to the interactions with the other biomass components.

Differences between the calculated kinetic parameters of BG, CS and OPS showed that biomass structure and molecular composition play a role in the biomass decomposition characteristics. Considering the nature of lignin, it could have an impact in the required energy to decompose hemicellulose and cellulose. The apparent activation energy for the three biomass pseudo-components followed the order BG E_a < CS E_a < OPS E_a; with OPS and BG being the highest lignin and lowest lignin content biomasses analyzed in this study, respectively. For the three studied materials, the model fitting error below 10% showed that the calculated kinetic parameters using model-free isoconversional methods are suitable for the description and prediction of the biomasses thermal decomposition.

Bibliography

[1] Kifayat Ullah, Vinod Kumar Sharma, Sunil Dhingra, Giacobbe Braccio, Mushtaq Ahmad, and Sofia Sofia. "Assessing the lignocellulosic biomass resources potential in developing countries: A critical review." In: *Renewable and Sustainable Energy Reviews* 51 (2015), pp. 682–698 (cit. on p. 52).

[2] Humberto Escalante, Janneth Orduz, Henry J. Zapata, Maria Cecilia Cardona, and Martha Duarte. "Potencial energético de la biomasa residual." In: *Atlas del Potencial Energético de Biomasa Residual en Colombia*. Ed. by Ministerio de Minas y Energia - Republica de Colombia. 2010. Chap. Anexo E, pp. 155–172 (cit. on p. 52).

[3] Jesus a. García N. and Edgar E. Yañez A. "Generación y uso de biomasa en plantas de beneficio de palma de aceite en Colombia - Power generation and use of biomass at palm oil mills in Colombia." In: *Revista Palmas* 31.2 (2010), pp. 41–48 (cit. on p. 52).

[4] Food and Agriculture Organisation of the United Nations. *FAO statistical yearbook 2014: Latin America and the Caribbean*. Santiago de Chile, 2014, p. 878 (cit. on p. 52).

[5] Lydia Fryda, Claudia Daza, Jan Pels, Arno Janssen, and Robin Zwart. "Lab-scale co-firing of virgin and torrefied bamboo species Guadua angustifolia Kunth as a fuel substitute in coal fired power plants." In: *Biomass and Bioenergy* 65 (June 2014), pp. 28–41 (cit. on pp. 52, 53).

[6] Ximena Londoño, Gloria C. Camayo, Néstor Riaño, and Yamel López. "Characterization of the anatomy of Guadua angustifolia (Poaceae: Bambusoideae) culms." In: *Bamboo Science and Culture* 16.1 (2002), pp. 18–31 (cit. on p. 52).

[7] Po-Chih Kuo, Wei Wu, and Wei-Hsin Chen. "Gasification performances of raw and torrefied biomass in a downdraft fixed bed gasifier using thermodynamic analysis." In: *Fuel* 117 (Jan. 2014), pp. 1231–1241 (cit. on p. 52).

[8] Thanasit Wongsiriamnuay, Nattakarn Kannang, and Nakorn Tippayawong. "Effect of operating conditions on catalytic gasification of bamboo in a fluidized bed." In: *International Journal of Chemical Engineering* 2013 (2013) (cit. on p. 52).

[9] Dengyu Chen, Dong Liu, Hongru Zhang, Yong Chen, and Qian Li. "Bamboo pyrolysis using TG–FTIR and a lab-scale reactor: Analysis of pyrolysis behavior, product properties, and carbon and energy yields." In: *Fuel* 148 (May 2015), pp. 79–86 (cit. on p. 52).

[10] Carlos A. Forero Núñez, Alexandra Cediel, Laura Carolina Hernández, José Ulises Castellanos, and Fabio Emiro Sierra Vargas. "Oil Palm Empty Bunch fruits and coconut shells gasification using a lab-scale downdraft fixed bed gasifier at Universidad Nacional de Colombia." In: *20th European Conference and Exhibition*. Milan, Italy, 2012, pp. 1112–1114 (cit. on p. 53).

[11] Lina María Romero Millán, María Alejandra Cruz Domínguez, and Fabio Emiro Sierra Vargas. "Efecto de la temperatura en el potencial de aprovechamiento energético de los productos de la pirólisis del cuesco de palma." In: *Revista Tecnura* 20.48 (2016), pp. 89–99 (cit. on p. 53).

[12] Prabir Basu. "Tar Production and Destruction." In: *Biomass Gasification, Pyrolysis and Torrefaction*. Elsevier, 2013. Chap. Chapter 6, pp. 177–198 (cit. on pp. 53, 58, 60).

[13] E. David and J. Kopac. "Activated carbons derived from residual biomass pyrolysis and their CO2 adsorption capacity." In: *Journal of Analytical and Applied Pyrolysis* 110 (2014), pp. 322–332 (cit. on p. 53).

[14] Liyi Ye, Jingmiao Zhang, Jie Zhao, Zhiming Luo, Song Tu, and Yingwu Yin. "Properties of biochar obtained from pyrolysis of bamboo shoot shell." In: *Journal of Analytical and Applied Pyrolysis* 114 (May 2015), pp. 172–178 (cit. on p. 53).

[15] Faisal Abnisa, Arash Arami-Niya, W.M.A. Wan Daud, J.N. Sahu, and I.M. Noor. "Utilization of oil palm tree residues to produce bio-oil and bio-char via pyrolysis." In: *Energy Conversion and Management* 76 (Dec. 2013), pp. 1073–1082 (cit. on p. 53).

[16] John E. White, W. James Catallo, and Benjamin L. Legendre. "Biomass pyrolysis kinetics: A comparative critical review with relevant agricultural residue case studies." In: *Journal of Analytical and Applied Pyrolysis* 91.1 (2011), pp. 1–33 (cit. on p. 53).

[17] Sergey Vyazovkin and Charles A Wight. "Model-free and model-fitting approaches to kinetic analysis of isothermal and nonisothermal data." In: *Thermochimica Acta* 340 (1999), pp. 53–68 (cit. on p. 53).

[18] Sergey Vyazovkin, Alan K. Burnham, José M. Criado, Luis A. Pérez-Maqueda, Crisan Popescu, and Nicolas Sbirrazzuoli. "ICTAC Kinetics Committee recommendations for performing kinetic computations on thermal analysis data." In: *Thermochimica Acta* 520.1 (2011), pp. 1–19 (cit. on pp. 53, 56, 57, 64).

[19] Xin Huang, Jing-Pei Cao, Xiao-Yan Zhao, Jing-Xian Wang, Xing Fan, Yun-Peng Zhao, and Xian-Yong Wei. "Pyrolysis kinetics of soybean straw using thermogravimetric analysis." In: *Fuel* 169 (Apr. 2016), pp. 93–98 (cit. on p. 53).

[20] Zhongqing Ma, Dengyu Chen, Jie Gu, Binfu Bao, and Qisheng Zhang. "Determination of pyrolysis characteristics and kinetics of palm kernel shell using TGA–FTIR and model-free integral methods." In: *Energy Conversion and Management* 89 (Jan. 2015), pp. 251–259 (cit. on p. 53).

[21] Katarzyna Slopiecka, Pietro Bartocci, and Francesco Fantozzi. "Thermogravimetric analysis and kinetic study of poplar wood pyrolysis." In: *Applied Energy* 97 (Sept. 2012), pp. 491–497 (cit. on p. 53).

[22] Xun Wang, Mian Hu, Wanyong Hu, Zhihua Chen, Shiming Liu, Zhiquan Hu, and Bo Xiao. "Thermogravimetric kinetic study of agricultural residue biomass pyrolysis based on combined kinetics." In: *Bioresource Technology* 219 (2016), pp. 510–520 (cit. on pp. 53, 66).

[23] Antonio Perejón, Pedro E Sánchez-Jiménez, Jose M. Criado, and Luis A Pérez-Maqueda. "Kinetic analysis of complex solid-state reactions. A new deconvolution procedure." In: *The journal of physical chemistry. B* 115.8 (2011), pp. 1780–91 (cit. on pp. 53, 60).

[24] Mian Hu, Zhihua Chen, Shengkai Wang, Dabin Guo, Caifeng Ma, Yan Zhou, Jian Chen, Mahmood Laghari, Saima Fazal, Bo Xiao, Beiping Zhang, and Shu Ma. "Thermogravimetric kinetics of lignocellulosic biomass slow pyrolysis using distributed activation energy model, Fraser–Suzuki deconvolution, and isoconversional method." In: *Energy Conversion and Management* 118 (June 2016), pp. 1–11 (cit. on pp. 53, 64, 66).

[25] Bojan Janković. "Devolatilization kinetics of swine manure solid pyrolysis using deconvolution procedure. Determination of the bio-oil/liquid yields and char gasification." In: *Fuel Processing Technology* 138 (2015), pp. 1–13 (cit. on p. 53).

[26] Mohammad Taghi Taghizadeh, Nazanin Yeganeh, and Mostafa Rezaei. "Kinetic analysis of the complex process of poly(vinyl alcohol) pyrolysis using a new coupled peak deconvolution method." In: *Journal of Thermal Analysis and Calorimetry* 118.3 (2014), pp. 1733–1746 (cit. on pp. 53, 56, 57).

[27] Alneira Cuéllar and Ismael Muñoz. "Fibra de guadua como refuerzo de matrices poliméricas - Bamboo fiber reinforcement for polymer matrix." In: *Dyna* 77.162 (2010), pp. 137–142 (cit. on p. 54).

[28] Q Mortley, W A Mellowes, and S Thomas. "Activated Carbons From Materials of Varying Morphological Structure." In: *Themochimica Acta* 129 (1988), pp. 173–186 (cit. on p. 54).

[29] J A García-Núñez, M García-Pérez, and K C Das. "Determination of Kinetic Parameters of Thermal Degradation of Palm Oil Mill By-Products Using Thermogravimetric Analysis and Differential Scanning Calorimetry." In: *Transactions of the ASABE* 51.2 (2008), pp. 547–557 (cit. on p. 54).

[30] Michael E. Brown. *Handbook of Thermal Analysis and Calorimetry. Volume 1. Principles and Practice*. Ed. by Michael Brown. First Edit. Elsevier, 1998, p. 725 (cit. on pp. 56, 62, 65).

[31] Andrés Anca-Couce, Anka Berger, and Nico Zobel. "How to determine consistent biomass pyrolysis kinetics in a parallel reaction scheme." In: *Fuel* 123 (2014), pp. 230–240 (cit. on p. 56).

[32] Andrés Anca-Couce, Nico Zobel, Anka Berger, and Frank Behrendt. "Smouldering of pine wood: Kinetics and reaction heats." In: *Combustion and Flame* 159.4 (2012), pp. 1708–1719 (cit. on pp. 56, 57).

[33] Roman Svoboda and Jiří Málek. "Applicability of Fraser–Suzuki function in kinetic analysis of complex crystallization processes." In: *Journal of Thermal Analysis and Calorimetry* 111.2 (Feb. 2013), pp. 1045–1056 (cit. on p. 57).

[34] P. Rajeshwari and T. K. Dey. "Advanced isoconversional and master plot analyses on non-isothermal degradation kinetics of AlN (nano)-reinforced HDPE composites." In: *Journal of Thermal Analysis and Calorimetry* 125.1 (2016), pp. 369–386 (cit. on p. 57).

[35] Francisco J Gotor, José M Criado, Jiri Malek, and Nobuyoshi Koga. "Kinetic Analysis of Solid-State Reactions: The Universality of Master Plots for Analyzing Isothermal and Nonisothermal Experiments." In: *Journal of Physical Chemistry A* 104 (2000), pp. 10777–10782 (cit. on p. 58).

[36] Pedro E. Sánchez-Jiménez, Luis A. Pérez-Maqueda, Antonio Perejón, and José M. Criado. "Generalized master plots as a straightforward approach for determining the kinetic model: The case of cellulose pyrolysis." In: *Thermochimica Acta* 552 (2013), pp. 54–59 (cit. on pp. 58, 66).

[37] Tao Kan, Vladimir Strezov, and Tim J. Evans. "Lignocellulosic biomass pyrolysis: A review of product properties and effects of pyrolysis parameters." In: *Renewable and Sustainable Energy Reviews* 57 (May 2016), pp. 1126–1140 (cit. on p. 58).

[38] Haiping Yang, Rong Yan, Hanping Chen, Dong Ho Lee, and Chuguang Zheng. "Characteristics of hemicellulose, cellulose and lignin pyrolysis." In: *Fuel* 86.12-13 (Aug. 2007), pp. 1781–1788 (cit. on p. 60).

[39] Wu-Jun Liu, Fan-Xin Zeng, Hong Jiang, and Xue-Song Zhang. "Preparation of high adsorption capacity bio-chars from waste biomass." In: *Bioresource technology* 102.17 (Sept. 2011), pp. 8247–52 (cit. on p. 60).

[40] Venugopal Mendu, Anne E Harman-Ware, Mark Crocker, Jungho Jae, Jozsef Stork, Samuel Morton, Andrew Placido, George Huber, and Seth Debolt. "Identification and thermochemical analysis of high-lignin feedstocks for biofuel and biochemical production." In: *Biotechnology for biofuels* 4 (2011), pp. 1–13 (cit. on p. 60).

[41] François-Xavier Collard and Joël Blin. "A review on pyrolysis of biomass constituents: Mechanisms and composition of the products obtained from the conversion of cellulose, hemicelluloses and lignin." In: *Renewable and Sustainable Energy Reviews* 38 (2014), pp. 594–608 (cit. on p. 64).

[42] Stylianos D. Stefanidis, Konstantinos G. Kalogiannis, Eleni F. Iliopoulou, Petros A. Pilavachi, Chrysoula M. Michailof, and Angelos A. Lappas. "A study of lignocellulosic biomass pyrolysis via the pyrolysis of cellulose, hemicellulose and lignin." In: *Journal of Analytical and Applied Pyrolysis* 105 (2014), pp. 143–150 (cit. on p. 64).

[43] Guozhan Jiang, Daniel J. Nowakowski, and Anthony V. Bridgwater. "A systematic study of the kinetics of lignin pyrolysis." In: *Thermochimica Acta* 498.1 (2010), pp. 61–66 (cit. on p. 64).

[44] J.A. Caballero, J.A. Conesa, R. Font, and A. Marcilla. "Pyrolysis kinetics of almond shells and olive stones considering their organic fractions." In: *Journal of Analytical and Applied Pyrolysis* 42.2 (July 1997), pp. 159–175 (cit. on p. 64).

[45] Zhihua Chen, Mian Hu, Xiaolei Zhu, Dabin Guo, Shiming Liu, Zhiquan Hu, Bo Xiao, Jingbo Wang, and Mahmood Laghari. "Characteristics and kinetic study on pyrolysis of five lignocellulosic biomass via thermogravimetric analysis." In: *Bioresource Technology* 192 (2015), pp. 441–450 (cit. on pp. 64, 66).

[46] Agustín García Barneto, José Ariza Carmona, José E. Martín Alfonso, and Rafael Sánchez Serrano. "Simulation of the thermogravimetry analysis of three non-wood pulps." In: *Bioresource Technology* 101.9 (2010), pp. 3220–3229 (cit. on p. 64).

[47] Carmen Branca, Alessandro Albano, and Colomba Di Blasi. "Critical evaluation of global mechanisms of wood devolatilization." In: *Thermochimica Acta* 429.2 (2005), pp. 133–141 (cit. on p. 64).

[48] Asri Gani and Ichiro Naruse. "Effect of cellulose and lignin content on pyrolysis and combustion characteristics for several types of biomass." In: *Renewable Energy* 32.4 (2007), pp. 649–661 (cit. on p. 64).

[49] Dangzhen Lv, Minghou Xu, Xiaowei Liu, Zhonghua Zhan, Zhiyuan Li, and Hong Yao. "Effect of cellulose, lignin, alkali and alkaline earth metallic species on biomass pyrolysis and gasification." In: *Fuel Processing Technology* 91.8 (Aug. 2010), pp. 903–909 (cit. on pp. 64, 66).

[50] Song Hu, Andreas Jess, and Minhou Xu. "Kinetic study of Chinese biomass slow pyrolysis: Comparison of different kinetic models." In: *Fuel* 86.17-18 (2007), pp. 2778–2788 (cit. on pp. 65, 66).

[51] Pedro E. Sanchez-Jimenez, Luis A. Pérez-Maqueda, Antonio Perej??n, and Jos?? M. Criado. "Generalized kinetic master plots for the thermal degradation of polymers following a random scission mechanism." In: *Journal of Physical Chemistry A* 114.30 (2010), pp. 7868–7876 (cit. on p. 65).

[52] Alan K Burnham, Xiaowei Zhou, and Linda J Broadbelt. "Critical Review of the Global Chemical Kinetics of Cellulose Thermal Decomposition." In: *Energy & Fuels* 29 (2015), pp. 2906–2918 (cit. on p. 66).

Chapter

4

Steam gasification behavior of tropical agrowastes: a new modeling approach based on the inorganic composition

This chapter was published as a research paper in an international journal, reference: Romero Millán LM, Sierra Vargas FE, Nzihou A. Steam gasification behavior of tropical agrowaste: A new modeling approach based on the inorganic composition. Fuel 2019;235:45–53. doi:10.1016/j.fuel.2018.07.053.

Abstract

The steam gasification and co-gasification reactivity and kinetics of coconut shells, oil palm shells and bamboo guadua were studied from an isothermal thermogravimetric analysis, with temperatures ranging from 750°C to 900°C, and steam partial pressures

from 3 to 10 kPa. In the analyzed experimental range, inorganics were identified as the most influential parameter in biomass reactivity and kinetics. Accordingly, a new modeling approach is proposed to predict the gasification behavior of lignocellulosic agrowastes based on their inorganic composition. A good agreement between the experimental and modeled data was found, showing that the proposed approach is suitable for the description and prediction of the gasification behavior of biomasses with different macromolecular structure and within a wide range of inorganic composition, and H/C and O/C ratios near 1.5 and 0.8 respectively. This kinetic model could constitute a valuable tool for reactor design and scale-up of steam gasification facilities using tropical lignocellulosic feedstocks.

4.1 Introduction

Tropical regions are rich in biodiversity thanks to their geographic location and climate conditions. In this regard, they are appropriate for the development of agricultural activities and cultivation of a great variety of crops. Several developing countries in tropical regions base their economy in agriculture and farming and produce great amounts of agro-wastes that usually remain under-exploited. These residues could be valorized as biofuels or transformed into value-added products, giving new development opportunities for local communities.

In this regard, gasification is a very interesting thermochemical process for the recovery of energy from agrowastes. In particular, steam gasification produces high heating value fuel gases that can be used for the generation of heat and power [1–4]. However, the valorization of agrowastes could have some restrictions. One of the most important is probably the fact that agricultural residues availability often depends on seasonal crops. Consequently, most gasification facilities should operate intermittently, or work with different kind of residues or even blends.

Several authors have highlighted the differences in the gasification behavior of chars from different biomasses. In particular, the inorganic elements are reported to be the most influential parameter in the steam gasification reactivity and conversion profile [5, 6]. Alkali and alkali earth metals (AAEM) like K, Na, Ca and Mg, which are present in indigenous biomass could have a catalytic effect on biomass gasification [7]. Among these elements, K has been reported to be the most active species for steam and CO_2 gasification of charcoal and biomass [8, 9]. In contrast, Si, Al or P may inhibit this catalytic effect, as they tend to react with AAEM [10, 11].

Most studies related with the impact of inorganics in the gasification behavior of biomasses use impregnation techniques to modify the composition of the samples [8, 12–15]. In general, these treatments allow a good understanding of the effects of inorganics on gasification. However, the behavior of impregnated inorganic elements may differ from the one of inorganic elements in their natural form and distribution in biomass. In this regard, Dupont et al. [16] studied 21 samples of woody biomasses, confirming the beneficial impact of K and the inhibitory effect of Si in the indigenous biomass. Generally, authors analyze the gasification behavior of biomasses individually. Nevertheless, most gasification applications in developing countries should work with different kind of residues or blends depending on their availability. In this context, the understanding of the impact of biomass characteristics and blends interactions in their

gasification behavior is important in order to properly adapt the process parameters and conditions to the application.

To describe the steam gasification behavior of biomasses, several authors have proposed different kinetic approaches, some of them incorporating the impact of inorganic elements. In this regard, Kajita et al. [17] considered that gasification occurs in a parallel reaction scheme and developed a dual Langmuir-Hinshelwood model, identifying K as the main catalytic element. This study highlighted the beneficial impact of K, but did not deal with other inorganic elements present in biomasses. For their part, Zhang et al. [10] analyzed the influence of AAEM and Si in the gasification behavior of different biomasses. They proposed a modified random pore model, introducing two dimensionless parameters that depends on the inorganic content of samples. Even when the calculation method of these parameters was not explicitly presented, the authors concluded that the gasification reactivities of biomasses are governed mainly by the amount of inorganic species. More recently, Dupont et al. [6] proposed a kinetic approach with two different kinetic laws for biomasses with inorganic ratio K/(Si+P) $>$ 1 and K/(Si+P) $<$ 1. A zeroth-order and a volumetric first-order model were found to describe the behavior of samples, respectively. Furthermore, in the case of biomasses with K/(Si+P) $>$ 1, the authors suggest that the gasification kinetics can be predicted simply through the knowledge of the K content of the sample. Even when the proposed approach in this work can satisfactorily estimate the behavior of biomasses within a wide range of inorganic compositions, the conversion of samples with intermediate values of inorganic ratio (K/(Si+P) $\sim$ 1) is not completely described. The authors stated that the decomposition of these biomasses can be estimated either with a zeroth or a first order law. Additionally, concerning the analysis of the simultaneous steam gasification of different kind of biomasses and their kinetic modeling, no studies have been found in the literature until now.

Accordingly, the aim of this work is to study the steam gasification behavior of three tropical lignocellulosic biomasses and their blends, from an isothermal thermogravimetric analysis. The influence of the gasification temperature and steam partial pressure on the gasification reactivity of biomasses was discussed. Also, the impact of biomasses and blends composition on the gasification reactivity and kinetics was analyzed. An approach using model-free isoconversional methods and generalized master plots was used to determine the gasification kinetic parameters of the samples and compare their decomposition behavior. As a result, a new model with a unique kinetic equation is proposed to describe and predict the steam gasification behavior of tropical lignocellulosic agrowastes based on their inorganic composition.

4.2 Materials and methods

4.2.1 Biomass samples

Three tropical lignocellulosic feedstocks were selected for this study: oil palm shells (OPS), coconut shells (CS) and bamboo guadua (BG). The samples were collected in Colombia, South America, and were provided by a palm oil extraction plant, a food processing industry, and a furniture and handicraft construction site, respectively. The origin of selected samples has been detailed on a previous work [18]. The chemical composition of the biomasses was determined according to the standards of solid biofuels with at least three replicates, and is presented in tables 4.1 and 4.2.

Table 4.1: Organic composition of studied biomasses

		OPS	CS	BG
Elemental Analysis (wt. % daf)	C	46.7±0.2	46.8 ±0.2	42.7±0.3
	H	6.5±0.1	5.8 ±0.1	5.4±0.1
	O*	46.2±0.1	47.1 ±0.1	51.5±0.1
	N	0.6±0.1	0.3 ±0.1	0.4±0.1
	O/C	0.7±0.1	0.7±0.1	0.9±0.1
	H/C	1.7±0.1	1.5±0.1	1.5±0.1
Proximate analysis (wt. %)	Moisture	9.5±0.4	10.2±0.2	9.0±0.3
	Volatile Matter	69.9±0.3	71.4±0.3	68.3±0.2
	Fixed Carbon*	19.0±0.3	17.1±0.2	18.1±0.3
	Ash	1.6±0.2	1.3±0.1	4.6±0.4
Molecular composition (wt % daf)	Cellulose	30.4	32.5	53.9
	Hemicellulose	12.7	20.5	13.5
	Lignin	49.8	36.5	25.1

* Calculated by difference

Table 4.2: Major inorganic composition of studied biomasses

		OPS	CS	BG
Inorganic composition (mg/kg dry basis)	Al	1 500±22	262±8	243±34
	Ca	54±6	391±73	441±99
	Fe	107 ±4	160±28	116±17
	K	1 006±15	2 808±44	5 360±85
	Mg	135±3	170±15	173±10
	Na	1.5±0.5	33±11	2±0.8
	P	270±7	397±40	829±62
	Si	5 600±39	309±43	19 372±354

Elemental composition (C, H, N, S, and O) was determined using a Themoquest NA 2000 elemental analyzer, while inorganic speciation was determined using an HORIBA Jobin Yvon Ultima 2 inductively coupled plasma optical emission spectrometer (ICP-OES), based on EN 16967 standard. Proximate analysis was calculated according to the standards EN ISO 18134-3, EN ISO 18123 and EN ISO 18122, respectively. Molecular composition of the biomasses is referred to literature reported values [19–21].

The raw biomasses were milled and sieved to a size range between 100 µm and 150 µm before TGA. The characteristic time analysis of the experiments showed that under the presented conditions, limitations by heat or mass transfer can be neglected. Bi-component biomass blends were prepared after milling and sieving using different proportions.

4.2.2 Isothermal TGA gasification experiments

Raw biomasses and biomass blends gasification under steam was performed using a Seratam TG-ATD 92 thermal analyzer, coupled with a Wetsys humid gas generator. Approximately 20 mg of each sample were placed in an aluminum crucible and heated from 25°C to the final gasification temperature (750°C, 800°C and 900°C) at a heating

rate of 10 °C/min, under an inert atmosphere. After 10 minutes, the measured mass loss of the sample was below 0.01%/min and then, it was considered that the pyrolysis stage has finished. The atmosphere was then switched to a mixture of H_2O/N_2 (steam partial pressure from 3.7 kPa to 10 kPa). The total flow rate was 4 l/h for all the experiments.

TGA experiments were conducted twice and averaged to verify their repeatability. A blank test was made for each experimental condition to exclude buoyancy effects. For each experimental condition, the repeatability was found to be satisfactory, as the calculated standard deviation of the mass loss was below 1%.

4.2.3 Reactivity and kinetic study

Theoretical background

The isothermal gasification experiments described are the basis of the kinetic analysis of biomasses decomposition under a steam atmosphere. The degree of conversion or reaction extent during gasification is defined as in Eq. 4.2.1:

$$\alpha = \frac{m_0 - m(t)}{m_0 - m_f} \tag{4.2.1}$$

Where m_0 is the mass of the sample at the beginning of the gasification stage, m_f the final mass, and m the current mass at a given time. According to this, the apparent gasification reactivity can be defined as a function of the conversion degree α:

$$R(\alpha) = \frac{1}{1-\alpha}\frac{d\alpha}{dt} \tag{4.2.2}$$

Moreover, the gasification reaction rate $d\alpha/dt$ can described as in Eq. 4.2.3:

$$\frac{d\alpha}{dt} = k(T)h(P_{H_2O})f(\alpha) \tag{4.2.3}$$

Where $k(T)$ is the Arrhenius equation, representing the temperature dependence of the process, $h(P)$ the relation expressing the gasification agent partial pressure dependence, and $f(\alpha)$ the reaction model function representing how the solid state decomposition process occurs. Different authors have suggested that the influence of the reactive atmosphere partial pressure in the reaction rate is described by a power law with a constant exponent value, for almost all conversion levels [22–24].

According to this, the reaction rate can be then written as follows:

$$\frac{d\alpha}{dt} = A\exp\left(\frac{-E_a}{RT}\right)P_{H_2O}^n f(\alpha) \tag{4.2.4}$$

Isoconversional model free approach

In this study, an isoconversional model-free approach was used to determine the Arrhenius parameters of steam gasification of biomasses. Isoconversional methods are based

on the hypothesis that the reaction rate at a constant degree of conversion is only a function of temperature and pressure, and then, the activation energy of the process can be calculated without a previous assumption of the reaction model [24, 25]. Also, the dependency of E_a with α can give information about the existence of a single-step or multi-step kinetics [26].

Besides the calculation of the apparent activation energy, the appropriate determination of the decomposition model describing the process is also important, as the wrong assumption of the decomposition mechanism could cause the misestimation of the kinetic parameters and an inaccurate interpretation of the process.

For biomass and coal gasification, three models are generally used in the literature for the description of char conversion. The volumetric model (VM), the shrinking core model (SCM), and the random pore model (RPM). Several studies have shown good agreement between experimental results and the three presented models, regardless of the differences in their theoretical background [27–30]. However, as there is not any relationship established between the biomass characteristics and the decomposition mechanism, no theoretical models were presupposed in this study. Isoconversional model-free methods and the generalized master-plots approach were used for the selection of the reaction expression that better describes the steam gasification process [31, 32]. Some solid-state reaction models used for char gasification or combustion description are presented in table 4.3.

Table 4.3: Most common reaction mechanisms used in solid state kinetic analysis [24,26]

	Model	$f(\alpha)$	$g(\alpha)$
Order based	Or1 - First order	$1-\alpha$	$-\ln(1-\alpha)$
	Or2 - Second order	$(1-\alpha)^2$	$[1/(1-\alpha)]-1$
	Or3 - Third order	$(1-\alpha)^3$	$(1/2)\left[1/(1-\alpha)^2\right]-1$
	Orn - nth order	$(1-\alpha)^n$	$[1/(n-1)]\left[(1-\alpha)^{(1-n)}-1\right]$
Diffusion	D1 – One dimensional	$1/(2\alpha)$	α^2
	D2 –Ttwo dimensional	$[-\ln(1-\alpha)]^{-1}$	$\alpha+(1-\alpha)\ln(1-\alpha)$
	D3 – Three dimensional	$(3/2)(1-\alpha)^{2/3}\left[1-(1-\alpha)^{1/3}\right]^{-1}$	$\left[1-(1-\alpha)^{1/3}\right]^2$
Geometrical contraction	R2 – Contracting area	$2(1-\alpha)^{1/2}$	$1-(1-\alpha)^{1/2}$
	R3 – Contracting volume	$3(1-\alpha)^{2/3}$	$1-(1-\alpha)^{1/3}$

For isothermal experiments, the reduced-generalized reaction rate expression $\lambda(\alpha)$ in Eq. 4.2.5 can be simplified and calculated without the previous knowledge of the activation energy E_a.

$$\lambda(\alpha)=\frac{f(\alpha)}{f(\alpha)_{\alpha=0.5}}=\frac{d\alpha/dt}{(d\alpha/dt)_{0.5}}\frac{\exp(E_a/RT)}{\exp(E_a/RT_{0.5})} \tag{4.2.5}$$

The most suitable $f(\alpha)$ model can be then identified as the best match between the experimental $\lambda(\alpha)$ values and the master-plots calculated from theoretical models. The generalized master-plots of the reaction models presented in table 3 and calculated according to Eq. 4.2.5, are presented in fig 4.1.

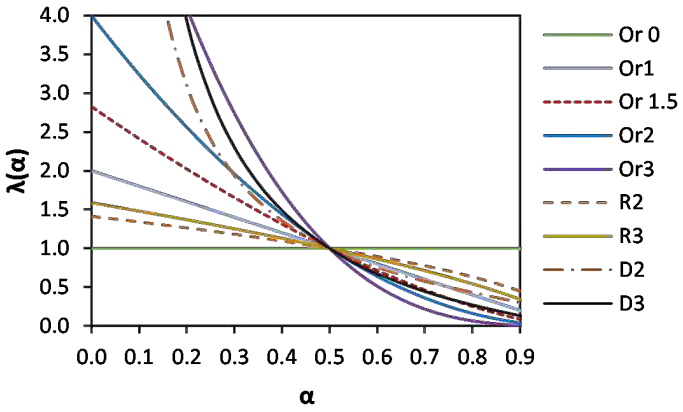

Figure 4.1: Generalized master-plots of the reaction models presented in table 4.1, calculated according to Eq. 4.2.5.

4.3 Results and discussion

4.3.1 Impact of temperature and steam partial pressure on gasification reactivity

Figure 4.2 presents the conversion degree α as a function of time of coconut shells (CS), at three different gasification temperatures and a steam partial pressure of 3.7 kPa. It is possible to observe that the gasification conversion rate is highly dependent on the temperature. An increase in the gasification temperature is associated with a reduction of the time required to reach a specific conversion degree. Accordingly, shorter reaction times are related to higher gasification reactivities.

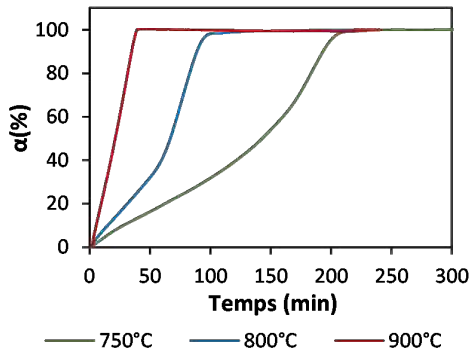

Figure 4.2: Conversion degree α vs. time of coconut shells (CS) at three different gasification temperatures and a steam partial pressure of 3.7 kPa.

In this regard, table 4.4 summarizes the steam gasification reactivity and reaction time at a conversion degree of 50% for the three raw biomasses analyzed. For all the samples, it is possible to observe that higher gasification temperatures are associated to higher reactivities and shorter reaction times. For instance, it is possible to notice that a temperature rise from 750°C to 800°C, increases twice the steam gasification reactivity of CS. Moreover, at 900°C, its reactivity is 6.6 times higher compared to 800°C. The same

trend was observed for BG and OPS. The results obtained in the analyzed temperature range are in accordance with those presented in the literature. As already described by several authors for CO_2 and steam atmospheres, at higher temperatures, the gasification process requires shorter times to be completed [33–36].

Regarding steam partial pressure, the conversion profile of coconut shells (CS) can be observed in figure 4.3 at three different steam partial pressures and an intermediate gasification temperature of 800°C. It can be noticed that an augmentation of this parameter is also associated with a decrease in the reaction time. Indeed, a higher steam partial pressure indicates a greater steam quantity available to react during the gasification stage, explaining the increase in the gasification rate of biomasses. At 800°C, CS reactivity at a conversion degree of 50% increased from 3.2 min^{-1} to 4.2 min^{-1} with a steam partial pressure rise from 3.7 kPa to 10 kPa. For its part, reaction time decreased from 67 min to 32 min, respectively. As observed with temperature, at higher steam partial pressures, the gasification process requires shorter times to be completed.

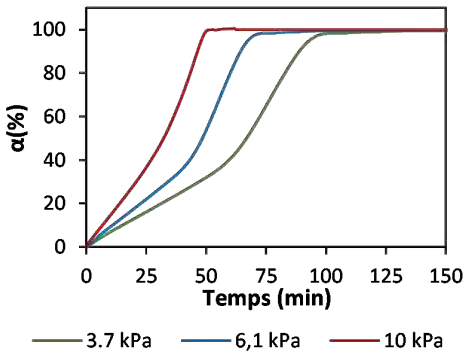

Figure 4.3: Conversion degree α vs. time of coconut shells (CS) at three different steam partial pressures and 800°C.

According to this and considering eq. 4.2.4, it is possible to determine the exponent n of the power law describing the influence of the steam partial pressure P_{H2O} on the reaction rate. For each conversion degree, this value was calculated from the slope of the plot $\ln(d\alpha/dt)$ vs $\ln(P_{H2O})$, using at least three gasification conditions. For the three raw biomasses analyzed, n remained nearly constant during all the conversion range, with a mean value of 0.5 and a standard deviation of 0.1. This result is in agreement

Table 4.4: Steam gasification reactivity and reaction time at 50% conversion. Steam partial pressure 3.7 kPa

	750°C		800°C		900°C	
Sample	**Reactivity (% min^{-1})**	**React. time (min)**	**Reactivity (% min^{-1})**	**React. time (min)**	**Reactivity (% min^{-1})**	**React. time (min)**
100%CS	0.5	142.8	1.3	66.7	8.7	21.0
100%BG	0.2	234.6	0.7	83.4	4.1	21.5
100%OPS	0.2	236.4	0.5	127.8	2.5	24.8

with the values reported by different authors between 0.4 and 0.8 for steam gasification of biomass and coal [16, 22, 37].

4.3.2 Impact of feedstock characteristics on steam gasification reactivity

The impact of the feedstock characteristics on the steam gasification reactivity was studied comparing the behavior of the three selected materials and their blends under different gasification conditions. As an example, the conversion profile of the raw biomasses at a gasification temperature of 800°C and a steam partial pressure of 3.7 kPa is presented in figure 4.4. It is possible to notice that the behavior of the three samples is notably different. In particular, CS conversion rate is nearly constant and tends to increase at high conversion levels, while OPS and BG conversion rate seems to decrease with time. This behavior was the same under all the analyzed experimental conditions.

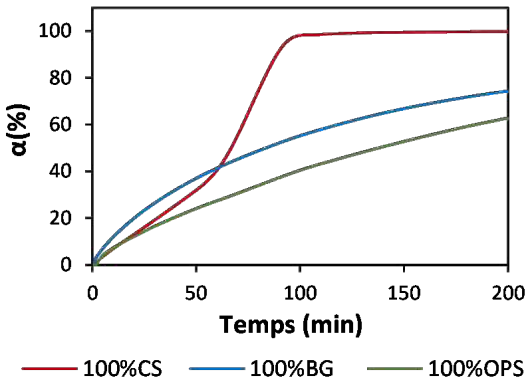

Figure 4.4: Conversion profile of the selected biomasses at 800°C and a steam partial pressure of 3.7 kPa.

Therefore, the gasification behavior does not seem to be related to the macromolecular composition of biomasses. Even when the hemicellulose, cellulose and lignin content of coconut shells and oil palm shells are similar, their gasification conversion profile are clearly different. Moreover, the behavior of oil palm shells and bamboo guadua are quite similar.

To better understand this, the figure 4.5 shows the conversion profile of coconut shells (CS) and bamboo guadua (BG), at three different gasification temperatures and a steam partial pressures of 10 kPa.

For the analyzed experimental conditions, it can be noticed that CS conversion rate is nearly constant and tends to increase at high conversion levels, as described previously. In contrast, BG conversion rate seems to decrease with time. Also, it can be observed that for a specific conversion degree, there is an important difference in the reaction time of both biomasses. For instance, at 800°C and 10 kPa, CS total conversion was reached after 55 minutes, while BG took more than 300 minutes. This behavior shows that CS have a higher gasification reactivity compared to BG. The reactivity of the three selected biomasses was already highlighted in table 4. It was possible to observe that CS reactivity is always higher compared with BG and OPS.

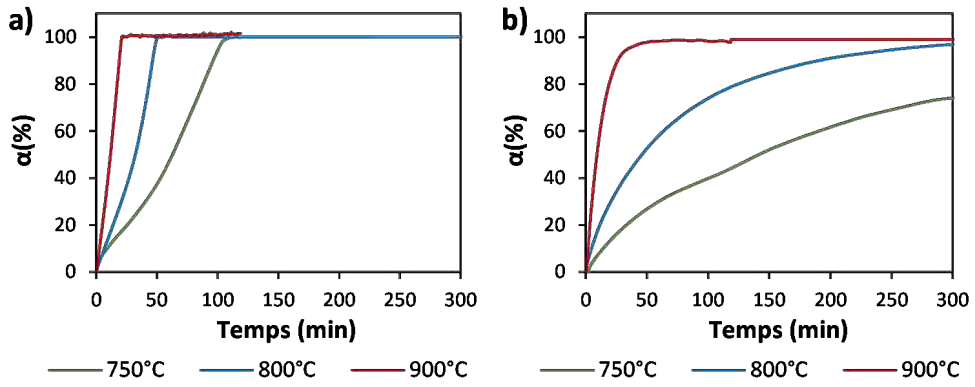

Figure 4.5: Conversion degree vs. time of CS and BG at different gasification temperatures. a) CS - 10 kPa, b) BG - 10 kPa

These differences can be related to the inherent inorganic content of raw biomasses. In particular, it is possible to notice from table 2, that coconut shells contain mainly K, Ca, Al and P, while oil palm shells and bamboo guadua are composed mainly of Si, Al, Ca and a little K. Different authors have identified the impact of inorganic elements in biomass gasification. Particularly, the catalytic effect of alkaline and alkaline earth metals (AAEM), and the inhibitory impact of Si, Al and P [9, 17, 38]. In this regard, Dupont et al [6], proposed a relevant correlation between the biomass gasification behavior and the inorganic ratio K/(Si+P). They found that biomasses with K/(Si+P) above 1 show a constant decomposition rate with a slightly increase at high conversion, while biomasses with K/(Si+P) below 1 have a decreasing rate along the whole conversion. According to this and taking into account that K has been reported to have the most beneficial impact on gasification reactivity among AAEM [39], the inorganic ratio K/(Si+P) will be used in this study to characterize and compare the inorganic composition of the selected biomasses.

The observed gasification behavior of the three analyzed biomasses may suggest that despite the differences in the macromolecular constituents, the inorganic composition of samples is the most important parameter that influences their steam gasification behavior. To better understand this impact, the gasification of different biomass blends was also studied. The inorganic ratio K/(Si+P) was calculated for each sample and is presented in table 4.5.

From experiments, it was possible to notice that the behavior of biomass blends is not clearly related to the mass blending ratio, but to the inorganic composition of the blend, calculated from the inorganic content of the individual samples.

The analysis of the gasification conversion profiles, showed that the behavior of blends is not additive, if compared to raw biomasses. Moreover, it is not possible to describe synergistic or inhibitory effects as a function of the biomass blend ratio. Since limitations by heat or mass transfer can be neglected under the presented experimental conditions, this behavior suggests that the interactions between biomasses are notably related to their inorganic content. For the analyzed biomasses and blends, it was noted that the conversion rate increased with the K/(Si+P) ratio of the sample. In this regard, a

Table 4.5: Calculated inorganic ratio K/Si+P of analyzed biomasses and blends

Biomass / blend	**K/(Si+P) (-)**
100% CS	3.98
100% BG	0.20
100% OPS	0.17
90%CS - 10%BG	1.18
85%CS - 15%BG	0.92
75%CS - 25%BG	0.61
50%CS - 50%BG	0.39
90%CS - 10%OPS	2.15
85%CS - 15%OPS	1.71
75%CS - 25%OPS	1.03
50%CS - 50%OPS	0.58

linear relationship was found between the biomass reactivity and the inorganic ratio K/(Si+P) of samples, in the analyzed temperature range, as observed in fig. 4.6. This result, confirms the fact that the inorganic species of the biomasses have an impact on their gasification behavior. The gasification reactivity increases with the inorganic ratio, highlighting the beneficial effect of K. In contrast, higher quantities of Si and P could react with K and other AAEM, inhibiting their impact in gasification reactions, and reducing the biomass gasification reactivity.

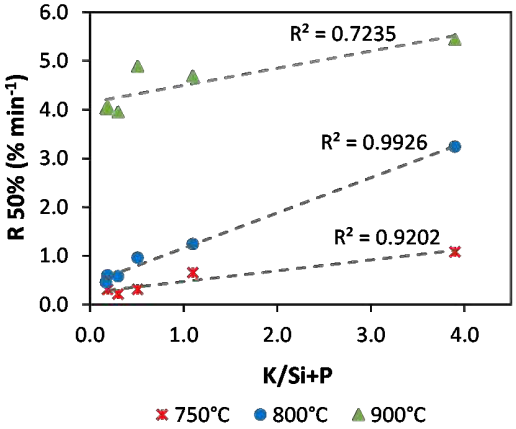

Figure 4.6: Steam gasification reactivity at a conversion degree of 50% of biomasses and blends at different temperatures and a steam partial pressure of 3.7 kPa

This observation may have an important impact in real gasification applications. As already discussed, biomasses with lower reactivities require longer gasification times or higher working temperatures to achieve a desired conversion level, impacting the energy consumption of the process. Thus, according to the feedstock characteristics, the process parameters and conditions should be properly adapted.

4.3.3 Steam gasification kinetic analysis

To better understand the impact of the inorganic composition on the biomass gasification behavior, a kinetic analysis was performed. As already presented, the decomposition curves (α Vs t) of biomasses or blends were analyzed using isoconversional methods in order to determine their kinetic triplet E_a, A and $f(\alpha)$.

Firstly, the most suitable reaction model that describes the biomasses gasification was determined using the generalized master plots approach. In general, it was observed that for all the analyzed materials, the decomposition model that best fit the gasification behavior is independent of the temperature and the steam partial pressure. This is the case for many solid-state reactions and was expected for steam gasification [26]. To better understand and compare the differences in the identified reaction models, the gasification behavior of the samples was described as a reaction order model, where n is the reaction order with respect to the reacting solid, as presented in table 3.

As already stated, for the analyzed biomasses and blends, it was observed that the identified reaction model depends on the inorganic composition. Figure 4.7a shows that the feedstocks with inorganic ratio closer or higher than 1 match closely the theoretical plot of a zeroth-order model (Or0) in almost all the conversion range. This result is in accordance with different authors that found that catalytic gasification can be properly described by a reaction order 0 with respect to the reactive solid [17, 40, 41]. The divergences observed at conversion levels above 60% are possibly related to the catalytic impact of K that becomes more evident at the end of the gasification, when the relative proportion of inorganics compared to carbon is higher.

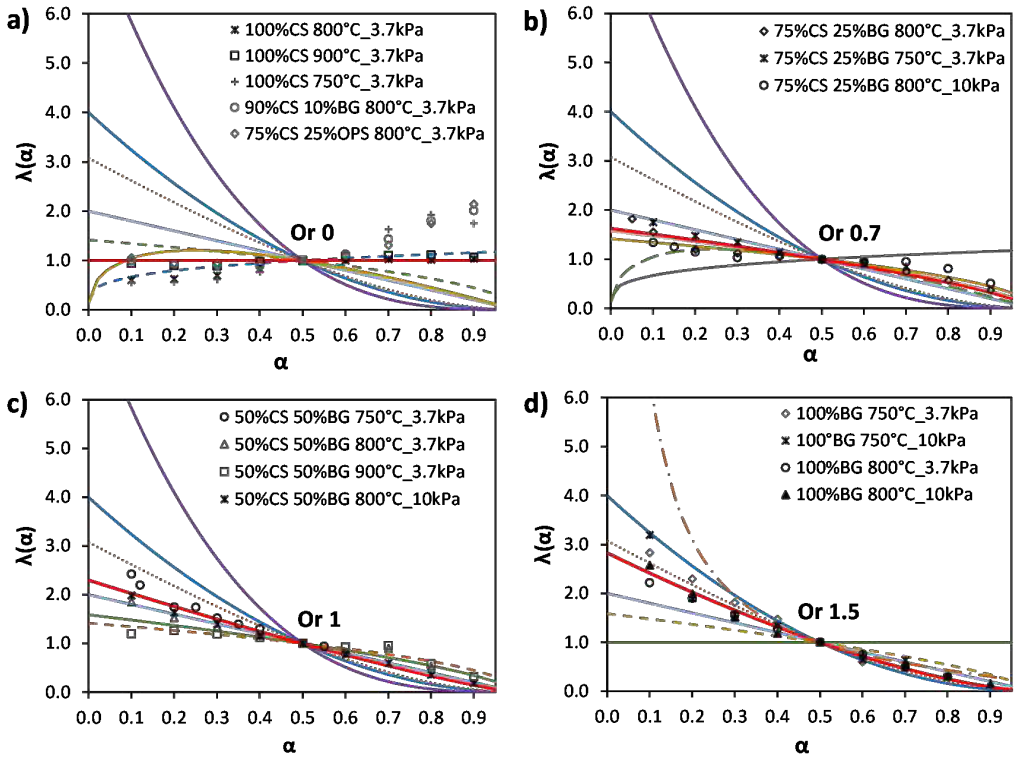

Figure 4.7: Comparison between the theoretical and experimental master plots of some analyzed samples and blends

In contrast, it can be noticed that for the biomasses and blends with inorganic ratio below 1 the most suitable reaction model identified with generalized master plots varies. With the decrease of the inorganic ratio, the reaction model moves away from a zeroth-order model and goes towards a second-order model. From figure 4.7b, c and d it is possible to observe that BG behavior is close to a reaction order 1.5, while the blends 50%CS - 50%BG and 75%CS - 25%BG approach a reaction order 1 and 0.7 respectively. From these results, it can be noticed that there is a linear and inverse relationship between the identified order of reaction and the inorganic ratio of the sample, as presented in figure 4.8.

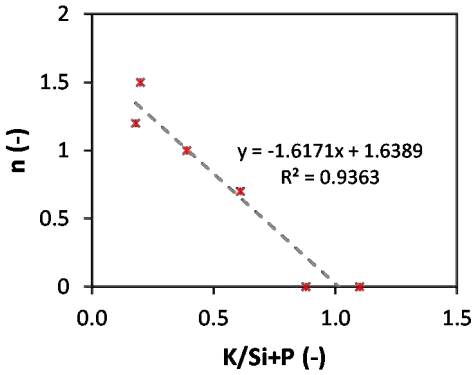

Figure 4.8: Identified reaction order vs. inorganic ratio of analyzed samples

The observed increase in the reaction order with the decrease in the inorganic ratio could be related to the inhibition of K catalytic impact by Si and P. The higher the Si and P content, the stronger the inhibition impact, and then, the lower the gasification reaction rate. This trend is in accordance with related studies which found that Si and P tend to react with AAEM reducing their catalytic impact in gasification behavior [39].

Similarly, in the case of samples with K/(Si+P) higher that one, the catalytic impact of steam gasification also depends on the inorganic ratio. Figure 4.9 shows that even when all the samples seem to follow a zeroth order reaction, the higher the K/(Si+P) content, the stronger the catalytic effect. Consequently, the total gasification time was the lowest for the biomass with the highest inorganic ratio. Moreover, the acceleration of gasification rate at the end of the conversion is more important for the biomass with the highest inorganic ratio. As already discussed, this behavior is possibly related to the catalytic impact of K that becomes more evident when the relative proportion of inorganics compared to carbon is higher.

According to these results and in agreement to previous work in the literature, it is possible to say that the steam gasification behavior of biomasses with K/(Si+P) below one follow a non-catalytic mechanism, contrary to biomasses with K/(Si+P) higher than one. The variation in the reaction order identified could be due to the interactions between the inorganic constituents of the biomass. In particular, Si and P could react with K and other AAEM to form alkali silicates, restraining their catalytic impact [10].

After the identification of the appropriate reaction model, the apparent activation energy Ea was determined from the slope of the isoconversional plots regression lines. For all

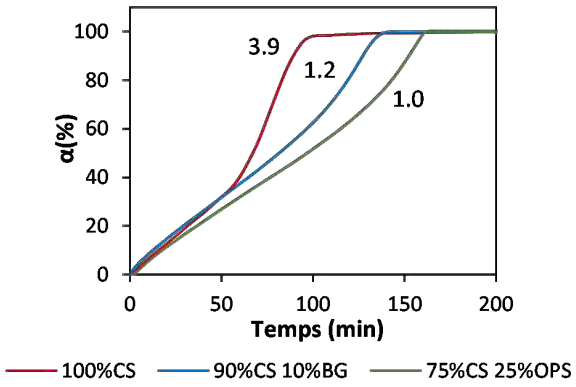

Figure 4.9: Conversion profile of different samples with inorganic ratio higher than 1 at 800°C and 3.7 kPa. The calculated inorganic ratio of the samples is indicated next to each curve.

the analyzed samples, the mean apparent E_a calculated was 134 kJ/mol, with a variation coefficient of 6% between the samples. The apparent activation energy calculated in this study is in agreement with different values reported in the literature for biomass steam gasification [16, 36, 42, 43].

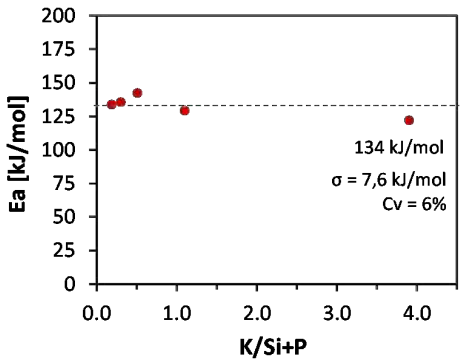

Figure 4.10: Apparent activation energy of analyzed samples as a function of the inorganic ratio.

According to figure 4.10, no relationship was found between the apparent activation energy and the inorganic coefficient of biomasses and blends. For all the analyzed samples, the calculated E_a remained almost constant with the reaction extent α, with variation coefficients below 15%. This result indicates that the E_a and the reaction model selected using master-plots approach are suitable for the description of the samples gasification during all the conversion range. Finally, the pre-exponential factor was determined from Eq. 4.2.4. A mean value of $13\,500\,\mathrm{min}^{-1}\ \mathrm{kPa}^{-0.5}$ was calculated for all the analyzed biomasses and blends. From these results, a kinetic equation that

describes the behavior of biomasses and blends as a function of their inorganic content is proposed:

$$\frac{d\alpha}{dt} = 13500 \exp\left(\frac{-134000}{RT}\right) P^{0.5}(1-\alpha)^n k_1 \tag{4.3.1}$$

Where P is the steam partial pressure in kPa, T the temperature in K, R the ideal gas constant in J mol^{-1} K^{-1}, n the theoretical model reaction order, and k_1 a coefficient that takes into account the differences observed between the gasification reaction rate of the biomasses that follow a zeroth-order model. Thus, the reaction order n and the coefficient k_1 depends on the inorganic ratio K/(Si+P) as follows:

If $K/(Si+P) \geq 1$

$$n = 0 \tag{4.3.2}$$

$$k_1 = 0.15\left(\frac{K}{Si+P}\right) + 0.7 \tag{4.3.3}$$

If $K/(Si+P) < 1$

$$n = -1.62\left(\frac{K}{Si+P}\right) + 1.64 \tag{4.3.4}$$

$$k_1 = 1 \tag{4.3.5}$$

Unlike the existing models that propose different kinetic laws for catalytic and non-catalytic gasification [6, 17], it is worth mentioning that the presented kinetic equation (Eq. 4.3.1) allows the description of the steam gasification behavior of biomasses within a wide range of inorganic compositions, including those with an inorganic ratio close to 1. Moreover, the coefficient k_1 was found to be proportional to the inorganic ratio K/(Si+P) and not to the K content, for the samples that follow a zeroth-order model. In this regard, the presented kinetic approach facilitates the understanding of the influence of biomass inorganic species and their interactions, on the steam gasification process. Furthermore, it confirms the validity of the inorganic ratio K/Si+P proposed by Hognon et al. [38] to describe biomasses and predict their steam gasification behavior.

The proposed kinetic equation was validated and used to reproduce the gasification behavior of the studied biomasses and their blends. For all the analyzed samples and gasification conditions, a good agreement was found between the experimental and the calculated data. The fit error E was determined according to Eq. 4.3.6,

$$Fit\ error(\%) = 100\left(\frac{\sqrt{\left(\left(\frac{d\alpha_i}{dT}\right)_{exp} - \left(\frac{d\alpha_i}{dT}\right)_{calc}\right)^2}}{\sqrt{N}\left(\frac{d\alpha_i}{dT}\right)_{exp,max}}\right) \tag{4.3.6}$$

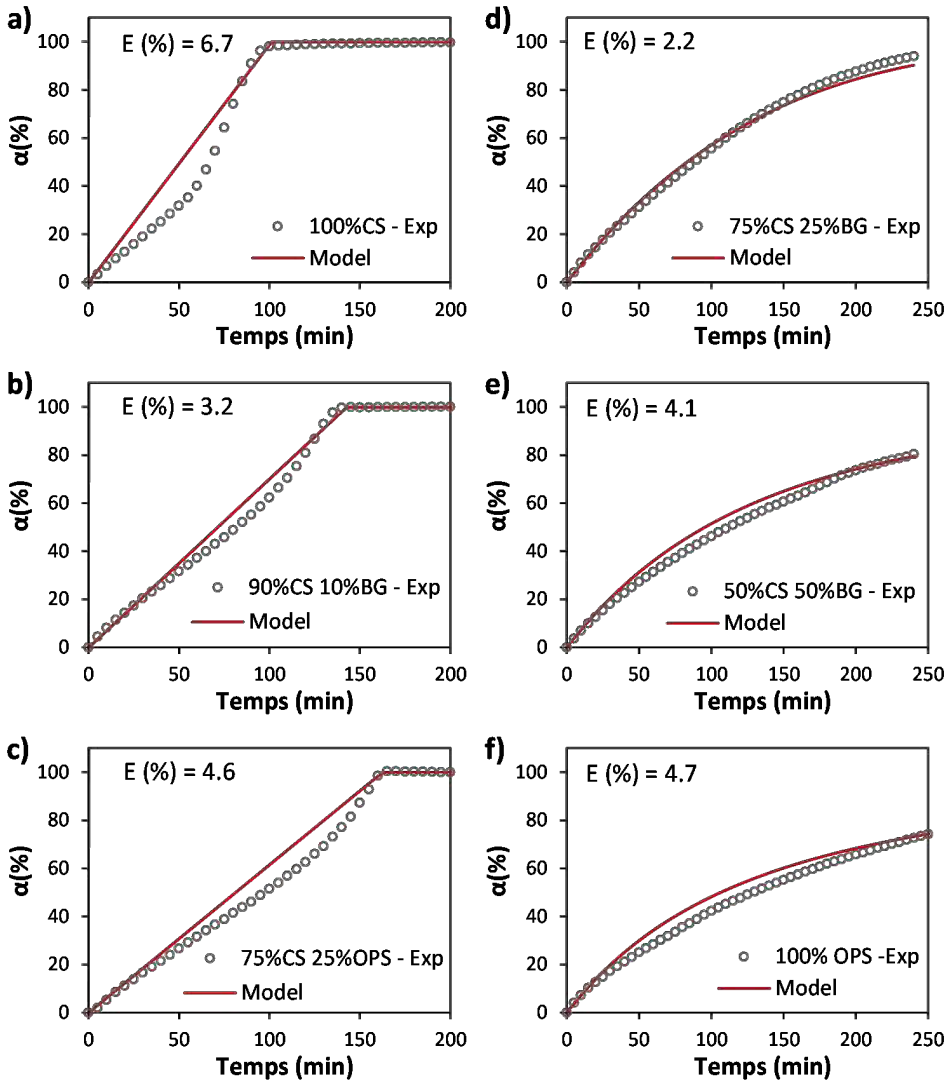

Figure 4.11: Comparison between the experimental and modeled decomposition curves of analyzed samples at 800°C and 3.7kPa.

Where $d\alpha/dt$ are the experimental and calculated values of the decomposition rate, and N is the total number of experimental points [44].

The calculated fitting error was below 7% in all cases. This value was considered reasonable, taking into account the heterogeneity of the biomasses and the incertitude in the measurement of their inorganic composition. Figure 4.11 shows the comparison between the experimental results and the model predictions of some analyzed samples. From this figure, it can be noticed that the conversion behavior of biomasses and blends is well described by the proposed kinetic model, highlighting the impact of inorganic composition on the steam gasification kinetics of lignocellulosic biomasses. The low fitting error showed that the presented kinetic equation (eq. 4.3.1) is suitable for the description and prediction of the gasification behavior of biomasses or blends based on their inorganic composition.

4.4 Conclusion

The steam gasification of coconut shells (CS), oil palms shells (OPS) and bamboo guadua (BG) was analyzed under different experimental conditions. Despite the differences in their macromolecular composition, inorganics showed to be the most important parameter influencing the biomass gasification reactivity and kinetics. The results confirmed the beneficial impact of K in gasification and the inhibitory effect of Si and P. Accordingly, a new kinetic equation considering the inorganic composition of feedstocks was proposed. This approach proved to be suitable for the description and prediction of the gasification behavior of lignocellulosic biomasses within a wide range of inorganic compositions, and H/C and O/C ratios near 1.5 and 0.8 respectively. Furthermore, it was evidenced that the co-gasification behavior of biomasses in the presented range can be predicted from the inorganic composition of the individual feedstocks. In future work, the presented approach can be expanded to other lignocellulosic residues and a wider range of blends.

As a result, the proposed kinetic model could constitute a valuable tool for reactor design and for the development and scale-up of steam gasification facilities using tropical lignocellulosic feedstocks. In particular, taking into account that residual biomass availability is variable, this approach could be useful in applications where different kind of residues should be gasified at the same time.

Bibliography

[1] Prabir Basu. "Gasification Theory." In: *Biomass Gasification, Pyrolysis and Torrefaction*. Elsevier Inc., 2013. Chap. Chapter 7, pp. 199–248 (cit. on p. 74).

[2] Juan Daniel Martínez, Khamid Mahkamov, Rubenildo V. Andrade, and Electo E. Silva Lora. "Syngas production in downdraft biomass gasifiers and its application using internal combustion engines." In: *Renewable Energy* 38.1 (2012), pp. 1–9 (cit. on p. 74).

[3] Emanuele Graciosa Pereira, Jadir Nogueira Da Silva, Jofran L. De Oliveira, and Cássio S. MacHado. *Sustainable energy: A review of gasification technologies*. 2012 (cit. on p. 74).

[4] Anwar Sattar, Gary A. Leeke, Andreas Hornung, and Joseph Wood. "Steam gasification of rapeseed, wood, sewage sludge and miscanthus biochars for the production of a hydrogen-rich syngas." In: *Biomass and Bioenergy* 69 (Oct. 2014), pp. 276–286 (cit. on p. 74).

[5] Colomba Di Blasi. "Combustion and gasification rates of lignocellulosic chars." In: *Progress in Energy and Combustion Science* 35.2 (2009), pp. 121–140 (cit. on p. 74).

[6] Capucine Dupont, Sylvain Jacob, Khalil Ould Marrakchy, Céline Hognon, Françoise Labalette, Maguelone Grateau, and Denilson Da Silva Perez. "How inorganic elements of biomass influence char steam gasification kinetics." In: *Energy* 109 (2016), pp. 430–435 (cit. on pp. 74, 75, 82, 87).

[7] Jose M Encinar, Juan F Gonzalez, Juan J Rodriguez, and Maria J Ramiro. "Catalysed and uncatalysed steam gasification of eucalyptus char: infuence of variables and kinetic study." In: *Fuel* 80 (2001), pp. 2025–2036 (cit. on p. 74).

[8] M Perander, N Demartini, A Brink, J Kramb, O Karlström, J Hemming, A Moilanen, J Konttinen, and M Hupa. "Catalytic effect of Ca and K on CO 2 gasification of spruce wood char." In: *Fuel* 150 (2015), pp. 464–472 (cit. on p. 74).

[9] Yanqin Huang, Xiuli Yin, Chuangzhi Wu, Congwei Wang, Jianjun Xie, Zhaoqiu Zhou, Longlong Ma, and Haibin Li. "Effects of metal catalysts on CO 2 gasification reactivity of biomass char." In: *Biotechnology Advances* 27 (2009), pp. 568–572 (cit. on pp. 74, 82).

[10] Y Zhang, M Ashizawa, S Kajitani, and K Miura. "Proposal of a semi-empirical kinetic model to reconcile with gasification reactivity profiles of biomass chars." In: *Fuel* 87 (2008), pp. 475–481 (cit. on pp. 74, 75, 85).

[11] Kentaro Umeki, Antero Moilanen, Alberto Gómez-Barea, and Jukka Konttinen. "A model of biomass char gasification describing the change in catalytic activity of ash." In: *Chemical Engineering & Technology* 207-208 (2012), pp. 616–624 (cit. on p. 74).

[12] Kawnish Kirtania, Joel Axelsson, Leonidas Matsakas, Paul Christakopoulos, Kentaro Umeki, and Erik Furusj. "Kinetic study of catalytic gasification of wood char impregnated with different alkali salts." In: *Energy* 118 (2017), pp. 1055–1065 (cit. on p. 74).

[13] Shuang Jia, Siyun Ning, Hao Ying, Yunjuan Sun, Wei Xu, and Hang Yin. "High quality syngas production from catalytic gasification of woodchip char." In: *Energy Conversion and Management* 151 (2017), pp. 457–464 (cit. on p. 74).

[14] Jason Kramb, Jukka Konttinen, Alberto Gómez-Barea, Antero Moilanen, and Kentaro Umeki. "Modeling biomass char gasification kinetics for improving prediction of carbon conversion in a fluidized bed gasifier." In: *Fuel* 132 (2014), pp. 10–115 (cit. on p. 74).

[15] Jason Kramb, Nikolai Demartini, Magnus Perander, Antero Moilanen, and Jukka Konttinen. "Modeling of the catalytic effects of potassium and calcium on spruce wood gasification in CO 2." In: *Fuel Processing Technology* 148 (2016), pp. 50–59 (cit. on p. 74).

[16] Capucine Dupont, Timothée Nocquet, José Augusto Da Costa, and Christèle Verne-Tournon. "Kinetic modelling of steam gasification of various woody biomass chars: Influence of inorganic elements." In: *Bioresource Technology* 102.20 (2011), pp. 9743–9748 (cit. on pp. 74, 81, 86).

[17] Makiko Kajita, Tokuji Kimura, Koyo Norinaga, Chun-Zhu Li, and Jun-Ichiro Hayashi. "Catalytic and Noncatalytic Mechanisms in Steam Gasification of Char from the Pyrolysis of Biomass." In: (2009) (cit. on pp. 75, 82, 84, 87).

[18] Lina Maria Romero Millan, Fabio Emiro Sierra Vargas, and Ange Nzihou. "Kinetic Analysis of Tropical Lignocellulosic Agrowaste Pyrolysis." In: *BioEnergy Research* (2017) (cit. on p. 75).

[19] Alneira Cuéllar and Ismael Muñoz. "Fibra de guadua como refuerzo de matrices poliméricas - Bamboo fiber reinforcement for polymer matrix." In: *Dyna* 77.162 (2010), pp. 137–142 (cit. on p. 76).

[20] Q Mortley, W A Mellowes, and S Thomas. "Activated Carbons From Materials of Varying Morphological Structure." In: *Themochimica Acta* 129 (1988), pp. 173–186 (cit. on p. 76).

[21] J A García-Núñez, M García-Pérez, and K C Das. "Determination of Kinetic Parameters of Thermal Degradation of Palm Oil Mill By-Products Using Thermo-

gravimetric Analysis and Differential Scanning Calorimetry." In: *Transactions of the ASABE* 51.2 (2008), pp. 547–557 (cit. on p. 76).

[22] F Marquez-Montesinos, T Cordero, Rodriguez-Mirasol, and J.J Rodriguez. "CO2 and steam gasification of a grapefruit skin char." In: *Fuel* 81 (2002), pp. 423–429 (cit. on pp. 77, 81).

[23] Mathieu Morin, Sébastien Pécate, Enrica Masi, and Mehrdji Hémati. "Kinetic study and modelling of char combustion in TGA in isothermal conditions." In: *Fuel* 203 (2017), pp. 522–536 (cit. on p. 77).

[24] Sergey Vyazovkin, Alan K. Burnham, José M. Criado, Luis A. Pérez-Maqueda, Crisan Popescu, and Nicolas Sbirrazzuoli. "ICTAC Kinetics Committee recommendations for performing kinetic computations on thermal analysis data." In: *Thermochimica Acta* 520.1 (2011), pp. 1–19 (cit. on pp. 77, 78).

[25] P Šimon. "ISOCONVERSIONAL METHODS Fundamentals, meaning and application." In: *Journal of Thermal Analysis and Calorimetry* 76 (2004), pp. 123–132 (cit. on p. 78).

[26] Michael E. Brown. *Handbook of Thermal Analysis and Calorimetry. Volume 1. Principles and Practice*. Ed. by Michael Brown. First Edit. Elsevier, 1998, p. 725 (cit. on pp. 78, 84).

[27] I I Ahmed and A K Gupta. "Kinetics of woodchips char gasification with steam and carbon dioxide." In: *Applied Energy* 88 (2011), pp. 1613–1619 (cit. on p. 78).

[28] Gartzen Lopez, Jon Alvarez, Maider Amutio, Aitor Arregi, Javier Bilbao, and Martin Olazar. "Assessment of steam gasification kinetics of the char from lignocellulosic biomass in a conical spouted bed reactor." In: *Energy* 107 (2016), pp. 493–501 (cit. on p. 78).

[29] Ganesh Samdani, Anuradda Ganesh, Preeti Aghalayam, R K Sapru, B L Lohar, and Sanjay Mahajani. "Kinetics of heterogeneous reactions with coal in context of underground coal gasification." In: *Fuel* 199 (2017), pp. 102–114 (cit. on p. 78).

[30] Joanne Tanner and Sankar Bhattacharya. "Kinetics of CO 2 and steam gasification of Victorian brown coal chars." In: *Chemical Engineering Journal* 285 (2016), pp. 331–340 (cit. on p. 78).

[31] Francisco J Gotor, José M Criado, Jiri Malek, and Nobuyoshi Koga. "Kinetic Analysis of Solid-State Reactions: The Universality of Master Plots for Analyzing Isothermal and Nonisothermal Experiments." In: *Journal of Physical Chemistry A* 104 (2000), pp. 10777–10782 (cit. on p. 78).

[32] Pedro E. Sánchez-Jiménez, Luis A. Pérez-Maqueda, Antonio Perejón, and José M. Criado. "Generalized master plots as a straightforward approach for determining the kinetic model: The case of cellulose pyrolysis." In: *Thermochimica Acta* 552 (2013), pp. 54–59 (cit. on p. 78).

[33] D.P. Ye, J.B. Agnew, and D.K. Zhang. "Gasification of a South Australian low-rank coal with carbon dioxide and steam: kinetics and reactivity studies." In: *Fuel* 77.11 (1998), pp. 1209–1219 (cit. on p. 80).

[34] Raymond C Everson, Hein W J P Neomagus, Rufaro Kaitano, Rosemary Falcon, and Vivien M Du Cann. "Properties of high ash coal-char particles derived from inertinite-rich coal: II. Gasification kinetics with carbon dioxide." In: *Fuel* 87 (2008), pp. 3403–3408 (cit. on p. 80).

[35] Kongvui Yip, Fujun Tian, Jun-Ichiro Hayashi, and Hongwei Wu. "Effect of Alkali and Alkaline Earth Metallic Species on Biochar Reactivity and Syngas Compo-

sitions during Steam Gasification." In: *Energy & Fuels* 24 (2010), pp. 173–181 (cit. on p. 80).
[36] CD Le and ST Kolaczkowski. "Steam gasification of a refuse derived char: Reactivity and kinetics." In: *Chemical Engineering Research and Design* 102.2 (2015), pp. 389–398 (cit. on pp. 80, 86).
[37] Massoud Massoudi Farid, Hyo Jae Jeong, and Jungho Hwang. "Co-gasification of coal-biomass blended char with CO2 and H2O: Effect of partial pressure of the gasifying agent on reaction kinetics." In: *Fuel* 162 (2015), pp. 234–238 (cit. on p. 81).
[38] Céline Hognon, Capucine Dupont, Maguelone Grateau, and Florian Delrue. "Comparison of steam gasification reactivity of algal and lignocellulosic biomass: Influence of inorganic elements." In: *Bioresource Technology* 164 (2014), pp. 347–353 (cit. on pp. 82, 87).
[39] Ange Nzihou, Brian Stanmore, and Patrick Sharrock. "A review of catalysts for the gasification of biomass char, with some reference to coal." In: *Energy* 58 (Sept. 2013), pp. 305–317 (cit. on pp. 82, 85).
[40] Bazardorj Bayarsaikhan, Jun-Ichiro Hayashi, Taihei Shimada, Chirag Sathe, Chun-Zhu Li, Atsushi Tsutsumi, and Tadatoshi Chiba. "Kinetics of steam gasification of nascent char from rapid pyrolysis of a Victorian brown coal." In: *Fuel* 84 (2005), pp. 1612–1621 (cit. on p. 84).
[41] Muhammad Shahbaz, Suzana Yusup, Abrar Inayat, David Onoja Patrick, and Muhammad Ammar. "The influence of catalysts in biomass steam gasification and catalytic potential of coal bottom ash in biomass steam gasification: A review." In: *Renewable & Sustainable Energy Reviews* 73 (2017), pp. 468–476 (cit. on p. 84).
[42] David G F Adamon, Latif A Fagbémi, Ammar Bensakhria, and Emile A Sanya. "Comparison of Kinetic Models for Carbon Dioxide and Steam Gasification of Rice Husk Char." In: *Waste and Biomass Valorization* (2017), pp. 1–9 (cit. on p. 86).
[43] C Guizani, F J Escudero Sanz, and S Salvador. "The gasification reactivity of high-heating-rate chars in single and mixed atmospheres of H2O and CO2." In: *Fuel* 108 (2013), pp. 812–823 (cit. on p. 86).
[44] Andrés Anca-Couce, Nico Zobel, Anka Berger, and Frank Behrendt. "Smouldering of pine wood: Kinetics and reaction heats." In: *Combustion and Flame* 159.4 (2012), pp. 1708–1719 (cit. on p. 88).

Chapter

5

Impact of feedstock characteristics on the steam gasification of lignocellulosic agrowaste

Abstract

The steam gasification of coconut shells, oil palm shells and bamboo guadua was studied under different experimental conditions in order to understand the impact of the biomass characteristics on the steam gasification product yield and gas composition. Gasification tests were performed in a fluidized bed reactor, with temperatures ranging from 750°C and 850°C. The experimental results showed that the inorganic content impact in a very important way the gasification reactivity and product yield of the samples. Gasification of samples with K/(Si+P) above 1 resulted in higher gas yields and gas efficiencies compared to samples with K/(Si+P) below 1. For its part, the organic composition, especially the H/C and O/C ratios seem to be related to the composition and heating value of the gaseous products. The produced gas obtained, with a heating value between 10 and 12 MJ/m^3, and a H_2/CO ratio between 2.5 and 4, is considered suitable for energy applications using gas turbines or internal combustion engines.

5.1 Introduction

The diverse climate conditions in tropical regions are associated with a great biodiversity and the possibility to develop agricultural and agroindustrial activities. In accordance, most developing countries in these areas base their economy in agriculture and related activities, producing great amounts of agrowastes. These residues are nevertheless barely valorized, and remain under-exploited. Taking into account that developing countries usually have particular energy needs in isolated areas, a possible valorization pathway for this materials could be their transformation in biofuels.

In this context, gasification is a very interesting process for the recovery of energy from agricultural and agroindustrial residues, as it produces fuel gases that can be used for the generation of heat or power [1–3]. In particular, steam gasification fuel gases have a higher heating value in comparison to air gasification [4–6], and then, the analysis and understanding of this process is of great importance in the presented context.

The main reactions involved in the steam gasification process are listed below [5]:

Water gas reaction:

$$\mathrm{C + H_2O \longrightarrow CO + H_2} \quad +131\,\mathrm{kJ/kmol} \tag{R5.1}$$

Water-gas shift reaction:

$$\mathrm{CO + H_2O \longrightarrow CO_2 + H_2} \quad -41.2\,\mathrm{kJ/kmol} \tag{R5.2}$$

Boudouard reaction:

$$\mathrm{C + CO_2 \longrightarrow 2\,CO} \quad +172\,\mathrm{kJ/kmol} \tag{R5.3}$$

Hydrogasification reaction:

$$\mathrm{C + 2\,H_2 \longrightarrow CH_4} \quad -74.8\,\mathrm{kJ/kmol} \tag{R5.4}$$

Methanation reactions:

$$\mathrm{2\,CO + 2\,H_2 \longrightarrow CH_4 + CO_2} \quad -247\,\mathrm{kJ/kmol} \tag{R5.5}$$

$$\mathrm{CO + 3\,H_2 \longrightarrow CH_4 + H_2O} \quad -206\,\mathrm{kJ/kmol} \tag{R5.6}$$

$$\mathrm{CO_2 + 4\,H_2 \longrightarrow CH_4 + 2\,H_2O} \quad -165\,\mathrm{kJ/kmol} \tag{R5.7}$$

Methane reforming reaction:

$$\mathrm{CH_4 + H_2O \longrightarrow CO + 3\,H_2} \quad +206\,\mathrm{kJ/kmol} \tag{R5.8}$$

The final gas composition of the steam gasification process is the result of the combination of the presented reactions. In general, steam gasification produces gases with heating value between 10 and 18 $\mathrm{MJ/m^3}$, and high $\mathrm{H_2}$ concentrations [5].

Despite the great potential of the steam gasification process, the valorization of agrowastes could have some restrictions associated with the availability of the feedstocks. Agricultural and agroindustrial activities are generally seasonal and then, the availability of the residues is not constant. In most cases, gasification facilities should operate

intermittently, or work with different kind of residues with different characteristics, or even blends. In consequence, the impact of the feedstock on the gasification behavior and products should be understood, in order to properly adapt the process parameters, according to the application requirements.

Several authors have investigated the effect of operating parameters and conditions on the performance of the gasification process, with different types of reactors and feedstocks [7–9]. Parameters like gasification temperature and steam quantity, have shown an important impact in the produced gas composition and quantity. Moreover, the impact of the indigenous inorganic elements of the raw materials on the steam gasification reactivity has been also reported [10, 11], and confirmed in a previous work [12].

Regarding the steam gasification product distribution and gas composition, several studies have been found in the literature associated with different kind of feedstocks like rice husk and straw [13], bagasse [14], wood [15], walnut and pistachio shells [16], or waste water sludge [17]. However, most of these studies deal with residues individually, without comparing different materials. A few references working with several biomasses, described some differences in the gas production rate and composition, which were attributed to the samples ash content and composition, volatile matter, particle porosity, or particle size [7, 18, 19]. Nevertheless, as the aim of these works was not the comparison of the gasification behavior of different feedstocks, the justification of these differences is not extensively detailed. In accordance, the understanding of the influence of the feedstock characteristics on the steam gasification behavior and product distribution still needs to be improved.

In this regard, the aim of the work developed in this chapter is to understand the impact of the biomass composition on the steam gasification behavior and product distribution. Three tropical lignocellulosic biomasses with different macromolecular and inorganic composition were analyzed and compared. A focus on the permanent gaseous products is made, analyzing its composition, heating value, and possible suitable applications in the presented context.

5.2 Materials and methods

5.2.1 Biomass samples

Three tropical lignocellulosic biomasses were selected for this study: oil palm shells (OPS), coconut shells (CS) and bamboo guadua (BG). The detailed origin of the samples, collected in Colombia-South America is described in a previous work[20]. The organic and inorganic chemical composition of the samples is presented in tables 5.1 and 5.2, as the average of three replicates.

The CHNS composition was determined using a Thermoquest NA 2000 elemental analyzer, while for the high heating value an IKA C 5000 automated bomb calorimeter was used. The inorganic composition was determined using an HORIBA Jobin Yon Ultima 2 inductively coupled plasma optical emission spectrometer (ICP-OES), base on the standard EN 16967. The proximate analysis was calculated according to the standards EN ISO 18134-3, EN ISO 18123, and EN ISO18122. Before the experimental tests the raw biomasses were ground and sieved to a size range between 2 mm and 4 mm.

Table 5.1: Organic composition and proximate analysis of studied biomasses

		OPS	CS	BG
Elemental Analysis (wt.% daf)	C	46.7±0.2	46.8 ±0.2	42.7±0.3
	H	6.5±0.1	5.8 ±0.1	5.4±0.1
	O*	46.2±0.1	47.1 ±0.1	51.5±0.1
	N	0.6±0.1	0.3 ±0.1	0.4±0.1
	O/C	0.7±0.1	0.7±0.1	0.9±0.1
	H/C	1.7±0.1	1.5±0.1	1.5±0.1
Proximate analysis (wt. % dry basis)	Volatile Matter	77.2±0.3	79.5±0.3	75.0±0.2
	Fixed Carbon*	20.9±0.3	19.0±0.2	19.9±0.3
	Ash	1.7±0.2	1.4±0.1	5.0±0.4
High heating value (MJ/kg)	HHV	19.6±0.2	18.7±0.3	18±0.3

* Calculated by difference

Table 5.2: Major inorganic composition of studied biomasses

		OPS	CS	BG
Inorganic composition (mg/kg dry basis)	Al	1 500±22	262±8	243±34
	Ca	54±6	391±73	441±99
	Fe	107 ±4	160±28	116±17
	K	1 006±15	2 808±44	5 360±85
	Mg	135±3	170±15	173±10
	Na	1.5±0.5	33±11	2±0.8
	P	270±7	397±40	829±62
	Si	5 600±39	309±43	19 372±354

5.2.2 Experimental setup

Pyrolysis and steam gasification experiments were carried out in a semicontinuous lab-scale fluidized bed gasifier. The reactor is made of stainless steel and is externally heated with an electrical furnance composed of two radiative covers. The height of the reactor is 60 cm and the internal diameter 6 cm. A porous disk in the bottom holds the biomass sample and allows the gasification atmosphere to pass through. The thermal regulation is ensured by an Eurotherm controller connected to a K-thermocouple in the center of the reactor.

The nitrogen gas flow supplied to the process is regulated by a mass flow controller calibrated between 0-5 Nm^3/h. Steam is supplied by a steam generator equipped with a water mass flow controller and a heating device producing superheated steam at 180°C. At the exit of the reactor, a gas conditioning unit based on the tar protocol [21] allowed the condensation of tars and steam. A series of 7 impinger bottles were used as presented in the experimental setup scheme 5.1. After the condensation train, a gas meter was used to measure the volume of produced permanent gases, before being released to the atmosphere. Every 5 minutes, the gas volume was registered and gas samples were taken using Tedlar®. bags in order to analyze their composition. For this

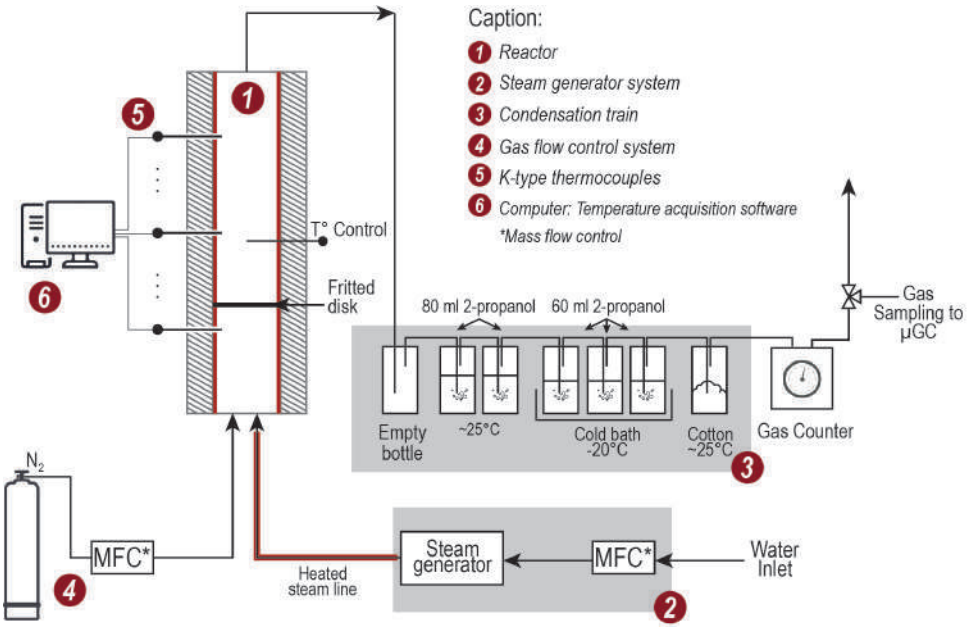

Figure 5.1: Schematic diagram of the gasification experimental setup

purpose, a micro-GC (MyGC Agilent) was used. The gas heating value was calculated from the CO, H_2, CH_4 and C_nH_m measured fractions.

For all the experiments, 80 g of biomass were placed inside the reactor and heated to the gasification temperature at a heating rate of 20°C/min, under nitrogen. When the gasification temperature was reached (from 750°C to 850°C), the atmosphere was switched to a mixture of H_2O/N_2 (from 50 to 300 g/h of steam - 15% to 90% of steam in the gasifying agent) and was maintained during all the gasification stage (t from 1h to 3h). The total flow rate was 0.7 m^3/h for all the experiments. After each test, the reactor was cooled down to room temperature under nitrogen. The remaining char was collected and weighted, as well as the impinger bottles and pipes, in order to determine the quantity of water and tars condensed and perform mass balances. For this purpose, prior to each test the condensation train impinger bottles and pipes were also weighted. The experimental program is presented in figure 5.2.

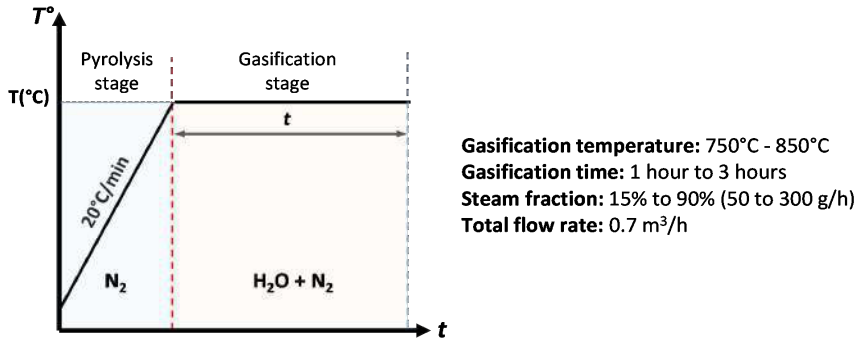

Figure 5.2: Pyrolysis and steam gasification experimental program

Pyrolysis-only tests were performed in order to determine the gas, solid and liquid yield at the end of the heating period (pyrolysis stage) for each gasification temperature. In order to verify the reproducibility, several tests were carried out twice. The repeatability was found to be satisfactory as the standard deviation of the gas composition and gas production was below 3% and 10% respectively.

5.2.3 Product distribution and reactivity analysis

Product mass yield and energy fraction

The mass balance for each experimental condition was calculated from the gravimetrically measured solid (char) and liquid yields (tar+water), and the registered gas volume production and composition. As the last bottles of the condensation train are placed in a -20°C cold bath, it is considered that the 2-propanol in the impingers is not volatilized during the experiment, and then, the liquid yield is determined from the mass difference between the condensation train before and after the test.

In the same way, considering that the nitrogen flow supplied to the thermo-conversion process is known and constant for each experiment, the total volume of permanent gases produced can be deduced, from the gas volume measured. The volume and mass of each gas species (H_2, CO, CO_2, CH_4) can be then determined from the measured gas composition. Taking into account that the repeatability was found to be satisfactory, the gas, liquid and solid mass measured for the pyrolysis-only tests are subtracted from the gasification experiments to obtain the product yield associated only to the gasification stage. Under all the tested conditions in this study, the mass balance closure for the gasification stage is in the range 88.6% and 103%, considered acceptable for the presented experimental setup. The schema of the inlet and outlet streams to and from the reactor during the gasification stage is presented in figure 5.3.

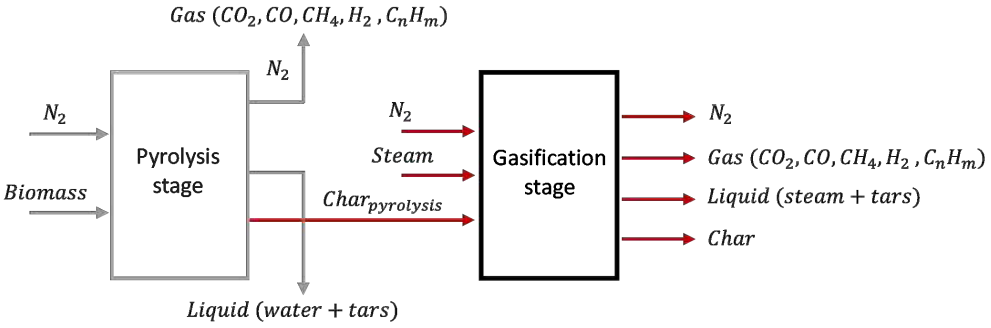

Figure 5.3: Inlet and outlet streams to and from the reactor during the gasification stage.

The gasification product yield as a function of the initial biomass and steam used in the pyro-gasification process was calculated according to equations 5.2.1 to 5.2.3

$$Char\ yield\ (\%) = \frac{m_{char}}{m_{biomass} + m_{steam}} \times 100 \tag{5.2.1}$$

$$Liquid\ yield\ (\%) = \frac{m_{liquid}}{m_{biomass} + m_{steam}} \times 100 \tag{5.2.2}$$

$$Gas\ yield\ (\%) = \frac{m_{gas}}{m_{biomass} + m_{steam}} \times 100 \tag{5.2.3}$$

Where m_{char} is the mass of the recovered char at the end of the experiment, and m_{liquid} and m_{gas} are the mass of liquid and gas produced during the gasification stage. For their part, $m_{biomass}$ and m_{steam} are the mass of the initial biomass used and the steam fed to the gasification process. For the present study, the gasification total product yield with respect to the initial biomass is below 100%, as only the gasification products are taken into account in the calculation procedure.

For all the experimental conditions, the energy fraction associated with the gas, liquid and solid by-products was determined. Their chemical energy, as well as their sensible or latent heat at the reactor temperature were taken into account, as presented below:

$$E_{prod} = E_{solid} + E_{gas} + E_{liquid} \tag{5.2.4}$$

$$E_{solid} = m_{char}(C_{p\,char}\,T_r + HHV_{char}) \tag{5.2.5}$$

$$E_{gas} = m_{gas}(h_{gas\,(T_r)} + HHV_{gas}) \tag{5.2.6}$$

$$E_{liquid} = m_{steam}(h_{steam\,(T_r)}) + m_{tars}(h_{tars\,(T_r)} + HHV_{tars}) \tag{5.2.7}$$

Where m_{char} and m_{gas} are the mass of the recovered char and gas at the end of the gasification process. $C_{p\,char}$ is the specific heat of the char, and T_r is the reactor temperature during the gasification stage. For their part, h_{gas} is the enthalpy of the produced gas at temperature T_r leaving the gasifier, and h_{steam} is the enthalpy of the unreacted steam also at temperature T_r. Finally, HHV_{char} and HHV_{gas} are the high heating value of the recovered char and gas. As the mass of tars could not be accurately determined during the gasification stage, it is assumed for the liquid energy fraction calculation that the recovered liquids correspond only to unreacted steam.

In accordance, the energy fraction of each gasification product is calculated according to equations 5.2.8 to 5.2.10.

$$E\%_{gas}(\%) = \frac{E_{gas}}{E_{prod}} \times 100 \tag{5.2.8}$$

$$E\%_{char}(\%) = \frac{E_{char}}{E_{prod}} \times 100 \tag{5.2.9}$$

$$E\%_{liquid}(\%) = \frac{E_{liquid}}{E_{prod}} \times 100 \tag{5.2.10}$$

Finally, considering the permanent gases as the targeted product, the gas efficiency of the gasification process is defined as follows:

$$Gas_{\,eff}\ (\%) = \frac{m_{gas}\,HHV_{gas}}{m_{biomass}\,HHV_{biomass} + m_{steam}\,h_{steam\,(T_r)}} \times 100 \tag{5.2.11}$$

Where, $m_{biomass}$ and m_{steam} are the mass of the initial biomass used and the total steam fed to the gasification process, HHV_{gas} and $HHV_{biomass}$ are the high heating value of the produced gas and the raw biomass, and $h_{steam\,(T_r)}$ is the enthalpy of the steam at the reactor temperature T_r during the gasification process.

Gasification reactivity analysis

To analyze the impact of the raw samples in their gasification behavior, an average reactivity study was performed for different gasification times. The degree of conversion of the char after the gasification stage is defined as in equation (5.2.12):

$$\alpha(t) = \frac{m_0 - m(t)}{m_0 - m_{ash}} \tag{5.2.12}$$

Where m_0 is the mass of the sample at the beginning of the gasification stage, $m(t)$ the mass at the end of the gasification period t, and m_{ash} the mass of ash in the sample. m_0 for each experimental condition is the mass of char in the reactor before the steam injection, determined from the pyrolysis-only tests.

The apparent gasification reactivity can be defined as a function of the conversion degree α, as presented in equation 5.2.13. Generally, reactivity comparisons are referred to a specific char conversion level. However, as the continuous monitoring of the mass loss of each biomass in not possible for the presented experimental setup, the gasification reactivity is presented in this study as an average for a defined gasification time, and is calculated according to the equation (5.2.14), where t is the time of the steam gasification stage, from 1h to 3h.

$$R(\alpha)_{(app)} = \frac{1}{1-\alpha(t)}\frac{d\alpha}{dt} \tag{5.2.13}$$

$$R_{(app)\ average} = \frac{1}{n}\sum_{t=1}^{n}\frac{1}{1-\alpha(t)}\frac{d\alpha}{dt} \tag{5.2.14}$$

5.3 Results and discussion

5.3.1 Mass and energy distribution of gasification products

Impact of steam fraction in the gasifying agent

To understand the impact of the biomass characteristics in its steam gasification behavior and product yield, different process conditions were analyzed and compared for the three selected materials: CS, BG, and OPS.

Firstly, the impact of the steam quantity on the gasification products distribution was studied at a process temperature of 750°C. Figure 5.4 presents the solid, gas, and liquid yield of the analyzed samples, in grams of by-product per grams of biomass initially fed to the process (g/g_{bio}). For the three samples, it was observed that the recovered char quantity at the end of each gasification experiment was reduced with the increase of the steam percentage, as presented in figure 5.4a. This trend was expected, considering that higher steam quantities available to react with carbon lead to higher carbon conversions and lower solid yields.

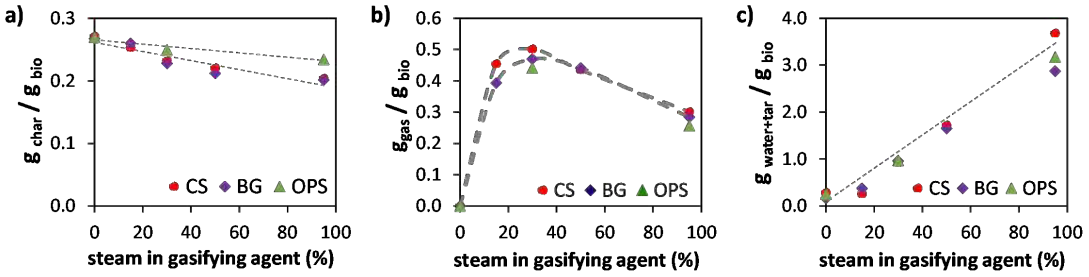

Figure 5.4: Evolution of the solid, gas and liquid products with the steam percentage in the gasification agent. Gasification temperature and time: 750°C, 1 hour. a) char, b) gas, c) liquid (water+tars)

For its part, the maximum gas production, of about 0.4 to 0.5 g/g_{bio} (0.6 to 0.8 Nl/g_{bio}) was observed between 15% and 30% of steam in the gasifying agent (figure 5.4c). Above these values, the produced gas quantity was reduced and an increase in the liquid fraction was noticed (figure 5.4c). In accordance, high steam quantities showed a negative impact in the gas production. This behavior is possibly related to a reduction in the reaction temperature that favors tars at the expense of permanent gases, and has been also observed by several authors [6, 22].

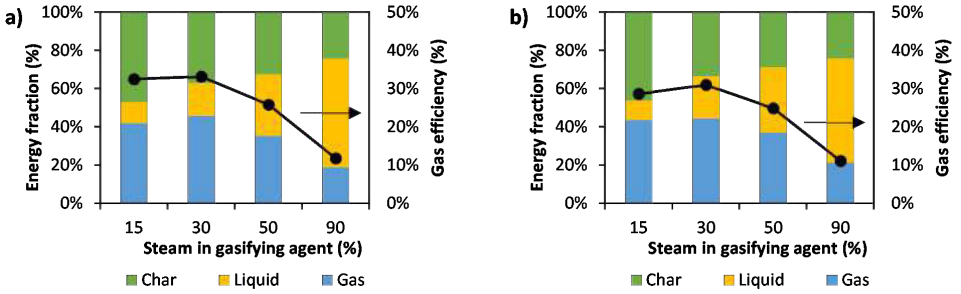

Figure 5.5: Energy distribution in the gasification products at 750°C as a function of the steam percentage in the gasifying agent. a) Coconut shells. b) Bamboo guadua

Furthermore, regarding the energy distribution of the gasification products, it is possible to observe from figure 5.5 that for the analyzed samples, the energy fraction contained in the liquid products increases with the steam percentage in the gasifying agent. Excess steam does not react with carbon and is recovered at the reactor exit, involving a greater energy consumption related to steam production and overheating. Accordingly, the energy fraction contained in the liquid products (water+tars) increases, being inconvenient for energy applications.

In accordance to the results presented in figure 5.5, the highest energy fraction and gas efficiency gas was also obtained for steam percentages between 15% and 30%, confirming that for the presented experimental setup, these conditions may be the most suitable for the study of the selected biomasses for energy applications. In consequence, the impact of temperature and time in the samples gasification will be analyzed thereafter for 30% of steam in the gasifying agent.

Impact of gasification temperature and feedstock

For the three analyzed biomasses, an rise in the gasification temperature resulted in an increase in the gas production and a decrease in the solid and liquid yields, as presented in figure 5.6.

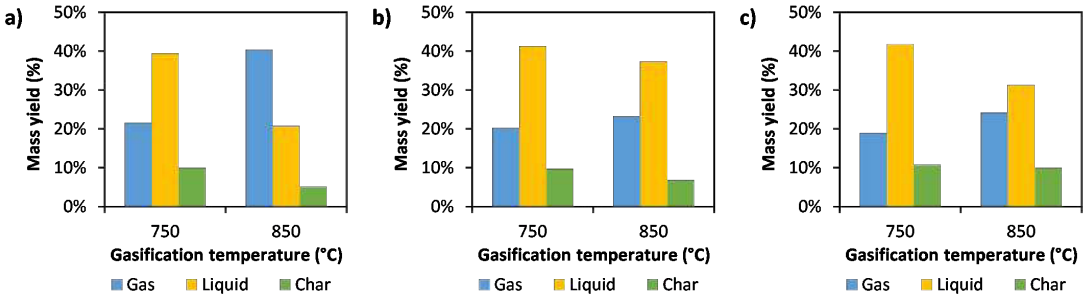

Figure 5.6: Evolution of the solid, liquid and gas yield with the gasification temperature. 1 hour gasification with 30% of steam in the gasifying agent. a) Coconut shells, b) Bamboo guadua, c) Oil palm shells

Indeed, with the temperature change from 750°C to 850°C, the gas yield increased from 0.50 to 0.94 g/g_{bio} (0.66 to 1.41 Nl/g_{bio}) for CS, from 0.47 to 0.54 g/g_{bio} (0.75 to 0.81 Nl/g_{bio}) for BG, and from 0.44 to 0.56 g/g_{bio} (0.79 to 0.84 Nl/g_{bio}) for OPS. This is an augmentation of 18, 3 and 5 percentage points respectively, while the liquid and solid yields decreased for the three samples. More specifically, the liquid yield showed a decrease of 19, 5 and 10 percentage points for CS, BG and OPS, with the temperature increase.

These results were expected, taking into account that endothermic steam gasification reactions are promoted by the temperature increase, resulting in a greater char and steam consumption, and an enhanced gas production. The described behavior has also been reported by different authors working with different kinds of biomass [8, 19, 23]. Furthermore, the rise in the gas yield observed for the same gasification time indicates an increase in the steam gasification reactivity of the samples with the temperature. From the average reactivity values calculated for the three analyzed feedstocks and summarized in table 5.3, a reactivity increase of more than 4 times is observed with the temperature change from 750°C to 850°C. This trend was already highlighted in a previous work, at a thermogravimetric scale [12] (Chapter 4).

Table 5.3: Calculated mean gasification reactivity during 3 hours in a 30% steam atmosphere

	Mean reactivity (%/min)		
Temperature	**CS**	**BG**	**OPS**
750°C	0.35	0.25	0.08
850°C	2.28	1.18	0.32

However, even when the described trend is the same for the three samples, some differences can be noticed. For the same gasification time, the increase in the gas production was greater for CS in comparison to OPS and BG when the gasification

temperature rose from 750°C to 850°C. Similarly, as shown in figure 5.7, the product energy fraction contained in the permanent gases augmented 28 percentage points for CS compared to only 10 and 5 for BG and OPS respectively. Moreover, the decrease in the energy fraction associated with the recovered solid and liquids is more important for CS.

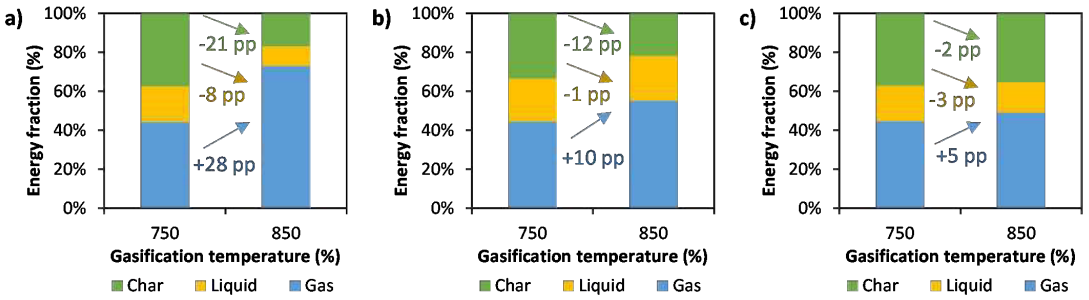

Figure 5.7: Evolution of the energy distribution in the gasification products with the temperature. 1 hour gasification with 30% of steam in the gasifying agent. a) Coconut shells, b) Bamboo guadua, c) Oil palm shells

Likewise, from the comparison of the gas production as a function of time, it can be observed that under the same gasification conditions the gas production evolution is different for the three samples (Figure 5.8). In particular, CS exhibited the highest gas yield in comparison to BG and OPS. This behavior can be better understood from the analysis of the average gasification reactivity values, already presented in table 5.3.

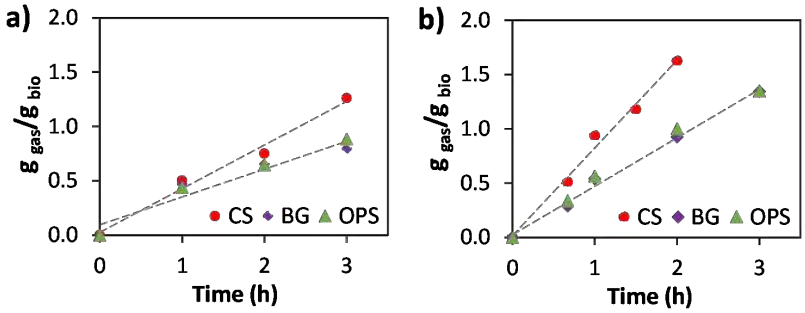

Figure 5.8: Gas production evolution with the gasification time. a) Gasification at 750°C and 30% of steam in the gasifying agent, b) Gasification at 850°C and 30% of steam in the gasifying agent.

Regardless the gasification temperature, the reactivity values of CS were always higher compared to BG and OPS, explaining the observed differences in the gas yield evolution with the gasification temperature and time. For instance, at 850°C, the BG and OPS reactivities correspond to only 51% and 14% of the CS value respectively. Accordingly, two different trends are identified: in one hand, CS with a high gasification reactivity, and in the other hand, BG and OPS with a lower reactivity. These differences may be related to the inherent inorganic content of the raw materials, considering that CS contain mainly K and Ca, while OPS and BG are principally composed of Si, Al, P. The catalytic effect of AAEM and the inhibitory impact of Si, Al and P on the steam gasification behavior of carbon materials has already been highlighted by different authors [24–26].

More specifically, the catalytic impact of alkali and alkali earth metals (AAEM) elements on the steam gasification reaction R5.1 (page 94) has been described as an oxygen transfer mechanism via the metal M, as presented below [26, 27]:

$$M_2CO_3 + 2\,C \longrightarrow 2\,M + 3\,CO$$
$$2\,M + 2\,H_2O \longrightarrow 2\,MOH + H_2$$
$$2\,MOH + CO \longrightarrow M_2CO_3 + H_2$$
$$2\,C + 2\,H_2O \longrightarrow 2\,CO + 2\,H_2$$

The enhanced oxygen transfer between the gasifying atmosphere and the reacting solid increases the carbon conversion rate, resulting in a higher reactivity and gas quantity produced under the same gasification conditions. Among the AAEM, K has been reported to be the most active element that promotes the steam gasification reactions in carbon materials [28, 29]. However, the described catalytic mechanism may be inhibited by elements like Si, Al, and P, as they tend to react with AAEM, reducing their beneficial effect in the gasification behavior [24, 30].

In this regard, several authors have proposed different reaction mechanisms between AAEM and Si, Al, and P compounds during biomass thermochemical conversion, as presented below [31–33]:

$$2\,MOH + P_2O_5 \longrightarrow 2\,MPO_3 + H_2O$$

$$2\,MOH + nSiO_2 \longrightarrow M_2O \cdot nSiO_2 + H_2O$$

$$2\,MOH + Al_2O_3\ 2\,SiO_2 \longrightarrow 2\,MAlSiO_4 + H_2O$$

In particular, the formation of alkali phosphates, silicates, and aluminosilicates may inhibit the oxygen transfer mechanism via the metal M, and then, may hinder the catalytic impact of AAEM on the steam gasification reactions.

In this respect, the inorganic ratio K/(Si+P) proposed by Hognon et al. [34] is adopted in this work to compare the inorganic composition of the analyzed samples and its impact on product yield. The validity of this ratio has been confirmed in a previous study at a thermogravimetric scale, where a kinetic expression was proposed to describe and predict the steam gasification behavior of lignocellulosic biomass as a function of its inorganic content (Chapter 4) [12]. More specifically, samples with K/(Si+P) higher than 1 showed a catalytic gasification behavior, contrary to samples with K/(Si+P) below 1, confirming the beneficial effect of AAEM (especially K), and the inhibitory impact of Si and P.

Regarding the analyzed samples, CS inorganic ratio is 3.9, while BG and OPS values are 0.2 and 0.17 respectively. These differences can explain the higher increase in the product energy fraction contained in permanent gases for CS, in comparison to the other two samples, as observed in figure 5.7. Therefore, the similarities between OPS and BG, and their differences with CS may be related to their K/(Si+P) ratio.

Similarly, the comparison of the three analyzed samples showed that the process gas efficiency calculated for gasification at 850°C, during 1 hour, and 30% of steam in the gasifying agent, is 20 percentage points higher for CS, in comparison to the values obtained for BG and OPS (55% in comparison to 33% and 35% respectively).

In this regard, to further illustrate the impact of the inorganic content of the raw biomass, the gas efficiency calculated for the analyzed samples and selected blends is

Table 5.4: Gasification products distribution and energy fraction for the analyzed experimental conditions

Raw sample	Product distribution			Product energy fraction			Gas Efficiency (%)
	Solid (g/g_{bio})	Liquid (g/g_{bio})	Gas (g/g_{bio})	Solid (%)	Liquid (%)	Gas (%)	
CS_30_750_1	0.23	0.92	0.50	37.1	18.4	45.0	33.2
CS_90_750_1	0.20	3.68	0.30	24.3	56.0	18.9	11.7
CS_30_750_2	0.20	1.98	0.75	23.3	30.1	46.2	37.1
CS_30_750_3	0.16	2.97	1.26	13.0	32.0	54.4	52.0
CS_30_850_1	0.12	0.48	0.94	16.9	10.1	73.0	54.6
CS_30_850_2	0.04	1.18	1.62	3.9	15.4	80.7	78.3
BG_30_750_1	0.23	0.97	0.47	33.4	21.9	44.7	31.0
BG_90_750_1	0.20	2.87	0.28	24.1	54.5	21.4	11.1
BG_30_750_2	0.21	2.11	0.65	21.4	34.4	44.2	34.4
BG_30_750_3	0.20	3.40	0.79	15.7	43.9	40.5	33.6
BG_30_850_1	0.15	0.85	0.54	21.8	22.9	55.4	33.3
BG_30_850_2	0.12	1.84	0.92	8.9	31.4	59.7	45.3
BG_30_850_3	0.08	2.76	1.34	3.4	34.5	62.0	53.8
OPS_30_750_1	0.25	0.97	0.44	37.1	18.2	44.8	35.5
OPS_90_750_1	0.23	3.17	0.26	29.2	50.8	20.0	11.9
OPS_30_750_2	0.24	2.12	0.65	25.1	27.1	47.8	45.9
OPS_30_750_3	0.24	3.11	0.88	19.4	31.9	48.7	49.3
OPS_30_850_1	0.23	0.73	0.56	35.3	15.5	49.2	35.1
OPS_30_850_2	0.20	1.62	1.00	19.8	21.7	58.5	54.5
OPS_30_850_3	0.16	2.62	1.35	12.6	27.4	60.0	60.3
Blends*							
50%CS_50%BG	0.16	0.65	0.76	24.2	13.7	62.1	46.5
50%CS_50%OPS	0.17	0.72	0.73	27.4	14.8	57.8	44.6
90%CS_10%BG	0.15	0.46	0.89	22.6	9.3	68.1	52.7
90%CS_10%OPS	0.12	0.68	0.86	19.0	14.1	66.9	51.2

Sample name nomenclature: Biomass_Steam fraction (%)_Temperature (°C)_Time (h)
* Blends were gasified at 850°C, during 1 hour, with a 30% steam atmosphere

presented in figure 5.9. Under the same process conditions, two different trends were clearly distinguished. At first, it can be noted that the gas efficiency of the process increases with K/(Si+P) for ratios below 1. In contrast, the highest gas efficiencies were observed for samples with K/(Si+P) close or higher than 1. It is worth noting that for samples with inorganic ratio higher than 1, the calculated gas efficiency remains almost constant.

From the analysis of the gas yield and gas efficiency obtained for each sample, it is not possible to evidence synergistic or inhibitory effects as a function of the biomass blend ratio. However, the experimental results highlight the evolution of the gasification behavior of samples as a function of their inorganic ratio. These findings confirm the validity of the inorganic ratio K/(Si+P) adopted in this work to classify and predict the behavior of lignocellulosic agrowaste.

From a practical point of view, this observation is important for real applications, as the process parameters and conditions should be adapted according to the feedstock

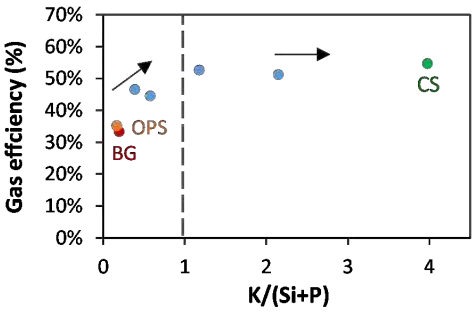

Biomass / blend	K/(Si+P) (-)
100%CS	3.98
100%BG	0.20
100%OPS	0.17
50%CS 50%BG	0.39
50%CS 50%OPS	0.58
90%CS 10%BG	1.18
90%CS 10%OPS	2.15

Figure 5.9: Calculated gas efficiency for pure biomass and selected blends at the same gasification conditions: 850°C, 1 hour, 30% of steam in the gasifying agent

characteristics. In particular, longer gasification times or higher temperatures are required for biomasses with low gasification reactivity, identified by an inorganic ratio K/(Si+P) lower than 1. Moreover, the behavior of biomass blends may be estimated from the knowledge of the inorganic composition of the individual feedstocks. The discussed experimental results are summarized in table 5.4 for all the analyzed samples. In the table, the sample name gives information about the raw biomass and the gasification conditions in the following order: steam fraction in the gasifying agent, gasification temperature, and gasification time.

5.3.2 Gas composition and heating value

For all the experimental conditions, no significant differences were identified between the three analyzed samples in terms of gas composition. The results obtained for gasification experiments with 30% of steam in the gasifying agent are presented in figure 5.10. As observed, the most representative gas is H_2, with an average fraction near 60%, followed by CO and CO_2 with 19% and 18% respectively, as expected for a steam gasification process [5]. Concentrations below 0.6% of CH_4 were also observed for the three samples, and below 0.02% of C_2H_4 for OPS. In all cases, the obtained gas composition is in accordance with literature reported values for the steam gasification of lignocellulosic materials under similar experimental conditions [13, 15, 35, 36].

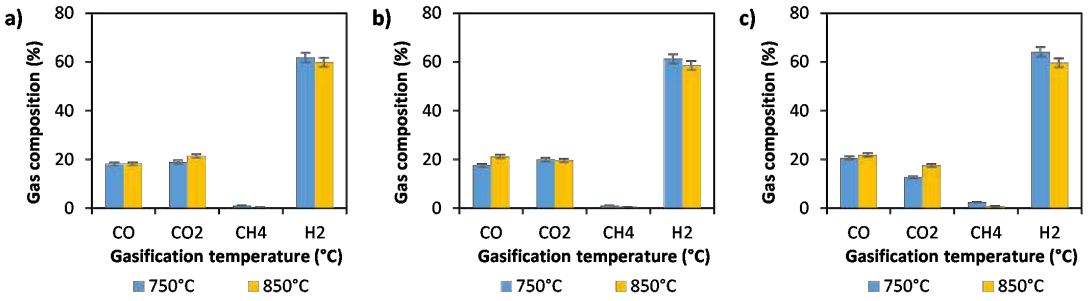

Figure 5.10: Produced gas average composition. 1 hour gasification with 30% of steam in the gasifying agent. a) Coconut shells, b) Bamboo guadua, c) Oil palm shells

For the three samples, a slight decrease between 2 and 5 percentage points in the H_2 fraction was observed with the temperature rise from 750°C to 850°C. This behavior may be related to the water-gas shift reaction (R5.2 - page 94) that could be disfavored with the temperature increase. In fact, this reaction is slightly exothermic, and has a higher equilibrium constant at lower temperatures, implying lower H_2 yields when the temperature increases [37–39]. In the same way, the CH_4 content in the gas slightly decreases with the gasification temperature, as it is produced by exothermic methanation reactions (R5.5 to R5.7 - page 94), whose equilibrium constant decreases with the temperature. Endothermic methane-reforming reaction (R5.8 - page 94) could also contribute to this result.

Concerning the average H_2/CO ratio of the produced gas, values between 2.5 and 4.5 were found for gasification experiments performed with a steam fraction of 30% in the gasifying agent. From table 5.5, it can be observed that the H_2/CO ratio decreases in a little extent with the increase in the biomass gasification temperature, in relation with the slight decrease in the H_2 fraction, mentioned previously. Moreover, an increase is also observed in the gas H_2/CO ratio with the rise in the steam fraction in the gasifying agent. In fact, the water-gas shift reaction (R5.2 - page 94) is favored with greater steam quantities available to react, resulting in higher H_2 concentrations and a decrease in the CO fraction. This behavior was more pronounced for CS, taking into account that the gasification reactivity of this sample is higher, in comparison to BG and OPS.

Despite these little changes, no remarkable differences were observed in the produced gas heating value with the temperature. For the three analyzed biomasses and under all the tested conditions, the calculated gas HHV was between 10 and 12 MJ/m^3, as presented in table 5.5, in accordance to the reported values for a steam gasification process [5]. OPS heating values are slightly higher compared to the other two samples, possibly due to the higher carbon content of the raw feedstock.

The similarities between the gas composition obtained from the steam gasification of coconut shells, bamboo guadua, and oil palm shells are possibly related to their close organic content, with H/C and O/C ratios near 1.5 and 0.8 respectively. Cao et al [40] found a correlation between the gasification produced gas H_2/CO ratio and the H/C ratio of different range coals. Particularly, in the case of the analyzed raw biomasses, the H/C ratio is very close; as well as the H/C ratio of the pyrolysis chars at the beginning of the gasification stage (e.g. 0.15 for CS pyrolysis chars at 850°C, 0.16 for BG chars, and 0.18 for OPS chars).

The required properties of the produced gas in terms of H_2/CO ratio are different for different applications and synthesis processes. According to several authors, ratios between 0.5 and 2 are suitable for Fischer Tropsch applications, while ratios between 2.5 and 4 are recommended for use as fuel in gas turbines or internal combustion engines [41–43]. Accordingly, the produced gas from the steam gasification of the selected feedstocks may be appropriate for energy applications in the presented context.

From the experimental results in the present work, it can be observed that the main differences identified in the produced gas from the three analyzed samples are principally associated with the obtained yield and not to the gas composition. Under the same gasification conditions, the gas production showed to be related to the sample reactivity, determined mainly by its inorganic content. For its part, the product gas composition and heating value may be related to the organic composition of the samples. In general

Table 5.5: Average gas composition and heating value obtained for the three analyzed samples

Raw sample	Gas composition				Gas H_2/CO (-)	Gas HHV (MJ/m^3)
	CO (% vol.)	CO_2 (% vol.)	CH_4 (% vol.)	H_2 (% vol.)		
CS_30_750_1	18.19	18.95	1.07	61.78	3.40	10.85
CS_90_750_1	13.32	22.78	0.71	63.20	4.75	10.02
CS_30_750_2	16.94	21.69	0.94	60.42	3.57	10.22
CS_30_750_3	13.80	23.17	0.49	62.53	4.53	9.91
CS_30_850_1	18.29	21.48	0.37	59.85	3.27	10.09
CS_30_850_2	16.98	21.58	0.42	61.02	3.59	10.09
BG_30_750_1	17.66	19.95	1.05	61.35	3.47	10.05
BG_90_750_1	15.20	22.51	0.82	61.56	4.05	10.08
BG_30_750_2	17.73	20.35	0.98	60.94	3.44	10.40
BG_30_750_3	15.56	22.44	0.77	61.22	3.93	10.08
BG_30_850_1	21.28	19.63	0.51	58.58	2.75	10.76
BG_30_850_2	17.17	21.71	0.55	60.55	3.53	10.11
BG_30_850_3	17.04	22.33	0.43	60.18	3.53	10.20
OPS_30_750_1	20.65	12.69	2.53	64.12	3.11	11.50
OPS_90_750_1	19.90	14.28	2.72	62.99	3.21	11.65
OPS_30_750_2	21.04	11.38	4.27	63.30	3.01	12.43
OPS_30_750_3	21.75	12.57	3.24	62.39	2.87	12.02
OPS_30_850_1	21.90	17.51	0.88	59.70	2.73	10.73
OPS_30_850_2	23.42	15.23	1.30	60.02	2.56	11.18
OPS_30_850_3	24.01	15.10	1.25	59.62	2.50	11.12
Blends*						
50%CS_50%BG	19.33	20.14	0.56	59.97	3.10	10.31
50%CS_50%OPS	19.29	20.35	0.64	59.70	3.09	10.84
90%CS_10%BG	17.45	21.98	0.45	60.12	3.45	10.73
90%CS_10%OPS	16.47	22.06	0.28	61.19	3.72	10.57

Sample name nomenclature: Biomass_Steam fraction (%)_Temperature (°C)_Time (h)
*Blends were gasified at 850°C, during 1 hour, with a 30% steam atmosphere

terms, it can be considered that according to its composition, the produced gas from the steam gasification of the analyzed samples is suitable for energy applications such as boilers, gas turbines, or internal combustion engines.

5.4 Conclusion

Coconut shells (CS), oil palm shells (OPS) and bamboo guadua (BG) were gasified in this work under different experimental conditions, in order to understand the impact of the biomass characteristics in their steam gasification behavior and product yield. The experimental results showed that the inorganic content impact in a very important way the gasification reactivity and product yield of the samples. For its part, the organic composition, especially the H/C and O/C ratios seem to be related to the composition and heating value of the produced gas.

The beneficial impact of AAEM, particularly K, in the steam gasification reactivity and gas yield was confirmed, as well as the inhibitory effect of Si and P. In this regard, the validity of the inorganic ratio K/(Si+P) to classify and predict the steam gasification behavior of lignocellulosic waste was verified. Gasification of samples with K/(Si+P) above 1 resulted in higher gas yields and gas efficiencies compared to samples with K/(Si+P) below 1.

Moreover, with similar H/C and O/C ratios, no significant differences were observed between the analyzed samples in terms of gas composition and heating value. In this regard, with a high heating value between 10 and 12 MJ/m^3, and a H_2/CO ratio between 2.5 and 4, the steam gasification produced gas from lignocellulosic feedstocks with H/C and O/C ratio near 1.5 and 0.8 respectively, is considered suitable for energy applications using boilers, gas turbines or internal combustion engines.

The experimental observations presented in this work could be an important reference for real gasification applications working with different kind of lignocellulosic residues, as the process parameters and conditions should be adapted according to the feedstock characteristics, and particularly, its inorganic content.

Bibliography

[1] Juan Daniel Martínez, Khamid Mahkamov, Rubenildo V. Andrade, and Electo E. Silva Lora. "Syngas production in downdraft biomass gasifiers and its application using internal combustion engines." In: *Renewable Energy* 38.1 (2012), pp. 1–9 (cit. on p. 94).

[2] Emanuele Graciosa Pereira, Jadir Nogueira Da Silva, Jofran L. De Oliveira, and Cássio S. MacHado. *Sustainable energy: A review of gasification technologies*. 2012 (cit. on p. 94).

[3] Tatiana Ramos Pacioni, Diniara Soares, Michele Di Domenico, Maria Fernanda Rosa, Regina de Fátima Peralta Muniz Moreira, and Humberto Jorge José. "Bio-syngas production from agro-industrial biomass residues by steam gasification." In: *Waste Management* (2016) (cit. on p. 94).

[4] Anwar Sattar, Gary A. Leeke, Andreas Hornung, and Joseph Wood. "Steam gasification of rapeseed, wood, sewage sludge and miscanthus biochars for the production of a hydrogen-rich syngas." In: *Biomass and Bioenergy* 69 (Oct. 2014), pp. 276–286 (cit. on p. 94).

[5] Prabir Basu. "Gasification Theory." In: *Biomass Gasification, Pyrolysis and Torrefaction*. Elsevier Inc., 2013. Chap. Chapter 7, pp. 199–248 (cit. on pp. 94, 106, 107).

[6] Prakash Parthasarathy and K Sheeba Narayanan. "Hydrogen production from steam gasification of biomass: Influence of process parameters on hydrogen yield e A review." In: *Renewable Energy* 66 (2014), pp. 570–579 (cit. on pp. 94, 101).

[7] Weijuan Lan, Guanyi Chen, Xinli Zhu, Xin Wang, Xuetao Wang, and Bin Xu. "Research on the characteristics of biomass gasification in a fluidized bed." In: *Journal of the Energy Institute* (2018) (cit. on p. 95).

[8] Feng Yan, Si-Yi Luo, Zhi-Quan Hu, Bo Xiao, and Gong Cheng. "Hydrogen-rich gas production by steam gasification of char from biomass fast pyrolysis in a fixed-bed reactor: Influence of temperature and steam on hydrogen yield and

syngas composition." In: *Bioresource Technology* 101 (2010), pp. 5633–5637 (cit. on pp. 95, 102).
[9] Elango Balu, Uisung Lee, and J.N. Chung. "High temperature steam gasification of woody biomass – A combined experimental and mathematical modeling approach." In: *International Journal of Hydrogen Energy* 40.41 (2015), pp. 14104–14115 (cit. on p. 95).
[10] Colomba Di Blasi. "Combustion and gasification rates of lignocellulosic chars." In: *Progress in Energy and Combustion Science* 35.2 (2009), pp. 121–140 (cit. on p. 95).
[11] Capucine Dupont, Sylvain Jacob, Khalil Ould Marrakchy, Céline Hognon, Françoise Labalette, Maguelone Grateau, and Denilson Da Silva Perez. "How inorganic elements of biomass influence char steam gasification kinetics." In: *Energy* 109 (2016), pp. 430–435 (cit. on p. 95).
[12] Lina María Romero Millán, Fabio Emiro Sierra Vargas, and Ange Nzihou. "Steam gasification behavior of tropical agrowaste: A new modeling approach based on the inorganic composition." In: *Fuel* 235.December 2017 (2019), pp. 45–53 (cit. on pp. 95, 102, 104).
[13] Filomena Pinto, Rui André, Miguel Miranda, Diogo Neves, Francisco Varela, and João Santos. "Effect of gasification agent on co-gasification of rice production wastes mixtures." In: *Fuel* 180 (2016), pp. 407–416 (cit. on pp. 95, 106).
[14] S. T. Chaudhari, A. K. Dalai, and N. N. Bakhshi. "Production of hydrogen and/or syngas (H2+ CO) via steam gasification of biomass-derived chars." In: *Energy and Fuels* 17.4 (2003), pp. 1062–1067 (cit. on p. 95).
[15] Sylvain Fremaux, Sayyed-Mohsen Beheshti, Hojat Ghassemi, and Rasoul Shahsavan - Markadeh. "An experimental study on hydrogen-rich gas production via steam gasification of biomass in a research-scale fluidized bed." In: *Energy Conversion and Management* 91 (2015), pp. 427–432 (cit. on pp. 95, 106).
[16] Hakan Karatas and Fehmi Akgun. "Experimental results of gasification of walnut shell and pistachio shell in a bubbling fluidized bed gasifier under air and steam atmospheres." In: *Fuel* 214 (2018), pp. 285–292 (cit. on p. 95).
[17] Nimit Nipattummakul, Islam Ahmed, Somrat Kerdsuwan, and Ashwani K. Gupta. "High temperature steam gasification of wastewater sludge." In: *Applied Energy* 87.12 (2010), pp. 3729–3734 (cit. on p. 95).
[18] Kongvui Yip, Fujun Tian, Jun-Ichiro Hayashi, and Hongwei Wu. "Effect of Alkali and Alkaline Earth Metallic Species on Biochar Reactivity and Syngas Compositions during Steam Gasification." In: *Energy & Fuels* 24 (2010), pp. 173–181 (cit. on p. 95).
[19] Javier Herguido, José Corella, and José González-Saiz. "Steam Gasification of Lignocellulosic Residues in a Fluidized Bed at a Small Pilot Scale. Effect of the Type of Feedstock." In: *Industrial and Engineering Chemistry Research* 31.5 (1992), pp. 1274–1282 (cit. on pp. 95, 102).
[20] Lina Maria Romero Millan, Fabio Emiro Sierra Vargas, and Ange Nzihou. "Kinetic Analysis of Tropical Lignocellulosic Agrowaste Pyrolysis." In: *BioEnergy Research* (2017) (cit. on p. 95).
[21] *CEN/TS 15439:2006. Biomass gasification - Tar and Particles in Product Gases - Sampling and Analysis.* Tech. rep. Brussels: European Commitee for Standardization, 2006 (cit. on p. 96).

[22] Pengmei Lv, Jie Chang, Zuhong Xiong, Haitao Huang, Chuangzhi Wu, Yong Chen, and Jingxu Zhu. "Biomass air-steam gasification in a fluidized bed to produce hydrogen-rich gas." In: *Energy and Fuels* 17.3 (2003), pp. 677–682 (cit. on p. 101).

[23] C Guizani, F J Escudero Sanz, and S Salvador. "The gasification reactivity of high-heating-rate chars in single and mixed atmospheres of H2O and CO2." In: *Fuel* 108 (2013), pp. 812–823 (cit. on p. 102).

[24] Y Zhang, M Ashizawa, S Kajitani, and K Miura. "Proposal of a semi-empirical kinetic model to reconcile with gasification reactivity profiles of biomass chars." In: *Fuel* 87 (2008), pp. 475–481 (cit. on pp. 103, 104).

[25] Makiko Kajita, Tokuji Kimura, Koyo Norinaga, Chun-Zhu Li, and Jun-Ichiro Hayashi. "Catalytic and Noncatalytic Mechanisms in Steam Gasification of Char from the Pyrolysis of Biomass." In: (2009) (cit. on p. 103).

[26] Ange Nzihou, Brian Stanmore, and Patrick Sharrock. "A review of catalysts for the gasification of biomass char, with some reference to coal." In: *Energy* 58 (Sept. 2013), pp. 305–317 (cit. on pp. 103, 104).

[27] Douglas W. McKee. "Mechanisms of the alkali metal catalysed gasification of carbon." In: *Fuel* 62.2 (Feb. 1983), pp. 170–175 (cit. on p. 104).

[28] M Perander, N Demartini, A Brink, J Kramb, O Karlström, J Hemming, A Moilanen, J Konttinen, and M Hupa. "Catalytic effect of Ca and K on CO 2 gasification of spruce wood char." In: *Fuel* 150 (2015), pp. 464–472 (cit. on p. 104).

[29] Yanqin Huang, Xiuli Yin, Chuangzhi Wu, Congwei Wang, Jianjun Xie, Zhaoqiu Zhou, Longlong Ma, and Haibin Li. "Effects of metal catalysts on CO 2 gasification reactivity of biomass char." In: *Biotechnology Advances* 27 (2009), pp. 568–572 (cit. on p. 104).

[30] Kentaro Umeki, Antero Moilanen, Alberto Gómez-Barea, and Jukka Konttinen. "A model of biomass char gasification describing the change in catalytic activity of ash." In: *Chemical Engineering & Technology* 207-208 (2012), pp. 616–624 (cit. on p. 104).

[31] Dan Boström, Nils Skoglund, Alejandro Grimm, Christoffer Boman, Marcus Öhman, Markus Broström, and Rainer Backman. "Ash transformation chemistry during combustion of biomass." In: *Energy and Fuels* 26.1 (2012), pp. 85–93 (cit. on p. 104).

[32] Yanqing Niu, Houzhang Tan, and Shi'En Hui. "Ash-related issues during biomass combustion: Alkali-induced slagging, silicate melt-induced slagging (ash fusion), agglomeration, corrosion, ash utilization, and related countermeasures." In: *Progress in Energy and Combustion Science* 52 (2016), pp. 1–61 (cit. on p. 104).

[33] D. Nutalapati, R. Gupta, B. Moghtaderi, and T. F. Wall. "Assessing slagging and fouling during biomass combustion: A thermodynamic approach allowing for alkali/ash reactions." In: *Fuel Processing Technology* 88.11-12 (2007), pp. 1044–1052 (cit. on p. 104).

[34] Céline Hognon, Capucine Dupont, Maguelone Grateau, and Florian Delrue. "Comparison of steam gasification reactivity of algal and lignocellulosic biomass: Influence of inorganic elements." In: *Bioresource Technology* 164 (2014), pp. 347–353 (cit. on p. 104).

[35] Hakan Karatas, Hayati Olgun, and Fehmi Akgun. "Experimental results of gasification of cotton stalk and hazelnut shell in a bubbling fluidized bed gasifier under air and steam atmospheres." In: *Fuel* 112 (2013), pp. 494–501 (cit. on p. 106).

[36] I Ahmed and A K Gupta. "Syngas yield during pyrolysis and steam gasification of paper." In: *Applied Energy* 86 (2009), pp. 1813–1821 (cit. on p. 106).
[37] Prabir Basu. *Biomass Gasification and Pyrolysis. Practical Design.* First Edit. Oxford: Elsevier, 2010, p. 364 (cit. on p. 107).
[38] Heidi C Butterman and Marco J Castaldi. "Influence of CO2 Injection on Biomass Gasification." In: *Industrial & Engineering Chemistry Research* 46.26 (2007), pp. 8875–8886 (cit. on p. 107).
[39] Dewi Tristantini, Dijan Supramono, and Ricky Kristanda Suwignjo. "Catalytic effect of K2CO3 in steam gasification of lignite char on mole ratio of H2/CO in syngas." In: *International Journal of Technology* 6.1 (2015), pp. 22–30 (cit. on p. 107).
[40] Yan Cao, Zhengyang Gao, Jing Jin, Hongchang Zhou, Marten Cohron, Houying Zhao, Hongying Liu, and Weiping Pan. "Synthesis Gas Production with an Adjustable H 2 /CO Ratio through the Coal Gasification Process: Effects of Coal Ranks And Methane Addition." In: *Energy & Fuels* 22.3 (2008), pp. 1720–1730 (cit. on p. 107).
[41] Heidi C. Butterman and Marco J. Castaldi. "CO2 as a Carbon Neutral Fuel Source via Enhanced Biomass Gasification." In: *Environmental Science & Technology* 43.23 (2009), pp. 9030–9037 (cit. on p. 107).
[42] Xueping Song and Zhancheng Guo. "Technologies for direct production of flexible H2/CO synthesis gas." In: *Energy Conversion and Management* 47.5 (2006), pp. 560–569 (cit. on p. 107).
[43] Bibhuti B. Sahoo, Niranjan Sahoo, and Ujjwal K. Saha. "Effect of H 2:CO ratio in syngas on the performance of a dual fuel diesel engine operation." In: *Applied Thermal Engineering* 49 (2012), pp. 139–146 (cit. on p. 107).

Chapter

6

Physico-chemical characterization of steam gasification chars from tropical lignocellulosic agrowaste

Abstract

In this study, the steam gasification chars from three lignocellulosic agrowastes with different macromolecular structure and inorganic composition were analyzed, in order to understand the impact of the raw biomass characteristics on the char physico-chemical properties. The experimental results showed that the produced chars are highly microporous materials with surface areas between 500 and 1000 m^2/g, comparable to activated carbons. The char properties can be modified by changing the gasification process conditions, including gasification temperature and time, as well as the steam fraction

in the gasifying agent. The principal differences observed between the three analyzed samples can be mainly attributed to their inorganic composition, and more specifically, to their inorganic ratio K/(Si+P). Under the same gasification conditions, samples with inorganic ratio above 1 showed higher surface areas, with greater proportions of surface oxygen-containing functional groups, in comparison to samples with ratios below 1. For its part, the macromolecular composition seems to have an influence in the pore size distribution of the gasification chars. The observations in this work could be an important reference for gasification applications working with several kind of residues, where the valorization of the solid by-product is intended.

6.1 Introduction

Tropical regions have a great potential for the development of agricultural and agroindustrial activities, thanks to their climate and geographic location. Developing countries in these areas have particular energy needs in rural and isolated zones, as several communities still lack access to reliable energy services. These populations base their economy in agricultural and related activities, and usually produce significant amounts of agrowastes that remain under-exploited. These residues could be valorized as biofuels in local applications to meet the communities energy needs. However, in most cases, the sustainability of biomass valorization projects in isolated areas depends on the creation of related productive activities that go beyond the energy supply, generating new incomes for local communities [1, 2]. Considering the existence of important amounts of agrowastes, simultaneous energy and business development opportunities around biomass valorization could be considered.

In this context, steam gasification seems to be a very interesting thermochemical process, as it produces high heating value fuel gases that can be used for heat or power generation [3–5], and a solid porous by-product that could also be valorized [6, 7]. Nevertheless, as the availability of agrowastes is often seasonal, gasification facilities should work with diverse residues, having different characteristics. In this regard, the understanding of the impact of the feedstock characteristics on the gasification behavior and by-products is of great importance, in order to properly adapt the process conditions to the application requirements.

Different authors have investigated the influence of the process conditions on the main properties of pyrolysis and gasification chars. The process temperature and time, as well as the reaction atmosphere, are reported to have a very important impact on the char physico-chemical characteristics [8, 9]. Among these parameters, the reaction atmosphere has probably the most important effect in the char porous structure and surface chemistry [10]. Air gasification chars show considerably lower specific surface areas in comparison to steam, CO_2, or air/steam gasification solid by-products. In particular, steam gasification chars are comparable to physical activated carbons, with high surface areas and pore volumes, and an important amount of surface functional groups. In the literature, the reported surface areas of steam gasification chars from different feedstocks are between 400 and 1000 m^2/g [11, 12], comparable to activated carbons with surfaces areas around 1000 m^2/g or higher. In contrast, air gasification chars, usually need to be upgraded by subsequent activation, to be used in adsorption or catalytic applications [13–15].

Moreover, the influence of the process conditions in the char properties have been widely analyzed for several lignocellulosic agrowastes like rice husk and straw [8], wood [16], coconut shells [17], switchgrass [18], and others. In contrast, the impact of the raw feedstocks in the properties of the gasification chars still needs to be investigated. Different authors have suggested that the macromolecular composition and the ash content of the samples may have an influence in the properties of activated carbons and chars [19]. However, as most studies deal with only one kind of feedstock, the understanding of this question needs to be improved.

In this regard, previous works have proven that the composition of the samples impact in a very important way their gasification reactivity [20, 21]. In particular, the inorganic content of the biomass could play a catalytic or an inhibitory role in the progress of the steam gasification reactions. More specifically, alkali and alkali earth metals (AAEM) like K, Ca, Na and Mg have a beneficial effect on biomass gasification [22, 23], that could be inhibited by elements like Al, Si and P [24, 25]. Nevertheless, the influence of inorganics in the gasification char properties is not clear. In the same way, regarding the macromolecular composition of the samples, a controversy exists in the literature in relation to the impact of the hemicellulose, cellulose and lignin content of the raw materials in the pore development and structure of chars and activated carbons [26–28].

In this regard, the aim of this work is to understand the influence of the biomass characteristics and composition on the physico-chemical properties of steam gasification chars. The steam gasification solid by-products from various lignocellulosic agrowastes with different macromolecular structure and within a wide range of inorganic composition were analyzed. Coconut shells (CS), bamboo guadua (BG) and oil palm shells (OPS) were used as feedstocks. The bulk organic and inorganic composition of the chars were analyzed, as well as the distribution of minerals in their surface. In addition, the surface area, pore structure, and surface chemistry were also evaluated and compared. Finally, the relationship between the char structure and surface chemistry was discussed for the three samples.

6.2 Materials and methods

6.2.1 Materials

The chars obtained from the steam gasification of three tropical lignocellulosic biomasses under different experimental conditions were characterized and analyzed in this study. Oil palm shells (OPS), coconut shells (CS) and bamboo guadua (BG) were selected as raw materials for the gasification experiments. The detailed origin of the samples, collected in Colombia-South America, as well as their organic and inorganic chemical composition are presented in a previous work [20, 29].

6.2.2 Experimental setup

Steam gasification experiments were carried out in a semicontinuous lab-scale fluidized bed gasifier. An externally heated stainless steel reactor of 60 cm height and 6 cm internal diameter, equipped with a porous disk in the bottom to hold the sample and allow the gasification atmosphere to pass through was used. The thermal regulation was ensured by an Eurotherm controller connected to a K-thermocouple in the center of

the reactor. A steam generator equipped of a water mass flow controller and a heating device producing superheated steam at 180°C, supplied the required steam for the gasification process. The detailed experimental setup has been presented in chapter 3.

For all the experiments, 80 g of biomass were placed inside the reactor and heated to the gasification temperature at a heating rate of 20°C/min, under nitrogen. When the gasification temperature was reached (from 750°C to 850°C), the atmosphere was switched to a mixture of H_2O/N_2 (from 15% to 90% of steam in the gasifying agent - 50 to 300 g/h of steam) and was maintained during all the gasification stage (t from 1h to 3h). The total flow rate was $0.7\,m/h^3$ for all the experiments. After each test, the reactor was cooled down to room temperature under nitrogen. The remaining char was collected, weighted, and stored for subsequent characterization. Pyrolysis tests were performed in order to determine the solid yield at the end of the heating period (pyrolysis stage) for each gasification temperature. In order to verify the reproducibility, several tests were carried out twice. The repeatability was found to be satisfactory as the standard deviation of the solid yield was below 3%

6.2.3 Char burn-off and gasification reactivity

For each steam gasification test, the char burn-off achieved at the end of the experiment was calculated according to equation 6.2.1:

$$Burn - off(\%) = \frac{m_0 - m_f}{m_0} \times 100 \tag{6.2.1}$$

Where m_0 is the mass of the sample at the beginning of the gasification stage, determined from the pyrolysis-only tests; and m_f the mass of the remaining char at the end of the experiment, on a dry ash free basis.

Likewise, from the measurement of the remaining char at the end of each gasification experiment, the average gasification reactiviy of the samples can be calculated for different gasification times. The degree of conversion of the char after the gasification stage is defined as in equation (6.2.2):

$$\alpha(t) = \frac{m_0 - m(t)}{m_0 - m_{ash}} \tag{6.2.2}$$

Where m_0 is the mass of the sample at the beginning of the gasification stage, $m(t)$ the mass at the end of the gasification period t, and m_{ash} the mass of ash in the sample.

The apparent gasification reactivity can be then defined as a function of the conversion degree α, as presented in equation 6.2.4. Generally, reactivity comparisons are referred to a specific char conversion level. However, as the continuous monitoring of the mass loss of each biomass in not possible for the presented experimental setup, the gasification reactivity is presented in this study as an average for a defined gasification time, and is calculated according to the equation (6.2.4), Where t is the time of the steam gasification stage, from 1h to 3h.

$$R(\alpha)_{(app)} = \frac{1}{1 - \alpha(t)} \frac{d\alpha}{dt} \tag{6.2.3}$$

$$R_{(app)\ average} = \frac{1}{n}\sum_{t=1}^{n}\frac{1}{1-\alpha(t)}\frac{d\alpha}{dt} \tag{6.2.4}$$

6.2.4 Char characterization

Proximate analysis and elemental composition

The elemental analysis (CHNS) of the collected chars was determined using a Thermoquest NA 2000 elemental analyzer. To determine the inorganic composition, 150mg of ground char (with a particle size below 500µm) were acid digested in close vessels at 220°C during 4h. Acid reagents H_2O_2, HNO_3, HF and H_3BO_3 were used according to EN 16967. Acid solutions were diluted with demineralized water to 50 ml and analyzed using an HORIBA Jobin Yvol Ultima 2 inductively coupled plasma optical emission spectrometer (ICP-OES). For its part, the ash content of the samples was calculated according to the standard EN ISO 18122. All the analysis were performed with at least three replicates.

Scanning Electron Microscopy (SEM) and Transmission Electron Microscopy (TEM)

The morphology of the chars was observed using a Hitachi TM3030 Plus tabletop scanning electron microscope (SEM), with an accelerating voltage of 15kV. The local chemical composition at a micro-scale was determined by using the energy dispersive X-ray spectroscopy (EDX) module in the same apparatus.

For its part, the carbon structure of the gasification chars at a nanometric scale was observed using a JEOL JEM-ARM200F transmission electron microscope (TEM). Elemental mapping of chemical species in the sample was performed using and EDX module in the same microscope. Powder char samples with particle size below 250 µm were dispersed in ethanol, then mixed in an ultrasonic bath. The samples were collected from the surface of the solution and deposited onto carbon support films.

X-Ray Diffraction (XRD)

X-ray diffraction (XRD) analyses of char powder samples (particle size below 250 µm) were carried out to analyze their global carbon structure. Experiments were performed using a Philips Panalytical X'pert Pro MPD diffractometer using a Cu Ka radiation source (1.543 Å) with a current of 45kV and an intensity of 40 mA. The diffraction patterns were collected between 2θ=10 and 2θ=70 with a step size of 0.05°.

Char pore structure and specific surface area

The pore structure of gasification chars was determined by nitrogen adsorption at 77K using a Micromeritics 3Flex high-resolution analyzer. Prior to measurements, the samples were degassed in vacuum at 90°C during 1h and then at 150°C during 10h. The surface area was calculated from the adsorption isotherms using the Brunauer-Emmett-Teller (BET) model. The t-plot model was used to determine the micropore volume of samples, and the Non-local Density Functional Theory (NLDFT) to determine the micropore size distribution.

Surface oxygen-containing functional groups (SOFG)

The oxygen-containing functional groups in the char surface were determined using the temperature programmed desorption (TPD) technique. Experiments were carried out in a Micromeritics AutoChem II chemisorption analyzer. Approximately, 150mg of char were placed in a quartz U-tube and heated under an helium atmosphere. The sample was kept at 150°C during 1 hour and then was heated to 1000°C with a heating rate of 5°C/min. The concentration of CO and CO_2 released was quantitatively analyzed using a MyGC Agilent micro-GC. Preliminary tests were performed to evaluate the impact of the sample mass and bed height on the TPD results, showing that under the presented experimental conditions, the results are repeatable and the diffusion limitations due to sample bed height can be neglected. In general, the repeatability of the TPD tests was found to be satisfactory as the maximum calculated standard deviation between two experiments was below 10%

The obtained CO and CO_2 desorption curves were deconvoluted to determine the contribution of each type of oxygen complex. The procedure presented in this work is based on the TPD spectra analysis proposed by Zhou et al [30], using 6 Gaussian peaks for the deconvolution of the CO desorption curve and 6 peaks for the CO_2 curve. Regarding the peak assignment, even though the reported decomposition temperatures for SOFG in carbon materials vary widely depending on the heating rate and the geometry of the experimental system used, some general trends have been identified in the literature [31].

It is generally stated that the CO_2 desorption at low temperatures is associated to carboxylic acids, while lactones decomposition results in CO_2 desorption at high temperatures. Also, carboxylic anhydrides decomposition is related to both CO and CO_2, while phenols, ethers and quinones result in CO desorption. Despite these trends, different authors have demonstrated that the desorption temperatures of the functional groups and their associated TPD peaks can also vary with their chemical and geometric local environment. Consequently, it may be difficult to clearly determine the content of each particular functional group from TPD patterns. Although, it is possible to quantify the global CO and CO_2 yielding groups and estimate their proportion in the char surface.

Accordingly, the CO desorption curves obtained were decomposed using Gaussian functions centered at 250±50°C and 380±50°C for carboxylic groups, 500±50°C for peroxydes, and 620±50°C, 750±50°C, and 800±50°C for lactones at different energetic sites. In the same way, the CO_2 curves were deconvoluted using functions centered at 400±50°C for acid anhydrides, 620±50°C for hydroxyl groups, 740±50°C for phenol groups, 860±50°C for ether groups, and 900±50°C and 970±50°C for quinone and pyrone groups respectively. The mentioned peak positions and a constraint over the peak width (55±5°C) were used for the optimization of the curve fitting. The fitting error between the experimental and the deconvoluted curve was always below 8%.

pH at the point of zero-charge (pH_{PZC})

The pH value at which the net charge of the chars surface is 0, or point of zero-charge (pH_{PZC}), was measured using a Malvern Pananalytical Zetasizer NanoZS. Char samples were ground into powder, with a particle size below 250 µm. About 15 mg of sample were used for each test with an approximate sample concentration of 0.5 mg/ml. Measurements were done at room temperature within the pH range from 2 to 11,

adjusted by the addition of a 0.25M HCl or 0.1M NaOH solution. The carbon pH_{PZC} was then defined as the pH at which the electrical charge density measured on the surface was zero.

6.3 Results and discussion

6.3.1 Composition of gasification chars

Table 6.1 reports the elemental composition of the gasification chars analyzed in the present study. In the table, the sample name gives information about the raw biomass and the gasification conditions in the following order: steam fraction in the gasifying agent, gasification temperature, and gasification time. In general, CS and OPS gasification chars are highly carbonaceous materials with carbon content above 80%. BG chars, with higher ash content exhibit lower carbon percentages from 70% to 36%.

Table 6.1: Organic and inorganic composition of the analyzed chars

	Elemental analysis (wt.% dry basis)					**Main inorganic constituents (mg/kg dry basis)**				
Sample	**C**	**H**	**N**	**O***	**Ash**	**Ca**	**K**	**Na**	**P**	**Si**
CS_30_750_1	87.7	1.3	0.3	6.8	3.9	390.0	8146.6	3130.0	242.7	1398.5
CS_90_750_1	84.6	1.4	0.3	9.2	4.5	205.7	12330.8	4010.0	495.1	1887.0
CS_30_750_2	81.1	1.4	0.2	9.6	7.7	910.2	10518.6	3050.0	141.7	1012.5
CS_30_750_3	82.3	1.5	0.2	10.0	6.0	497.1	19495.8	4580.8	358.1	1222.1
CS_30_850_1	79.2	1.3	0.0	11.3	8.2	491.1	20393.8	4188.7	269.7	779.8
CS_30_850_2	80.7	1.2	0.1	10.9	7.1	381.4	16845.7	4102.0	305.4	1695.5
BG_30_750_1	69.7	1.2	0.3	5.2	23.6	984.2	15438.4	432.7	804.4	56563.7
BG_90_750_1	68.5	1.1	0.4	6.8	23.2	850.8	22200.1	554.9	1124.2	81173.2
BG_30_750_2	67.1	1.0	0.2	7.2	24.5	1281.0	21991.1	447.8	884.9	73697.0
BG_30_750_3	67.6	1.0	0.2	6.5	24.8	1127.8	22397.8	427.8	925.8	77031.0
BG_30_850_1	60.8	0.8	0.3	6.6	31.5	1316.5	30501.5	376.5	1662.9	86598.5
BG_30_850_2	49.1	0.6	0.1	6.2	44.0	670.9	64937.1	525.9	5786.5	96860.0
BG_30_850_3	36.7	0.6	0.1	4.8	57.9	880.3	84258.2	603.1	8563.0	120697.0
OPS_30_750_1	87.0	1.3	0.7	6.6	4.4	1234.2	3984.6	35.4	1304.2	12623.1
OPS_90_750_1	84.9	1.4	0.6	7.7	5.5	1500.8	4201.2	41.3	1443.4	13052.2
OPS_30_750_2	87.5	1.3	0.5	6.0	4.6	1425.8	4003.1	51.3	1305.5	13906.2
OPS_30_750_3	87.6	1.3	0.5	5.8	4.8	1506.3	4512.3	61.2	1654.8	13748.2
OPS_30_850_1	85.2	0.8	0.5	8.6	4.9	1560.9	6375.3	101.2	2255.6	13477.0
OPS_30_850_2	83.8	0.8	0.4	9.3	5.6	1651.3	7425.8	101.1	2187.3	15624.1
OPS_30_850_3	81.0	0.8	0.3	9.6	8.3	1589.4	8495.6	90.2	2874.2	16879.0

* Calculated by difference

The mineral composition of the chars is in accordance with the composition of the raw materials. CS chars are mainly composed of K and Na, while BG and OPS chars show greater amounts of Si. The dispersion of minerals in the char surface are presented in the SEM-EDX micrographs in figure 6.1, for 1 hour gasification chars obtained at 850°C with 30% of steam in the gasifying agent.

SEM-EDX images are in accordance with the information obtained from the ICP-OES results and show that minerals in the CS chars are well dispersed in the surface. In general, K and Na were the dominant elements detected, with some traces of Ca.

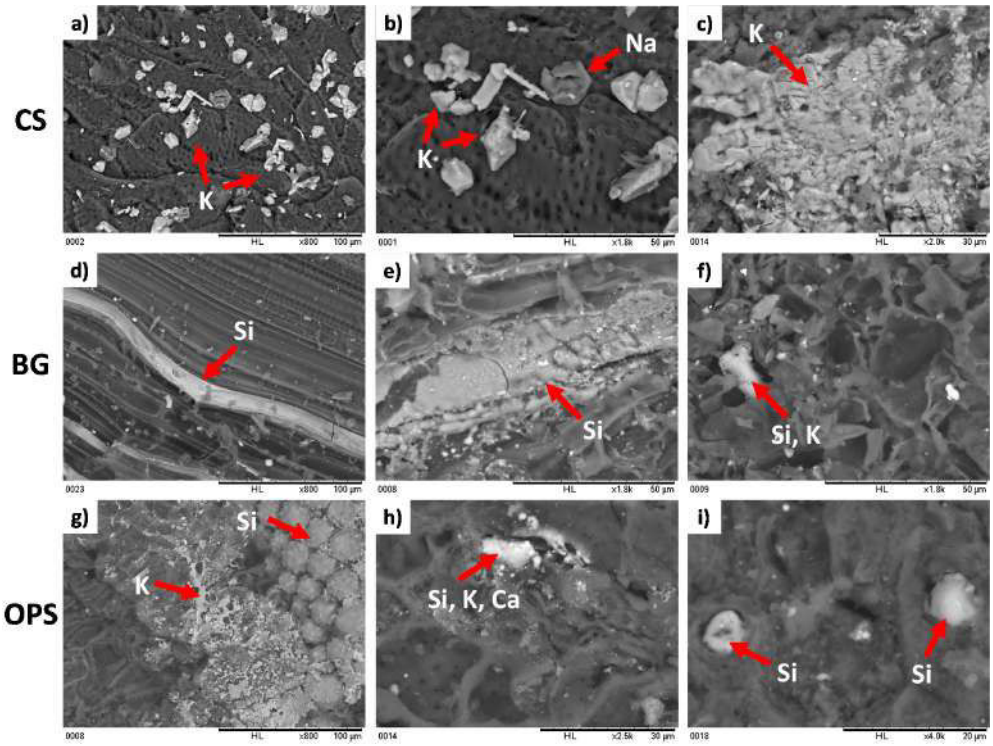

Figure 6.1: SEM-EDX micrographs of analyzed chars. Gasification conditions: 1 hour, 850°C, 30% steam in the gasifying agent

Furthermore, Si was the main element observed in OPS chars, as well as some Ca and K. Finally, SEM-EDX analyzes confirmed the higher mineral content of BG chars. In this case, Si was detected in almost all the char surface, probably as SiO_2, or associated to K.

6.3.2 Char yield and burn-off

To understand the impact of the biomass characteristics in the gasification char properties, different process conditions were analyzed and compared.

For the three biomasses, the recovered char at the end of the gasification process was reduced with the increase of the steam fraction in the gasifying agent, the temperature and the gasification time. The impact of these parameters in the gasification behavior of CS, BG and OPS was analyzed previously in a thermogravimetric scale [20], and is in accordance with the experimental results obtained in this work. Higher gasification temperatures and steam quantities are related to higher reactivities, an then, to higher carbon conversions and lower char yields. In the same way, longer gasification times also allow higher carbon conversions, resulting in less recovered char at the end of the experiment.

In this regard, from a general point of view, the impact of the process parameters on the steam gasification solid yield and burn-off, defined in equation 6.2.1, is the same for the three studied biomasses. From figure 6.2, it can be observed that the three materials exhibit a linear correlation between the gasification time and the char burn-off.

However, for the same experimental conditions, the calculated char burn-off is always considerably higher for CS compared to BG and OPS. These results are in accordance with Daud and Ali [26], who analyzed the activation behavior of CS and OPS chars under a steam atmosphere, and observed a greater burn-off evolution of CS compared to OPS, with the activation time.

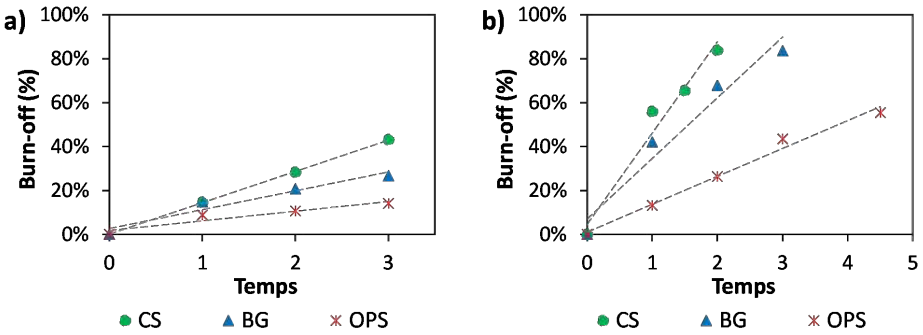

Figure 6.2: Char burn-off Vs. time of studied biomasses gasified in a 30% steam atmosphere. a) 750°C, b) 850°C

This experimental observation is supported by the results of the calculated average steam gasification reactivity of the three samples, summarized in table 6.2. In fact, regardless of the gasification temperature, the reactivity values of CS were always higher compared to BG and OPS. For instance, at 850°C, the BG and OPS reactivities correspond to only 51% and 14% of the CS value respectively, explaining the lower solid yield and higher char burn-off observed for CS under the same experimental conditions.

Table 6.2: Calculated mean gasification reactivity during 3 hours in a 30% steam atmosphere

	Mean reactivity (%/min)		
Temperature	**CS**	**BG**	**OPS**
750°C	0.35	0.25	0.08
850°C	2.28	1.18	0.32

As discussed in a previous work, the differences in the steam gasification reactivities of the samples can be mainly attributed to the inorganic composition of the raw materials [20]. Coconut shells main inorganic constituents are K and Ca, that have a catalytic impact on the steam gasification reactions [24, 32, 33], while oil palm shells and bamboo are mainly composed of Si and P, that tend to react with AAEM and inhibit their beneficial effect [34, 35].

More specifically, the inorganic ratio K/(Si+P) proposed by Hognon et al. [21] was employed in this work to analyze and compare the impact of the inorganic composition of the samples in their gasification reactivity. Coconut shells, with an inorganic ratio of 3.9 (K/(Si+P) $>$ 1), have a higher proportion of K in relation to Si and P, and then, follow a catalytic gasification behavior. In contrast, BG and OPS, with inorganic ratios 0.2 and 0.17 respectively (K/(Si+P) $<$ 1), have a higher proportion of Si and P that inhibit the beneficial impact of AAEM (principally K). In accordance to this, the

TEM-EDX cartography in figure 6.3, shows the distribution of inorganic elements in BG chars produced at 850°C. It is possible to observe that K and Ca, with potential catalytic impact on steam gasification, may be associated with Si, explaining the inhibition of their beneficial effect. In this regard, the inorganic ratio K/(Si+P) can explain the differences observed between the char burn-off evolution of CS in comparison to BG and OPS. TEM-EDX results are in accordance with SEM-EDX micrographs presented in fig.6.1.

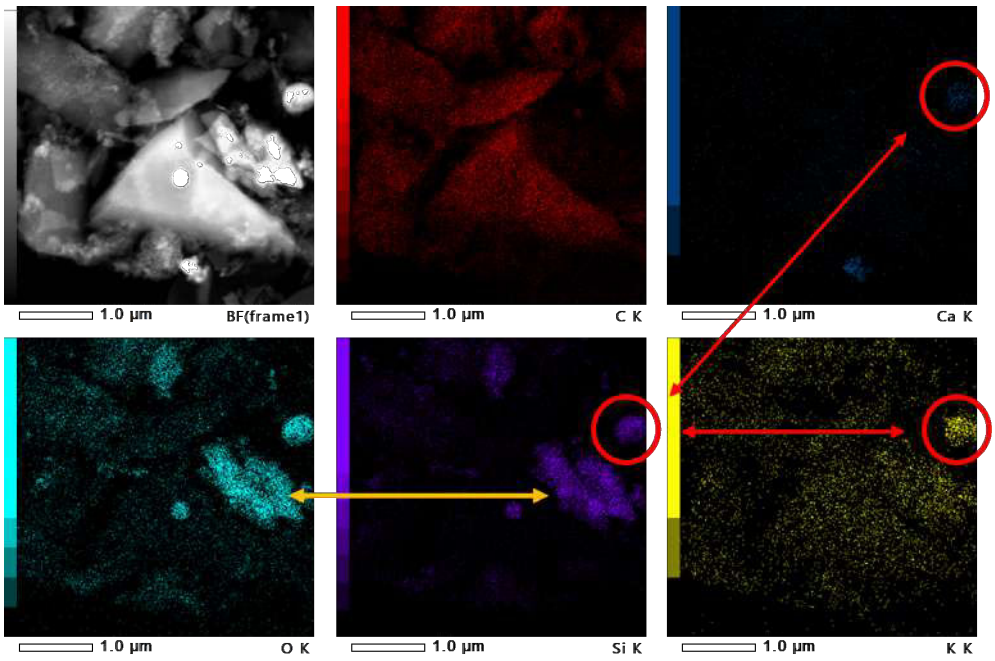

Figure 6.3: TEM-EDX cartographic images of BG char. Gasification conditions: 1 hour, 850°C, 30% steam in the gasifying agent

6.3.3 Char specific surface area and pore structure

From the N_2 adsorption experiments, the specific surface area of the gasification chars was determined. As expected, an increase in the BET char surface area was observed with the char burn-off. Indeed, the progress of the gasification reactions is related to carbon atoms consumption with the subsequent formation of pores in char structure [36]. This is in fact, the basis of the production of activated carbon through physical or thermal activation, attributed mainly to reaction R6.1, in the case of steam as the reacting atmosphere:

$$C + H_2O \longrightarrow CO + H_2 \qquad \text{(R6.1)}$$

This reaction generates CO and H_2 as gasification fuel gases and creates a porous network in the char. Gasification can also result in the chemisorption of oxygen and hydrogen in the char structure, creating surface oxygen complexes that influence in an important way the physico-chemical properties of chars [37].

Accordingly, in figure 6.4, it is possible to observe that for the three biomasses, there is a linear increase in the BET surface area with the char burn-off, for values below

60%. Then, the BET surface area begins to decrease. The maximum BET surface area attained was 1041.8 m^2/g for CS, 1014.0 m^2/g for OPS and 807.7 m^2/g for BG. Then, the subsequent decline may be due to the weakening and collapse of the char structure due to the progress of the gasification reactions [38–41].

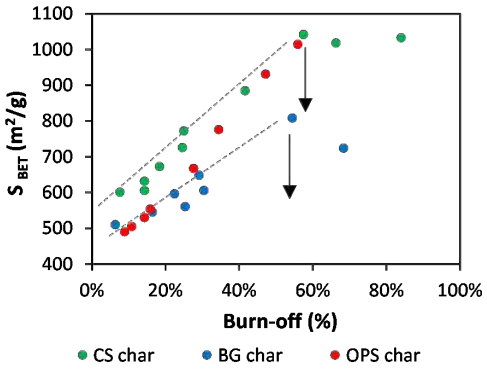

Figure 6.4: BET surface area of gasification chars in relation to burn-off

For burn-off degrees below 30%, CS chars developed nearly 35% more surface area compared to BG and OPS chars. In contrast, above 30%, OPS surface area approached the CS char values. The behavior observed at low burn-off degrees may be attributed to the differences in the gasification reactivity of the samples, while the results obtained for higher burn-off degrees could be related to the raw biomass structure and the ash content of chars. In particular, the high ash content of BG chars (higher than 30%), may explain the lower surface area development in comparison to CS and OPS, for burn-off degrees above 30% [42].

Nevertheless, it is worth mentioning that due to the differences in the gasification reactivity of the samples, the burn-off degree attained is not the same under identical experimental conditions and then, the developed char surface area is also different. From table 6.3, it can be observed that CS surface area is always higher in comparison to similarly produced BG and OPS chars. In this regard and as stated previously, two trends can be identified related to the inorganic composition of the samples. Under the same gasification conditions, feedstocks with inorganic ratio K/(Si+P) above 1 follow a catalytic gasification behavior and then, develop higher surface areas compared to samples with K/(Si+P) below 1.

From the analysis of N_2 adsorption tests, it was also found that for the three samples, the gasification chars obtained for burn-off degrees below 30% are highly microporous, with at least 85% of their surface area attributed to micropores. In contrast, for higher burn-off degrees, the microporosity of BG is reduced to 70%, while CS and OPS continue to show microporosity percentages above 87% and 82%, respectively. In fact, BG chars isotherms showed a higher development of narrow mesopores with the progress of the gasification process, as presented in figure 6.5.

To better understand the porous structure of the gasification chars, the pore-size distribution (PSD) calculated using the NLDFT model is presented in figure 6.6 for two different burn-off degrees. In both cases, it can be observed that the chars obtained from the three feedstocks are highly microporous. At a burn-off near 28% (figure 6.6a), it can be noticed that the surface area of CS and OPS chars can be mainly attributed

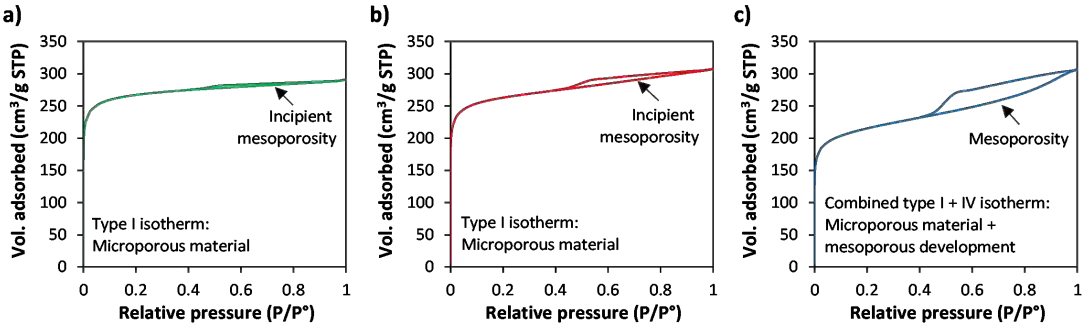

Figure 6.5: N_2 adsorption isotherms of chars at ∼ 55% burn-off. a) Coconut shells (CS_30_850_1), b) Oil palm shells (OPS_30_850_4.5), c) Bamboo guadua (BG_30_850_1)

to narrow microporosity (<1.0nm), while BG chars show also the existence of incipient mesopores. With the increase in the burn-off degree (figure 6.6b), the BG char pore-size distribution becomes larger, and the surface area attributed to narrow microporosity decreases considerably. In contrast, there is an increase in the proportion of micropores between 1-2 nm, and mesopores. For its part, CS still show a high proportion of narrow micropores and pores between 1-2 nm, with no visible development of mesoporosity. Finally, the OPS chars surface area is mostly associated to narrow micropores, with a lower proportion of pores between 1-2 nm, compared to the other feedstocks.

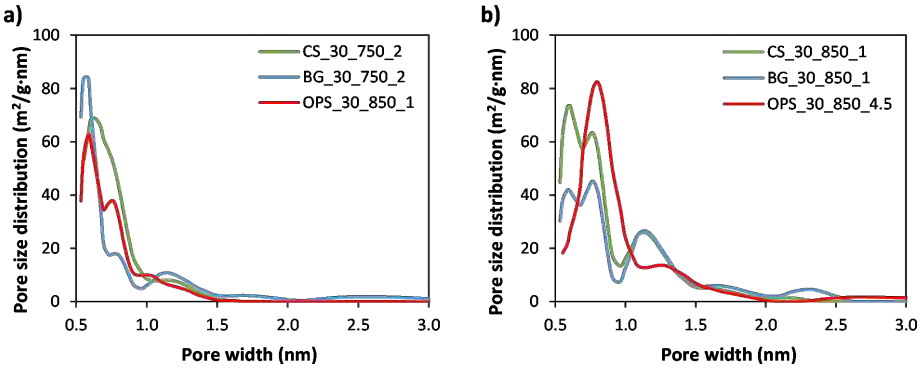

Figure 6.6: Pore size distribution of gasification chars. a) ∼ 28% burn-off. b) ∼ 55% burn-off

These differences may be related to the structure of the raw materials and their initial macromolecular composition. In fact, BG is a fibrous grass with high hemicellulose and cellulose content (>50%) [43]. Therefore, the thermal decomposition of these components during the pyrolysis stage may generate a more open char structure, resulting in a higher proportion of mesopores in the char. In contrast, CS and OPS are high-lignin endocarp feedstocks [44, 45].

In accordance to this, the micrographs in figure 6.7, present the surface morphology of the obtained chars at a burn-off degree near 55%. It is possible to observe that the structure of BG is visibly different from CS and OPS. In particular, BG shows

an irregular and open structure with visible macroporosity, while CS and OPS have a relatively smooth surface with some macropores, and a more compact structure.

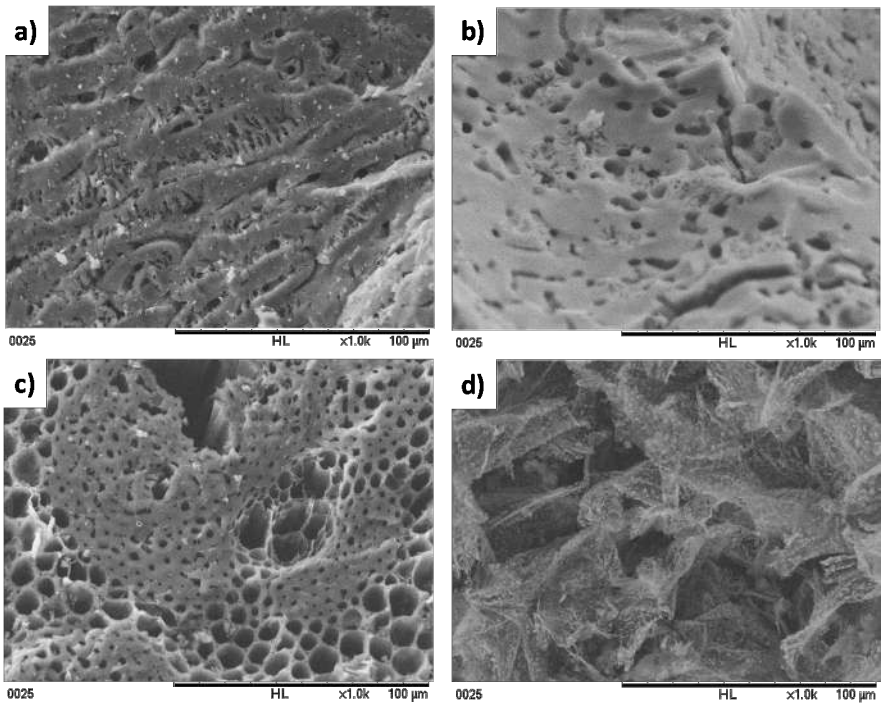

Figure 6.7: SEM micrographs of gasification chars at a burn-off degree near 55%. a) coconut shells, b) oil palm shells, c) bamboo guadua - cross-section view, d) bamboo guadua - longitudinal view

As reported by Rodriguez-Reinoso [46], the pore development process during char gasification begins with the creation of micropores followed by their subsequent widening, and then the creation of new pores. In this regard, a less compact structure as in the case of BG, facilitates the access of steam into the char structure and the widening of the existing pores, developing meso and macropores. Unlike some reported studies that attribute the development of macro and mesopores to the lignin content of the feedstock [26, 47], in the present study, the highest development of mesoporosity was observed for the samples with the highest hemicellulose and cellulose content.

In general terms, it can be said that the steam gasification of the analyzed feedstocks produces a highly microporous solid by-product with surface areas from 500 to 1000 m^2/g, close to literature reported activated carbon values [47], or gasification chars produced under similar conditions [11]. The main characteristics of the analyzed gasification chars are summarized in table 6.3.

6.3.4 Char global carbon structure

The global carbon structure of the gasification chars was analyzed using X-ray diffraction (XRD) and transmission electron microscopy (TEM). The diffraction profiles of all the analyzed chars exhibited two broad peaks at $2\theta \sim 23°$ and $2\theta \sim 44°$, attributed to graphite bands (0 0 2) and (1 0 0) respectively. The first peak is associated to the stacking of graphitic basal planes, and the latter one to graphite-like atomic order within

Table 6.3: Surface and structure characteristics of the analyzed gasification chars

	Char burn-off	Pore structure			TPD CO and CO_2 desorption		
Sample	**(%)**	**S_{BET} (m^2/g)**	**S_{micro} (m^2/g)**	**V_{micro} (cm^3/g)**	**CO_2 (mmol/g)**	**CO (mmol/g)**	**Total (mmol/g)**
CS_30_750_1	14.7	631.5	550.2	0.21	0.57	0.57	1.14
CS_90_750_1	25.5	725.6	603.1	0.23	0.50	0.78	1.28
CS_30_750_2	28.4	772.3	684.2	0.26	0.47	0.76	1.22
CS_30_750_3	43.2	884.0	779.0	0.30	0.69	1.04	1.73
CS_30_850_1	57.0	1041.8	898.9	0.34	0.83	0.57	1.41
CS_30_850_2	84.6	1032.6	952.0	0.38	0.76	1.56	2.32
BG_30_750_1	16.5	544.9	468.9	0.18	0.36	0.18	0.53
BG_90_750_1	25.3	560.0	500.0	0.16	0.35	0.55	0.90
BG_30_750_2	29.1	648.2	539.4	0.21	0.31	0.30	0.62
BG_30_750_3	30.4	605.4	497.8	0.20	0.37	0.61	0.98
BG_30_850_1	52.0	807.7	592.8	0.24	0.39	0.59	0.98
BG_30_850_2	68.4	723.5	508.1	0.21	0.35	0.54	0.90
BG_30_850_3	78.5	[a]	-	-	0.25	0.15	0.41
OPS_30_750_1	8.9	490.0	450.9	0.17	0.20	0.21	0.40
OPS_90_750_1	15.9	553.7	479.0	0.18	0.30	0.64	0.80
OPS_30_750_2	10.8	504.2	476.4	0.18	0.23	0.45	0.68
OPS_30_750_3	14.3	529.9	503.1	0.19	0.23	0.48	0.71
OPS_30_850_1	27.7	667.4	550.0	0.25	0.19	0.38	0.58
OPS_30_850_2	34.5	776.0	687.6	0.26	0.17	0.33	0.50
OPS_30_850_3	47.2	931.0	830.0	0.32	0.17	0.35	0.51
OPS_30_850_4.5	56.0	1014.0	883.0	0.35	0.18	0.36	0.55

[a] N_2 adsorption test did not yield acceptable results, possibly due to the high ash content of the sample

a single plane. To illustrate this, the X-ray diffraction patterns of CS, BG and OPS gasification chars obtained at 850°C are presented in figure 6.8

The observed broad peaks indicate that the analyzed chars have a short-range graphite-like structure, also denoted as turbostratic structure by several authors. Likewise, the background intensity suggests the existence of non-aromatic or amorphous carbon in the carbon matrix [48].

In this regard, the gasification chars from the three analyzed feedstocks have a similar disordered carbon structure. Some differences are observed in the peak intensity of the diffraction profiles, probably related to the carbon content of the samples. OPS char, with a carbon content of 85.2% shows the highest (0 0 2) and (1 0 0) peak intensity, followed by CS and BG, with carbon contents of 79.2% and 60.8% respectively.

The quantitative analysis of the XRD patterns of carbon materials has been widely discussed in the literature. In the case of biochars and activated carbons, the assessment of structural parameters of the carbon structure is not easy due to the low crystallinity of the samples and their porous nature [49]. Several authors suggest that the analysis of the height, width and symmetry of the (0 0 2) and (1 0 0) peaks can give information about the crystalline structure of turbostratic carbons. In particular, the interlayer spacing of aromatic layers and the "crystallite" size [48, 50–52]. However, several discrepancies

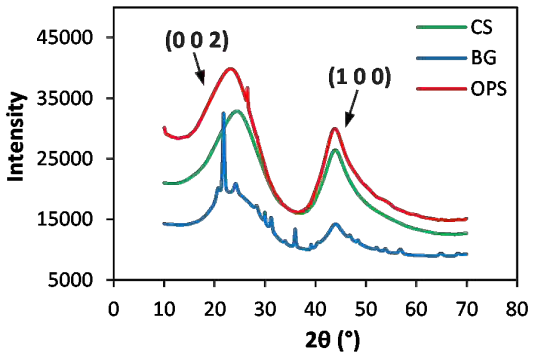

Figure 6.8: Diffraction profiles of chars produced at 850°C during 1h gasification with 30% of steam in the gasifying agent

exist in relation to the validity and physical meaning of the "crystallite" concept and the obtained results [36].

In the case of the analyzed chars, the quantitative analysis and comparison of the carbon structure from the height, width and symmetry of the (0 0 2) peak is not appropriate, as errors related to the inorganic content of the samples can be introduced. In particular, for BG chars, the existence of amorphous silica can also show a broad peak near 22° that can not be separated from the carbon peak [53, 54].

In general, the XRD results are in accordance with the high resolution TEM micrographs of the samples. From the images in figure 6.9, it can be observed that the carbon structure of the three chars is very similar, with visible randomly oriented graphene-like layers. This short-range order has been reported by several authors as one of the characteristics of microporous chars, and is in agreement with the porous structure assessed using N_2 adsorption [50, 55].

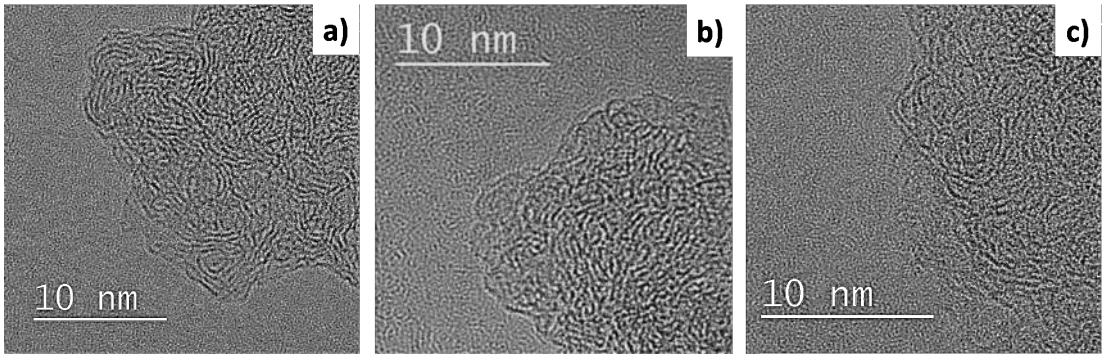

Figure 6.9: High-resolution transmission electron microscopy of chars produced at 850°C during 1h gasification with 30% of steam in the gasifying agent. a) CS, b) BG, c) OPS.

Due to the high inorganic content of BG char, some mineral peaks can be observed in the XRD diffraction patterns. According to the JCPDS data base, these peaks correspond to SiO_2 with a tetragonal crystal arrangement (01-082-0512). In fact, for chars treated at temperatures below 600°C, the Si in the structure is mainly amorphous,

while at higher temperatures, crystalline polymorphs can be formed[53, 56, 57]. In the case of CS and OPS chars, carbon peaks may hide XRD peaks of existing crystalline structures.

6.3.5 Char surface oxygen-containing functional groups

The thermal programmed desorption analysis confirmed the existence of a certain amount of oxygen-containing functional groups in the surface of chars. This result was expected, taking into account that the char gasification reactions can also result in the chemisorption of oxygen and hydrogen in the carbon matrix. For all the gasification conditions, the CO and CO_2 desorption of CS chars was higher compared to OPS and BG, suggesting the presence of a higher amount of surface oxygen complexes. This result is consistent with the steam gasification reactivity of the samples, since CS reactivity is considerably higher than OPS and BG. In accordance, under the same conditions, the steam gasification reactions proceed faster, resulting in higher char conversions and activation degrees.

The observed differences between the three char samples were reduced with the increase of the steam percentage in the gasifying agent, as a greater steam quantity was available to react with the carbon matrix. As presented in figure 6.10, with 30% of steam in the gasifying agent, BG and OPS chars CO and CO_2 desorption was 53% and 64% lower than CS respectively. In contrast, with 90% of steam this difference was reduced to 29% and 31%.

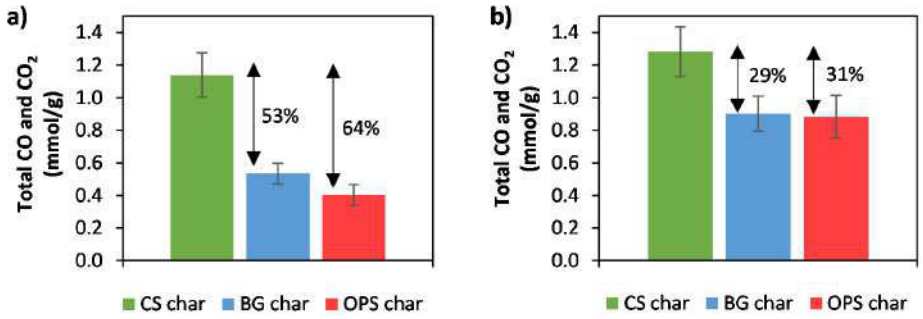

Figure 6.10: Total CO and CO_2 desorption of steam gasification chars during TPD analysis. Gasification conditions: a) 1 hour at 750°C with 30% of steam in the gasifying agent. b) 1 hour at 750°C with 90% of steam in the gasifying agent.

The differences between the samples are still visible with the increase in the gasification temperature. The figure 6.11 shows the evolution of the total CO and CO_2 desorption with the gasification time for processes at 750°C and 850°C with 30% of steam in the gasifying agent. In all cases, the amount of oxygen-containing functional groups in the char surface is higher for CS, as well as the amount increase with the gasification time. For CS, an augmentation in the gasification time from 1h to 2h at 850°C resulted in an increase of 60% in the CO and CO_2 desorption. In contrast, this trend is not observed for BG and OPS. Likewise, for 1h gasification, the gas desorption of CS is 30% and 65% higher in comparison to BG and OPS respectively. In figure 6.11b, it should be noted that no CS data are presented for 3 hours, as under these experimental conditions all the sample was consumed and no char was recovered.

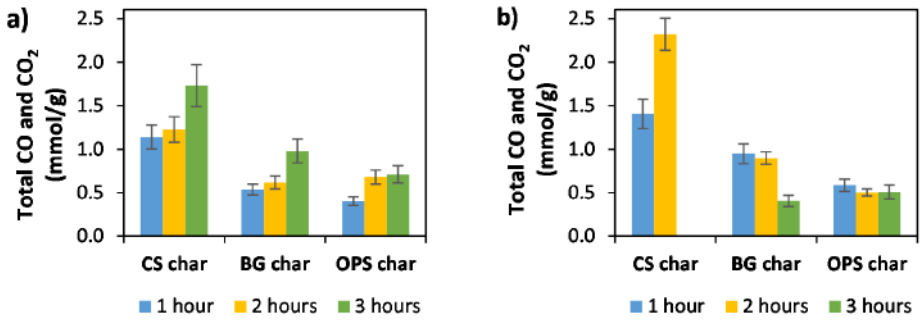

Figure 6.11: Evolution of total CO and CO_2 desorption with time of steam gasification chars during TPD analysis. a) gasification at 750°C with 30% of steam in the gasifying agent. b) gasification at 850°C with 30% of steam in the gasifying agent.

As presented in table 6.3, for all the gasification chars analyzed, the maximum total CO and CO_2 desorption observed was 2.32 and 0.98 mmol/g for CS and BG at 850°C and 30% of steam in the gasifying agent, and 0.8 mmol/g for OPS at 750°C and 90% of steam. These values, in the same range of literature reported amounts for steam activated carbons from lignocellulosic precursors [58, 59], confirm the potential of steam gasification chars as value-added by-products for different applications.

It is important to note that for the analyzed conditions, even at the same burn-off degree, the observed CO and CO_2 desorption of chars was always in the order CS < BG < OPS. This trend is most likely associated to the reactivity of the samples, and particularly, to the inorganic composition of the raw materials. As discussed earlier, CS is an AAEM rich feedstock while BG and OPS main inorganic constituents are Si and P. More precisely, the defined inorganic ratio K/(Si+P) of the raw samples is 3.9, 0.2 and 0.17 respectively, following the order CS < BG < OPS.

A more detailed analysis of the CO and CO_2 desorption curves showed that the surface of the gasification chars contains an important proportion of acidic oxygen functional groups. In particular, the presence of carboxylic acids, peroxides, lactones and phenols was identified. Furthermore, ether, quinone and pyrone-like functional groups, reported to have a basic and neutral character [60–62], were also identified. These characteristics of chars are in line with the gasification conditions. The introduction of acidic groups (e.g., carboxylic acids) in the char surface has been associated by several authors to their steam treatment or activation [63].

In agreement with this observation, the measured pH_{PZC} of the analyzed chars is in the acidic region, with values between 2 and 3, suggesting also the dominance of acidic groups over basic groups in the char surface [64, 65]. No particular trends were observed with the gasification conditions, and in all cases, the measured values were in the described range. The low pH_{PZC} values observed indicate that the samples surface will be negatively charged in almost all the pH range (pH values above pH_{PZC}), suggesting that steam gasification chars may be suitable for applications where the adsorption or retention of cations is required.

6.3.6 Relationship between char structure and surface chemistry

Finally, comparing the BET surface area and the TPD results of the analyzed chars, it was possible to notice that under the same gasification conditions, higher surface areas are also associated to a greater content of oxygen-containing functional groups in the char surface, as presented in figure 6.12.

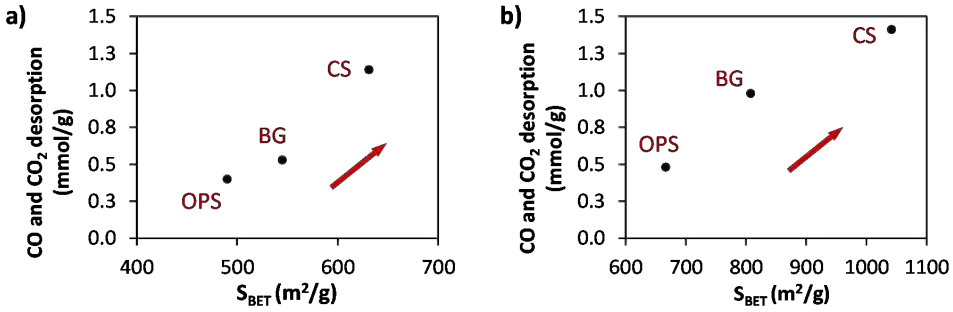

Figure 6.12: Total CO and CO_2 desorption Vs. BET surface area of chars at the same gasification conditions. a) 30% steam in the gasification agent, 750°C and 1h of gasification time. b) 30% steam in the gasification agent, 850°C and 1h of gasification time.

The observed relationship between the total CO and CO_2 desorption and the BET surface of the analyzed chars can be explained by the fact that the progress of the steam gasification reactions remove carbon atoms from the char matrix, developing a porous structure and including at the same time, oxygen-containing surface complexes [50, 66]. Once gain, the inorganic composition of the raw sample could play an important role in the development of oxygen-containing surface groups, as it impacts the char steam gasification reactivity. According to Marsh [36], the enhanced rate of gasification reactions produced by AAEM and some transition metals may be attributed to the enhanced rate of formation of chemisorbed oxygen in the char matrix. This could explain the fact that for all the analyzed experimental conditions, CS chars showed the highest CO and CO_2 desorption. In this regard, the inorganic content of the raw biomass impacts not only its gasification rate, but also the properties of the gasification solid by-product.

In the context of developing countries, possible char applications related to soil amendment, carbon sequestration or waste water treatment could be considered according to the observed characteristics of gasification chars. Notably, soil applications may be of particular interest, taking into account the surface structure and chemistry of the analyzed chars and their important inorganic content.

6.4 Conclusion

The steam gasification chars produced from three different lignocellulosic agrowastes were analyzed in this work in order to understand the impact of the raw biomass characteristics in the properties of the gasification solid by-product. Coconut shells (CS), bamboo guadua (BG) and oil palm shells (OPS) were used as feedstocks.

The experimental results showed that the inorganic composition has an important impact on the gasification reactivity of the samples, and in consequence, an influence on the porous structure development and surface chemistry of the gasification chars. For samples with inorganic ratio K/(Si+P) above 1, the beneficial impact of AAEM (specially K) in the steam gasification reactions resulted also in higher surface area development and oxygen-containing functional groups in the char surface, in comparison to samples with inorganic ratio below 1. For its part, the pore size distribution of the chars seems to have a relation with the nature and the macromolecular composition of the raw feedstocks.

In general, the analyzed gasification chars are highly microporous carbonaceous materials, with specific surface areas between 500 and 1000 m^2/g. A dominance of acidic oxygenated functional groups in the char surface, with pH_{PZC} values below 3 was observed in all cases. Accordingly, chars could be considered an interesting gasification by-product that could be valorized in applications where the adsorption or retention of cations is required. Moreover, the important inorganic content of chars suggests also their valorization in soil applications.

The experimental observations presented in this work could be an important reference for real gasification applications working with different kind of residues, when a simultaneous valorization of the gaseous and solid by-products is searched. According to the nature and composition of the samples, the gasification parameters and conditions could be adapted to obtain the application required by-products proportion, with the char needed characteristics. Future work will include the analysis of possible char applications according to their production conditions and properties.

Bibliography

[1] Julia Terrapon-Pfaff, Carmen Dienst, Julian Koenig, and Willington Ortiz. "A cross-sectional review: Impacts and sustainability of small-scale renewable energy projects in developing countries." In: *Renewable & Sustainable Energy Reviews* 40 (2014), pp. 1–10 (cit. on p. 114).

[2] Ana María González, Harrison Sandoval, Pilar Acosta, and Felipe Henao. "On the acceptance and sustainability of renewable energy projects-a systems thinking perspective." In: *Sustainability (Switzerland)* 8.11 (2016) (cit. on p. 114).

[3] Prabir Basu. "Gasification Theory." In: *Biomass Gasification, Pyrolysis and Torrefaction*. Elsevier Inc., 2013. Chap. Chapter 7, pp. 199–248 (cit. on p. 114).

[4] Juan Daniel Martínez, Khamid Mahkamov, Rubenildo V. Andrade, and Electo E. Silva Lora. "Syngas production in downdraft biomass gasifiers and its application using internal combustion engines." In: *Renewable Energy* 38.1 (2012), pp. 1–9 (cit. on p. 114).

[5] Tatiana Ramos Pacioni, Diniara Soares, Michele Di Domenico, Maria Fernanda Rosa, Regina de Fátima Peralta Muniz Moreira, and Humberto Jorge José. "Bio-syngas production from agro-industrial biomass residues by steam gasification." In: *Waste Management* (2016) (cit. on p. 114).

[6] Yafei Shen. "Chars as carbonaceous adsorbents / catalysts for tar elimination during biomass pyrolysis or gasi fi cation." In: 43 (2015), pp. 281–295 (cit. on p. 114).

[7] Duo Wang, Wenqiao Yuan, and Wei Ji. "Char and char-supported nickel catalysts for secondary syngas cleanup and conditioning." In: *Applied Energy* 88.5 (May 2011), pp. 1656–1663 (cit. on p. 114).

[8] D Dias, N Lapa, M Bernardo, D Godinho, I Fonseca, M Miranda, F Pinto, and F Lemos. "Properties of chars from the gasification and pyrolysis of rice waste streams towards their valorisation as adsorbent materials." In: *Waste Management* 65 (2017), pp. 186–194 (cit. on pp. 114, 115).

[9] In Hee Hwang, Jun Kobayashi, and Katsuya Kawamoto. "Characterization of products obtained from pyrolysis and steam gasification of wood waste, RDF, and RPF." In: *Waste Management* 34.2 (2014), pp. 402–410 (cit. on p. 114).

[10] C. Guizani, F.J. Escudero Sanz, M. Jeguirim, R. Gadiou, and S. Salvador. "The effects of textural modifications on beech wood-char gasification rate under alternate atmospheres of CO2 and H2O." In: *Fuel Processing Technology* 138 (2015), pp. 687–694 (cit. on p. 114).

[11] Naomi Klinghoffer, Marco J. Castaldi, and Ange Nzihou. "Catalyst Properties and Catalytic Performance of Char from Biomass Gasification." In: *I&EC* (2012), pp. 13113–13122 (cit. on pp. 114, 125).

[12] Veronika Hansen, Dorette Müller-Stöver, Jesper Ahrenfeldt, Jens Kai Holm, Ulrik Birk Henriksen, and Henrik Hauggaard-Nielsen. "Gasification biochar as a valuable by-product for carbon sequestration and soil amendment." In: *Biomass and Bioenergy* 72.1 (2015), pp. 300–308 (cit. on p. 114).

[13] Thawatchai Maneerung, Johan Liew, Yanjun Dai, Sibudjing Kawi, Clive Chong, and Chi-Hwa Wang. "Activated carbon derived from carbon residue from biomass gasification and its application for dye adsorption: Kinetics, isotherms and thermodynamic studies." In: *Bioresource technology* 200 (Oct. 2015), pp. 350–359 (cit. on p. 114).

[14] Vittoria Benedetti, Francesco Patuzzi, and Marco Baratieri. "Gasification Char as a Potential Substitute of Activated Carbon in Adsorption Applications." In: *Energy Procedia* 105 (2017), pp. 712–717 (cit. on p. 114).

[15] Sari Kilpimaa, Hanna Runtti, Teija Kangas, Ulla Lassi, and Toivo Kuokkanen. "Physical activation of carbon residue from biomass gasification: Novel sorbent for the removal of phosphates and nitrates from aqueous solution." In: *Journal of Industrial and Engineering Chemistry* 21 (2015), pp. 1354–1364 (cit. on p. 114).

[16] Naomi Klinghoffer, Marco J. Castaldi, and Ange Nzihou. "Beneficial use of ash and char from biomass gasification." In: *19th Annual North American Waste-to-Energy Conference, NAWTEC19*. Lancaster, Pennsylvania, 2011, pp. 13–17 (cit. on p. 115).

[17] Wei Li, Kunbin Yang, Jinhui Peng, Libo Zhang, Shenghui Guo, and Hongying Xia. "Effects of carbonization temperatures on characteristics of porosity in coconut shell chars and activated carbons derived from carbonized coconut shell chars." In: *Industrial Crops and Products* 28.2 (2008), pp. 190–198 (cit. on p. 115).

[18] Catherine E Brewer, Klaus Schmidt-Rohr, Justinus A Satrio, and Robert C Brown. "Characterization of Biochar from Fast Pyrolysis and Gasification Systems." In: *American Insti-tute of Chemical Engineers Environ Prog* 28 (2009), pp. 386–396 (cit. on p. 115).

[19] Silvia Román, Beatriz Ledesma, Andrés Álvarez-Murillo, Awf Al-Kassir, and Talal Yusaf. "Dependence of the microporosity of activated carbons on the lignocellulosic composition of the precursors." In: *Energies* 10.4 (2017) (cit. on p. 115).

[20] Lina María Romero Millán, Fabio Emiro Sierra Vargas, and Ange Nzihou. "Steam gasification behavior of tropical agrowaste: A new modeling approach based on the inorganic composition." In: *Fuel* 235.December 2017 (2019), pp. 45–53 (cit. on pp. 115, 120, 121).

[21] Céline Hognon, Capucine Dupont, Maguelone Grateau, and Florian Delrue. "Comparison of steam gasification reactivity of algal and lignocellulosic biomass: Influence of inorganic elements." In: *Bioresource Technology* 164 (2014), pp. 347–353 (cit. on pp. 115, 121).

[22] M Perander, N Demartini, A Brink, J Kramb, O Karlström, J Hemming, A Moilanen, J Konttinen, and M Hupa. "Catalytic effect of Ca and K on CO 2 gasification of spruce wood char." In: *Fuel* 150 (2015), pp. 464–472 (cit. on p. 115).

[23] Kawnish Kirtania, Joel Axelsson, Leonidas Matsakas, Paul Christakopoulos, Kentaro Umeki, and Erik Furusj. "Kinetic study of catalytic gasification of wood char impregnated with different alkali salts." In: *Energy* 118 (2017), pp. 1055–1065 (cit. on p. 115).

[24] Makiko Kajita, Tokuji Kimura, Koyo Norinaga, Chun-Zhu Li, and Jun-Ichiro Hayashi. "Catalytic and Noncatalytic Mechanisms in Steam Gasification of Char from the Pyrolysis of Biomass." In: (2009) (cit. on pp. 115, 121).

[25] Jose M Encinar, Juan F Gonzalez, Juan J Rodriguez, and Maria J Ramiro. "Catalysed and uncatalysed steam gasification of eucalyptus char: influence of variables and kinetic study." In: *Fuel* 80 (2001), pp. 2025–2036 (cit. on p. 115).

[26] Wan Mohd Ashri Wan Daud and Wan Shabuddin Wan Ali. "Comparison on pore development of activated carbon produced from palm shell and coconut shell." In: *Bioresource technology* 93.1 (May 2004), pp. 63–9 (cit. on pp. 115, 121, 125).

[27] Benoît Cagnon, Xavier Py, André Guillot, Fritz Stoeckli, and Gérard Chambat. "Contributions of hemicellulose, cellulose and lignin to the mass and the porous properties of chars and steam activated carbons from various lignocellulosic precursors." In: *Bioresource technology* 100.1 (Jan. 2009), pp. 292–8 (cit. on p. 115).

[28] Sabornie Chatterjee and Tomonori Saito. "Lignin-Derived Advanced Carbon Materials." In: *ChemSusChem* 8.23 (2015), pp. 3941–3958 (cit. on p. 115).

[29] Lina Maria Romero Millan, Fabio Emiro Sierra Vargas, and Ange Nzihou. "Kinetic Analysis of Tropical Lignocellulosic Agrowaste Pyrolysis." In: *BioEnergy Research* (2017) (cit. on p. 115).

[30] Jing-Hong Zhou, Zhi-Jun Sui, Jun Zhu, Ping Li, De Chen, Ying-Chun Dai, and Wei-Kang Yuan. "Characterization of surface oxygen complexes on carbon nanofibers by TPD, XPS and FT-IR." In: *Carbon* 45.4 (2007), pp. 785–796 (cit. on p. 118).

[31] Takafumi Ishii and Takashi Kyotani. "Temperature Programmed Desorption." In: *Materials Science and Engineering of Carbon*. Vol. 2011. Tsinghua University Press Limited, 2011. Chap. 14, pp. 287–305 (cit. on p. 118).

[32] Colomba Di Blasi. "Combustion and gasification rates of lignocellulosic chars." In: *Progress in Energy and Combustion Science* 35.2 (2009), pp. 121–140 (cit. on p. 121).

[33] Capucine Dupont, Sylvain Jacob, Khalil Ould Marrakchy, Céline Hognon, Françoise Labalette, Maguelone Grateau, and Denilson Da Silva Perez. "How inorganic elements of biomass influence char steam gasification kinetics." In: *Energy* 109 (2016), pp. 430–435 (cit. on p. 121).

[34] Kentaro Umeki, Antero Moilanen, Alberto Gómez-Barea, and Jukka Konttinen. "A model of biomass char gasification describing the change in catalytic activity of ash." In: *Chemical Engineering & Technology* 207-208 (2012), pp. 616–624 (cit. on p. 121).
[35] Y Zhang, M Ashizawa, S Kajitani, and K Miura. "Proposal of a semi-empirical kinetic model to reconcile with gasification reactivity profiles of biomass chars." In: *Fuel* 87 (2008), pp. 475–481 (cit. on p. 121).
[36] H Marsh. *Activated carbon*. First. Elsevier Science & Technology Books, 2006, p. 542 (cit. on pp. 122, 127, 130).
[37] Roop Chand Bansal and Meenakshi Goyal. *Activated Carbon Adsorption*. CRC Press, May 24, 2005 (cit. on p. 122).
[38] Anchan Paethanom and Kunio Yoshikawa. "Influence of Pyrolysis Temperature on Rice Husk Char Characteristics and Its Tar Adsorption Capability." In: *Energies* 5.12 (2012), pp. 4941–4951 (cit. on p. 123).
[39] Natthaya Punsuwan, Chaiyot Tangsathitkulchai, and Takayuki Takarada. "Low Temperature Gasification of Coconut Shell with CO 2 and KOH : Effects of Temperature , Chemical Loading , and Introduced Carbonization Step on the Properties of Syngas and Porous Carbon Product." In: 2015 (2015) (cit. on p. 123).
[40] J F Kwiatkowski. *Activated Carbon: Classifications, Properties and Applications*. 2011 (cit. on p. 123).
[41] Adrian M Cunliffe and Paul T Williams. "Influence of Process Conditions on the Rate of Activation of Chars Derived from Pyrolysis of Used Tires." In: *Energy & Fuels* 13 (1999), pp. 166–175 (cit. on p. 123).
[42] Catalina Rodriguez Correa, Thomas Otto, and Andrea Kruse. "Influence of the biomass components on the pore formation of activated carbon." In: *Biomass and Bioenergy* 97 (2017), pp. 53–64 (cit. on p. 123).
[43] Yan-Juan Zhang, Zhen-Jiao Xing, Zheng-Kang Duan, and Yin Wang. "Effects of steam activation on the pore structure and surface chemistry of activated carbon derived from bamboo waste." In: *Applied Surface Science* 315 (Oct. 2014), pp. 279–286 (cit. on p. 124).
[44] Anne E. Harman-Ware, Mark Crocker, Robert B. Pace, Andrew Placido, Samuel Morton, and Seth DeBolt. "Characterization of Endocarp Biomass and Extracted Lignin Using Pyrolysis and Spectroscopic Methods." In: *BioEnergy Research* 8.1 (Mar. 2015), pp. 350–368 (cit. on p. 124).
[45] Venugopal Mendu, Anne E Harman-Ware, Mark Crocker, Jungho Jae, Jozsef Stork, Samuel Morton, Andrew Placido, George Huber, and Seth Debolt. "Identification and thermochemical analysis of high-lignin feedstocks for biofuel and biochemical production." In: *Biotechnology for biofuels* 4 (2011), pp. 1–13 (cit. on p. 124).
[46] F Rodriguez Reinoso. "Controlled gasification of carbon and pore structure development." In: *Fundamental Issues in Control of Carbon Gasification Reactivity*. 1991, pp. 533–571. arXiv: `arXiv:1011.1669v3` (cit. on p. 125).
[47] Mohd Adib Yahya, Z Al-Qodah, and C W Zanariah Ngah. "Agricultural bio-waste materials as potential sustainable precursors used for activated carbon production: A review." In: *Renewable and Sustainable Energy Reviews* 46 (2015), pp. 218–235 (cit. on p. 125).
[48] L Lu, V Sahajwalla, C Kong, and D Harris. "Quantitative X-ray diffraction analysis and its application to various coals." In: *Carbon* 39.12 (Oct. 2001), pp. 1821–1833 (cit. on p. 126).

[49] N Yoshizawa, K Maruyama, Y Yamada, and M Zielinska-Blajet. "XRD evaluation of CO 2 activation process of coal-and coconut shell-based carbons." In: *Fuel* 79 (2000), pp. 1461–1466 (cit. on p. 126).

[50] P González-García. "Activated carbon from lignocellulosics precursors: A review of the synthesis methods, characterization techniques and applications." In: *Renewable and Sustainable Energy Reviews* 82.1 (2018), pp. 1393–1414 (cit. on pp. 126, 127, 130).

[51] Badie S Girgis, Yassin M Temerk, Mostafa M Gadelrab, and Ibrahim D Abdullah. "X-ray Diffraction Patterns of Activated Carbons Prepared under Various Conditions." In: *Carbon Science* 8.2 (2007), pp. 95–100 (cit. on p. 126).

[52] H Takagi, K Maruyama, N Yoshizawa, Y Yamada, and Y Sato. "XRD analysis of carbon stacking structure in coal during heat treatment." In: *Fuel* 83 (2004), pp. 2427–2433 (cit. on p. 126).

[53] S Chandrasekhar, K G Satyanarayana, P N Pramada, P Raghavan, and T N Gupta. "Review Processing, properties and applications of reactive silica from rice husk—an overview." In: *Journal of Materials Science* 38 (2003), pp. 3159–3168 (cit. on pp. 127, 128).

[54] Yue Chen, Yanchao Zhu, Zichen Wang, Ying Li, Lili Wang, Lili Ding, Xiaoyan Gao, Yuejia Ma, and Yupeng Guo. "Application studies of activated carbon derived from rice husks produced by chemical-thermal process—A review." In: *Advances in Colloid and Interface Science* 163 (2011), pp. 39–52 (cit. on p. 127).

[55] J.R. Fryer. "The micropore structure of disordered carbons determined by high resolution electron microscopy." In: *Carbon* 19.6 (1981), pp. 431–439 (cit. on p. 127).

[56] Anthony R West. *Solid State Chemistry and its Applications*. Second edi. Wiley, 2014, p. 453. arXiv: `arXiv:1011.1669v3` (cit. on p. 128).

[57] M M Haslinawati, K A Matori, Z A Wahab, H A A Sidek, and A T Zainal. "Effect of Temperature on Ceramic from Rice Husk Ash." In: *International Journal of Basic & Applied Sciences IJBAS-IJENS* 09.22 (2009) (cit. on p. 128).

[58] M Molina-Sabio, M T Gonzalez, F Rodriguez-Reinoso, and A Sepiijlveda-Escribano. "Effect of steam and carbon dioxide activation in the micropore size distribution of activated carbon." In: *Carbon* 34.4 (1996), pp. 505–509 (cit. on p. 129).

[59] Imen Ghouma, Mejdi Jeguirim, Sophie Dorge, Lionel Limousy, Camé lia Matei Ghimbeu, Abdelmottaleb Ouederni, and Tunisia C R. "Activated carbon prepared by physical activation of olive stones for the removal of NO 2 at ambient temperature Pre´paration par voie physique de carbones active´s obtenus a ' partir de noyaux d'olives destine´s a ' l'adsorption de NO 2 a ' tempe´rature ambiante." In: *Comptes rendus - Chimie* 18 (2015), pp. 63–74 (cit. on p. 129).

[60] M. A. Montes-Morán, D. Suárez, J. A. Menéndez, and E. Fuente. "On the nature of basic sites on carbon surfaces: An overview." In: *Carbon* 42.7 (2004), pp. 1219–1224 (cit. on p. 129).

[61] Larissa A. Alves, Arthur H. De Castro, Fernanda G. De Mendonça, and João P. De Mesquita. "Characterization of acid functional groups of carbon dots by nonlinear regression data fitting of potentiometric titration curves." In: *Applied Surface Science* 370 (2016), pp. 486–495 (cit. on p. 129).

[62] Jakub Ederer, Pavel Janoš, Petra Ecorchard, Václav Štengl, Zuzana Bělčická, Martin Šťastný, Ognen Pop-Georgievski, and Vlastimil Dohnal. "Quantitative

determination of acidic groups in functionalized graphene by direct titration." In: *Reactive and Functional Polymers* 103 (June 2016), pp. 44–53 (cit. on p. 129).
[63] Mohammad Saleh Shafeeyan, Wan Mohd Ashri Wan Daud, Amirhossein Houshmand, and Ahmad Shamiri. "A review on surface modification of activated carbon for carbon dioxide adsorption." In: *Journal of Analytical and Applied Pyrolysis* 89 (2010), pp. 143–151 (cit. on p. 129).
[64] Ali Gundogdu, Celal Duran, H. Basri Senturk, Mustafa Soylak, Mustafa Imamoglu, and Yunus Onal. "Physicochemical characteristics of a novel activated carbon produced from tea industry waste." In: *Journal of Analytical and Applied Pyrolysis* 104 (Nov. 2013), pp. 249–259 (cit. on p. 129).
[65] Tahira Mahmood, Abdul Naeem, Muhammad Hamayun, Madeeha Aslam, and Rahmat Ali. "Potential of used Camellia sinensis leaves as precursor for activated carbon preparation by chemical activation with H3PO4; optimization using response surface methodology." In: *Process Safety and Environmental Protection* 109.2 (2017), pp. 548–563 (cit. on p. 129).
[66] Mohd Adib Yahya, Z Al-Qodah, and C W Zanariah Ngah. "Agricultural bio-waste materials as potential sustainable precursors used for activated carbon production: A review." In: *Renewable and Sustainable Energy Reviews* 46 (2015), pp. 218–235 (cit. on p. 130).

Chapter

7

Characterization of steam gasification chars for soil amendment applications

Abstract

In this study, steam gasification chars from coconut shells (CS), bamboo guadua (BG), and oil palm shells (OPS), were analyzed in order to determine their suitability to be used in soil amendment and remediation applications. In general, the three analyzed chars showed high pH values between 9 and 11, and an interesting potential for the improvement of acidic soils characteristics. Moreover, the relatively high inorganic content of gasification chars from agrowastes suggests that these materials may also be a source of nutrients, that could impact soil fertility and crop yield. The experimental results showed that the inorganic content of the samples impacts in a great extent their

cation exchange and neutralization capacities. In particular, char from bamboo guadua, with an ash content above 30%, exhibited the most notable properties with regard to soil applications, with a cation exchange capacity (CEC) of 45 $cmol_c/kg$ and an acid neutralization capacity (ANC) of 125 cmol H^+/kg. The observations in this work give an useful insight regarding a promising valorization pathway for steam gasification chars from lignocellulosic agrowastes.

7.1 Introduction

In the context of most developing countries, steam gasification of agricultural and agroindustrial residues could be an interesting thermochemical process for the simultaneous production of energy [1–3], and the development of business opportunities for local communities. In particular, considering the importance of agroindustrial activities for the economy of developing countries, the use of gasification chars in soil amendment and remediation applications may be an effective strategy to enhance soil fertility and improve crop yield.

Biochars are carbon-rich and porous materials that have been widely recognized as beneficial for soil amendment and remediation applications [4, 5]. In particular, biochars usually show a high cation exchange capacity (CEC), associated to an important ability to adsorb and retain cations, and in consequence, to the improvement of nutrient retention if applied to soils [6]. Furthermore, the CEC of chars may also be important to the removal and immobilization of heavy metals in soils, making them unavailable for leaching or plant uptake [7].

The high alkalinity of most biochars, may also suggest the use of these materials in acidic soils, to improve their physico-chemical properties and productivity. Several authors have found that the incorporation of biochars in acidic soils increased their acid neutralization or pH buffering capacity (ANC) and enhanced the availability of nutrients for plant uptake, improving their retention in soils and avoiding their leaching [8–10].

Nevertheless, the impact of biochars in soils largely depends on their physico-chemical characteristics, generally determined by the raw materials and the production process [11, 12]. For instance, in the case of pyrolysis chars, high cation exchange capacities have been observed for low temperature treatments, considering the low devolatilization extent attained. In contrast, a decrease in the cation exchange capacity with the increase of the pyrolysis temperature has been reported. In consequence, low temperature pyrolysis biochars usually show a better performance in soil applications, in comparison to high temperature pyrolysis samples [13].

Contrary to pyrolysis chars, steam gasification chars are generally produced at higher temperatures and under a reactive atmosphere, and thus, may have different physico-chemical properties that should be analyzed with care in order to determine their suitability for soil amendment applications.

The use of gasification chars is not often reported in the literature, considering that gasification process is usually focused on gas production for energy applications. However, a higher soil amendment and remediation effectiveness has been observed for different activated carbons in comparison to pyrolysis biochars [14–17], suggesting that steam gasification chars could also have interesting properties in this field. In particular,

steam gasification chars develop large specific surface areas and may have an important amount of oxygen-containing functional groups, that could enhance properties like their cation exchange and acid neutralization capacities [18–20]. Moreover, due to the high mineral content of agrowastes, gasification chars from these feedstocks could be also a direct source of nutrients, promoting soil fertility and plant growth [21, 22]. More specifically, according to the raw biomass composition, biochar application to soils may supply different amounts of macro and micronutrients (e.g. N, P, S, Ca, Mg, Zn, Mn, Cu, B, Mo, Co, Fe, and Ni), considered essential for plant nutrition, and other beneficial elements for plant growth (e.g. Na, Co, Si, Se, and V). In the particular case of micronutrients (Zn, Mn, Cu, B, Mo, Co, Fe, and Ni), it is worth noting that even though they are essential for plant growth, they may become toxic beyond a threshold concentration [23].

In this regard, the aim of this work is to evaluate the physico-chemical properties of steam gasification chars produced from three different agrowastes, in order to determine their suitability to be used in soil amendment and remediation applications. Coconut shells (CS), bamboo guadua (BG) and oil palm shells (OPS) have been chosen as raw materials. The pH and buffering capacities of chars were analyzed, as well as their cation exchange capacity (CEC) and mineral release at different pH conditions. Accordingly, the agronomical implications of the observed gasification char properties were discussed, providing new insights to steam gasification chars valorization pathways.

7.2 Materials and methods

7.2.1 Materials

The steam gasification chars obtained from three tropical lignocellulosic biomasses were characterized and analyzed in this study, in order to determine their potential to be used in soil amendment applications. Oil palm shells (OPS), coconut shells (CS) and bamboo guadua (BG) were selected as raw materials. The detailed origin of the raw biomass, collected in Colombia-South America, as well as its organic and inorganic chemical composition are presented in a previous work [24].

7.2.2 Gasification experiments

Gasification experiments were performed at 850°C with a steam fraction of 30% in the gasifying atmosphere, considering that these conditions allow the production of high heating value fuel gases, with a relatively high gas efficiency, as presented in chapter 5. The gasification process was stopped after 1 hour, in order to maximize the quantity of recovered char for further analysis.

The steam gasification experimental setup was described previously in chapter 3. Briefly, 80g of biomass were placed inside a semicontinuous lab-scale fluidized bed reactor and heated to 850°C at 20°C/min, under nitrogen. When the temperature was reached, the atmosphere was switched to a mixture of 30% steam/70%N_2 (vol.%), with a steam mass flow rate of 100 g/h at 180°C. After 1 hour, the reactor was cooled down to room temperature under nitrogen. Finally, the remaining char was collected, weighted and stored in a desiccator for subsequent analysis. The collected char particle size was between 1mm and 3mm.

7.2.3 Char characterization

Elemental composition and ash content

The elemental analysis (CHNS) of the collected chars was determined using a Thermoquest NA 2000 elemental analyzer. To determine the inorganic composition, 150mg of ground char (with a particle size below 250µm) were acid digested in close vessels at 220°C during 4h. Acid reagents H_2O_2, HNO_3, HF and H_3BO_3 were used according to EN 16967. Acid solutions were diluted with demineralized water to 50 ml and analyzed using an HORIBA Jobin Yvol Ultima 2 inductively coupled plasma optical emission spectrometer (ICP-OES). For its part, the ash content of the samples was calculated according to the standard EN ISO 18122. All the analysis were performed with at least three replicates.

The local chemical composition of the samples at a micro-scale was also analyzed using a Hitachi TM3030 Plus tabletop scanning electron microscope (SEM), with an energy dispersive X-ray spectroscopy (EDX) module in the same apparatus.

pH

The pH of chars in aqueous solution was measured following the experimental protocol proposed by Denyes et al [25], by adding 0.25g of char to 25ml of distilled water. The suspension was shaken for two minutes and then centrifuged to collect the supernatant. The pH was measured using a calibrated Hach PHC725 probe.

pH at the point of zero-charge pH_{PZC}

The pH value at which the net charge of the chars surface is 0, or point of zero-charge (pH_{PZC}), was measured using a Malvern Pananalytical Zetasizer NanoZS. Char samples were ground into powder, with a particle size below 250 µm. About 15 mg of sample were used for each test with an approximate sample concentration of 0.5 mg/ml of deionized water. Measurements were done at room temperature within the pH range from 2 to 11, adjusted by the addition of a 0.25M HCl or 0.1M NaOH solution. The carbon pH_{PZC} was then defined as the pH at which the electrical charge density measured on the surface was zero.

Cation exchange capacity

In order to determine the ability of chars to retain nutrients in soils, their cation exchange capacity (CEC) was measured according to the sodium acetate method described by Laird and Fleming [26]. In general terms, this method involves the saturation of the char samples with Na^+ ions that replace the exchangeable cations in the char surface, followed by the subsequent displacement of Na^+ ions by a replacement solution. The amount of displaced Na^+ ions is measured using inductively coupled plasma-atomic emission spectrometry (ICP-OES). Specifically, 0.2 g of raw char (not ground) were placed in a 50ml centrifuge tube and washed three times with a 1M NaOAc solution with a pH adjusted to 8.2. The samples were then rinsed with a 80% isopropanol solution followed by a 100% isopropanol solution, until the measured electrical conductivity of the supernatant was below µS/cm. Finally, the retained Na^+ is displaced washing the sample 3 times with a 0.1M NH_4Cl replacing solution. The extracted sodium content

was analyzed, and the CEC of the samples in cmol/kg was calculated as presented in equation 7.2.1

$$CEC = \frac{100 \cdot C \cdot V}{W \cdot m_m} \tag{7.2.1}$$

Where C is the measured Na concentration in mg/L, V is the dilution volume of the analyzed solution in L, W is the sample mass in g, and m_m is the sodium molar mass in g/mol.

Acid neutralization capacity (ANC) and mineral release

In order to establish the char potential to resist acidification and to supply nutrients to soils, the char acid neutralization capacity (ANC) and the leaching behavior of inorganic constituents were determined using the protocol described in the NF EN 14429 standard [27]. Char samples were leached with water solutions containing pre-selected amounts of acid or base, in order to reach specific pH values at the end of a 48h extraction period, within the pH range from 2 to 12. Preliminary titration tests were performed to determine the acid and base quantities required to obtain at least, 8 final pH values within the analyzed range. For this purpose, the maximum acid and base consumption to attain a final pH value of 2 and 12 where determined and then, divided by the number of pH intended to be tested. 5M HNO_3 and 2.5M NaOH solutions were used.

For each test, 750 mg of raw char (not ground) were leached with a liquid to solid ratio of 10 L/kg. The suspensions were mixed using a GLF 3040 rotating shaker at 6 rpm during 48h. At the end of the test, the pH of the suspensions was measured using a Hach PHC725 probe. The liquid phases were separated from the solid by filtration, and analyzed using inductively coupled plasma-atomic emission spectrometry (ICP-OES).

7.3 Results and discussion

7.3.1 Composition of gasification chars

Table 7.1 reports the organic composition and ash content of the gasification chars analyzed in the present study. It can be observed that the three samples are highly carbonaceous materials with carbon content between 60% and 85%. BG char, with the highest ash content (above 30%) exhibits also the lowest carbon percentage, in comparison to CS and OPS chars.

Table 7.1: Organic composition of analyzed chars

	Elemental analysis (wt.% dry basis)				
Sample	**C**	**H**	**N**	**O***	**Ash**
CS char	79.2	1.3	0.0	11.3	8.2
BG char	60.8	0.8	0.3	6.6	31.5
OPS char	85.2	0.8	0.5	8.6	4.9

*Calculated by difference

Table 7.2: Mineral constituents of the analyzed chars

			CS char	BG char	OPS char
Essential plant nutrients (mg/kg dry basis)	Primary macronutrients	**P**	269.7	1 662.9	2 255.6
		K	20 393.8	30 501.5	6 375.3
	Secondary macronutrients	**Ca**	491.1	1 316.5	1 560.9
		Mg	320.1	785.8	1 623.2
	Micronutrients	**Mo**	17.1	16.6	41.4
		Zn	162.8	178.9	0.0
		Mn	170.9	184.5	129.0
		Cu	561.2	632.4	276.1
		Ni	189.1	35.8	444.8
		Fe	1270.0	1 332.2	888.6
	Beneficial nutrients	**Na**	4 188.7	376.5	101.2
		Si	779.8	86 598.5	13 477.0

In relation to inorganic composition, table 7.2 presents the main mineral constituents of the analyzed chars, relevant for agricultural applications and plant growth. It can be observed that the three samples contain non-negligible amounts of macro and micronutrients, and other beneficial elements for plants. Moreover, it can be noticed that the mineral constituents of the chars are in accordance with the composition of the raw materials. In particular, CS char is mainly composed of K, Ca and Na, while BG and OPS chars main constituents are Si, P, and K.

7.3.2 Char pH and pH_{PZC}

The table 7.3 shows the pH and pH_{PZC} values measured for the analyzed chars. It can be noted that the three samples have very similar pH values in the alkaline region, between 9 and 11. The high observed pH range could be mainly related to the inorganic composition of the chars, and particularly to the presence of alkali and alkaline earth metals as principal inorganic constituents [28, 29]. However, no particular correlations were found between the alkalinity of the samples and their ash content.

Table 7.3: Biochar pH in deionized water and pH_{PZC}

	CS	BG	OPS
pH (H_2O)	10.9	10.2	9.8
pH_{PZC}	2.2	1.6	3.1

Regarding the pH_{PZC}, the three chars showed similar values in the acidic region, between 1.5 and 3. Considering that the pH_{PZC} represents the pH value at which the net surface of the char is 0, cationic adsorption will be favored at pH values above pH_{PZC}, and anionic adsorption at values below. Accordingly, the low pH_{PZC} observed indicates that the surface of the chars is negatively charged in almost all the pH range, and then, the samples may favor the adsorption or retention of cations in soil applications.

The low pH_{PZC} measured values are in agreement with the TPD analysis of the chars, performed in a previous work (chapter 3), that confirmed the existence of a certain

amount of acid oxygen-containing functional groups in the char surface. The presence of carboxylic acid, peroxides, lactones and phenols was identified, and may contribute to the negative charge in the char surface at pH > pH_{PZC}.

7.3.3 Cation exchange capacity (CEC)

The cation exchange capacity (CEC) of the steam gasification chars was also analyzed in order to determine their suitability to be used in soil amendment applications. Generally, CEC may represent the ability of chars to retain nutrients in the soil matrix and avoid their leaching. The three analyzed samples showed CEC values between 10 cmol/kg and 45 cmol/kg, as observed in figure 7.1. BG char exhibited the highest value with 44.2 cmol/kg, followed by CS and OPS chars with 15.8 and 11.5 cmol/kg respectively.

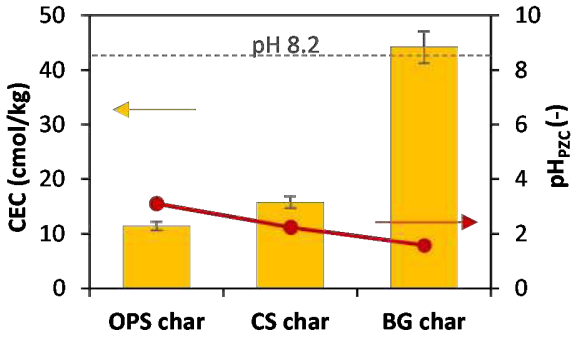

Figure 7.1: Cation exchange capacity (CEC) and pH_{PZC} of the analyzed chars

From figure 7.1, it can also be noted that the CEC values of the samples are in agreement with their low measured pH_{PZC}. In fact, according to the sodium acetate method, the CEC of the chars was measured at a pH of 8.2. At this value, the surface of the three samples is negatively charged and then, they can retain and exchange cations.

Nevertheless, it can be observed that the cation exchange capacity of BG char is three times and four times higher than CS and OPS chars respectively. These differences could be mainly related to the inorganic content of the samples, considering that BG char has a high ash content (>30%). In particular, from the SEM-EDX analysis of the samples, it was possible to determine that SiO_2 is one of the main mineral constituents of BG char, as presented in figure 7.2. SiO_2 may contribute in an important way to the cation exchange capacity, considering that this compound is negatively charged even at low pH, due to its very low pH_{PZC} value ($\sim$ 2.0) [30, 31]

For their part, considering the low ash content of CS and OPS chars (<10%), their cation exchange capacity may be mainly related to the oxygen-containing functional groups in their surface [18, 32]. Weakly acid carboxylic and phenolic functional groups can dissociate and form negatively charged sites in the char surface, contributing to the cation exchange capacity. In this regard, as CS char has a considerably higher amount of oxygen-containing functional groups than OPS char, the former one exhibits also a higher CEC.

Although CEC is not an intrinsic property of chars and strongly depends on the measurement method used, the obtained results for the analyzed samples are in accordance with the values presented in the literature for several biochars from different feedstocks.

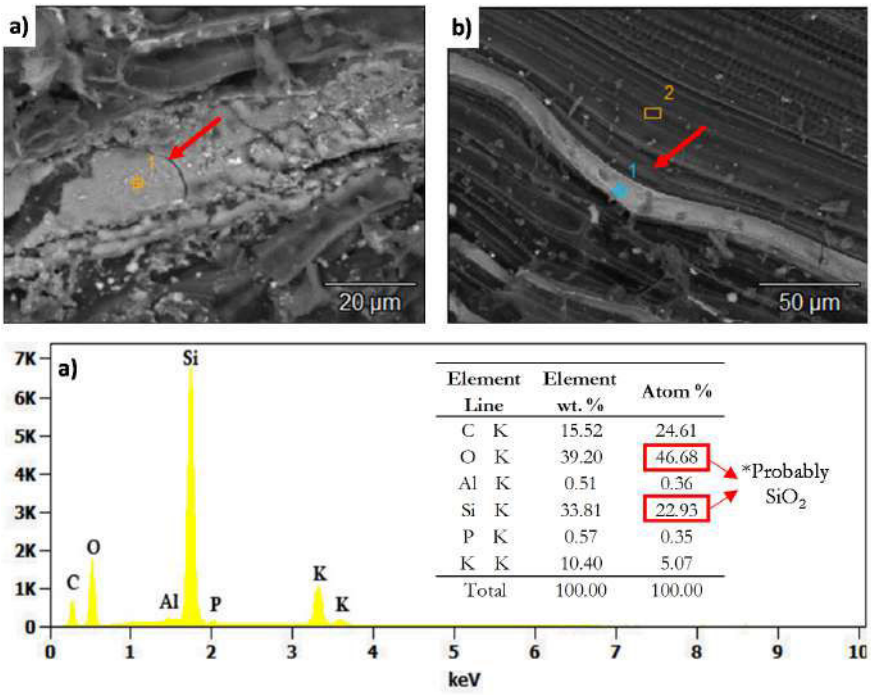

Figure 7.2: SEM-EDX analysis of BG steam gasification chars.

From table 7.4, it can be observed that the analyzed samples and in particular BG char, show similar CEC values than those observed for low-temperature pyrolysis chars.

Several authors have reported that low-temperature biochars exhibit higher CEC values than high-temperature biochars, as most of the oxygen-containing functionalities in the char surface are lost with the thermal treatment. However, considering that steam gasification process can result in the creation of oxygen-containing complexes in the char surface, the analyzed samples show a cation exchange capacity comparable to low-temperature pyrolysis biochars.

Moreover, from the comparison of the pH and CEC values obtained for the analyzed chars and some reported acidic soils, it is possible to observe that gasification chars could have an interesting potential to be used in soil amendment applications. More specifically, it can be noticed from table 7.5, that the three analyzed char samples have higher pH and CEC values in comparison to the ones reported for most acidic soils. In accordance, their application may result in the increase of the soil pH and CEC.

In particular, acidic soils may present several problems to plant growth and crop yields, mainly related to aluminum (Al) and manganese (Mn) toxicity to plants, and an important deficiency of essential nutrients like phosphorous (P), potassium (K), calcium (Ca) and magnesium (Mg) [34]. Therefore, it is important to prevent soil acidification in agricultural activities, or remediate already degraded soils. Several authors have reported an increase in the CEC and pH of soils in the presence of biochar, providing benefits to soil fertility and crop yield [35, 36].

Although the validation of the beneficial effect of the analyzed chars in soil pH and CEC needs further agronomic analysis, the present work gives a useful insight to a

Table 7.4: Cation exchange capacity (CEC) and pH of agricultural residues biochar

Char feedstock	Production process	Temperature (°C)	pH (-)	CEC (cmol/kg)	Ref.
Corn stover	Pyrolysis	450°C	-	26.4	[32]
Corn stover	Air gasification	700°C	-	10.2	[32]
Peanut straw	Pyrolysis	400	10.28	146.8	[9]
Corn straw	Pyrolysis	500	-	50	[33]
Corn stover	Pyrolysis	400	-	23.9	[13]
Corn stover	Pyrolysis	700	-	6.5	[13]
Sawdust	Pyrolysis	500	10.5	41.7	[12]
Peanut shell	Pyrolysis	500	10.5	44.5	[12]
Wheat straw	Pyrolysis	500	10.2	95.5	[12]
Coconut shells	Steam gasification	850	10.9	15.8	This work
Oil palm shells	Steam gasification	850	9.8	11.5	This work
Bamboo guadua	Steam gasification	850	10.2	44.2	This work

Table 7.5: Cation exchange capacity (CEC) and pH of some acidic soils

Soil	Location	pH (-)	CEC (cmol/kg)	Ref.
Ultisol - Ternary red sandstone	China	4.96	6.34	[9]
Ultisol - Quaternary red earth	China	4.78	12.4	[9]
Oxisol - Basalt	China	4.62	6	[37]
Ultisol - Granite	China	4.52	4.4	[37]
Andisol - Sandy loam	Colombia	4.8	19	[38]
Inceptisol - Sandy loam	Colombia	4.8	25	[38]
Entisol - Sandy loam	Colombia	5.3	9	[38]
Ferrosol - Sandy loam	Australia	6.14	11.6	[39]

possible valorization pathway for the steam gasification solid by-product, in line with most developing countries context.

In addition to the presented benefits to soil fertility, the relatively high CEC of the analyzed chars may be also important to the removal of inorganic contaminants from soils. In particular, the adsorption of cationic heavy metals could be favored, making them unavailable for leaching or plant uptake [20, 40]. Considering the low pH_{PZC} values of steam gasification chars from agrowastes, heavy metal adsorption may be associated to electrostatic attraction between cationic metals and the negatively charged surface, as well as cation exchange between metal ions and mineral ions (K^+, Na^+, Ca^{2+} and Mg^{2+}). In the particular case of BG char, its high mineral content could significantly favor heavy metal removal or immobilization through electrostatic adsorption, as reported by different authors [41–43].

7.3.4 Acid neutralization capacity (ANC)

The acid neutralization capacity of chars was analyzed in order to establish their capability to resist acidification, if potentially applied to soils. The acid-base titration curves for the three samples, presented in figure 7.3, indicate the amount of acid

consumed by each char to decrease its pH to a value of 2. In accordance, a higher acid consumption is related to a greater char buffering capacity.

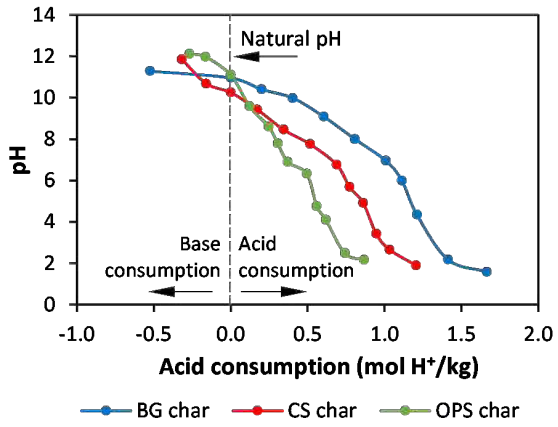

Figure 7.3: Changes in biochar suspension pH as a function of acid-base titration

In general, the acid neutralization capacity (ANC) of a biochar is defined as the quantity of acid or base (cmol/kg) required to shift the initial pH of the sample to a pH of 4 [44]. In the case of the analyzed chars, with a basic natural pH, BG char showed the highest acid neutralization capacity (ANC), consuming 125 cmol/kg of H^+ protons, while CS and OPS values were 24% and 50% lower, with 95 cmol/kg and 62 cmol/kg respectively.

Likewise, in all the analyzed pH range, from 2 to 12, BG chars also showed the highest acid consumption, with 170 cmol/kg of H^+ protons, followed by CS and OPS, with 120 cmol/kg and 90 cmol/kg respectively.

The acid neutralization capacity of chars may be attributed to the acidic oxygen-containing functional groups in the char surface, and their mineral content, existing either as discrete phases or associated with functional groups [9, 45]. In this regard, organic anions of weak acid functional groups like carboxyl ($-COO^-$) or hydroxyl ($-O^-$) groups may accept protons, increasing the char resistance to acidification. Moreover, alkali salts dissolution may also contribute in a very important extent to the char buffering capacity, as well as soluble silicate minerals [8].

Despite the fact that CS char has 30% more oxygen-containing functional groups than BG char, and 66% more than OPS char, BG char showed the highest acid neutralization capacity. In relation to this, it can be noted that BG char has a considerably higher inorganic content (>30% ash), in comparison to CS and OPS (<10% ash).

To better understand this behavior, the release of minerals during the acid-base titration experiments was analyzed and compared for the three samples. From figure 7.4, it can be observed that in all cases, the total sum of K^+, Na^+, Ca^{2+} and Mg^{2+} (base cations) released remained almost constant with the acid addition, while the soluble Si in the suspensions decreased with the pH. Despite the observed common trends, some differences were noticed between the three samples. In particular, it can be noted that the amount of base cations released by CS and BG chars was approximately 4 times higher than OPS. Moreover, the Si release was higher for BG in almost all the pH range.

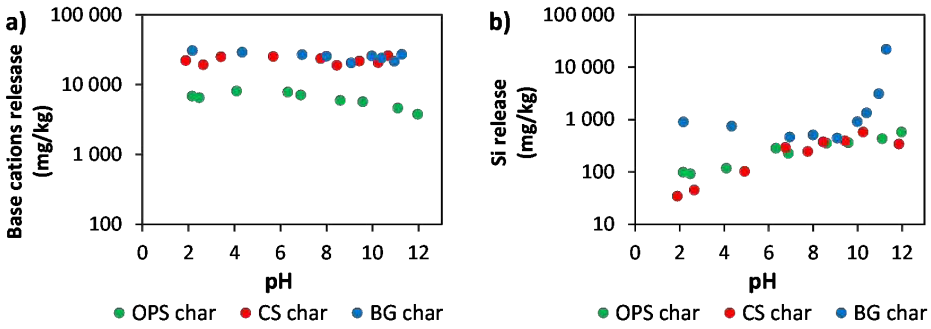

Figure 7.4: Mineral release during the acid-base titration experiments. a) Sum of base cations (K^+, Na^+, Ca^{2+} and Mg^{2+}), b) Soluble Si.

The base cations release may be related to the dissolution of alkali salts and oxides present in the char as discrete phases or associated with functional groups. The contribution of base cations release to the buffering capacity has been already described by several authors [8, 46], and may explain the fact that OPS char, with the lowest amount of K^+, Na^+, Ca^{2+} and Mg^{2+} released, is also the sample that exhibits the lowest proton consumption during tests.

Moreover, the greater Si release observed for BG in comparison to CS, may be related to its higher acid neutralization capacity. In fact, at high pH, soluble Si is present in the solution as $H_3SiO_4^-$, which is transformed into H_4SiO_4 and precipitates when the pH decreases, consuming protons [47, 48].

These results suggest that inorganics play a primary role on buffering capacity of the analyzed gasification chars. The acid neutralization capacity of the analyzed samples is in accordance with some reported values in the literature for pyrolysis biochars from crop residues (100 - 200 cmol H^+/kg)[6, 8], showing the interesting potential of steam gasification chars for acidic soil amendment applications.

7.3.5 pH dependent mineral release

In addition to the cation exchange and acid neutralization capacity, the significant inorganic content of steam gasification chars from agrowastes is also a relevant characteristic that suggests their use in soil amendment applications. More specifically, the elemental analysis of the samples revealed the presence of non-negligible amounts of essential nutrients that could be available for plant uptake.

However, the mineral availability is not immediate, and depends on the environmental conditions, soil type, and char characteristics. In this regard, the analysis of the chars mineral release at different pH values may give an insight to their associated nutrient availability at different soil conditions. The measured mineral release of the three samples, for a 48 hours leaching test and pH values between 2 and 12, is presented in figure 7.5.

In all cases, the release of a certain amount of K, P, Ca, Mg, Na, and Si from the char matrix was observed, suggesting the potential increase of nutrient availability in soils, if treated with the analyzed chars. In contrast, only a slight liberation of Mo was observed

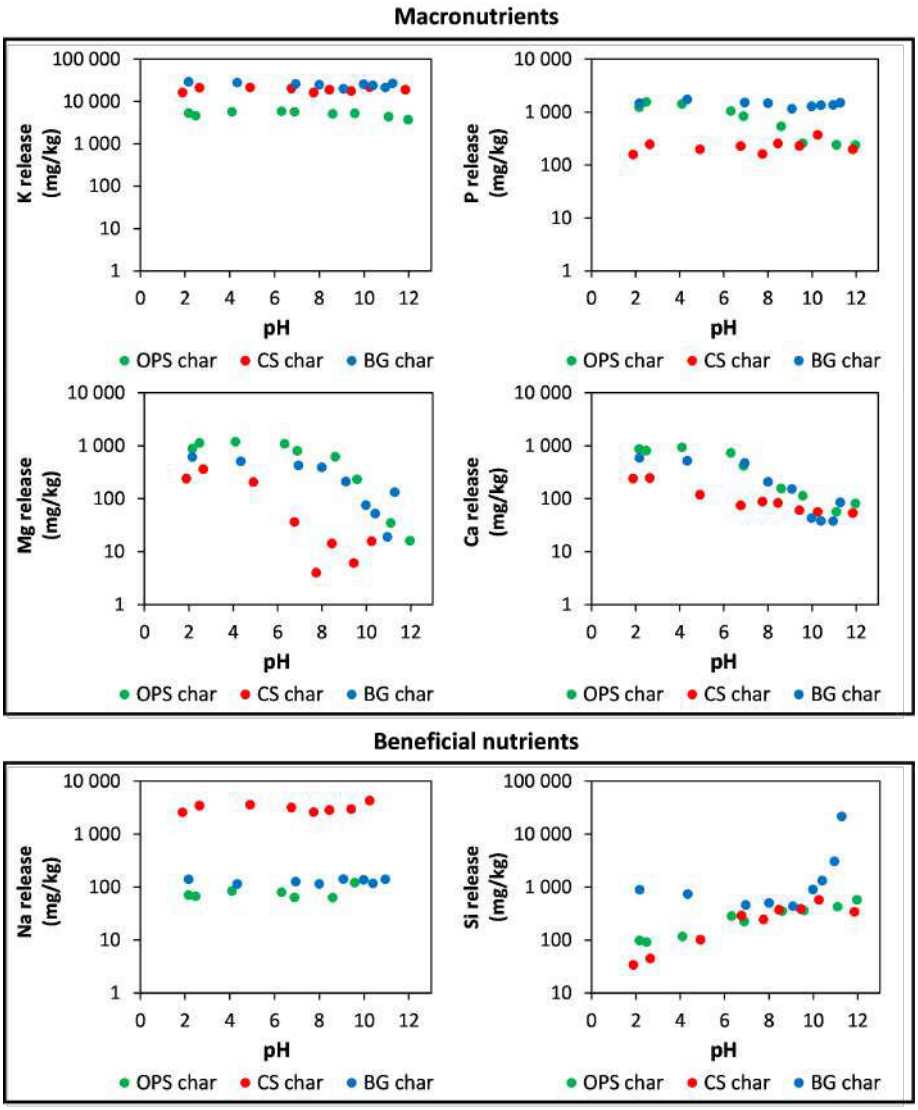

Figure 7.5: Effect of pH on the K, Ca, Mg, Na, P, and Si release from gasification chars.

at pH higher than 7. Moreover, no significant release of Zn, Mn, Cu, Ni, or Fe was measured during the leaching tests, even though these elements were identified in the char composition.

In relation to the mineral release behavior, it can be noticed that for the three samples, the K and Na release was pH independent, while Ca and Mg release exhibited an increase with the solution acidity. The opposite trend was observed for Si, whose availability decreased with the pH. In the case of P, the leaching behavior of CS and BG was pH independent while a slight increase was observed for OPS with the pH decrease.

Furthermore, the amount leached of each element is in agreement with the initial composition of the chars. For instance, the highest K content in the leaching solution was observed for BG char in all the pH range, considering that this sample has the

highest K content. The same trend was observed for the other analyzed elements with the three samples. Similar observations were reported by Ding et al.[49], suggesting that the composition of the chars could give a first insight to their mineral leaching potential and nutrient value.

Nevertheless, it is worth noting that the recovered amount of minerals is not necessarily the total initial content present in the chars. The mineral leachability may depend on different parameters related to the char morphology, and the occurrence forms and distribution of minerals [50]. On one side, the char morphological structure (e.g. pore structure, surface area) may affect the mineral accessibility, impacting also the observed release. On the other side, the solubility of minerals depends on their occurrence form (chemical form) and bonding to the carbon matrix [51].

In order to better understand the nutrient leaching potential of the analyzed chars, the amount released of each element is presented in figure 7.6, as a percentage of the total amount originally available in the char. A neutral pH has been chosen as a reference, considering that the optimum soil pH range is between 5.5 and 7.5 [52].

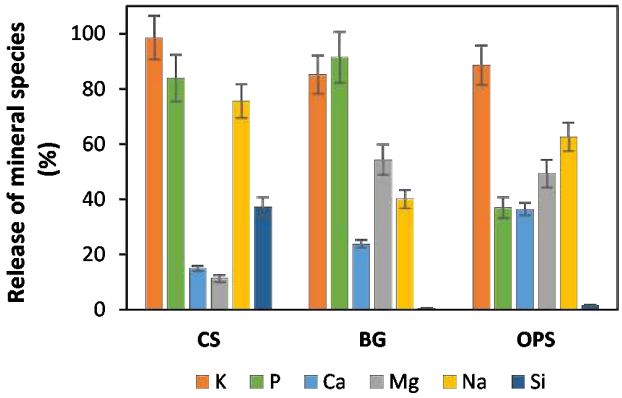

Figure 7.6: Release percentage of mineral species from chars at a pH = 7, during a 48h leaching test with a liquid to solid ratio of 10 L/kg

It can be observed that under the present conditions, K, P, and Na are the minerals that exhibit the highest availability, with a recovery percentage from 40% to nearly 100%. In particular, the recovered fraction of K was above 85% for the three samples, indicating that this element is mostly present in the char structure as soluble K-containing salts [51]. In the case of Si, CS char showed a higher availability compared to BG and OPS. Considering that the solubility of amorphous silica is higher than that of crystalline silica [48], the leached amounts may correspond principally to the amorphous fraction present in chars. Taking into account the considerably higher amount of Si in BG and OPS chars in comparison to CS, the low leaching percentage observed for BG and OPS could indicate that an important amount of crystalline Si is present in their structure.

The results obtained in the present study are in accordance with some literature reported values, showing that the recyclability of Na and K is relatively high for biochars from different agrowastes [21, 50]. Nevertheless, the recovered percentages cannot be directly compared, as different solid to liquid ratios have been used for leaching studies, resulting in deviations caused by solubility and saturation limitations.

In this regard, despite the fact that the leaching behavior of the analyzed biochars in real soil applications may differ from the presented values, this study gives an useful insight regarding the possible nutrient contribution of gasification chars from agrowastes.

7.3.6 Agronomical implications of char properties

The observed leaching behavior suggests that the gasification chars from the analyzed feedstocks may be a significant source of plant nutrients to soils. In the particular case of primary macronutrients (e.g. N, K, and P), the studied chars showed a high K and P availability, considering their leaching percentages. In the same way, secondary macronutrients such as Ca and Mg may be also supplied in some extent. Regarding micronutrients, also essential for plant metabolism and growth, only a slight release of Mo was observed for the analyzes chars.

Similarly, even though they are not essential for some plants, beneficial nutrients such Na and Si showed also a non-negligible release. In particular, Na is essential for the metabolism of some plants, and may improve the taste and texture of several crops. For its part, Si provides protection to plants from biotic and abiotic stress, and may improve their strength and productivity [23].

Considering that the recommended rates of biochar amendments in soils are between 5-50 ton char/ha [53, 54], gasification chars could reduce the consumption of conventional fertilizers, notably regarding primary macronutrients (P and K). As an example, with a mean char application rate of 10 tons/ha, and assuming similar conditions to those of the leaching tests performed in this work, the average available mineral quantities that could be supplied to soil for plant uptake at a pH of 7, are presented in table 7.6.

Table 7.6: Average mineral release available for plant uptake with a rate of biochar amendment of 10 tons/ha

		Average supply potential (kg/ha)		
Inorganic elements		**CS char**	**BG char**	**OPS char**
Primary macronutrients	**P**	2.3	15.2	8.3
	K	201.0	259.8	56.5
Secondary macronutrients	**Ca**	0.7	3.1	5.7
	Mg	0.4	4.3	8.0
Micronutrients	**Mn**	0.0	0.0	0.2
	Mo	0.1	0.1	0.1
Beneficial nutrients	**Na**	31.7	1.3	0.6
	Si	2.9	4.6	2.3

As observed, the amount of K released is significant for the three samples, as well as the P released by BG char. In this regard, considering the average macronutrients consumption reported for different crops, the analyzed gasification chars could partially replace conventional K and P fertilizers. In particular, CS and BG chars may supply up to 100% and 60% of the K and P needs of some low-input crops, presented in table 7.7.

Table 7.7: Primary macroutrients consumption of selected crops [55, 56]

		Macronutrient consumption* (kg/ha)		
Crop	**Plants ha^{-1}**	**N**	**K**	**P**
Fresh tomatoes	12 000	250	370	24
Eggplant	12 500	290	380	33
Lettuce	100 000	110	250	22
Sweet corn	75 000	240	320	40
Carrot	400 000	279	604	73
Celery	90 000	150	224	36
Broccoli	33 000	202	165	26

*Throughout the growing season

Besides the potential nutrient supply of gasification chars, their beneficial effects are also related to their high pH and their interesting cation exchange capacity (CEC) and acid neutralization capacity (ANC). In particular, the significant CEC measured for the samples indicates that gasification chars may increase the retention capacity of plant nutrients in soils, when supplied by conventional procedures (e.g. traditional fertilizers). This behavior can improve the fertilizer use efficiency, ameliorating the soil fertility. Moreover, the high pH observed for chars, as well as their significant acid neutralization capacity, suggest that the analyzed samples could be used for acidic soils amendment and remediation.

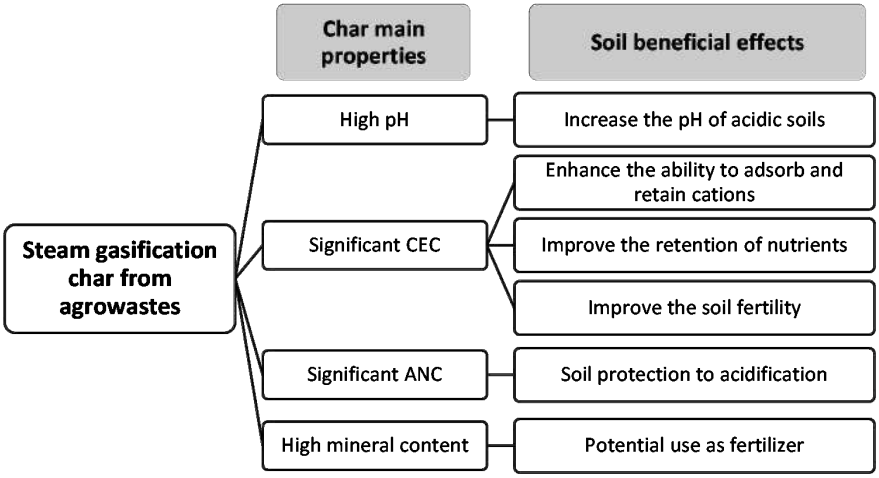

Figure 7.7: Steam gasification chars properties and associated soil beneficial effects

According to the observed characteristics of the steam gasification chars analyzed in this study, figure 7.7 summarizes the possible benefits associated to their application to soils. Although the behavior of chars in real applications may differ from the one observed during the laboratory characterization, the present work gives an useful insight regarding a promising valorization pathway for steam gasification chars. In the context

of most developing countries, the application of chars to the appropriate soils may improve crop production, boosting local economies.

7.4 Conclusion

Steam gasification chars from different lignocellulosic agrowastes were analyzed in this study, in order to determine their suitability to be used in soil amendment and remediation applications. Coconut shells (CS), bamboo guadua (BG) and oil palm shells (OPS) were used as feedstocks.

The three analyzed chars showed an interesting potential to be used in soil amendment applications. In particular, their high pH values between 9 and 11, and their significant acid neutralization capacity above 62 cmol H^+/kg, suggest the char capacity for the improvement of acidic soil characteristics. Moreover, their cation exchange capacity values between 11 and 45 cmol/kg may enhance the nutrient retention and fertility of several kinds of soils.

Experimental results showed that the inorganic content of the samples plays a primary role on the char properties with regard to soil applications. In particular, BG chars, with an ash content above 30%, exhibited the highest cation exchange and acid neutralization capacities, in comparison to chars with lower ash content.

The mineral release analysis of the three gasification chars revealed that these materials could be a source of essential and beneficial plant nutrients that could also impact the soil fertility and crop yield. Thanks to their high mineral content, CS and BG chars may supply up to 100% and 60% of the K and P needs of some low-input crops. In this regard, even when the inorganic composition of the chars does not necessarily reflect their total mineral availability to plants, this information could give a first approach to their nutrient supply potential.

Although the behavior of chars in real applications may differ from the one observed during the laboratory characterization, the present work gives an useful insight regarding a promising valorization pathway for steam gasification chars from different lignocellulosic agrowastes.

Bibliography

[1] Juan Daniel Martínez, Khamid Mahkamov, Rubenildo V. Andrade, and Electo E. Silva Lora. "Syngas production in downdraft biomass gasifiers and its application using internal combustion engines." In: *Renewable Energy* 38.1 (2012), pp. 1–9 (cit. on p. 138).

[2] Emanuele Graciosa Pereira, Jadir Nogueira Da Silva, Jofran L. De Oliveira, and Cássio S. MacHado. *Sustainable energy: A review of gasification technologies*. 2012 (cit. on p. 138).

[3] Tatiana Ramos Pacioni, Diniara Soares, Michele Di Domenico, Maria Fernanda Rosa, Regina de Fátima Peralta Muniz Moreira, and Humberto Jorge José. "Bio-syngas production from agro-industrial biomass residues by steam gasification." In: *Waste Management* (2016) (cit. on p. 138).

[4] Jin Sun Cha, Sung Hoon Park, Sang-Chul Jung, Changkook Ryu, Jong-Ki Jeon, Min-Chul Shin, and Young-Kwon Park. "Production and utilization of biochar: A review." In: *Journal of Industrial and Engineering Chemistry* 40 (2016), pp. 1–15 (cit. on p. 138).

[5] Fernanda R Oliveira, Anil K Patel, Deb P Jaisi, Sushil Adhikari, Hui Lu, and Samir Kumar Khanal. "Environmental application of biochar: Current status and perspectives." In: *Bioresource Technology* 246 (2017), pp. 110–122 (cit. on p. 138).

[6] Jin-Hua Yuan, Ren-Kou Xu, and Hong Zhang. "The forms of alkalis in the biochar produced from crop residues at different temperatures." In: *Bioresource Technology* 102.3 (Feb. 2011), pp. 3488–3497 (cit. on pp. 138, 147).

[7] Hongbo Li, Xiaoling Dong, Evandro B Da Silva, Letuzia M De Oliveira, Yanshan Chen, and Lena Q Ma. "Mechanisms of metal sorption by biochars: Biochar characteristics and modifications." In: *Chemosphere* 178 (2017), pp. 466–478 (cit. on p. 138).

[8] Ren-yong Shi, Zhi-neng Hong, Jiu-yu Li, Jun Jiang, M Abdulaha-Al Baquy, Ren-kou Xu, and Wei Qian. "Mechanisms for Increasing the pH Buffering Capacity of an Acidic Ultisol by Crop Residue-Derived Biochars." In: *Journal of Agricultural and Food Chemistry* 65 (2017), pp. 8111–8119 (cit. on pp. 138, 146, 147).

[9] Ren-yong Shi, Zhi-neng Hong, Jiu-yu Li, Jun Jiang, Muhammad Aqeel Kamran, Ren-kou Xu, and Wei Qian. "Peanut straw biochar increases the resistance of two Ultisols derived from different parent materials to acidification: A mechanism study." In: *Journal of Environmental Management* 210 (Mar. 2018), pp. 171–179 (cit. on pp. 138, 145, 146).

[10] Nikola Teutscherova, Jakub Houška, Mariela Navas, Alberto Masaguer, Marta Benito, and Eduardo Vazquez. "Leaching of ammonium and nitrate from Acrisol and Calcisol amended with holm oak biochar: A column study." In: *Geoderma* 323 (2018), pp. 136–145 (cit. on p. 138).

[11] Hongguang Cheng, Davey L. Jones, Paul Hill, Mohd Saufi Bastami, and Cheng long Tu. "Influence of biochar produced from different pyrolysis temperature on nutrient retention and leaching." In: *Archives of Agronomy and Soil Science* 0.0 (2017), pp. 1–10 (cit. on p. 138).

[12] Ling Zhao, Xinde Cao, Ondřej Mašek, and Andrew Zimmerman. "Heterogeneity of biochar properties as a function of feedstock sources and production temperatures." In: *Journal of Hazardous Materials* 256-257 (July 2013), pp. 1–9 (cit. on pp. 138, 145).

[13] C. Banik, M. Lawrinenko, S. Bakshi, and D.A. Laird. "Impact of pyrolysis temperature and feedstock on surface charge and functional group chemistry of biochars." In: *Journal of Environmental Quality* 47.3 (2018), pp. 452–461 (cit. on pp. 138, 145).

[14] Michał Kołtowski, Isabel Hilber, Thomas D. Bucheli, Barbara Charmas, Jadwiga Skubiszewska-Zięba, and Patryk Oleszczuk. "Activated Biochars Reduce the Exposure of Polycyclic Aromatic Hydrocarbons in Industrially Contaminated Soils." In: *Chemical Engineering Journal* 310 (Feb. 15, 2017), pp. 33–40 (cit. on p. 138).

[15] Michał Kołtowski, Isabel Hilber, Thomas D Bucheli, and Patryk Oleszczuk. "Effect of activated carbon and biochars on the bioavailability of polycyclic aromatic hydrocarbons in different industrially contaminated soils." In: *Environmental Science and Pollution Research* () (cit. on p. 138).

[16] N. Borchard, A. Wolf, V. Laabs, R. Aeckersberg, H. W. Scherer, A. Moeller, and W. Amelung. "Physical activation of biochar and its meaning for soil fertility and nutrient leaching - a greenhouse experiment." In: *Soil Use and Management* 28.2 (2012), pp. 177–184 (cit. on p. 138).

[17] James W Lee, Bob Hawkins, Michelle K Kidder, Barbara R Evans, A C Buchanan, and Danny Day. "Characterization of biochars produced from peanut hulls and pine wood with different pyrolysis conditions Background." In: *Bioresour. Bioprocess* 3 (2016) (cit. on p. 138).

[18] Minori Uchimiya, Sechin Chang, and K Thomas Klasson. "Screening biochars for heavy metal retention in soil: Role of oxygen functional groups." In: *Journal of Hazardous Materials* 190 (2011), pp. 432–441 (cit. on pp. 139, 143).

[19] Matthew Smith, Su Ha, James E. Amonette, Ian Dallmeyer, and Manuel Garcia-Perez. "Enhancing cation exchange capacity of chars through ozonation." In: *Biomass and Bioenergy* 81 (2015), pp. 304–314 (cit. on p. 139).

[20] Lokesh P Padhye. "Influence of surface chemistry of carbon materials on their interactions with inorganic nitrogen contaminants in soil and water." In: *Chemosphere* 184 (2017), pp. 532–547 (cit. on pp. 139, 145).

[21] Saran P Soh and Teri E Angst. "Establishing release dynamics for plant nutrients from biochar." In: *GCB Bioenergy* 5 (2013), pp. 221–226 (cit. on pp. 139, 149).

[22] Natália Aragão De Figueredo, Liovando Marciano Da Costa, Leônidas Carrijo, Azevedo Melo, Evair Antônio Siebeneichlerd, and Jairo Tronto. "Characterization of biochars from different sources and evaluation of release of nutrients and contaminants." In: *Revista Ciencia Agronomica* 48.3 (2017), pp. 395–403 (cit. on p. 139).

[23] M Naeem, Abid A Ansari, and Sarvajeet Singh, eds. *Essential Plant Nutrients. Uptake, Use efficiency, and Management*. 1st ed. Springer, 2017, p. 569 (cit. on pp. 139, 150).

[24] Lina María Romero Millán, Fabio Emiro Sierra Vargas, and Ange Nzihou. "Steam gasification behavior of tropical agrowaste: A new modeling approach based on the inorganic composition." In: *Fuel* 235.December 2017 (2019), pp. 45–53 (cit. on p. 139).

[25] Mackenzie J Denyes, Michèle A Parisien, Allison Rutter, and Barbara A Zeeb. "Physical, Chemical and Biological Characterization of Six Biochars Produced for the Remediation of Contaminated Sites Video Link." In: *Journal of Visualized Experiments* 93 (2014), pp. 1–12 (cit. on p. 140).

[26] David Laird and Pierce Fleming. "Analysis of Layer Charge, Cation and Anion Exchange Capacities, and Synthesis of Reduced Charge Clays." In: *Methods of Soil Analysis. Part 5. Mineralogical Methods*. 2008. Chap. 16, pp. 485–508 (cit. on p. 140).

[27] NF EN 14429:2015. *Characterization of waste - Leaching behaviour test - Influence of pH on leacing with inicial acid/base addition*. 2015 (cit. on p. 141).

[28] Rivka B Fidel, David A Laird, Michael L Thompson, and Michael Lawrinenko. "Characterization and quantification of biochar alkalinity." In: *Chemosphere* 167 (2017), pp. 367–373 (cit. on p. 142).

[29] Ling Zhao, Xinde Cao, Wei Zheng, Qun Wang, and Fan Yang. "Endogenous minerals have influences on surface electrochemistry and ion exchange properties of biochar." In: *Chemosphere* 136 (2015), pp. 133–139 (cit. on p. 142).

[30] Donald L Sparks. *Environmental soil chemistry*. Second edi. Elsevier Science & Technology Books, 2003, p. 367 (cit. on p. 143).

[31] Yiliang Xu and Baoliang Chen. "Organic carbon and inorganic silicon speciation in rice-bran-derived biochars affect its capacity to adsorb cadmium in solution." In: *Journal of Soils and Sediments* 15 (2015), pp. 60–70 (cit. on p. 143).

[32] James W. Lee, Michelle Kidder, A. C. Buchanan, Charles T Garte, and Robert Brown. "Characterization of Biochars Produced from Cornstovers for Soil Amendment." In: *Environ. Sci. Technol.* 44 (2010), pp. 7970–7974 (cit. on pp. 143, 145).

[33] A Silver, I Levkovitch, and E.R. Graber. "pH-Dependent Mineral Release and Surface Properties of Cornstraw Biochar: Agronomic Implications." In: *Environ. Sci. Technol.* 44.24 (2010), pp. 9318–9323 (cit. on p. 145).

[34] Somchai Butnan, Jonathan L Deenik, Banyong Toomsan, Michael J Antal, and Patma Vityakon. "Biochar characteristics and application rates affecting corn growth and properties of soils contrasting in texture and mineralogy." In: *Geoderma* 237-238 (2015), pp. 105–116 (cit. on p. 144).

[35] K Y Chan, A Downie, : S Joseph, and A Cowie. "Effects of biochar from slow pyrolysis of papermill waste on agronomic performance and soil fertility." In: *Plant Soil* 327 (2010), pp. 235–246 (cit. on p. 144).

[36] J. H. Yuan and R. K. Xu. "The amelioration effects of low temperature biochar generated from nine crop residues on an acidic Ultisol." In: *Soil Use and Management* 27.1 (2011), pp. 110–115 (cit. on p. 144).

[37] Ren kou Xu, An zhen Zhao, Jin hua Yuan, and Jun Jiang. "pH buffering capacity of acid soils from tropical and subtropical regions of China as influenced by incorporation of crop straw biochars." In: *Journal of Soils and Sediments* 12.4 (2012), pp. 494–502 (cit. on p. 145).

[38] Alvaro García-Ocampo. "Fertility and soil productivity of Colombian soils under different soil management practices and several crops." In: *Archives of Agronomy and Soil Science* 58.sup1 (Oct. 2012), S55–S65 (cit. on p. 145).

[39] Fangjie Qi, Zhaomin Dong, Dane Lamb, Ravi Naidu, Nanthi S Bolan, Yong Sik Ok, Cuixia Liu, Naser Khan, M A H Johir, and Kirk T Semple. "Effects of acidic and neutral biochars on properties and cadmium retention of soils." In: *Chemosphere* 180 (2017), pp. 564–573 (cit. on p. 145).

[40] Mahtab Ahmad, Anushka Upamali Rajapaksha, Jung Eun Lim, Ming Zhang, Nanthi Bolan, Dinesh Mohan, Meththika Vithanage, Sang Soo Lee, and Yong Sik Ok. "Biochar as a sorbent for contaminant management in soil and water: A review." In: (2014) (cit. on p. 145).

[41] Xinde Cao and Willie Harris. "Properties of dairy-manure-derived biochar pertinent to its potential use in remediation." In: *Bioresource Technology* 101.14 (July 2010), pp. 5222–5228 (cit. on p. 145).

[42] Liyi Ye, Jingmiao Zhang, Jie Zhao, Zhiming Luo, Song Tu, and Yingwu Yin. "Properties of biochar obtained from pyrolysis of bamboo shoot shell." In: *Journal of Analytical and Applied Pyrolysis* 114 (May 2015), pp. 172–178 (cit. on p. 145).

[43] Zhenyu Wang, Guocheng Liu, Hao Zheng, Fengmin Li, Huu Hao Ngo, Wenshan Guo, Cui Liu, Lei Chen, and Baoshan Xing. "Investigating the mechanisms of biochar's removal of lead from solution Complexation with functional groups Pb 2+-π interaction." In: *Bioresource* 177 (2015), pp. 308–317 (cit. on p. 145).

[44] A Venegas, A Rigol, and M Vidal. "Viability of organic wastes and biochars as amendments for the remediation of heavy metal-contaminated soils." In: *Chemosphere* 119 (2015), pp. 190–198 (cit. on p. 146).
[45] Xiaoyun Xu, Yinghao Zhao, Jingke Sima, Ling Zhao, Ondřej Mašek, and Xinde Cao. "Indispensable role of biochar-inherent mineral constituents in its environmental applications: A review." In: *Bioresource Technology* 241 (Oct. 2017), pp. 887–899 (cit. on p. 146).
[46] K W T Goulding. "Soil acidification and the importance of liming agricultural soils with particular reference to the United Kingdom." In: *Soil Use and Management* 32 (2016), pp. 390–399 (cit. on p. 147).
[47] Lela Munjas Jurkić, Ivica Cepanec, Sandra Kraljević Pavelić, and Krešimir Pavelić. "Biological and therapeutic effects of ortho-silicic acid and some ortho-silicic acid-releasing compounds: New perspectives for therapy." In: *Nutrition and Metabolism* 10.1 (2013), pp. 1–12 (cit. on p. 147).
[48] Brenda Tubaña and Joseph Raymond Heckman. "Silicon in Soils and Plants." In: *Silicon and Plant Diseases*. 2015. Chap. 2, pp. 1–148 (cit. on pp. 147, 149).
[49] Yang Ding, Yunguo Liu, Shaobo Liu, Zhongwu Li, Xiaofei Tan, Xixian Huang, Guangming Zeng, Lu Zhou, and Bohong Zheng. "Biochar to improve soil fertility. A review." In: *Agronomy for Sustainable Development* 36 (2016), p. 36 (cit. on p. 149).
[50] Zhaoying Kong, Sui Boon Liaw, Xiangpeng Gao, Yun Yu, and Hongwei Wu. "Leaching characteristics of inherent inorganic nutrients in biochars from the slow and fast pyrolysis of mallee biomass." In: *Fuel* 128 (July 2014), pp. 433–441 (cit. on p. 149).
[51] Hongwei Wu, Kongvui Yip, Zhaoying Kong, Chun-Zhu Li, Dawei Liu, Yun Yu, and Xiangpeng Gao. "Removal and Recycling of Inherent Inorganic Nutrient Species in Mallee Biomass and Derived Biochars by Water Leaching." In: *Ind. Eng. Chem. Res* 50 (2011), pp. 12143–12151 (cit. on p. 149).
[52] Cornell University Cooperative Extension. *Soil pH for Field Crops - Agronomy Fact Sheet Series - Fact Sheet 5*. Tech. rep. Cornell University Cooperative Extension, p. 2 (cit. on p. 149).
[53] Mahmood Laghari, Muhammad Saffar Mirjat, Zhiquan Hu, Saima Fazal, Bo Xiao, Mian Hu, Zhihua Chen, and Dabin Guo. "Effects of biochar application rate on sandy desert soil properties and sorghum growth." In: (2015) (cit. on p. 150).
[54] Julie Major. *Guidelines on Practical Aspects of Biochar Application to Field Soil in Various Soil Management Systems*. Tech. rep. International Biochar Initiative, 2010, p. 23. arXiv: `j.geoderma.2011.04.021 [10.1016]` (cit. on p. 150).
[55] CFI - Canadian fertilizer institute. *Nutrient uptake and removal by field crops*. Tech. rep. 1998, p. 2 (cit. on p. 151).
[56] B. Bar-Yosef. "Advances in Fertigation." In: *Advances in Agronomy* 65 (1999), pp. 1–77 (cit. on p. 151).

General conclusion and prospects

Conclusion

In the current world energy, environmental, and economic context, agricultural and agroindustrial wastes represent an interesting, low-cost, and renewable resource for the production of biofuels and value-added products in both developing and developed countries.

In particular, considering the great variety of lignocellulosic agrowaste sources, the understanding of the impact of the biomass organic and inorganic composition on the pyro-gasification behavior is of great importance to adapt the process parameters to the available feedstocks and application requirements. Moreover, the understanding of the influence of biomass characteristics on the pyro-gasification by-products is also essential to determine their most suitable valorization pathways.

The pyrolysis analysis performed at a thermogravimetric scale, revealed that the macromolecular composition of the samples is the main factor that influences their pyrolysis behavior and product yield. Notably, the kinetic analysis performed showed that the lignin content may have an impact on the energy required to decompose the samples, considering that lignin is the binding agent of the biomass fibers. In this regard, oil palm shells, with the highest lignin content showed also the highest pyrolysis activation energy.

In contrast, in the case of gasification, despite the differences in their macromolecular composition, inorganics showed to be the most important parameter influencing the biomass reactivity and kinetics. Principally, the inorganic ratio K/(Si+P) proved to be suitable to describe the biomass steam gasification behavior. Samples with an inorganic ration below 1 exhibited a low gasification reactivity and a non-catalytic behavior, contrary to biomasses with inorganic ratio higher than 1. This observation is related to the interactions between the inorganic constituents of the samples. In particular, Si and P could react with K and other alkali and alkali earth metals (AAEM) to form silicates, restraining the known catalytic impact of the latter ones.

Regarding the produced gas, the differences observed between the analyzed samples were mainly related to the gas yield and not to the gas composition. In fact, under the same experimental conditions, biomasses with higher reactivities produced also greater gas quantities, impacting the gas efficiency of the process. In this regard, it can be said that the inorganic composition of the samples also impacts the steam gasification gas efficiency, and then, is an important parameter to take into account in the design and operation of gasification facilities.

In relation to this, a new kinetic model was proposed to describe the steam gasification behavior of lignocellulosic biomass from the knowledge of its inorganic composition. This model could constitute a valuable tool for reactor design, and for the development and scale-up of gasification facilities working with different kind of agrowastes or blends.

The experimental results also showed that even though the inorganic content of the samples impact in a very important way the gasification reactivity and gas yield, the organic composition, and specially the H/C and O/C ratios seem to be related to the composition and heating value of the producer gas. With similar H/C and O/C ratios, no remarkable differences were observed between the analyzed samples in terms of gas composition. In all cases, the producer gas H_2/CO ratio between 2.5 and 4, suggests that steam gasification gas may be used in electricity generation applications using boilers, gas turbines, or internal combustion engines.

For its part, the analysis of the char produced from the steam gasification process revealed that the biomass characteristics also impact the char physico-chemical properties. For samples with inorganic ratio K/(Si+P) above 1, the beneficial impact of AAEM (specially K) on the steam gasification reactions resulted also in a higher specific surface area development and a greater content of oxygen-containing functional groups in the char surface, in comparison to samples with inorganic ratio below 1. For its part, the pore size distribution of the chars seems to have a relation with the nature and the macromolecular composition of the raw feedstocks.

In all cases, the produced steam gasification chars exhibited a high microporosity, with surface areas between 500 and 1000 m^2/g, similar to several activated carbons. Moreover, the significant mineral content of chars and the dominance of acidic oxygen-containing functional groups in their surface, with low pH_{PZC} values, suggest the possibility to use these materials in applications where the adsorption or retention of cations is required, such as soil amendment or remediation applications.

In accordance, the specific characterization of three selected steam gasification chars for soil applications revealed that these materials could have an interesting potential, particularly in the case of bamboo guadua. In this regard, the experimental results showed that the inorganic content of the samples plays a primary role on the char properties with regard to soil applications. In particular, bamboo guadua chars, with an ash content above 30%, exhibited the highest cation exchange and acid neutralization capacities, in comparison to chars with lower ash content. Moreover, the mineral release analysis of the three samples revealed that these materials could be a source of nutrients that could also impact the soil fertility and crop yield. Thanks to their high mineral content, CS and BG chars may supply up to 100% and 20% of the K and P needs of some low-input crops.

In general, the results obtained in the present work contributed to a better understanding of the steam gasification process of lignocellulosic agrowastes, and highlighted the important role of inorganics in their gasification behavior and by-products properties. Moreover, the present research showed that steam gasification could be considered as a suitable technique for the simultaneous valorization of lignocellulosic residues in energy applications, and the production of value-added products, that could represent an opportunity to implement productive activities in the context of both developing and developed countries.

In accordance, the design and operation of agrowaste gasification facilities should take into account the organic and inorganic composition of the feedstocks, in order to properly adapt the process parameters to ensure the production of the required by-products yield and properties.

Prospects

Steam gasification has proved to be an interesting alternative for the energy valorization of agrowastes and the simultaneous production of value-added products. The results obtained in the present work brought to light new challenges for further studies, as discussed below:

- Co-gasification experiments at a thermogravimetric scale could be extended to other agrowastes within a wider range of H/C and O/C ratios, in order to extend the application limits of the proposed kinetic model. In this study, only steam as gasifying agent was analyzed. However, in several applications, mixed atmospheres with air, steam, and CO_2 may be required or imposed by the reactor design (e.g. autothermal reactors). In accordance, the analysis of the impact of the biomass composition on the gasification behavior under mixed atmospheres should also be explored. In this regard, the gasification kinetic model proposed could be extended to take into account a reacting agent composed of different proportions of CO_2 or CO_2/steam mixtures.

  Moreover, in order to understand the impact of mixed reacting atmospheres on the yield and properties of the gasification by-products from lignocellulosic agrowastes, gasification experiments could also be performed at a laboratory scale, using the described fluidized bed reactor. A tar analysis and comparison between the selected samples could be considered. Likewise, the detailed physico-chemical characterization of the resulting chars will be required to determine their suitability in soil amendment and remediation applications, or other uses.

- The analysis of the steam gasification behavior of lignocellulosic agrowastes at a laboratory scale is extremely important to fully understand the physico-chemical mechanisms involved in the process. In this regard, the results obtained in the present work could constitute a valuable tool for the future scale-up of the steam gasification process using tropical lignocellulosic agrowastes. In particular, the analysis of different gasification technologies (e.g. updraft fixed bed gasifier, downdraft fixed bed gasifier, etc) may also be an interesting work to develop in the future, in order to determine the most suitable conditions adapted to

real applications in developing countries. A life cycle analysis approach could be considered for the comparison of gasification technologies and by-products valorization pathways.

Considering other gasification technologies, the evaluation of the steam gasification process using the autothermal downdraft reactor described at the beginning of the present document could also be an interesting work in the future, taking into account that this technology is widely employed for small scale gasification facilities. In this regard, the development of the present work has been the starting point of several financing possibilities at the Colombian National University to redesign, adapt, and adjust the existing reactor for steam gasification tests and subsequent char recovery.

- In relation to the evaluation of the steam gasification char potential to be used in soil amendment applications, the mineral release analysis of the selected samples revealed that chars could be a non-negligible source of nutrients that could impact the soil fertility. The nutrient extraction tests in the present work were performed using a fixed solid to liquid ratio, and extraction time. Even though these conditions gave a first insight of the char nutrient availability, their release dynamics could not be established. In order to determine the long term availability of char nutrients to soils, various leaching times and solid to liquid ratios should be tested. Moreover, a leaching kinetic analysis could also be performed in order to better predict the char mineral release in real soil applications.

  Moreover, an analysis concerning the influence of char morphology and inorganic chemical forms in the mineral leaching potential and nutrient availability could be performed.

- Considering their relatively high mineral content and cation exchange capacity, the suitability of steam gasification chars from lignocellulosic residues to be used in soil remediation applications could be also an interesting research approach for future work. Principally, their ability to adsorb and retain inorganic contaminants from soils, such as heavy metals. In the particular case of Colombia, several agricultural soils are polluted by Cu, Ni, Pb, Cd, Hg, and Zn, principally due to mining activities, validating the interest of the proposed approach. Moreover, in developed countries, heavy metal pollution may also be important in some locations due to anthropogenic activities.

- The physico-chemical characterization of gasification chars revealed their potential to be used in soil amendment applications. Despite the fact that incubation experiments to evaluate the effect of chars on real soils are not under the scope of the present work, future interdisciplinary projects including agronomic research specialists may help to determine the real impact of chars in soils. In particular, a recent research cooperation accord with the agronomy school of the National University of Colombia may allow the laboratory characterization and analysis of different steam gasification chars and acidic soils blends. Moreover, incubation plant growth experiments could be also performed.

Annexes

Appendix

Publications related to this work

Publications in international journals

1. Romero Millan Lina Maria, Sierra Vargas Fabio Emiro, Nzihou Ange. Kinetic Analysis of Tropical Lignocellulosic Agrowaste Pyrolysis. **BioEnergy Research** 2017; 10:832-45 doi:10.1007/s12155-017-9844-5.

2. Romero Millan Lina Maria, Sierra Vargas Fabio Emiro, Nzihou Ange. Steam gasification behavior of tropical agrowaste: A new modeling approach based on the inorganic composition. **Fuel** 2019;235:45–53. doi:10.1016/j.fuel.2018.07.053.

Publications in international conferences

1. Romero Millan Lina Maria, Maria Alejandra Cruz, Sierra Vargas Fabio Emiro. Valorization of oil palm shells and industrial residual wood for energy production in Colombian rural zones via gasification. 6th International Conference on Engineering for Waste Valorization. May 23-26, 2016, Albi, France (Oral presentation).

2. Romero Millan Lina Maria, Sierra Vargas Fabio Emiro, Nzihou Ange. Steam gasification of tropical lignocellulosic agrowastes. XXVI International Materials Research Congress. Advances on Biofuels: Materials, Characterization, Processing and Testing Symposium. August 20-25, 2017, Cancun, Mexico (Oral presentation).

3. Romero Millan Lina Maria, Sierra Vargas Fabio Emiro, Nzihou Ange. Kinetic analysis of tropical lignocellulosic biomass steam gasification. 7th International Conference on Engineering for Waste Valorization. July 2-5, 2018, Prague, Czech Republic (Oral presentation).

4. Romero Millan Lina Maria, Sierra Vargas Fabio Emiro, Nzihou Ange. Impact of tropical lignocellulosic biomass composition on steam gasification char properties. 7th International Conference on Engineering for Waste Valorization. July 2-5, 2018, Prague, Czech Republic (Poster - Best poster award).

Appendix

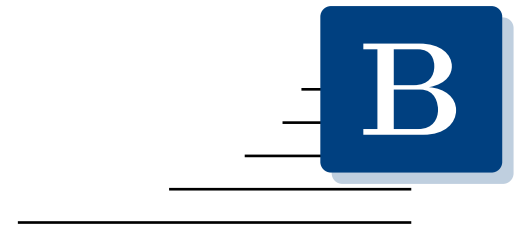

TPD spectra deconvolution of selected samples

In this section, an example of the TPD curves deconvolution process is presented for three selected gasification chars obtained from coconut shells (CS), bamboo guadua (BG), and oil palm shells (OPS). As previously described in chapter 6, CO and CO_2 desorption patterns were deconvoluted using 6 Gaussian functions respectively (Equation B.0.1), in order to determine the contribution of each type of oxygen complex.

Gaussian function:

$$f(x) = a \exp\left[-\frac{1}{2}\left(\frac{x-b}{c}\right)^2\right] \tag{B.0.1}$$

Regarding the parameters of the Gaussian function, a is the amplitude of the peak in molar percentage ; b is the peak central temperature in °C, and c the width of the peak in °C.

In accordance, the CO_2 desorption curves were decomposed using 6 peaks centered at 250±50°C and 380±50°C for carboxylic groups, 500±50°C for peroxydes, and 620±50°C, 750±50°C, and 850±50°C for lactones at different energetic sites.

In the case of the CO curves, peaks centered at 400±50°C for acid anhydrides, 620±50°C for hydroxyl groups, 740±50°C for phenol groups, 860±50°C for ether groups, and 900±50°C and 970±50°C for quinone and pyrone groups were used respectively. A constraint over the peak width (55±5°C) was fixed for the optimization of the curve fitting.

In this regard, Figures B.1 to B.3 present the TPD spectra obtained for the selected chars and the associated deconvolution peaks. Moreover, the fitting parameters and identified oxygen complexes are summarized in tables B.1 to B.3.

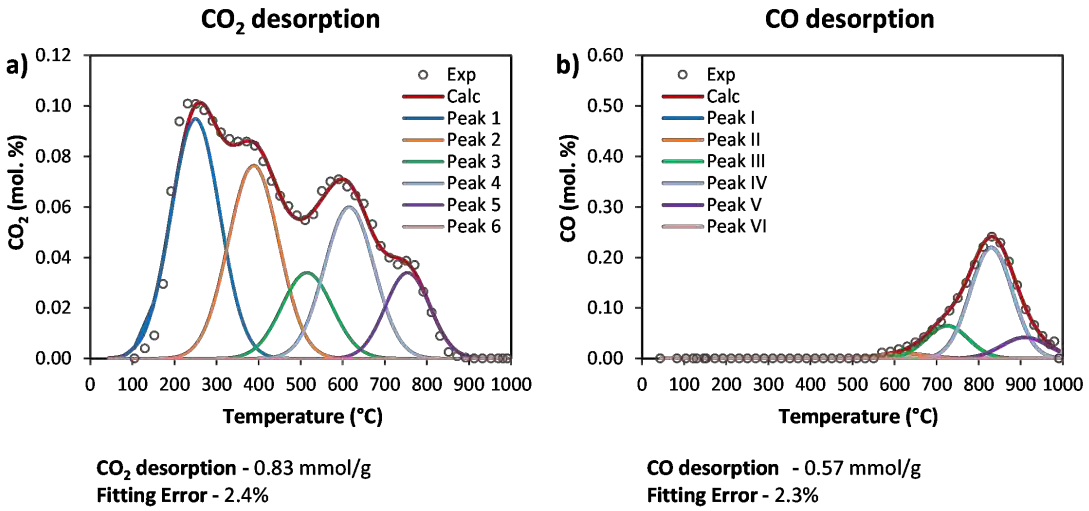

Figure B.1: TPD spectra and deconvolution of CS chars produced at 850°C with a steam fraction of 30% in the gasifying agent. 1 hour gasification time. a) CO_2 desorption, b) CO desorption.

Table B.1: Deconvolution fitting parameters of CS chars presented in figure B.1

	CO_2					
	Carboxylic		**Peroxyde**	**Lactone**	**Lactone**	**Lactone**
Gaussian parameters	**Peak 1**	**Peak 2**	**Peak 3**	**Peak 4**	**Peak 5**	**Peak 6**
a	0.0950	0.0765	0.0340	0.0600	0.0340	0.0000
b	250.0	388.0	515.0	615.5	754.0	900.0
c	58.0	60.0	60.0	59.0	53.0	60.0
Desorption (mmol/g)	0.097	0.123	0.125	0.067	0.126	0.296

	CO					
	Anhydrides	**Hydroxyle**	**Phenol**	**Ether**	**Quinone**	**Pyrones**
Gaussian parameters	**Peak I**	**Peak II**	**Peak III**	**Peak IV**	**Peak V**	**Peak VI**
a	0.0000	0.0100	0.0900	0.4500	0.0300	0.0000
b	400.0	620.0	710.0	808.0	910.0	970.0
c	60.0	50.0	50.0	50.0	50.0	55.0
Desorption (mmol/g)	0.000	0.000	0.023	0.033	0.105	0.414

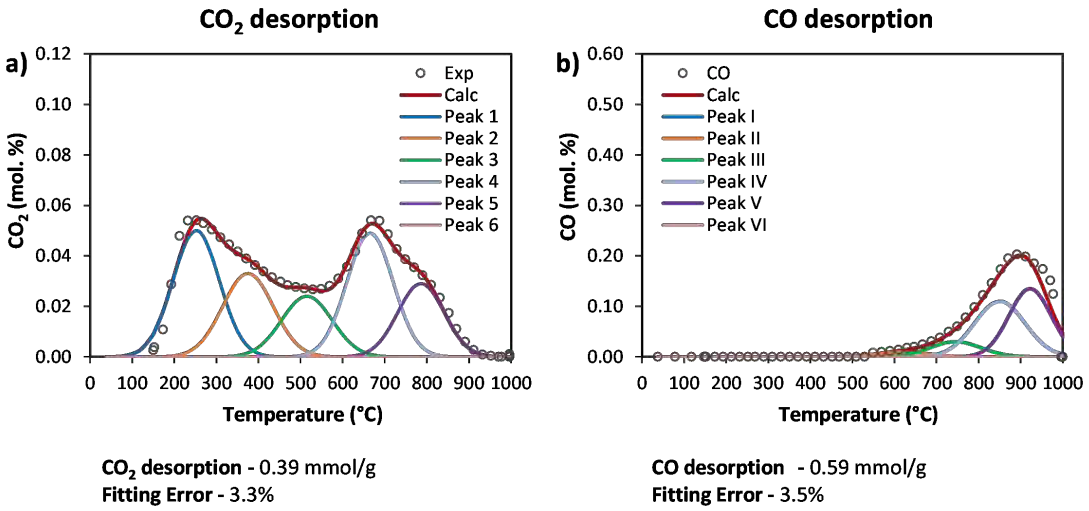

Figure B.2: TPD spectra and deconvolution of BG chars produced at 850°C with a steam fraction of 30% in the gasifying agent. 1 hour gasification time. a) CO_2 desorption, b) CO desorption.

Table B.2: Deconvolution fitting parameters of BG chars presented in figure B.2

	CO_2					
	Carboxylic		**Peroxyde**	**Lactone**	**Lactone**	**Lactone**
Gaussian parameters	**Peak 1**	**Peak 2**	**Peak 3**	**Peak 4**	**Peak 5**	**Peak 6**
a	0.0500	0.0330	0.240	0.0490	0.0290	0.0000
b	252.0	375.0	515.0	665.5	786.0	883.0
c	55.0	60.0	60.0	55.0	55.0	55.0
Desorption (mmol/g)	0.100	0.075	0.054	0.102	0.060	0.000

	CO					
	Anhydrides	**Hydroxyle**	**Phenol**	**Ether**	**Quinone**	**Pyrones**
Gaussian parameters	**Peak I**	**Peak II**	**Peak III**	**Peak IV**	**Peak V**	**Peak VI**
a	0.0000	0.0100	0.0300	0.1100	0.1350	0.0000
b	500.0	620.0	745.0	850.0	922.0	980.0
c	60.0	60.0	60.0	60.0	50.0	50.0
Desorption (mmol/g)	0.000	0.023	0.068	0.247	0.237	0.000

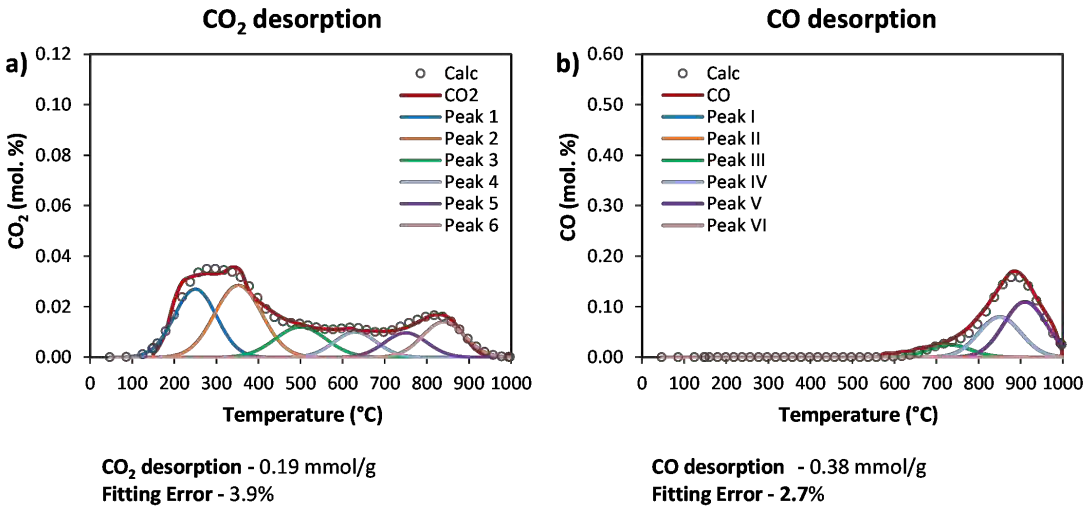

Figure B.3: TPD spectra and deconvolution of OPS chars produced at 850°C with a steam fraction of 30% in the gasifying agent. 1 hour gasification time. a) CO_2 desorption, b) CO desorption.

Table B.3: Deconvolution fitting parameters of OPS chars presented in figure B.3

	CO_2					
	Carboxylic		**Peroxyde**	**Lactone**	**Lactone**	**Lactone**
Gaussian parameters	**Peak 1**	**Peak 2**	**Peak 3**	**Peak 4**	**Peak 5**	**Peak 6**
a	0.0270	0.0285	0.0120	0.0100	0.0097	0.0140
b	250.0	352.0	500.0	630.5	750.0	840.0
c	50.0	56.0	60.0	50.0	50.0	50.0
Desorption (mmol/g)	0.049	0.059	0.026	0.018	0.017	0.026

	CO					
	Anhydrides	**Hydroxyle**	**Phenol**	**Ether**	**Quinone**	**Pyrones**
Gaussian parameters	**Peak I**	**Peak II**	**Peak III**	**Peak IV**	**Peak V**	**Peak VI**
a	0.0000	0.0000	0.0300	0.0800	0.1100	0.0000
b	500.0	620.0	735.0	850.0	910.0	970.0
c	60.0	62.0	50.0	50.0	50.0	50.0
Desorption (mmol/g)	0.000	0.000	0.046	0.148	0.194	0.000

List of Figures

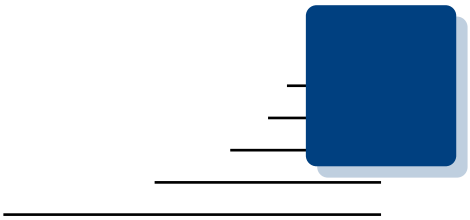

List of Tables

Steam gasification of tropical lignocellulosic agrowaste: impact of biomass characteristics on the gaseous and solid by-products

In the context of most developing countries, steam gasification could be a very interesting process for both energy generation in isolated areas and the production of value-added products from lignocellulosic agrowaste. Considering that the availability of agricultural residues is often seasonal, gasification facilities should operate with different feedstocks. In consequence, this work is focused on the understanding of the impact of biomass characteristics on the gasification process and the properties of the gaseous and solid by-products. Three lignocellulosic agrowastes with different macromolecular structure and inorganic composition were selected for this study: Coconut shells (CS), bamboo guadua (BG) and oil palm shells (OPS). The thermal decomposition kinetics of the selected feedstocks was analyzed in a thermogravimetric scale under inert and steam atmosphere. Despite the differences in their macromolecular composition, inorganics showed to be the most important parameter influencing the steam gasification reactivity and kinetics of the samples. The beneficial impact of AAEM was confirmed, as well as the inhibitory effect of Si and P. More specifically, the ratio K/(Si+P) proved to be suitable to describe and compare the steam gasification behavior of lignocellulosic agrowastes. In accordance, a new kinetic modeling approach was proposed to predict the gasification behavior of samples, from the knowledge of their inorganic composition. The validity of the ratio K/(Si+P) to classify and predict the biomass steam gasification behavior was also confirmed from experiments in a lab-scale fluidized bed gasifier. Samples with K/(Si+P) above 1 exhibited higher gasification reactivities compared to samples with ratios below 1, resulting in greater gas yields and higher gas efficiencies. Moreover, inorganics impacted not only the gasification rate of the samples, but also the properties of the gasification solid by-products. In particular, higher gasification reactivities were related to greater char surface areas and contents of oxygenated surface functional groups. A temperature of 850°C and a steam fraction of 30% in the reacting atmosphere proved to be the most suitable gasification conditions for the simultaneous production of fuel gases for energy applications, and a valuable char that could be valorized in soil amendment applications. The gasification model and experimental results presented in this work might be an important reference for real gasification applications working with different kind of residues, when both the gaseous and solid by-products valorization is intended. Moreover, in the presented context, steam gasification of lignocellulosic agrowaste may improve the energy access in rural isolated areas, and simultaneously promote the development of productive projects that could generate new incomes for local communities.

Keywords: Steam gasification, Gasification reactivity, Lignocellulosic agrowaste, Inorganic composition, Biochar.

Gazéification sous vapeur d'eau de résidus agricoles : impact des caractéristiques de la biomasse sur les propriétés des sous-produits gazeux et solides

Dans le contexte économique de la plupart des pays en voie de développement, la gazéification sous vapeur d'eau de résidus agricoles lignocellulosiques pourrait être un procédé intéressant, à la fois pour la génération d'énergie dans des régions isolées et pour la production des produits à valeur ajoutée. Étant donné que la disponibilité des résidus agricoles est souvent saisonnière, différents types de biomasse doivent être utilisés pour assurer le fonctionnement des installations de gazéification. A cet égard, ce travail est axé sur la compréhension de l'impact des caractéristiques de la biomasse sur le procédé de gazéification et les propriétés des sous-produits gazeux et solides. Trois biomasses lignocellulosiques à composition macromoléculaire et inorganique différentes ont été sélectionnées pour cette étude : coques de noix de coco (CS), bambou guadua (BG) et coques de palmier à huile (OPS). La cinétique de décomposition thermique des biomasses a été étudiée une échelle thermogravimétrique sous atmosphère inerte et sous vapeur d'eau. Malgré les différences dans la structure macromoléculaire des échantillons, la composition inorganique s'est avérée être le paramètre le plus important influençant la réactivité et la cinétique de gazéification. L'impact bénéfique des métaux alcalins et alcalino-terreux a été confirmé, ainsi que l'effet inhibiteur du Si et du P. Plus précisément, le ratio K/(Si + P) est considéré approprié pour décrire et comparer le comportement des biomasses pendant la gazéification sous vapeur d'eau. En conséquence, une nouvelle approche pour la modélisation de la cinétique de gazéification à partir de la composition inorganique de l'échantillon a été proposée. La validité du ratio K/(Si + P) pour classifier et prédire le comportement des biomasses a également été confirmée par des expériences dans un réacteur à lit fluidisé à l'échelle laboratoire. Les échantillons avec un ratio K/(Si + P) au-dessus de 1 ont montré des réactivités de gazéification supérieures à celles des échantillons dont le ratio était inférieur à 1, et donc, une production de gaz et un rendement énergétique plus élevés. De plus, la composition inorganique a non seulement impacté le taux de gazéification des échantillons, mais également les propriétés du sous-produit solide. En particulier, une réactivité de gazéification plus élevée est liée à des chars avec une surface spécifique et un nombre de groupes fonctionnels plus importants. Une température de 850°C et une fraction de vapeur de 30% dans l'agent de réaction ont été identifiées comme les conditions les plus adaptées à la production simultanée de gaz combustible et de char pouvant être valorisé dans des applications agricoles. Le modèle de gazéification sous vapeur d'eau et les résultats expérimentaux présentés dans ce travail peuvent être une référence pour des applications réelles de gazéification travaillant avec différents types de résidus. Par ailleurs, dans le contexte présenté, la gazéification sous vapeur d'eau de déchets lignocellulosiques peut améliorer l'accès à l'énergie des zones rurales isolées, en promouvant simultanément le développement de projets productifs susceptibles de générer de nouveaux revenus pour les communautés locales.

Mots-clés : Gazéification sous vapeur d'eau, Réactivité, Biomasse lignocellulosique, Composition inorganique, Biochar.